JAMS

JOURNAL OF ASSOCIATED MEDICAL SCIENCES

Volume 54 Number 3 September-December 2021 E-ISSN: 2539-6056

Journal of Associated Medical Sciences

Aims and scope

The Journal of Associated Medical Sciences belongs to Faculty of Associated Medical Sciences (AMS), Chiang Mai University, Thailand. The journal specifically aims to provide the platform for medical technologists, physical therapists, occupational therapists, radiologic technologists, speech-language pathologists and other related professionals to distribute, share, discuss their research findings, inventions, and innovations in the areas of:

1. Medical Technology
2. Physical Therapy
3. Occupational Therapy
4. Radiologic Technology
5. Communication Disorders
6. Other related fields

Submitted manuscripts within the scope of the journal will be processed strictly following the double-blinded peer review process of the journal. Therefore, the final decision can be completed in 1-3 months average, depending on the number of rounds of revision.

Objectives

The Journal of Associated Medical Sciences aims to publish integrating research papers in areas of Medical Technology, Physical Therapy, Occupational Therapy, Radiologic Technology, and related under peer-reviewed via double-blinded process by at least two internal and external reviewers.

Types of manuscript

Manuscripts may be submitted in the form of review articles, original articles, short communications, as an approximate guide to length:

- **Review articles** must not exceed 20 journal pages (not more than 5,000 words), including 6 tables/figures, and references (maximum 75, recent and relevant).
- **Original articles** must not exceed 15 journal pages (not more than 3,500 words), including 6 tables/figures, and 40 reference (maximum 40, recent and relevant).
- **Short communications** including technical reports, notes, and letters to the editor must not exceed 5 journal pages (not more than 1,500 words), including 2 tables/figures, and references (maximum 10, recent and relevant).

Peer review process

By submitting a manuscripts to Journal of Associated Medical Sciences, the authors agree to subject it to the confidential double-blinded peer-review process. Editors and reviewers are informed that the manuscripts must be considered confidential. After a manuscripts is received, it is assigned by a specific Associate Editor. The Associate Editor prepares a list of expert reviewers, which may include some suggested by the Editor-in-Chief. Authors can indicate specific individuals whom they would like to have excluded as reviewers. Generally, requests to exclude certain potential reviewers will be honored except in fields with a limited number of experts. All potential reviewers are contacted individually to determine availability. Manuscripts files are sent to at least two expert reviewers. Reviewers are asked to complete the review of the manuscripts within 2 weeks and to return a short review form. Based on the reviewers' comments, the Associate Editor recommends a course of action and communicates the reviews and recommendations to the Editor-in-Chief for a final decision.

The Associate Editor considers the comments made by the reviewers and the recommendation of the Editor-in-Chief, selects those comments to be shared with the authors, makes a final decision concerning the manuscripts, and prepares the decision letter for signature by the Editor-in-Chief. If revisions of the manuscripts are suggested, the Associate Editor also recommends who should review the revised paper when resubmitted. Authors are informed of the decision by e-mail; appropriate comments from reviewers and editors are appended.

Publication frequency

Journal of Associated Medical Sciences publishes 3 issues a year

Issue 1: January-April
Issue 2: May-August
Issue 3: September-December

Journal Impact Factor
The journal's 2017 Impact Factor is 0.237

Journal website
Homepage https://www.tci-thaijo.org/index.php/bulletinAMS/index

Journal E-ISSN:
2539-6056

Editorial Office
Faculty of Associated Medical Sciences, Chiang Mai University
110 Inthawaroros Road, Suthep, Muang, Chiang Mai, 50200
Phone 053 935072 Facsimile 053 936042

Journal of Associated Medical Sciences

Vol. 54 No. 3 : September 2021

Content

Content

Journal of Associated Medical Sciences 2021; 54 (3): 1-10

JAMS
Journal of Associated Medical Sciences

Thai-Journal Citation Index Centre (TCI) & ASEAN Citation Index (ACI)

Journal of Associated Medical Sciences

Journal homepage: https://www.tci-thaijo.org/index.php/bulletinAMS/index

Determination of the reference range of whole blood cholinesterase activities in Thai postmortem cases

Wichuda Pathomrattanasiri Surattana Houngtong Peerayuht Phuangphung*

Department of Forensic Medicine, Faculty of Medicine, Siriraj Hospital, Mahidol University, Bangkok, Thailand.

ARTICLE INFO

Article history:
Received 10 February 2021
Accepted as revised 26 April 2021
Available online 3 May 2021

Keywords:
Cholinesterase activities, whole blood, postmortem, Thai

ABSTRACT

Background: Whole blood cholinesterase activities are biomarkers for diagnosis of organophosphate and carbamate poisoning. The reference ranges for these biomarkers in Thai people were available for living people. However, there is no baseline data for these biomarkers in Thai postmortem cases.

Objectives: The objective of this study is to study the reference range of whole blood cholinesterase activities in Thai postmortem cases and factors influencing enzyme activities.

Materials and methods: Postmortem blood samples were collected from Thai dead bodies who were 18-60 years old and were sent for medico-legal autopsies at the Department of Forensic Medicine, Siriraj Hospital, Mahidol University between 9th June 2020 and 31st December 2020. Data including gender, age, postmortem interval (PMI) and liver pathology were recorded. Whole blood cholinesterase activities were analyzed by using UV-visible spectrophotometer. Whole blood cholinesterase activities were analyzed using descriptive statistics. Mann-Whitney U test and Kruskal-Wallis H test were also tested for comparison between each factor using statistical significance at p<0.05.

Results: There were 176 subjects recruited in this study (121 males and 55 females). Whole blood cholinesterase activities in all subjects were 3514.32-7771.13 IU/mL and the mean and median values were 6150.27 and 6326.78 IU/mL, respectively. There was significant difference among classified four age groups (p value=0.014). Whole blood cholinesterase activities of two lower age groups (18-30 and 31-40 years old) were significantly lower than the third age group (41-50 years old) (p value=0.027 and 0.005, respectively). Whole blood cholinesterase activities were also significantly related to PMI (p value=0.042). The values from early PMI (0-8 hours) period was significantly lower than the values from the second PMI (8-16 hours) period (p value=0.043). In addition, postmortem cases with fatty change >50% significantly presented lower enzyme activities than those with fatty change <50% (p value=0.042).

Conclusion: Whole blood cholinesterase activities in Thai postmortem cases whose age ranged from 18 to 60 years old were 3514.32-7771.13 IU/mL. Age, PMI and liver pathology were three factors that affect whole blood cholinesterase activities in Thai postmortem cases.

* **Corresponding author.**
Author's Address: *Department of Forensic Medicine, Faculty of Medicine, Siriraj Hospital, Mahidol University, Bangkok, Thailand.*
** **E-mail address:** peerayuht.phu@mahidol.ac.th
doi: 10.14456/jams.2021.17
E-ISSN: 2539-6056

Introduction

Cholinesterase enzymes (EC 3.1.1.x) are enzymes found in normal human bodies and belong to serine hydrolase superfamilies.[1] They can be categorized into two types including acetylcholinesterase (AChE, EC 3.1.1.7) and butyrylcholinesterase (BuChE, EC 3.1.1.8). AChE is normally found in erythrocyte, neuro-muscular junction and central nervous system whereas BuChE is mainly found in liver and plasma.[1] Cholinesterase activities can be employed as the biomarker for organophosphate and carbamate poisoning because these two insecticides result in cholinesterase inhibition.[2] Thus, cholinesterase activities should be decreased after the exposure to organophosphate and carbamate insecticides. However, the levels of cholinesterase activities can be affected by several underlying diseases, drugs, malnutrition and genetic variabilities.[1] Thus, the analysis of cholinesterase activities should be carefully interpreted and inter-personal variation and underlying diseases should be also considered.

The analysis of cholinesterase activities can be performed by two methods. The first method is the analysis for whole blood or red blood cell cholinesterase activities which is used for determination of AChE activities.[3] The second method is the analysis for plasma or serum cholinesterase activities which is applied for BuChE activities.[3] Although the determination of AChE activities is preferred for the diagnosis of organophosphate and carbamate poisoning, the analysis of BuChE activities can be performed in some context like the detection of exposure to insecticides or monitoring for clinical recovery.[2,4] However, the detection of BuChE activities may not be suitable for the diagnosis of organophosphate and carbamate poisoning in postmortem cases because of the occurrence of hemolysis in postmortem blood particularly in prolonged postmortem intervals.[5] Thus, the analysis of whole blood cholinesterase activities should be more appropriate for the diagnosis of organophosphate and carbamate poisoning in postmortem cases.

The studies of cholinesterase activities in Thai people from previous publications were conducted in healthy Thai living people who were not exposed to pesticides and the authors reported that means and ranges of AChE activities in healthy Thai people were 3320-5136 IU/mL[6,7] and 3684-6588 IU/mL,[6] respectively. However, there is no information for whole blood cholinesterase activities in normal Thai postmortem cases. Klette KL et al reported that the mean and range of whole blood cholinesterase activities in postmortem cases were 4800 IU/mL and 2000-7400 IU/mL.[8] Postmortem changes may affect whole blood cholinesterase activities in dead bodies due to the effect of postmortem blood hemolysis[5] and the effect of bacterial cholinesterase activities[9] from bacterial translocation into blood stream after death.[10] Therefore, this study aims to determine the baseline reference values of whole blood cholinesterase activities in Thai postmortem cases for the application to the diagnosis of organophosphate and carbamate poisoning in Thai postmortem cases.

Materials and methods

Study subjects

Blood samples were collected from Thai medico-legal cases who were sent for medico-legal autopsies at Department of Forensic Medicine, Siriraj Hospital, Mahidol University between 9th June 2020 and 31st December 2020. Inclusion criteria for this study were Thai postmortem cases who were between 18 and 60 years old with no histories of any underlying diseases and had declared postmortem intervals not greater than 24 hours (no signs of decomposition). Exclusion criteria consisted of 5 types including:

1. Dead bodies who were agriculturists
2. Dead bodies who were suspicious for organophosphate or carbamate poisoning
3. Dead bodies who had the history of hospital admission greater than 24 hours
4. Dead bodies who had signs of sepsis from medical records or autopsy findings
5. Dead bodies who were given for cholinesterase inhibitor drugs.

This study was approved by the Siriraj Institutional Review Board, Faculty of Medicine, Siriraj Hospital, Mahidol University (Certificate of Approval No. Si 389/2020).

Sample collection

Blood samples were taken from femoral vein access during autopsy procedures. Blood samples approximately 7-10 mL were collected into blood tubes without any anticoagulants. Then, blood samples were transferred to keep in the refrigerator at 4 °C. Whole blood cholinesterase activities were analyzed by using UV-visible spectrophotometer in the next day. Before blood sample was analyzed, the blood tube was gently overturned back and forth around 8-10 times. Next, the blood tube was slightly inclined and liquid blood sample was slowly taken out approximately 2-3 mL into the other tube which was sufficient for analysis. Any blood clot inside the blood tube was avoided during blood pipetting to ensure that liquid blood form was transferred. Then, transferred blood sample was mixed using blood vortex mixer to obtain blood homogeneity for analysis. The analysis was performed in duplicated and the mean values were determined and recorded as whole blood cholinesterase activities for blood samples.

Subject data including gender, age, postmortem interval (PMI), liver pathology and cause of death were recorded for each blood sample for statistical analysis. The age in this study was classified into four categories: 18-30, 31-40, 41-50 and 51-60 years old. PMI was categorized into three groups: 0-8, 8-16 and 16-24 hours. Liver pathology could be defined based on gross and microscopic findings and then divided into two groups: liver with fatty change less than 50% and liver with fatty change more than 50% (Figure 1).

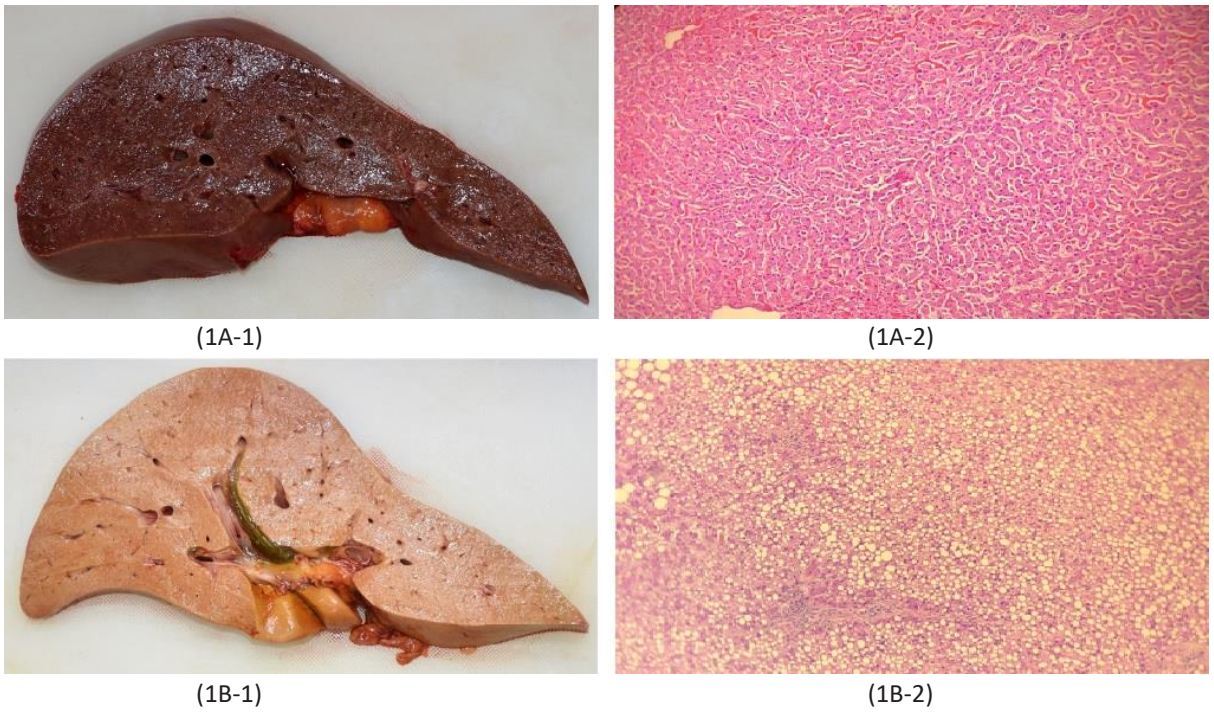

Figure 1. *Gross and microscopic findings for liver pathology. 1A: fatty change <50%, 1A-1: gross findings, 1A-2: microscopic findings, 1B: fatty change >50%, 1B-1: gross findings, 1B-2: microscopic findings.*

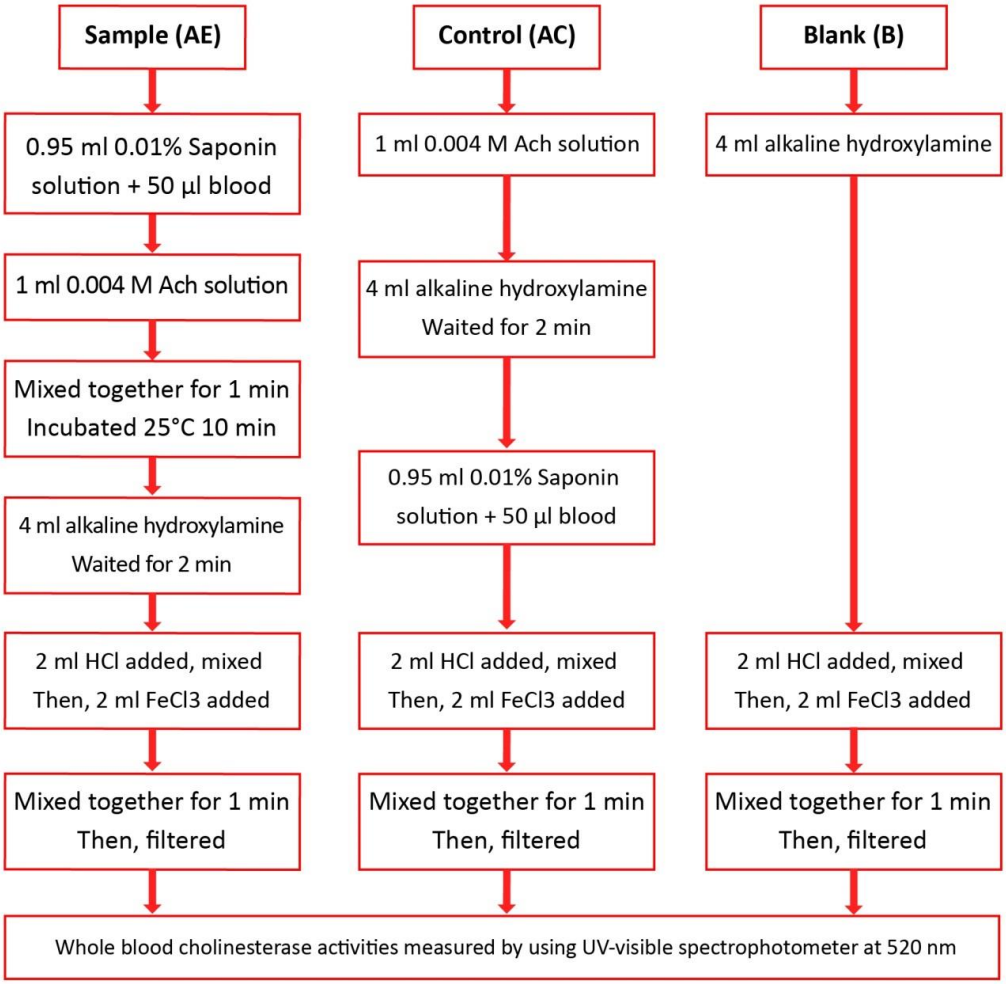

Figure 2. *Experimental steps for the analysis of whole blood cholinesterase activities*[3].

Chemicals and reagents

Acetylcholine chloride (Ach) 99%, sodium acetate AR grade, glacial acetic acid AR grade, disodium hydrogen phosphate pentahydrate AR grade, potassium dihydrogen phosphate anhydrous AR grade, sodium hydroxide (NaOH) AR grade, hydrochloric acid (HCl) 37%, ferric chloride ($FeCl_3$) anhydrous 98%, hydroxylamine hydrochloride 99%, saponin permeating solution (0.5% w/v solution in phosphate buffer solution) and Whatman filter paper number 41 with diameter 110 millimeters (mm) were purchased from U&V Holding (Thailand) Co., Ltd. Deionized water was generated from Merck Millipore Direct-Q® 3 UV-R Water Purification System.

Sample preparation for the analysis of whole blood cholinesterase activities[3]

The analysis of whole blood cholinesterase activities was performed in three sample groups for each blood sample including sample group (AE), control group (AC) and blank group (B). Experimental steps in these three sample groups were described in Figure 2.

After all sample groups were filtered by Whatman paper, all sample groups were taken into quartz cuvette with path length 10 mm. Then, all three sample groups were measured for whole blood cholinesterase activities using the Agilent Cary 8454 UV-visible spectrophotometer at 520 nanometers (nm) within 10 minutes.

Blank group was used for zero adjustment in measurement. Next, control group (AC) and sample group (AE) were measured against blank group to obtain cholinesterase activities. Then, whole blood cholinesterase activities were calculated by using equation 1 as described below

Whole blood cholinesterase activities (IU/mL) = [4-(4AE/AC)]x2000 IU/mL (**Equation 1**)

The analysis was performed in duplicate for each blood sample. Next, %coefficient of variation (%CV) was determined for these two results. Acceptable %CV in this study should not be greater than 15% based on method validation guidelines. Then, these two results were calculated for the mean value of each blood sample and this mean value was recorded and used for the statistical analysis.

External quality control from proficiency testing (PT) samples

Two external quality control samples that were supplied as PT samples were used for verification of this laboratory method and these two samples were kindly supported by the Department of Medical Sciences. These two samples were analyzed for whole blood cholinesterase activities. The results from these two PT samples were compared with the results from the Department of Medical Sciences. All results obtained from the laboratory method should be in good agreement with acceptable criteria for the application to postmortem blood samples.

Statistical analysis

The data for whole blood cholinesterase activities were analyzed using IBM SPSS® Statistics for Window version 26. Descriptive statistics including mean, median, and standard deviation (SD) were analyzed. Normality test was performed using Kolmogorov-Smirnov test. After normality test, data set in this study did not meet the criteria of normal distribution and the equality of variances. Thus, the Mann-Whitney U test and Kruskal-Wallis H test were performed for data comparison where it was appropriate. Statistical significance was set at p value <0.05.

Results

The results of two PT samples compared with the results from all participant laboratories reported in the certificate from the Department of Medical Sciences were shown in Table 1.

Table 1 The results of PT samples compared with the results from the Department of Medical Sciences.

PT sample	Results from all laboratories participated in PT schemes (N = 6) (IU/mL)	Results from this study (IU/mL)
PT NIH/AChE 1/63	2847±791	3338.34
	(Median Xi = 2839, MAD = 338)	(Criterion=1.48)
PT NIH/AChE 2/63	2440±663	3095.99
	(Median Xi=2474, MAD=420)	(Criterion=1.48)

According to the certificate, the Department of Medical Sciences employed median absolute deviation (MAD) method to analyze the results and the acceptable criterion was:

$$\text{Criterion: } \frac{|Xi\text{-}median\ (xi)|}{MAD} < 5$$

When the results from this study were applied for the criterion, it was found that all of these two results were in acceptable ranges. Thus, this method was able to apply for postmortem blood samples.

There were 176 blood samples recruited for the analysis of whole blood cholinesterase activities in this study. The subjects were 121 males (68.75%) and 55 females (31.25%). The mean ages of male and female subjects were 45 and 46 years old, respectively. Whole blood cholinesterase activities in all subjects ranged from 3514.32 to 7771.13 IU/mL and the mean and median values were 6150.27 and 6326.78 IU/mL, respectively. The range, mean and median of whole blood cholinesterase activities in male and female subjects were shown in Table 2. Data for whole blood cholinesterase activities were present in histogram chart as shown in Figure 3.

Table 2 Whole blood cholinesterase activities in all subjects classified by gender.

Sex	N	Range (IU/mL)	Mean±SD (IU/mL)	Median (IU/mL)
Female	55	3642.52-7693.23	6153.86±1098.14	6305.92
Male	121	3514.32-7771.13	6148.64±991.56	6350.23
Total	176	3514.32-7771.13	6150.27±1022.89	6326.78

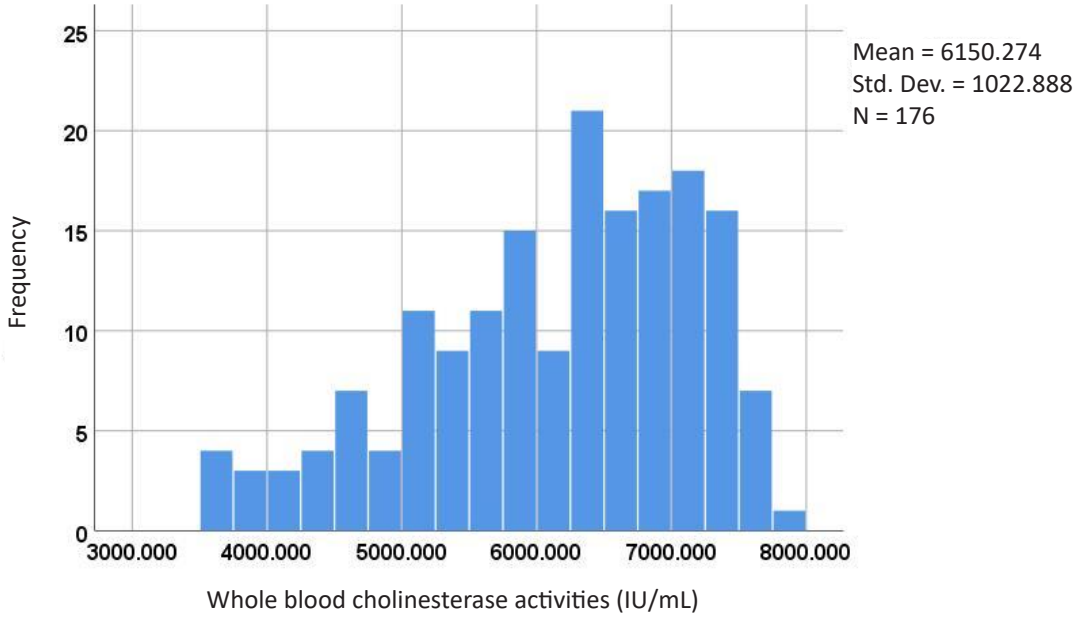

Figure 3. *Histogram of whole blood cholinesterase activities in this study.*

Comparison of whole blood cholinesterase activities between Thai male and female subjects was analyzed by using Mann-Whitney U test and it was found that the values in male subjects were not significantly different from those in female subjects (*p* value=0.812) as shown in Figure 4.

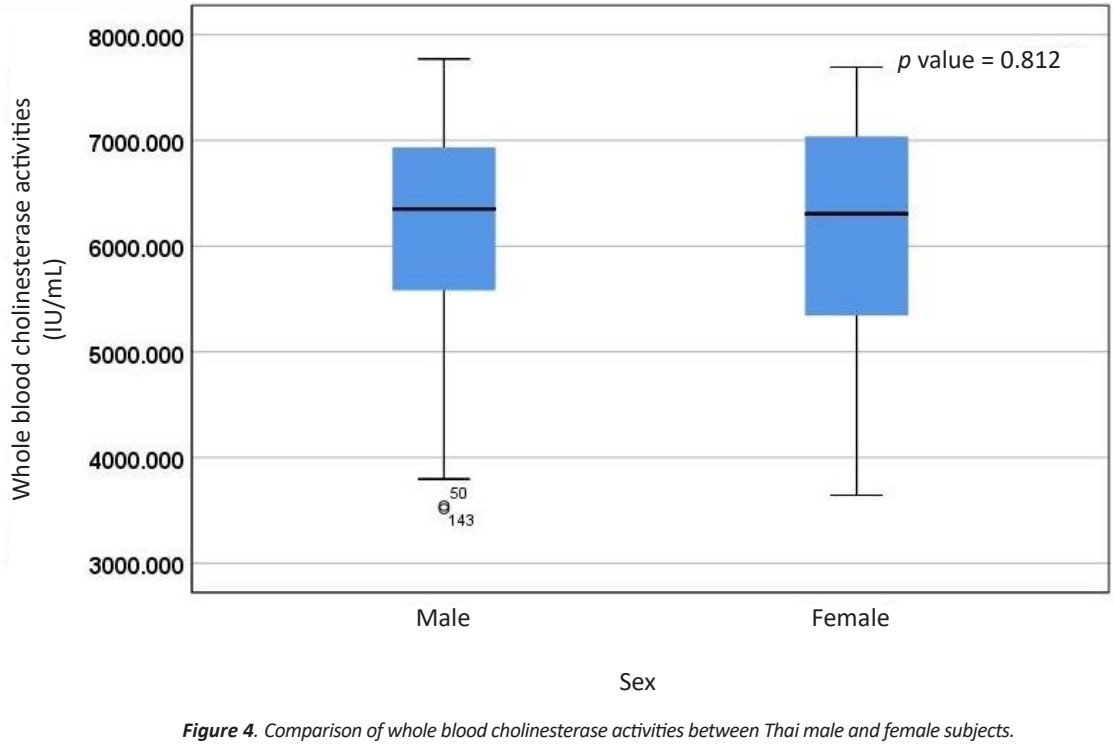

Figure 4. *Comparison of whole blood cholinesterase activities between Thai male and female subjects.*

Whole blood cholinesterase activities in four age groups classified in this study were shown in Table 3. Then, the comparison of whole blood cholinesterase activities among these four age groups was analyzed by using Kruskal-Wallis H test and it was found that there was significant difference among these four age groups (*p* value=0.014) as shown in Figure 5. When the comparison between each group was considered, it was found that the values in the first two lower age groups (18-30 and 31-40 years old) were significantly different from the values in the third age group (41-50 years old) (*p* value=0.027 and 0.005, respectively). In addition, the values in the second age group (31-40 years old) were also significantly different from the values in the fourth age group (51-60 years old) (*p* value=0.022).

Table 3 Whole blood cholinesterase activities in four age groups.

Age (years old)	N	Range (IU/mL)	Mean±SD (IU/mL)	Median (IU/mL)
18-30	48	3514.32–7600.95	6306.91±988.49	6528.72
31-40	43	4510.02–7771.13	6475.01±854.66	6636.21
41-50	41	3542.62–7502.21	5835.67±1060.30	5945.70
51-60	44	3642.52–7693.23	5955.20±1079.24	6144.62
Total	176	3514.32-7771.13	6150.27±1022.89	6326.78

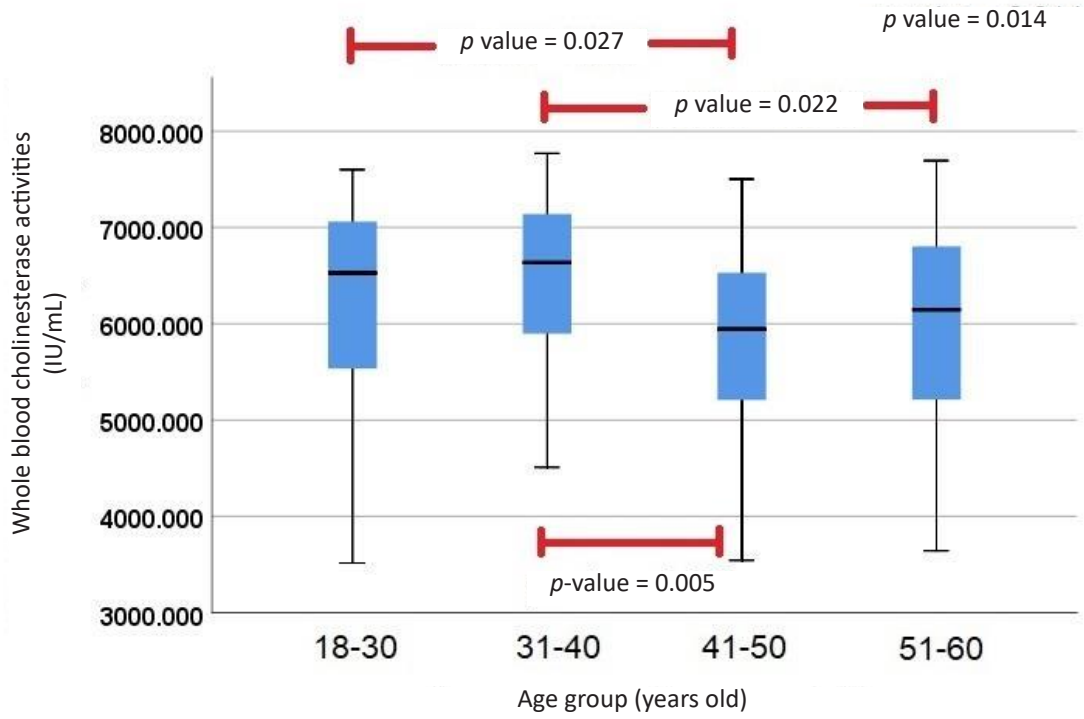

Figure 5. *Comparison of whole blood cholinesterase activities among four age groups.*

Whole blood cholinesterase activities in three PMI groups were shown in table 4. When the analysis by Kruskal-Wallis H test was performed for these three PMI groups, it was found that there was significant difference among these three PMI groups (*p* value=0.042) as shown in figure 6. It was found that the values in the first PMI group (0-8 hours) were lower than the other two groups. The values in the second PMI group were significantly higher than the first PMI group (*p* value=0.043). According to Table 4, the values in the third PMI group were lower than the second PMI group but still higher than the first PMI group. However, this difference did not have statistical significance.

Table 4 Whole blood cholinesterase activities in three PMI groups.

PMI (hours)	N	Range (IU/mL)	Mean±SD (IU/mL)	Median (IU/mL)
0-8	44	3514.32-7568.96	5883.69±1124.99	6003.32
8-16	56	3642.52-7771.13	6413.85±936.88	6538.77
16-24	76	3714.47-7693.23	6110.39±988.38	6340.43
Total	176	3514.32-7771.13	6150.27±1022.89	6326.78

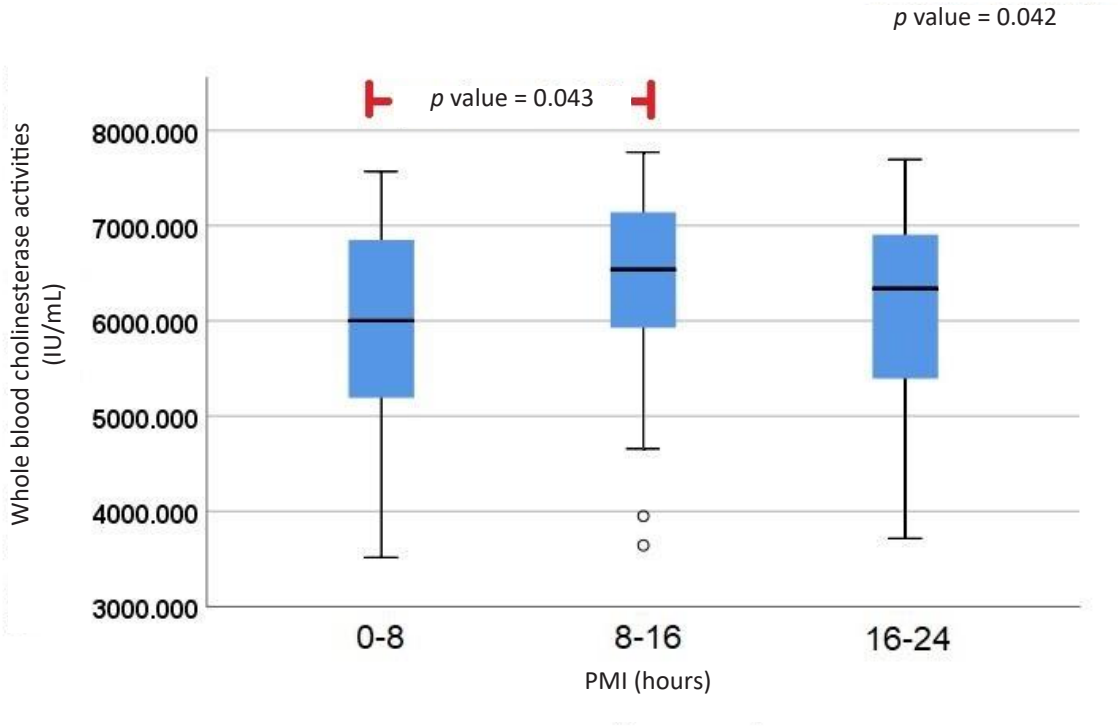

Figure 6. *Comparison of whole blood cholinesterase activities among three PMI groups.*

Whole blood cholinesterase activities in two groups of liver pathology were shown in Table 5. After the analysis with Mann-Whitney U test, it was found that there was significant difference between the group with fatty change less than 50% and the group with fatty change greater than 50% (*p* value=0.042) as shown in Figure 7.

Table 5 Whole blood cholinesterase activities in two groups of liver pathology.

Liver pathology	N	Range (IU/mL)	Mean±SD (IU/mL)	Median (IU/mL)
Fatty change <50%	116	3514.32-7771.13	6269.33±982.94	6368.58
Fatty change >50%	60	3642.52-7493.35	5920.10±1066.99	6168.97
Total	176	3514.32-7771.13	6150.27±1022.89	6326.78

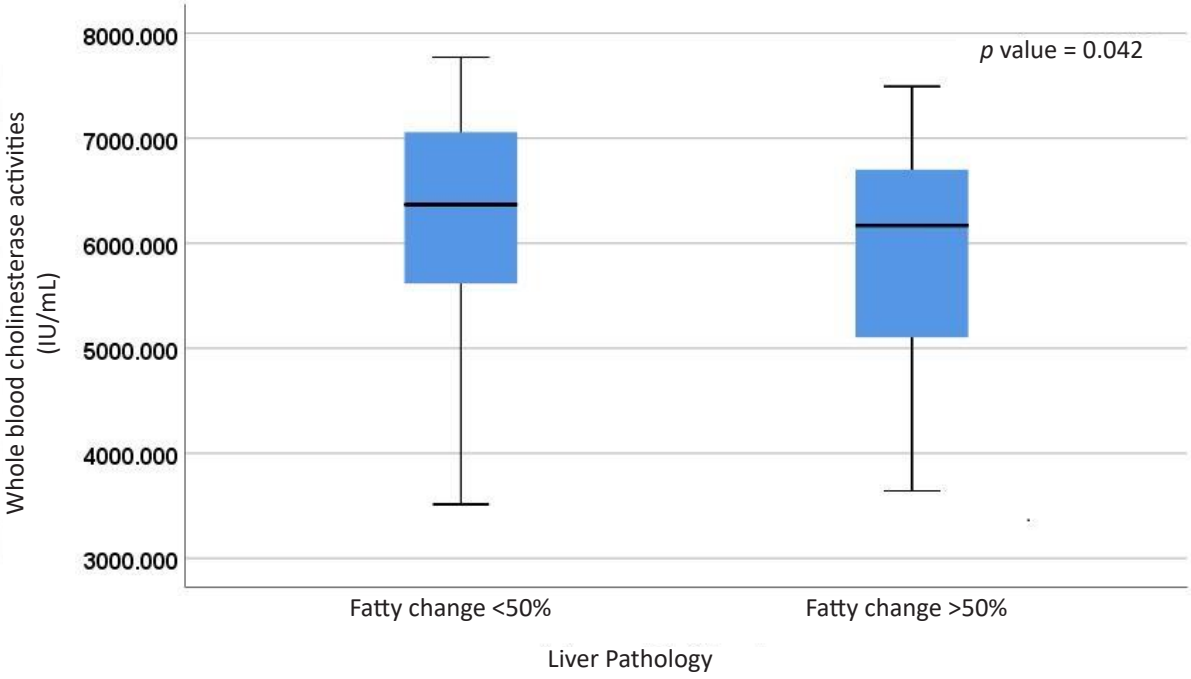

***Figure 7**. Comparison of whole blood cholinesterase activities between two groups of liver pathology.*

Discussion

Whole blood cholinesterase activities in Thai postmortem cases in this study ranged from 3514.32 to 7771.13 IU/mL and the mean and median values were 6150.27 and 6326.78 IU/mL, respectively. These values were slightly higher than AChE activities in healthy Thai living people reported by Singhatong S.[6] This finding might be explained by the effect of bacterial activities following the progression of postmortem change. The process of postmortem change began with early period consisting of cellular death, the reduction of body temperature, loss of adenosine triphosphate (ATP) and circulation cease.[5] This process produced supravital reaction, postmortem cooling, postmortem rigidity and postmortem lividity, respectively[5]. When PMI increased, protein degradation and bacterial translocation due to loss of integrity of intestinal mucosa occurred and these led to secondary flaccidity and transition state before decomposition.[5,10] After 24 hours (1 day), decomposition process was mostly developed in postmortem cases under ambient temperature (20 °C).[5] Putrefaction played an important role in decomposition as a result of bacteria and other microorganisms.[5] According to this process, bacterial translocation from gastro-intestinal (GI) tract into bloodstream occurred after death following increased PMI.[5,10] There were many bacterial strains in GI tract as normal intestinal flora. *Pseudomonas aeruginosa* was reported that it could be detected as normal intestinal flora in GI tract but it had low infectivity because it was unable to attach to normal intestinal epithelium.[11] The previous study showed that some bacterial strains like *Pseudomonas spp*. could produce acetylcholine-hydrolyzing enzymes.[9] Thus, it could be possible that translocation of intestinal flora like *Pseudomonas*. aeruginosa into postmortem blood was responsible for slightly higher cholinesterase activities after death.

This study showed that whole blood cholinesterase activities in male and female subjects were not significantly different and this result was consistent with the previous study.[3] In contrast to gender, this study showed that the younger age groups tended to have greater whole blood cholinesterase activities than the older age groups. Previous studies demonstrated that cholinesterase activities in the brains of younger humans and younger rats were higher than those of older humans and older rats.[12,13] In addition, it was reported that AChE activities in younger age group were higher than older age group although it was not statistically significant.[14] Thus, it might be possible that whole blood cholinesterase activities were age-related in Thai postmortem cases.

This study demonstrated that the trend of whole blood cholinesterase activities changed following increased PMI. In early PMI period (0-8 hours), whole blood cholinesterase activities were lower than those in the next two PMI periods. Whole blood cholinesterase activities were increased significantly in the second PMI period (8-16 hours). Then, whole blood cholinesterase activities declined in the last PMI period (16-24 hours) but the values were still slightly higher than the values in the early PMI period with no statistical significance. This result could be explained by the effect of bacterial translocation and protein denaturation. In the first PMI period (0-8 hours), whole blood cholinesterase activities were not affected by acetylcholine-hydrolyzing enzymes from some bacterial strains[9] due to minor effect of bacterial translocation in early postmortem period. When PMI increased, bacterial translocation significantly

occurred[10] and it might be hypothesized that some bacterial strains like *Pseudomonas aeruginosa* from GI tract could enter the bloodstream and produce cholinesterase activities as mentioned above. When PMI was progressively increased, the secondary flaccidity after rigor mortis occurred because of muscle breakdown and protein denaturation process.[5] Due to the effect of protein denaturation, all human proteins would be denatured and the protein functions should be decreased. Thus, it should be explained that the reduction of whole blood cholinesterase activities in the last PMI group resulted from enzyme denaturation even though the decrease of whole blood cholinesterase activities was not statistically significant. Further study should be conducted in the late PMI period (greater than 24 hours) which would prove the trend of whole blood cholinesterase activities after protein denaturation.

Whole blood cholinesterase activities in the group with fatty change in liver less than 50% significantly higher than those in the group with fatty change in liver more than 50%. AChE was normally synthesized in nervous tissue, nerve fiber, and erythropoiesis.[1] However, AChE was a glycoprotein which contained protein and carbohydrate (10-15% of its molecule).[1] This indicated that the synthesis of AChE required these two nutrients. The previous study reported that the deficiency of some amino acids could be related to fatty change in liver, for example, tryptophan and methionine.[15] AChE had two active sites and one of them was quaternary ammonium binding site for choline.[1] The key amino acid residue in this site was tryptophan.[1] Thus, it might be hypothesized that fatty change greater than 50% in liver affected synthetic capacity of some nutrients and had an effect on whole blood cholinesterase activities.

This study had some limitations. Firstly, there were small proportions of Thai female subjects in this study. Thus, the interpretation that whole blood cholinesterase activities in Thai male and female populations was not different should be carefully performed because there were some studies indicating that gender also affected ChE activities.[14] In addition, whole blood cholinesterase activities in this study were analyzed using the conventional method which did not have AChE extraction process from erythocytes[16] and the previous study stated that the conventional method could suffer from hemoglobin interference which might affect the method accuracy.[1] However, this conventional method consisted of simple analytical steps and more suitable for application in many laboratories. Thus, the analysis of whole blood cholinesterase activities should be carefully interpreted and case information should be also considered.

Conclusion

Whole blood cholinesterase activities in Thai postmortem cases whose age ranged from 18 to 60 years old were 3514.32-7771.13 IU/mL and the mean and median values were 6150.27 and 6326.78 IU/mL, respectively. Age, PMI and liver pathology were three factors that affect whole blood cholinesterase activities in Thai postmortem cases. Thus, these three factors should be considered when the analysis of whole blood cholinesterase activities was performed in Thai postmortem cases.

Conflict of interest

The authors declare no conflicts of interest.

Acknowledgments

This research project was supported by Siriraj Research Fund, Grant number (IO) R016331048, Faculty of Medicine, Siriraj Hospital, Mahidol University. In addition, the authors were indebted to the Department of Medical Sciences for the provision of two PT samples.

References

[1] Assis CRD, Linhares AG, Cabrera MP, Oliveira VM, Silva KCC, Marcuschi M, Maciel Carvalho EVM, Bezerra RS, Carvalho LB Jr. Erythrocyte acetylcholinesterase as biomarker of pesticide exposure: new and forgotten insights. Environ Sci Pollut Res Int. 2018; 25(19): 18364-76. doi: 10.1007/s11356-018-2303-9.

[2] Eddleston M, Buckley NA, Eyer P, Dawson AH. Management of acute organophosphorus pesticide poisoning. Lancet. 2008; 371(9612): 597-607. doi: 10.1016/S0140-6736(07)61202-1.

[3] Kala M. Chapter 16 Pesticides. In: Moffat AC, Osselton MD, Widdop B. editors. Clarke's Analysis of Drugs and Poisons. 4th Ed. London, UK: Pharmaceutical Press; 2011: 258-87.

[4] Aurbek N, Thiermann H, Eyer F, Eyer P, Worek F. Suitability of human butyrylcholinesterase as therapeutic marker and pseudo catalytic scavenger in organophosphate poisoning: a kinetic analysis. Toxicology. 2009; 259(3): 133-9. doi: 10.1016/j.tox.2009.02.014.

[5] Madea B. Methods for determining time of death. Forensic Sci Med Pathol. 2016; 12(4): 451-85. doi: 10.1007/s12024-016-9776-y.

[6] Singhatong S. Acetylcholinesterase and butyrylcholinesterase levels of healthy volunteers who not exposed to pesticides in Chiang Mai Province. J Assoc Med Sci. 2017; 50(2): 168-75.

[7] Hongsibsong S, Kerdnoi T, Polyiem W, Srinual N, Patarasiriwong V, Prapamontol T. Blood cholinesterase activity levels of farmers in winter and hot season of Mae Taeng District, Chiang Mai Province, Thailand. Environ Sci Pollut Res Int. 2018; 25(8): 7129-34. doi: 10.1007/s11356-015-4916-6.

[8] Klette KL, Levine B, Dreka C, Smith ML, Goldberger BA. Cholinesterase activity in postmortem blood as a screening test for organophosphate/chemical weapon exposure. J Forensic Sci. 1993; 38(4): 950-5.

[9] Tani Y, Nagasawa T, Oda H, Ogata K. Distribution and Some Properties of Bacterial Cholinesterase. Agricultural and Biological Chemistry. Agr Biol Chem. 1975; 39(1): 105-11.

[10] Palmiere C, Egger C, Prod'Hom G, Greub G. Bacterial Translocation and Sample Contamination in Postmortem Microbiological Analyses. J Forensic Sci. 2016; 61(2): 367-74. doi: 10.1111/1556-4029.12991.

[11] Pachori P, Gothalwal R, Gandhi P. Emergence of antibiotic resistance Pseudomonas aeruginosa in intensive care unit; a critical review. Genes Dis. 2019 Apr; 6(2): 109-19. doi: 10.1016/j.gendis.2019.04.001.

[12] Janeczek M, Gefen T, Samimi M, Kim G, Weintraub S, Bigio E, Rogalski E, Mesulam MM, Geula C. Variations in Acetylcholinesterase Activity within Human Cortical Pyramidal Neurons Across Age and Cognitive Trajectories. Cereb Cortex. 2018; 28(4): 1329-37. doi: 10.1093/cercor/bhx047.

[13] Meneguz A, Bisso GM, Michalek H. Age-related changes in acetylcholinesterase and its molecular forms in various brain areas of rats. Neurochem Res. 1992; 17(8): 785-90. doi: 10.1007/BF00969013.

[14] Karasova JZ, Maderycova Z, Tumova M, Jun D, Rehacek V, Kuca K, Misik J. Activity of cholinesterases in a young and healthy middle-European population: Relevance for toxicology, pharmacology and clinical praxis. Toxicol Lett. 2017; 277: 24-31. doi: 10.1016/j.toxlet.2017.04.017.

[15] King DW, Socolow EL, Bensch KG. The relation between protein synthesis and lipide accumulation in L strain cells and Ehrlich ascites cells. J Biophys Biochem Cytol. 1959; 5(3): 421-31. doi: 10.1083/jcb.5.3.421.

[16] Linhares AG, Assis CR, Siqueira MT, Bezerra RS, Carvalho LB Jr. Development of a method for extraction and assay of human erythrocyte acetylcholinesterase and pesticide inhibition. Hum Exp Toxicol. 2013; 32(8): 837-45. doi: 10.1177/0960327112468906.

Journal of Associated Medical Sciences 2021; 54 (3): 11-17

JAMS
Journal of Associated Medical Sciences

Thai-Journal Citation Index Centre (TCI) & ASEAN Citation Index (ACI)

Journal of Associated Medical Sciences

Journal homepage: https://www.tci-thaijo.org/index.php/bulletinAMS/index

Activities of daily living performance in stroke survivors receiving services from the trained village health volunteers at Doi Lor Community Rehabilitation Center, Doi Lor District, Chiang Mai Province, Thailand

Pisak Chinchai[1*] **Siriphan Kongsawasdi**[2]

[1]*Department of Occupational Therapy, Faculty of Associated Medical Sciences, Chiang Mai University, Chiang Mai Province, Thailand*
[2]*Department of Physical Therapy, Faculty of Associated Medical Sciences, Chiang Mai University, Chiang Mai Province, Thailand*

ARTICLE INFO

Article history:
Received 17 April 2021
Accepted as revised 29 April 2021
Available online 3 May 2021

Keywords:
Functional performance, community rehabilitation, activities of dailylLiving, Stroke

ABSTRACT

Background: Stroke is a major health problem in Thailand. The majority of stroke survivors suffer a sequela of the disease such as muscle weakness, sensory deficits, visual problems, and perceptual and cognitive function disorders. All of these lead to poor performance in activities of daily living for those survivors. Community-based rehabilitation is considered a potential approach that promotes functional performance in stroke individuals.

Objectives: The purpose of the current study was to investigate the effectiveness of rehabilitation services provided by trained village health volunteers (VHVs) in activities of daily living performance for stroke patients.

Materials and methods: This study was a one-group pre-test and post-test research design. Eleven stroke subjects were recruited by purposive sampling from Doi Lor Community Rehabilitation Center in Chiang Mai Province. Their activities of daily living performance were compared before and after the treatment program. The instrument used was The Activities of Daily Living Assessment Tool. Statistics used were descriptive and included the Wilcoxon Signed Ranks Test.

Results: Results demonstrated that the basic activities of daily living performance in stroke participants increased significantly from pre-intervention to post-test (z=-2.223, p<0.05). Also, scores in the instrumental activities of daily living of these individuals increased from pre-test to post-test significantly (z=-2.805, p<0.05).

Conclusion: It was indicated that Doi Lor Community Rehabilitation Center run by trained VHVs could provide effective improvement in activities of daily living performance in stroke clients.

* **Corresponding author.**
Author's Address: *Department of Occupational Therapy, Faculty of Associated Medical Sciences, Chiang Mai University, Chiang Mai Province, Thailand.*
** **E-mail address:** pisak.c@cmu.ac.th
doi: 10.14456/jams.2021.18
E-ISSN: 2539-6056

Introduction

Stroke is a major health problem in Thailand. It is the leading cause of death. Stroke is also the leading cause of long-term disability in those who survive. In 2012, rates of stroke mortality were 30.7 per 100,000 people,[1] and this increased to 44.8 per 100,000 people in 2014,[2] and 47.8 per 100,000 people in 2017.[3] In 2011, the total recordable incident rate of stroke was 330.6 per 100,000 people, which in 2014 escalated to 352.3 per 100,000 people and 425.2 per 100,000 people in 2015.[3, 4] Approximately 90% of stroke victims suffer a sequela of stroke such as weakness of the muscles, sensory deficits, perceptual problems and cognitive dysfunction, visual disorders, dysphagia, and aphasia.[5-7] All of these lead to poor performance in activities of daily living for these individuals.

Rehabilitation services in Thailand occur mainly in institutional settings. Especially in major and general hospitals in urban areas, while less attention was paid to disabled persons living at home and out in the rural community, especially ones who live in remote rural areas.[8] It is a characteristic of Thai culture that family caregivers and relatives tend to help disabled persons under their care instead of encouraging individuals to be independent in life.[9] There are few numbers of occupational therapists in Thailand compared to the total population of individuals who need occupational therapy treatment, especially for those in rural areas. Telerehabilitation can be used as alternative treatment method for clients who live far from urban areas.[10] However, many Thai people who live in remote areas do not have communication devices and a lot of them cannot access the internet to receive treatment via telerehabilitation.

Local government organizations Such as Sub-district Administrative Organizations (SAO) and Sub-district municipalities in Thailand are permitted by the government to establish a community rehabilitation center(s) with their own budget. These sub-district-rehabilitation centers can facilitate basic treatment programs provided by village health volunteers (VHVs). These centers can also be a place to advocate the human rights of people with disabilities.[11] Therefore, some Sub-district Municipalities, and SAO, where the mayor, chief executive, and officers agree on the needs of people for rehabilitation in their areas, provide the funding to establish rehabilitation centers. However, the Thai government does not require these centers to hire health professionals such as occupational and physical therapists because of the limitations of budget in maintaining the continuum of rehabilitation services.

Doi Lor Sub-district at Doi Lor District, Chiang Mai Province in Thailand is located approximately 60 kilometers away from the Chiang Mai city area. There were 223 persons with disabilities in this Sub-district, among 12,227 of the total population, who desperately waited for rehabilitation outreach since there was only one physical therapist providing services for people with disabilities in the whole district.[12] Regarding limited financial support from the government, there was no occupational therapist working in Doi Lor District. The chief executive of Doi Lor SAO, officials and heads of the villages agreed together to set up the Rehabilitation Center in their own area and trained the village health volunteers (VHVs) to work as rehabilitation workers.

Researchers, for this study, were interested in the effectiveness of services run by the trained VHVs at Doi Lor Community Rehabilitation Center in terms of functional performance for stroke survivors. Specifically, this study aimed to explore the effectiveness of rehabilitation services run by the trained VHVs on activities of daily living performance in stroke clients.

Materials and methods

Study design

This study was a single group, pre-test and post-test research design. It was comparing the activities of daily living performance of stroke clients before receiving services, from VHVs at Doi Lor Community Rehabilitation Center, and 8 weeks after receiving this intervention.

Participants

Sixteen stroke participants who received services at Doi Lor Community Rehabilitation Center in Chiang Mai Province, Thailand, were selected using purposive sampling. After the Community Rehabilitation Center agreed to participate in this research project, the principal investigator recruited participants corresponding to the inclusion and exclusion criteria.

All participants were required to meet the following inclusion criteria: 1) first stroke incident 2) the first admission to the center, 3) stable medical symptoms, 4) age between 20 and 80 years, 5) were able to participate in the program for one and a half hours each time, twice a week, for 8 consecutive weeks, and 6) could follow a three-part command. Participants were excluded if they: 1) had aphasia, and 2) participated in rehabilitation programs from other institutes at the same time as this study. The withdrawal criterion was the stroke survivors who participated less than 80 percent of the whole program.

All of the participants were informed about the procedure of the research project and each of them signed a consent form prior to starting the study.

Instruments

The Activities of Daily Living Assessment Tool (ADL–AT)

This instrument was developed by Apichai et al.[13] to provide a measure of ability on activities of daily living in stroke patients. This included both basic activities of daily living (BADL) and instrumental activities of daily living (IADL). Scores were measured by rating scales ranging from 1 to 5; 1 referring to dependence, 2 referring to maximal assistance, 3 referring to moderate assistance, 4 referring to minimal assistance, and 5 referring to independence with or without supervision. The BADL in this test is divided into 3 aspects consisting of self-care activities, functional mobility, and sexual expression. There are 23 items in the complete BADL. Possible scores in the BADL range from 23 to 115. There are 12 items in the IADL e.g. care of others, child-rearing, care of pets, communication management, community mobility, financial management, etc. Possible scores in the IADL range from 12 to 60. The total scores of this instrument range from 35 to 175. The items that are not applicable to measure can be

marked as "not applicable or N/A." The whole scores are calculated in percentage to determine the level of activities of daily living performance. The higher percentage scored demonstrates the higher performance of activities of daily living performance. Psychometric property of the ADL-AT in Thai stroke patients has shown an excellent inter-rater and test-retest reliability (ICC=0.98, 0.93, respectively). The analysis of Cronbach's alpha coefficient revealed high internal consistency (α=0.88). In addition, this tool displayed a positive correlation with Barthel index (r=0.90; p<0.001). In known-groups validity, stroke patients obtained lower ADL–AT scores compared to normal subjects (p<0.001).[13]

The VHVs in Thailand: Roles and Responsibilities

VHVs are considered the hallmark of community health care in Thailand.[14] They have contributed to a broad range of health promotion and health prevention activities in the country. In 2010 there were approximately 800,000 active volunteers, covering over 12 million households 15 and this number increased to 1,040,000 in the year 2020 throughout every Province in Thailand.[16] In the beginning, village health volunteers were chosen by local officials and given primary-care training to fulfill the mission of creating good change in the healthcare sector, propagating knowledge, coordinating for healthcare-development activities, and providing public health services. The initial training is 43 hours of classroom work and 15 days of specialized on-the-job training in health promotion, infectious disease surveillance and control, consumer protection, as well as traditional health knowledge. Following this training, each VHV is responsible for 10 households on average in their community. They assist the local health workers in promoting health and preventing diseases as well as in providing basic health services to local communities. The VHVs are supervised by on-site local health workers or public health officials.[17] At present, public health problems such as malnutrition and consumer health problems are continuously decreasing in Thailand,[18, 19] and the VHVs are encouraged to focus their duty in areas of prevention and management of chronic diseases.

Doi Lor Community Rehabilitation Center, Chiang Mai Province, Thailand

Doi Lor Community Rehabilitation Center was established with the funding of Doi Lor SAO who financial support from the Thai government. This established center aims to provide health promotion and basic rehabilitation to people with disabilities and the elderly in their own area.[20] Doi Lor Community Rehabilitation Center provides free transportation for clients. Caregivers do not need to take care of stroke survivors under their care on the day that stroke clients come to receive services at the Rehabilitation Center, so caregivers can take a rest or do another work as they prefer. There are four trained VHVs who provide services from 9 am to 4 pm, 2 days a week, on Tuesday and Friday.

Stroke Rehabilitation Education for the VHVS at Doi Lor Rehabilitation Center

There were 30 VHVs from 26 villages in Doi Lor Sub-district who applied to attend a stroke rehabilitation education program. The research team (five occupational therapists and five physical therapists) conducted stroke rehabilitation education for two and a half days including both theory and practice in the sessions. There were 4 topics of stroke rehabilitation provided for the VHVs in this study. These were comprising of 1) fundamental knowledge of stroke, 2) physical exercise and gait training for stroke, 3) upper extremity function training, and 4) ADL performance in stroke survivors. The topic of "fundamental knowledge of stroke," covered etiology, risk factors, physical symptoms, motor recovery, medical management, and possible complications. This was conducted on the first day between 9 am and 12 pm by the occupational therapists. The topic of "physical exercise and gait training for stroke" was conducted by physical therapists on the second day. This covered therapeutic exercise, walking gait and gait pattern, walking training, and postural control. The theory session was in the morning, and went from 9 am to 12 pm, then took a one-hour break for lunch from 12 pm to 1 pm. The practice session on "physical exercise and gait training for stroke" was conducted in the afternoon and went from 1 pm to 5 pm. In this session, 5 medically stable stroke survivors who lived in Doi Lor Sub-district were invited to be subjects for the VHVs in the training room. The trainers included five physical therapists. Each trainer was responsible for 6 VHVs in order to encourage more participation and discussion within the group. Therefore, a group of 6 VHVs each had one stroke subject. The topics of "upper extremity function training" and "ADL performance in stroke survivors" were conducted by occupational therapists on the third day. The theory session was in the morning and went from 9 am to 12 pm. The upper extremity function training emphasized general movement of the arm and hand, consist of reaching out for, holding, carrying, and releasing objects. The ADL performance in stroke survivors emphasized both BADL such as self-care, bed mobility, transferring, locomotion, sexual expression, and IADL such as care of pets, communication management, community mobility, meal preparation and clean up. All audiences took one hour break for lunch between 12 pm and 1 pm. The practice session on "upper extremity function training" and "ADL performance in stroke survivors" conducted in the afternoon went from 1 pm to 5 pm. In this session, the same 5 medically stable stroke subjects who participated in the practice program on the previous day were invited again to join the training session of upper extremity function and ADL performance in stroke at the meeting venue. The trainers in this session were five occupational therapists. Each trainer was responsible for 6 VHVs and a group of 6 VHVs each had one stroke subject.

In the rehabilitation education program for the VHVs, both occupational and physical therapists distributed a manual for stroke rehabilitation to all VHVs.The manual provided information concerning stroke comprising of epidemiology, causes and risk factors, types of stroke, physical symptoms, and treatment modalities. It illustrated rehabilitation for stroke patients such as ADL training, active and passive range of motion movement, therapeutic exercise, locomotion and walking training, upper extremity function practice programs, and the modification of home environment. The manual demonstrated precise definitions, clear color pictures, concise explanations, and wording in texts that were easily understood

by people who were not in the medical field. The VHVs were motivated to use this manual both in the theory and the practice sessions. In order to promote easy understanding in the training program, the trainers, who were occupational and physical therapists, provided a mostly structured training program to the VHVs so that they could quickly understand and easily apply the therapeutic treatment methods to use with those with stroke.

After the rehabilitation education, all VHVs took a paper examination concerning the theory and practice skills they had learned. Only the top 4 rankings among 30 VHVs were recruited to be rehabilitation workers at Doi Lor Community Rehabilitation Center. All these 4 VHVs provided rehabilitation services to stroke clients one week after finishing the training program. Prior to providing treatment to each client, occupational and physical therapists demonstrated how to evaluate and train stroke survivors in front of the 4 VHVs case by case, so that they could perform the treatment by themselves easily soon after. The occupational and the physical therapists in the research team visited Doi Lor Rehabilitation Center once every two weeks, for a period of 8 weeks, to give more guidance to the 4 VHVs if there were any questions.

Procedure

The process of the research project was conducted step by step as follows: 1) After the ethics approval, the principal investigator contacted the chief executive and officials at Doi Lor SAO to ask for permission to provide stroke rehabilitation education for the VHVs, 2) The education program was held at Doi Lor SAO near to the home of the VHVs, 3) After the completion of rehabilitation education, the research team selected the top 4 VHVs, who received higher test scores than the rest, to be health providers at the Rehabilitation Center, 4) The research team made contact with the director of the Sub-district Health Promotion Hospitals in Doi Lor area to ask for permission to access statistics, name's list, and addresses of stroke survivors, 5) The research team made appointments with the VHVs in the villages to visit the houses of stroke survivors under their care. They screened these patients correspondingly with the inclusion and exclusion criteria and invited them into the research project, 6) All subjects signed the consent form prior to receiving services at the Community Rehabilitation Center, 7) Four trained VHVs provided rehabilitation for stroke subjects for a period of 8 weeks, twice a week, one and a half hours each time, 8) Data collection was performed by 2 trained research assistants (RA), one collected data 7 days before intervention and the other collected data within 7 days after the program completion, 9) During the 8-weeks that services were provided, the research team, including occupational and physical therapists, visited Doi Lor Rehabilitation Center once every two weeks to offer advice to the 4 trained VHVs regarding any obstacles.

Data Collection

Data collection was conducted by 2 trained RAs who were not aware of the study's goal and were not involved in the rehabilitation education program. The principal investigator and the research team screened stroke subjects in accordance with the inclusion and exclusion criteria and notified the first RA, who was an occupational therapist, to collect data within 7 days before intervention at the Rehabilitation Center. Data collection was conducted by actual performance testing in the BADL and interviewing in the IADL. After 8 weeks of intervention, the principal investigator notified the other RA to collect data at post-test within 7 days following program completion at the Rehabilitation Center. The data collection procedure was the same between pre-test and post-test.

Statistical Analysis

Demographic characteristics of stroke participants were calculated using descriptive statistics. The comparisons of outcome variables at pre and post intervention were analyzed using the Wilcoxon Signed Ranks Test. The level of statistical significance was set at 0.05.

Results

There were 16 stroke participants recruited into the study. However, 5 of them could participate less than 80 percent in the whole program. Therefore, only 11 subjects were eligible for data analysis. All results were captured in tabular format as follows.

The analysis of sociodemographic data in 11 stroke survivors demonstrated that the majority of the participants were male and most of them finished elementary school. Almost all of the participants had right hemiplegia with the diagnosis of hemorrhagic stroke (Table 1).

The results also indicated that scores for BADL and IADL in stroke participants at post-intervention were significantly higher than those at pre-test (p<0.05), as shown in Table 2.

Table 1 Sociodemographic data of stroke participants. (n=11).

Sociodemographic data	Variables	Numbers (percentage)
Gender	Male	8 (72.70)
	Female	3 (27.30)
Age (years)	41-50	4 (36.30)
	51-60	3 (27.30)
	61-70	3 (27.30)
	71-80	1 (9.10)
Marital status	Single	3 (27.30)
	Married	6 (54.50)
	Divorced	2 (18.20)
Educational level	Elementary school	8 (72.70)
	Secondary school	3 (27.30)
Affected side	Left hemiplegia	3 (27.30)
	Right hemiplegia	8 (72.70)
Diagnosis	Hemorrhagic stroke	8 (72.70)
	Thrombotic stroke	1 (9.10)
	Embolic stroke	2 (18.20)
Time length since onset	<1 year	2 (18.20)
	1-2 years	4 (36.30)
	>2 years	5 (45.50)

Table 2 Comparison of activities of daily living performance: BADL and IADL in stroke participants at pre and post intervention. (n=11).

Variables		Mean (SD)	Mean rank	Z	Sig. (2-tailed)
1. BADL	Post-test	75.50 (21.17)	8.00	-2.22	0.026*
	Pretest	67.41 (23.31)	5.80		
2. IADL	Post-test	51.64 (23.02)	0.00	-2.81	0.005*
	Pretest	39.09 (16.13)	5.50		

**p<0.05*

Discussion

Activities of Daily Living Performance

Activities of daily living performance in the present study measured both the BADL and the IADL. Results indicated that the BADL performance in stroke participants increased significantly from pre-intervention to post–test (z=-2.22, p<0.05). Likewise, scores in the IADL of these individuals increased from pre-test to post–test significantly (z=-2.81, p<0.05).

The BADL components consist of fundamental daily activities such as eating, dressing, grooming, personal hygiene, toileting, bathing, bed mobility, transferring and locomotion, etc. Many of these activities can be easily performed with one hand if those with stroke receive appropriate advice from the health care providers. Samples of activities that can be accomplished by one hand e.g. eating activity, drinking from a glass, teeth brushing, and grooming. Some of the stroke participants in the present study do not have the opportunity to act by themselves, instead, their caregivers assist them throughout the day within reason, due to time constraints. Scoring for the ADL–AT used in this study began at zero for the ones who could or would not perform activities by themselves. In contrast, when these stroke survivors received advice and the training program from the VHVs, they learned how to do these activities independently and the score for functional performance changed from zero to five.

The components in the IADL comprised care of others, child-rearing, care of pets, communication management, community mobility, meal preparation and clean up, for example. The trained VHVs who work at the Community Rehabilitation Center applied their knowledge received from occupational and physical therapists to advise stroke clients in performing these activities successfully. For example, the VHVs suggested meal preparation using a one-hand cutting board and taught individuals with stroke to use a smartphone

for communication. All these techniques promoted higher functional performance in stroke clients who received services at Doi Lor Rehabilitation Center. Consistent with a study of Chinchai, Jindakham, Apichai[21] who investigated the BADL function in 25 stroke participants who received services from the trained VHVs at four Community Rehabilitation Centers in Chiang Mai Province. Results demonstrated that stroke participants improved their functional abilities at three months post-intervention compared to pre-test abilities significantly (p<0.05). Congruent with a study of Park and Lee[22] who examined the effects of the community-based rehabilitation program in 11 chronic stroke patients. Results demonstrated that subjects who received the community-based rehabilitation program ten times in ten months improved activities of daily living performance significantly (p<0.05). Compatible with a study by Ru, et al.,[23] who explored the effectiveness of community-based rehabilitation on daily activities of stroke patients in Beijing, China. There were 50,000 stroke survivors who participated in the study, divided into 2 groups based upon which community the participants lived in. One was the experimental group where stroke participants received rehabilitation intervention from health professionals, the other was the control group where there was no special health service from the research team. Results revealed that stroke survivors in the intervention group increased their function in daily activities significantly (p<0.05) compared to the control group. Results of the present study were also supported by a study of Chinchai, Sirisatayawong, Jindakum[24] who investigated community integration in terms of home integration, social integration, and productive activities in 25 stroke subjects who received a 3-month rehabilitation service from the trained VHVs in Thailand. Results revealed that activities of daily living skills, as part of the home integration section, in stroke participants increased significantly after the intervention program (p<0.05).

Limitations

The present study was a one-group pre-test and post-test research design. There was no control stroke participant for the comparison of outcome variables and this could be a limitation of this study. Researchers, therefore, set the inclusion criteria to gather stroke clients with as much homogeneity among the subjects as possible. The study also used different research assistants, who were unaware of the study's goal, for collecting data before and after the intervention program in order to enhance the reliability of the research project. However, it is recommended that the inclusion of a control subject should be considered for future study. Another limitation in the present study were the small numbers of the participants. Therefore, its results may not be generalizable to the population of stroke survivors who received services from other Community Rehabilitation Centers. In further study, the larger sample size should be considered.

Conclusion

The study of activities of daily living performance in stroke clients who received services from the trained VHVs at Doi Lor Community Rehabilitation Center, Doi Lor District, Chiang Mai Province, demonstrated that participants with stroke had significantly improved activities of daily living performance after an intervention (p<0.05). The results suggested that rehabilitation services provided by the trained VHVs at the Community Rehabilitation Center that was established by the Sub-district administrative organization was helpful for functional performance in stroke clients.

Acknowledgments

The authors would like to thank the Dean and the Executive Team, Faculty of Associated Medical Sciences, Chiang Mai University, Thailand, for their support and grants that made this project possible..

Conflict of interest

The authors report no conflicts of interest. The authors alone are responsible for the content and writing of the paper.

Ethics approval

The research project was approved by the Ethics Committee, Faculty of Associated Medical Sciences, Chiang Mai University, Thailand. Project number: AMSEC–63EX–027, ethics clearance number: 289/2563.

Funding

The study was supported by the Faculty of Associated Medical Sciences, Chiang Mai University, Chiang Mai, Thailand. The funders claimed no role in this study.

References

[1] Suwanwela NC. Stroke Epidemiology in Thailand. Journal of Stroke. 2014; 16(1): 1-7.

[2] Srivanichakorn S. Morbidity and mortality situation of non-communicable diseases (diabetes type 2 and cardiovascular diseases) in Thailand during 2010-2014. Disease Control Journal. 2017; 43(4): 379-90.

[3] Number and mortality rate of non-communicable diseases Year 2016-2018 (Hypertension, diabetes, ischemic heart disease, cerebrovascular disease, bronchitis and chronic obstructive pulmonary disease) [Internet]. 2021, Mar [cited Mar 22, 2021]. Available from: http://www.thaincd.com/2016/mission/documents-detail.php?id=13486&tid=32&gid=1-020.

[4] Division of Policy and Strategy Office of the Permanent Secretary Ministry of Public Health. Numbers and motality rate in non-communicable diseases and trauma in year 2015. Bangkok: Division of Policy and Strategy, Office of the Permanent Secretary Ministry of Public Health; 2016.

[5] Bunyamark T. Occupational therapy in stroke. In: Chinchai P, Bunyamark T, editors. The occupational therapy for persons with neurological conditions. 4th Ed. Chiang Mai: Siam Pimnana Company Limited; 2017.

[6] Gillen G. Cerebrovascular accident/stroke. In: Pendleton HM, Schultz-Krohn W, editors. Pedretti's Occupational Therapy: Practice Skills for Physical Dysfunction. 7th Ed. St. Louis, MO: Elsevier Mosby; 2013. p. 844-80.

[7] Gillen G. Cerebrovascular accident (Stroke). In: Pendleton HM, Schultz-Krohn W, editors. Occupational Therapy: Practice Skills for Physical Dysfunction 8th ed. St. Louis, MO: ELSEVIER; 2018. p. 809-40.

[8] Chinchai P, Marquis R, Passmore A. Functional performance, depression, anxiety, and stress in people with spinal cord injuries in Thailand: A transition from hospital to home. Asia Pacific Disabil Rehabil J, 2003; 14(1): 30-40.

[9] Pakdee P, Chinchai P. The influence of home visit program on functional abilities and quality of life in persons with disabilities resulting from stroke. Bull Chiang Mai Assoc Med Sci, 2016; 49(2): 276-85.

[10] Hung K, G., Fong K. Effects of telerehabilitation in occupational therapy practice: A systematic review. Hong Kong J Occup Ther, 2019; 32(1): 3-21.

[11] Empowerment of Persons with Disabilities Act, B.E. 2550 (2007, September 27).

[12] Office of the Chief Administrator of the Subdistrict Administrative Organization. History and general information of the Doi Lor Subdistrict Administrative Organization 2021 [cited 2020. Available from: http://www.doilor.org/about.php?id=1.

[13] Apichai S, Chinchai P, Dhippayom JP, Munkhetvit P. A new assessment of activities of daily living for Thai stroke patients. CMU J Nat Sci. 2020; 19(2): 176-90.

[14] Chuengsatiansup K, Suksuth P. Health volunteers in the context of change: potential and developmental strategies. J Health Systems Res. 2007; 1(3-4): 268-79.

[15] Bhutta ZA, Lassi ZS, Pariyo G, Huicho L. Global experience of community health workers for delivery of health related millennium development goals: A systematic review, country case studies, and recommendations for integration into national health systems. Global Health Workforce Alliance, World Health Organization. 2010; 1: 249-61.

[16] Administrator of Human Resource Development Office. Village Health Volunteers are Hard-to-Imitate: Worker Ants in Thailand's Healthcare System [updated 23 April 2020; cited 2563 23 April]. Available from: https://hrdo.org/en/village-health-volunteers-are-hard-to-imitate-worker-ants-in-thailands-healthcare-system/.

[17] Kauffman KS, Myers DH. The changing role of village health volunteers in northeast Thailand: An ethnographic field study. Int J Nurs Stud. 1997; 34 (4): 249-55.

[18] Dans A, Ng N, Varghese C, Tai E, Firestone R, Bonita R. The rise of chronic non-communicable diseases in southeast Asia: Time for action. The Lancet. 2011; 377(9766): 680-9.

[19] Kowitt SD, Emmerling D, Fisher EB, Tanasukarn C. Community health workers as agents of health promotion: Analyzing Thailand's village health volunteer program. J Community Health. 2015; 40(4): 780-8.

[20] Doilo Subdistrict Administrative Organization. Annual Report 2020. Chiang Mai: Doilo Subdistrict Administrative Organization; 2020.

[21] Chinchai P, Jindakham N, Apichai S. Functional abilities of stroke survivors receiving services at community rehabilitation center. J Assoc Med Sci. 2017; 50(3): 336-46.

[22] Park YJ, Lee CY. Effects of community-based rehabilitation program on activities of daily living and cognition in elderly chronic stroke survivors. J Phys Ther Sci. 2016; 28: 3264-6.

[23] Ru X, Dai H, Jiang B, Li N, Zhao X, Hong Z, et al. Community-based rehabilitation to improve stroke survivors' rehabilitation participation and functional recovery. Am J Phys Med Rehabil. 2017; 96(7): e123-e9.

[24] Chinchai P, Sirisatayawong P, Jindakum N. Community integration and quality of life: stroke survivors as recipients of rehabilitation by village health volunteers (VHVs) in Thailand. Occup Ther in Health Care. 2020; 34(3): 277-90.

Journal of Associated Medical Sciences 2021; 54 (3): 18-26

JAMS
Journal of Associated Medical Sciences

Thai-Journal Citation Index Centre (TCI) & ASEAN Citation Index (ACI)

Journal of Associated Medical Sciences

Journal homepage: https://www.tci-thaijo.org/index.php/bulletinAMS/index

Anti-HMG-CoA reductase and antioxidant activities of Sacha inchi (*Plukenetia volubilis* L.) nutshell extract

Wattanapong Prasongsub[1] **Nattaporn Pimsan**[1] **Chantanatda Buranapattarachote**[1] **Khanittha Punturee**[1,2*]

[1]*Division of Clinical Chemistry, Faculty of Associated Medical Sciences, Chiang Mai University, Chiang Mai Province, Thailand*
[2]*Cancer Research Unit of Associated Medical Sciences (AMS-CRU), Faculty of Associated Medical Sciences, Chiang Mai University, Chiang Mai Province, Thailand*

ARTICLE INFO

Article history:
Received 26 April 2021
Accepted as revised 21 May 2021
Available online 28 May 2021

Keywords:
Sacha inchi, Plukenetia volubilis, HMG-CoA reductase inhibitor, antioxidant, hypercholesterolemia

ABSTRACT

Background: Hypercholesterolemia is one of the major risks of cardiovascular diseases (CVDs). Hypercholesterolemia and oxidative stress are involved in the pathogenesis of atherosclerosis. Thailand has high percentage of unawareness of hypercholesterolemia, with low percentage of treatment and control. HMG-CoA reductase is a rate limiting step enzyme in cholesterol biosynthesis. Synthetic drugs such as statin are normally used to lower cholesterol level, however it causes adverse effects on the liver and muscle. Thus, HMG-CoA reductase inhibitors of plant origin are needed. *Plukenetia volubilis* Linneo, commonly known as Sacha inchi or inca peanut is a potential oilseed crop. The seeds of this plant are rich in omega-3 fatty acid. Some studies have shown that consuming Sacha inchi could reduce blood cholesterol. However, the exact mechanism of their lipid lowering activity is still unknown.

Objectives: This study aimed to investigate the anti-HMG-CoA reductase, anti-cholesterol esterase and antioxidant activities of different parts of Sacha inchi extracts.

Materials and methods: Hot water extracts of 3 different parts of Sacha inchi (nutshell, baby nut and leaf) and Sacha inchi nut oil were evaluated the anti-HMG-CoA reductase and antioxidant activities. HMG-CoA reductase inhibitory activity was determined spectrophotometrically by NADPH oxidation, using HMG-CoA as a substrate. HMG-CoA reductase inhibitory mechanism was also analyzed by using Lineweaver-Burk plot. Antioxidant activity was determined by ABTS and DPPH radical scavenging assay. Total phenolic content was also measured by Folin-Ciocalteu reagent. Moreover, cholesterol esterase inhibition assay was also performed.

Results: Sacha inchi nutshell extract revealed the highest anti-HMG-CoA reductase activities at about 99% at concentration of 250 µg/mL, with uncompetitive inhibition in Lineweaver-Burk plot analysis. It also showed the highest cholesterol esterase inhibitory activity around 38% at concentration of 125 µg/mL. Moreover, Sacha inchi nutshell extract also showed the highest antioxidant activity by both ABTS and DPPH assay. Antioxidant activity was correlated to total phenolic content.

Conclusion: The experimental data suggested that Sacha inchi nutshell extract is a source of antioxidant compound and may lower cholesterol level by inhibiting HMG-CoA reductase and cholesterol esterase enzymes. Investigation in an *in vivo* model could further confirm the potential use of Sacha inchi nutshell extract as a supplement for treatment of hypercholesterolemia.

* **Corresponding author.**
Author's Address: *Division of Clinical Chemistry, Faculty of Associated Medical Sciences, Chiang Mai University, Chiang Mai Province, Thailand.*
** **E-mail address:** khanittha.taneyhill@cmu.ac.th
doi: 10.14456/jams.2021.19
E-ISSN: 2539-6056

Introduction

Cardiovascular diseases (CVDs) are becoming a leading cause of death in developing countries due to demographic transition and lifestyle changes.[1] The prevalence of CVDs has increased rapidly. According to WHO fact sheet in 2016, there are 17.9 million people died from CVDs around the world. In Thailand, the prevalence and mortality rate have also increased and most of CVDs patients are adults.[2] A lack of income, reduced productivity, and increased health care costs lead to overall economic losses. Thus, the prevention of CVDs can save not only billions for the economy but also many lives. Major risk factors of CVDs include dyslipidemia, diabetes, smoking, high blood pressure, and family history of atherosclerotic cardiovascular diseases (ASCVD). Moreover, additional risks of CVDs have also been reported such as alcohol consumption, unhealthy diet, sedentary lifestyle, obesity, stress, and air pollution.[3] Pathogenesis of CVDs begins with the development of atherosclerosis causing by an accumulation of cholesterol in the intima layer of blood vessel. Low density lipoprotein (LDL) contains the highest amount of cholesterol compare to other lipoprotein particles. Accumulation of LDL in intima layer of blood vessel and modification of LDL particle by free radical and carbohydrate trigger the development of atherosclerosis. Thus, hypercholesterolemia and oxidative stress status directly involved in atherosclerosis. Moreover, excess adipose tissue in obesity can cause inflammation, induce oxidative stress by releasing of pro-inflammatory cytokines and induce insulin resistant which leads to type 2 diabetes mellitus (T2DM).[4,5] Lowering cholesterol level and improving oxidative stress status can prevent CVDs and T2DM.

The 3-hydroxy-3-methylglutaryl-coenzyme A (HMG CoA) reductase is a rate limiting step enzyme in cholesterol biosynthesis pathway. Inhibition of this enzyme can lower cholesterol level in blood. Statin, HMG-CoA reductase inhibitor, is effectively used for treatment of hypercholesterolemia. However, statins increased risk of liver and muscle-related adverse effects in long-term use such as myalgia, myopathy and rhabdomyolysis.[6] Thus, HMG-CoA reductase inhibitors of plant origin are needed. Medicinal plant that contains flavonoids showed anti-atherosclerotic effect.[7] Another way to reduce cholesterol level is inhibition of cholesterol esterase (CE). The hydrolysis of dietary cholesterol ester into cholesterol by CE in the intestinal lumen is an essential process for absorption. Therefore, inhibition of cholesterol esterase enzyme activity could inhibit absorption of dietary cholesterol esters.[8-10]

Sacha inchi (*Plukenetia volubilis* L.) belongs to the family Euphorbiaceae. It is also known as inca peanut. It is a tropical rain forest Amazonian plant. Sacha inchi becomes an economic crop in Southeast Asia especially in Thailand. Sacha inchi seeds contain mainly oil and protein. Commercially available Sacha inchi oil is beneficial for health. Sacha inchi oil contains high amount of long-chain n-3 fatty acids and antioxidant compounds such as tocopherol and vitamin A.[11-13] In addition, dried Sacha inchi leaves and nutshell are available as tea. Many customers who consumed Sacha inchi products experienced good controlled of blood glucose, decreased cholesterol level especially LDL-cholesterol and increased high-density lipoprotein cholesterol (HDL-cholesterol).[14] Sacha inchi seeds showed antioxidant activity[15] and immunomodulatory activity,[16] however other parts of plant have never been studied before. This study aimed to investigate anti-HMG-CoA reductase, anti-cholesterol esterase and antioxidant effects of Sacha inchi extracts (dried leaves, nutshells, and baby nuts) as well as Sacha inchi oil

Materials and methods

Chemicals

The 2,2-azino-bis (3-ethylbenzothiazoline-6-sulfonic acid (ABTS), gallic acid, 2,2-diphenyl-1-picrylhydrazyl (DPPH), 4-nitrophenyl butyrate (pNPB), cholesterol esterase from porcine pancreas and HMG-CoA reductase assay kit were purchased from Sigma-Aldrich (St. Louis, MO, USA). Ethanol and isopropanol were purchased from MERCK (Darmstadt, Germany). L-ascorbic acid (vitamin C), and sodium hydrogen phosphate were obtained from Ajax Finechem Pty Limited (Taren Point, New South Wales, Australia). Acetonitrile and sodium chloride were purchased from RCI Labscan Limited (Bangkok, Thailand). Sodium fluoride (NF) was acquired from BDH Laboratory Supplied (Poole, England). Triton X-100 was purchased from Amresco (Solon, Ohio, USA) All reagents were analytical or HPLC grade. Distilled water and ultrapure water were used for all experiments.

Plant materials and extracts

Sacha inchi leaves, nutshells, and baby nuts were provided by Oil Star Tak Limited Partnership, Tak province, Thailand. Each part of plant was dried and ground to powder. One hundred grams of Sacha inchi leaf, nutshell, and baby nut powder was extracted by boiling with 1 liter of distilled water for 15 minutes and further incubated for 4 hours. Solution was filtered through straining cloth and centrifuged at 3,500 rpm for 5 minutes. After centrifugation, supernatant was filtered through Whatman paper filter no.1. The filtrate was completely dried in a freeze-dryer and stored at -20°C until further use. The total yield percentage of the Sacha inchi extract was calculated by the formula, yield percentage (%) = (weight of extract obtained)/ (total weight of sample loaded)×100.

Sacha inchi nuts were mainly used to produced sacha inchi oil which contain high amount of polyunsaturated fatty acid and antioxidant compounds such as tocopherol and vitamin A. Cold pressed Sacha inchi oil was received from Oil Star Tak limited partnership, Tak province, Thailand. The Sacha inchi oil was stored at room temperature. The oil was dissolved in isopropanol into the desired concentration before performing any experiments or added directly into the reaction mix in the volume that meet the desired concentration.

Total phenolic content (TPC)

The TPC of Sacha inchi extracts were analyzed spectrophotometrically using modified Folin-Ciocalteau colorimetric method.[17] Sacha inchi extracts were dissolved to the concentration of 1 mg/mL with deionized (DI) water. Samples (100 µL)

were mixed with 100 µL of Folin-Ciocalteau's phenol reagent (Sigma-Aldrich, MO). Then, 300 µL of 20% sodium carbonate solution were added into the reaction and incubated at room temperature for 15 min. After incubation, 100 µL of DI water were added into the reaction and centrifuged at 1,250 ×g at 25˚C for 5 min. Supernatant were collected and measured an absorbance at 765 nm by using UV-Visible spectrophotometer (SPECORD PLUS 250, Germany). Diluted extracts were used as sample blank. Gallic acid (0-300 µg/ml) was used as a standard. Calibration curve was plot against concentration of gallic acid and absorbance at 765 nm. TPC of extracts were expressed as mg of gallic acid equivalents/gram dried weight (mg of GAE/g).

2,2'-azinobis-(3-ethylbenzothiazoline-6-sulfonate) (ABTS) assay

This study aimed to evaluate the free radical scavenging capacity of each Sacha inchi extracts, to reduce the radical cation $ABTS^{+}$ to ABTS according to the method described by Kokina *et al*.[18] Briefly, ABTS stock solution was prepared by mixing ammonium persulfate (4.9 mM) and ABTS (7 mM) in equal ratio and incubating at RT in dark for 12-16 hrs. The working $ABTS^{+}$ solution was prepared by dilution of the stock solution with 80% methanol to absorbance at 734 equals to 0.700±0.020. Different concentrations (1-20 mg/mL) of Sacha inchi extract (10 µL) were added to 990 µL of $ABTS^{+}$ working solution. An absorbance (734 nm) was measured at 1 min after incubation by using UV-Visible spectrophotometer. L-ascorbic acid was used as a standard. Calibration curve was plot against concentration of ascorbic acid and absorbance at 734 nm. The results were expressed as mg of ascorbic acid equivalent/gram dried weight.

2,2-Diphenyl-1-picrylhydrazyl (DPPH) assay

Free radical scavenging activity of Sacha inchi extract was investigated using DPPH assay as described by Hajlaoui *et al*.[19] Sacha inchi extracts (40 µL) at various concentration (1-20 mg/mL) were mixed with 1.2 mL of DPPH reagent and incubated at room temperature for 15 min. Samples were centrifuged at 1,250 ×g at 25˚C for 5 min after incubation. The supernatants were collected and measured absorbance at 517 nm by using UV-Visible spectrophotometer. Diluted extracts were used as sample blank. Gallic acid was used as a standard. Calibration curve was plot against concentration of gallic acid and absorbance at 517 nm. Results were expressed as mg of gallic acid equivalents/gram dried weight (mg of GAE/g).

HMG-CoA reductase activity assay

This study aimed to investigate inhibitory effect of Sacha inchi extracts on HMG-CoA reductase enzyme activity. The HMG-CoA reductase catalyzed HMG-CoA into mevalonate using NADPH. The HMG-CoA reductase activity was measured by the reduction of NADPH at 340 nm. Briefly, 4 µL of NADPH, 1 µL of samples, 12 µL of HMG-CoA substrate, and 181 µL of assay buffer were mixed. Pravastatin at final concentration of 0.2 µg/mL was used as inhibition control. To initiate the reaction, HMG-CoA reductase catalytic domain was added into reaction mixture. The absorbance (340 nm) was measured at 37 °C every 15 sec for 5 min by UV-Visible spectrophotometer. For blank, the assay buffer was added into reaction tube instead of HMG-CoA reductase. The enzyme activity was calculated using the following equation:

$$\text{Units/mgP} = \frac{(\Delta A_{340}/\text{min}_{\text{sample}} - \Delta A_{340}/\text{min}_{\text{blank}}) \times TV}{12.44 \times V \times 0.6 \times LP}$$

where ΔA: change of absorbance, TV: total volume of the reaction in mL, 12.44: coefficient of NADPH, V: volume of enzyme used in the assay, 0.6: enzyme concentration in mg-protein, LP: light path in cm.

Cholesterol esterase activity assay

Cholesterol esterase inhibitory activity of Sacha inchi extracts was evaluated spectrophotometrically at 25 °C using the method of Asmaa and Ream[20]. The cholesterol esterase from porcine pancreas (CEase) was solubilized in 1 mL of 0.1 M sodium phosphate buffer pH 7.0 and stored at -80˚C as a stock CEase. Prior to use, working CEase was prepared by diluting a stock CEase to 5 µg/mL with the same buffer. The reaction mixture consisted of 500 µL of Triton X-100 (5% w/w), 20 µL of p-nitrophenyl butyrate (0.05 M in acetonitrile), 40 µL of 2% acetonitrile in 400 µL of assay buffer (100 mM sodium phosphate, 100 mM sodium chloride, pH7.0) and 20 µL samples. The mixture was mixed and incubate at 25 °C for 5 min. The reaction was initiated by adding of 20 µL of working CEase (5 µg/mL). After 15 min of incubation at 25°C, the absorbance was measured by spectrophotometer at 405 nm. NaF was used as inhibition control. The percentage of inhibition were calculated using the following formula:

$$\%\text{Inhibition} = \frac{\text{Abs}_{\text{Activity}} - \text{Abs}_{\text{Sample}}}{\text{Abs}_{\text{Activity}}} \times 100$$

Statistical analysis

Data were expressed as mean±standard deviation (SD) of three independent experiments. The data were analyzed by one-way ANOVA. $p<0.05$ was considered to be statistically significant.

Results

Total phenolic content and antioxidant activity of Sacha inchi extracts

Leaves, baby nuts and nutshells of Sacha inchi were extracted with hot water. Total yield percentage of the Sacha inchi extracts were calculated. Leaf extract showed the highest yield percentage followed by baby nuts and nutshells, respectively (Table 1). The characteristic of leaves, nutshells and baby nuts hot water extracts were shown in Figure 1.

Table 1 Total yield percentage of hot water extracts of each part of Sacha inchi.

Sacha inchi	Yield of extract (%)
Leaves	19.73
Nutshells	12.64
Baby nuts	14.57

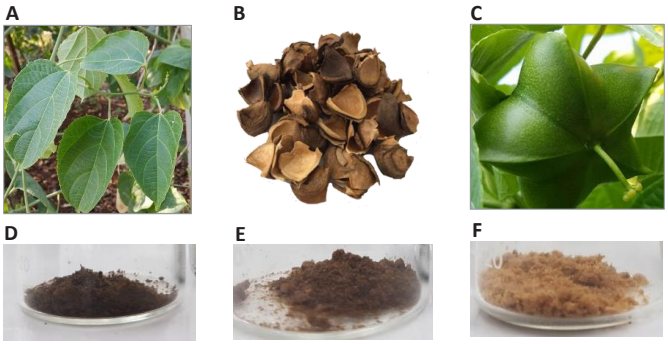

Figure 1. *Characteristic of tested materials. A: leaves, B: nutshells, C: baby nuts of Sacha inchi, D-F: corresponding dried hot water extracts (D-F).*

TPC was determined using Folin-Ciocalteu calorimetric assays. Sacha inchi nutshell and baby nut extracts showed much higher TPC compared to others, which were about 74.8 mg and 63.6 GAE/100 g dried weight, respectively. Sacha inchi leaf extracts and oil showed lower TPC which were 18.2 and 10.0 mg GAE/100 g dried weight (Figure 2).

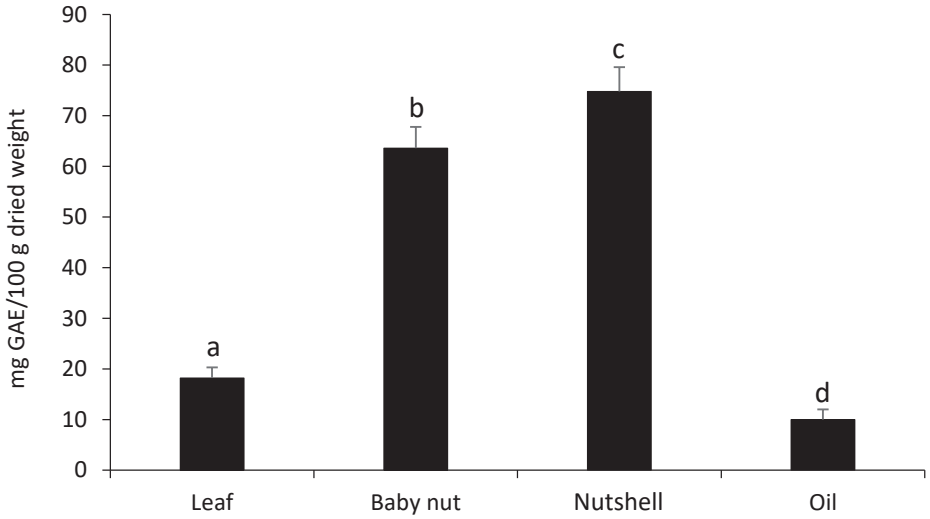

Figure 2. *Total phenolic content of different parts of Sacha inchi extracts and Sacha inchi oil at concentration of 1 mg/mL. The data were expressed as the mean±SD of sample tested in 3 independent experiments. Values having different letters differ significantly (p<0.05).*

The antioxidant activity was determined by DPPH and ABTS radical scavenging assay. Results from antioxidant activity by both methods were similar to the results from TPC. Sacha inchi nutshell extracts presented the highest DPPH and ABTS radical scavenging activity which were 78 mg GAE/100 g dried weight and 450 mg ascorbic acid equivalent/ 100 g dried weight, respectively. In contrast, Sacha inchi oil had the lowest antioxidant activity (Figure 3 and Figure 4).

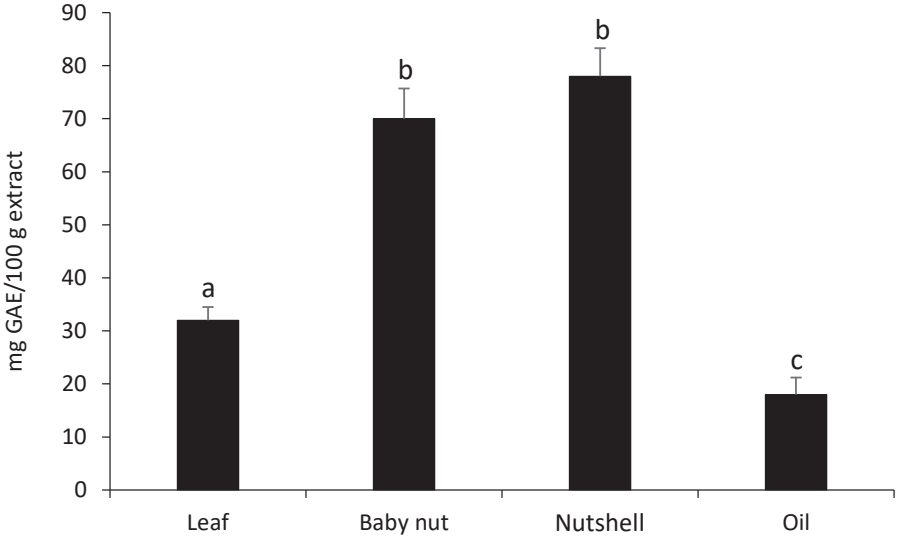

Figure 3. *DPPH radical scavenging activity of different parts of Sacha inchi extracts and Sacha inchi oil at concentration of 1 mg/mL. The data were expressed as the mean±SD of sample tested in 3 independent experiments. Values having different letters differ significantly (p<0.05).*

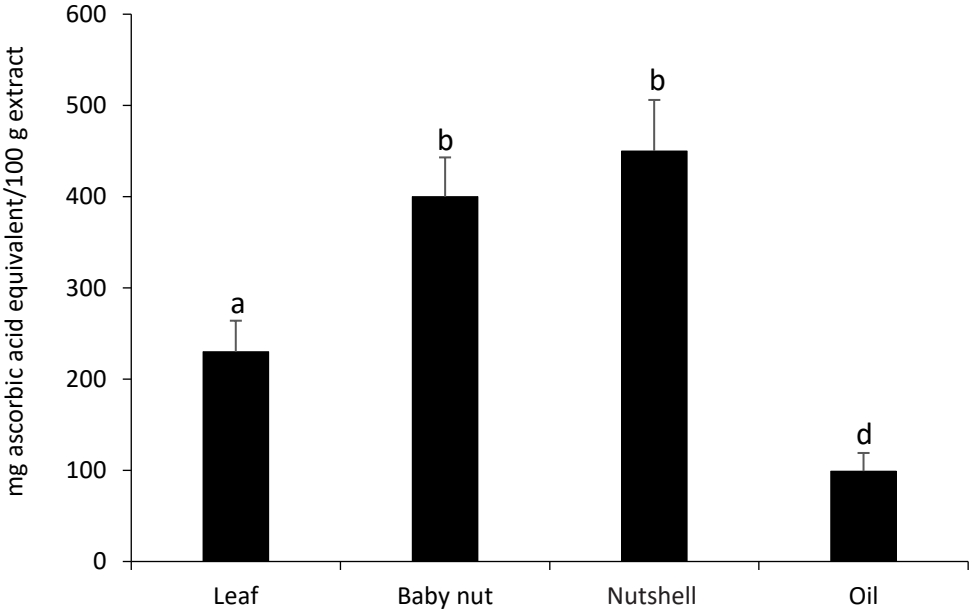

Figure 4. *ABTS radical scavenging activity of different parts of Sacha inchi extracts and Sacha inchi oil at concentration of 1 mg/mL. The data were expressed as the mean±SD of sample tested in 3 independent experiments. Values having different letters differ significantly (p<0.05).*

HMG-CoA reductase inhibitory activity

The HMG-CoA reductase inhibitory effect of Sacha inchi extracts and Sacha inchi oil were evaluated. Pravastatin was used as an inhibitory control which can inhibit HMG-CoA reductase activity for 75%. Only, Sacha inchi extract from nutshells presented HMG-CoA reductase inhibitory activity about 65% at the concentration of 125 µg/mL (Figure 5). The rest of the Sacha inchi extracts and Sacha inchi oil had no effect on HMG-CoA reductase activity. Inhibition of HMG-CoA reductase activity by Sacha inchi nutshell extract was dose-dependent manner. It inhibited HMG-CoA reductase activity up to 99% at the concentration of 250 µg/mL (Figure 6).

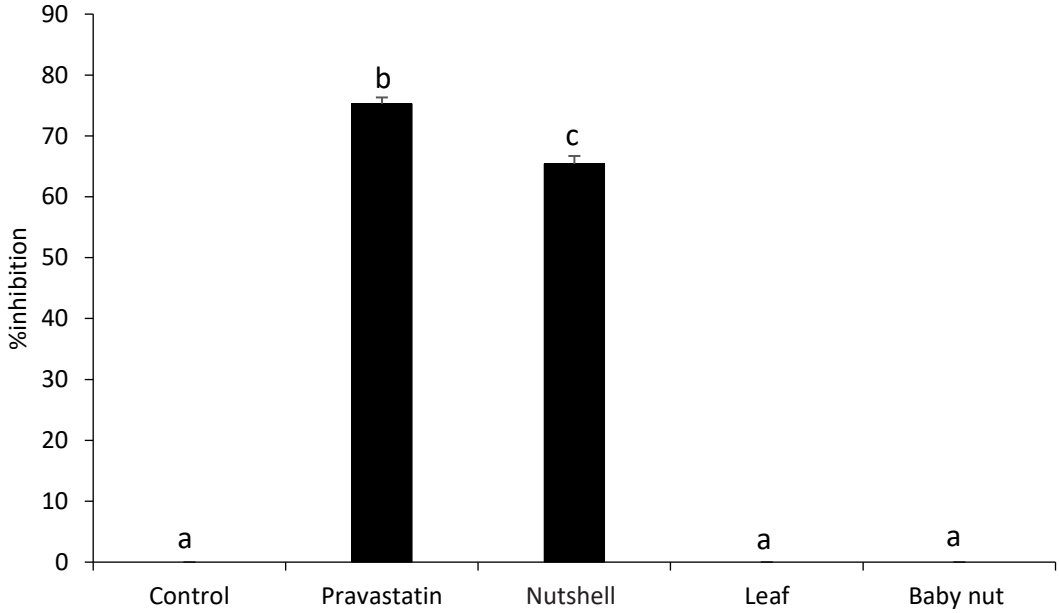

Figure 5. *HMG-CoA reductase inhibitory activity of different parts of Sacha inchi extracts (125 µg/mL). Distilled water was used as a negative control and pravastatin (0.2 µg/mL) was used as a positive control. All data were expressed as the mean±SD of sample tested in 3 independent experiments. Values having different letters differ significantly (p<0.05).*

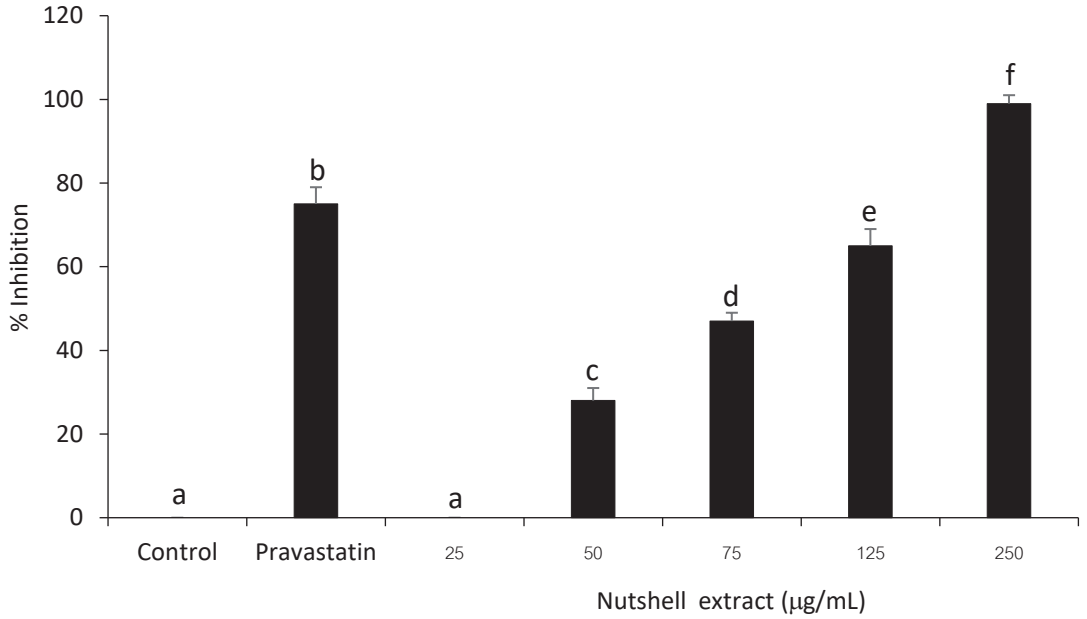

Figure 6. *Inhibition of HMG-CoA reductase activity by various concentrations of Sacha inchi nutshell extracts. Distilled water was used as a negative control and pravastatin was used as a positive control. All data are presented as the mean±SD of samples tested in 3 independent experiments. Values having different letters differ significantly (p<0.05).*

Sacha inchi nutshell extract was further analyzed the type of enzymatic inhibition by Lineweaver-Burk plot analysis. The Lineweaver-Burk plot analysis showed parallel line pattern (Figure 7), indicating the uncompetitive inhibition.

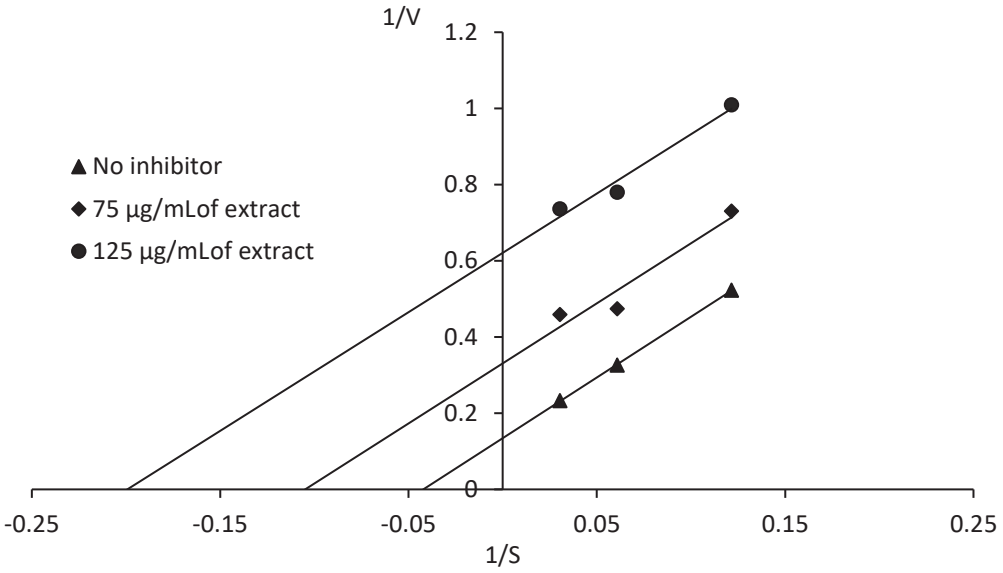

Figure 7. *Lineweaver-Burk plot analysis for HMG-CoA reductase in the presence of different concentrations of HMG-CoA (8, 16 and 32 mM) and two different concentrations of Sacha inchi nutshell extract (75 and 125 µg/mL). Data represents mean+SD of 3 independent experiments.*

Cholesterol esterase inhibitory activity

Sacha inchi extracts and Sacha inchi oil were evaluated for their cholesterol esterase inhibition activity. NaF used as a positive control markedly inhibited the cholesterol esterase about 26.0%. Among Sacha inchi extracts, only nutshell and baby nut extracts revealed cholesterol esterase inhibitory activity by 38.1 and 24.1%, respectively (Figure 8). Sacha inchi oil (750 µg/mL) had no effect on cholesterol esterase inhibition (data not shown).

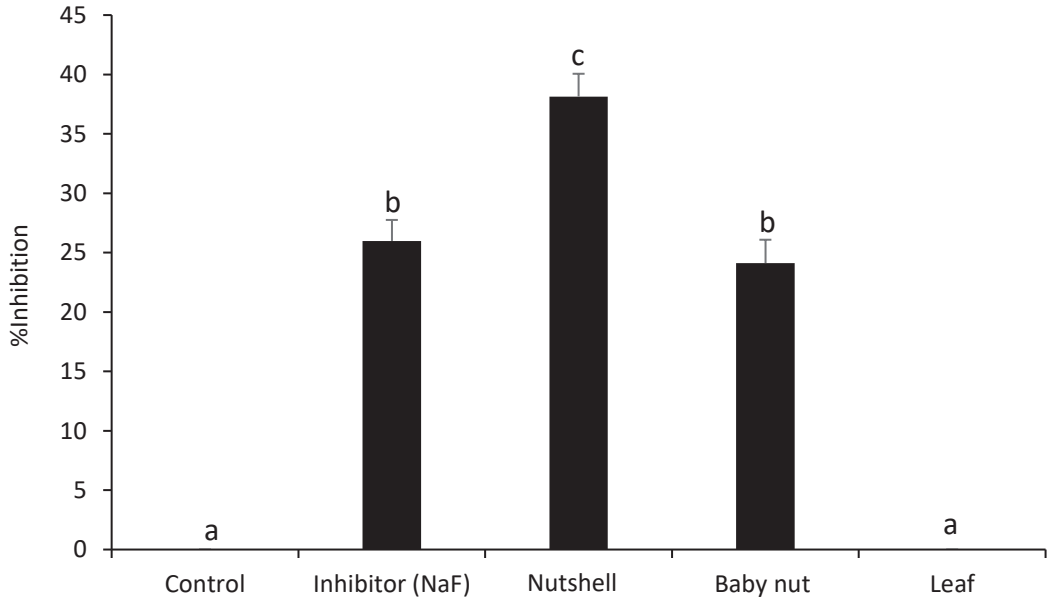

Figure 8. *Effect of Sacha inchi extracts (125 µg/mL) on cholesterol esterase activity. Percentage of enzyme inhibition were calculated. Control was represented the condition without inhibitor. Data represents mean+SD of 3 independent experiments. Values having different letters differ significantly (p<0.05).*

Discussion

Various parts of Sacha inchi are edible. Products of Sacha inchi in the market include roasted nut, cold press nut oil, and tea that made from leaves and nut shells.[11] Plants which contain antioxidant activity have been reported to also exert lipid lowering property.[21] As both oxidative stress and hyperlipidemia are involved in atherosclerosis, plant that exert both effects might be useful for CVDs prevention. Among various parts of Sacha inchi and sacha inchi oil, nutshell extract showed the highest antioxidant activity as well as total phenolic content. This data suggested that phenolic compound might be the active ingredient in Sacha inchi nutshell extract.

Sacha inchi products have been claimed to reduce cholesterol level. However, the scientific data and the exact mechanism are still limited. HMG-CoA reductase, a rate limiting step enzyme in cholesterol biosynthesis, is the target for treatment of hypercholesterolemia. Statins are synthetic drugs that competitively inhibit HMG-CoA reductase.[22] Statins are commonly used to treat hypercholesterolemia. However, the adverse side effects from long term use are in a great concern.[23] Thus, HMG-CoA reductase inhibitors from natural origin are in a great interest.[24]

This is the first report on anti-HMG-CoA reductase activity from Sacha inchi nutshell. Hot water extract of Sacha inchi nutshell inhibited HMG-CoA reductase activity ranging from 28-99% according to the concentrations of the extract (50-250 µg/mL). Previous studies on HMG-CoA reductase inhibitors from plant origin have been reported. HMG-CoA reductase inhibitory activity of crude extract of *Quercus infectoria*, *Basella alba, Rosa damascene*, *Myrtus communis*, and *Amaranthus viridis* leaf were 84%, 74%, 70%, 62% and 72%, respectively.[25-27] Fraction 18 of methanolic *Ficus virens* Ait extract showed a large number of HMG-CoA reductase inhibition about 98%.[28] Therefore, anti-HMG CoA reductase compounds from plant origin was very interesting because they can be used to lower blood cholesterol level. Cholesterol lowering effect of Sachi inchi via HMG-CoA reductase inhibition was firstly investigated in this study. The mechanism of enzyme inhibition of Sacha inchi nutshell extract was also studied. Unlike statin drug which competitively inhibit HMG-CoA reductase,[29] Sacha inchi nutshell extract showed uncompetitive inhibition pattern. This type of inhibitor is more specific and efficient compare to other types of inhibitors.[30] Uncompetitive inhibitors bind only to the enzyme-substrate complex, while competitive inhibitors have affinity for the enzyme and compete for substrate binding.

Besides inhibition of HMG-CoA reductase, inhibition of enzymes that control cholesterol absorption and transportation is important target for lowering blood cholesterol. Cholesterol esterase is one of those enzymes that plays an important role in the regulation of cholesterol metabolism by extending cholesterol intestinal absorption and transportation to enterocytes.[20] Sacha inchi nutshell extract showed the strongest anti-cholesterol esterase activity. Inhibition of cholesterol esterase could block cholesterol absorption and finally lower the blood cholesterol level. In this study Sacha inchi oil did not have either anti-HMG CoA reductase (data not shown) or strong antioxidant activity. However, previous studies have reported lipid lowering properties of Sacha inchi oil *in vivo*.[11,31] These data indicated that the mechanism of cholesterol lowering activity of Sacha inchi

oil did not cause by direct inhibition of HMG-CoA reductase.

All data suggested that Sacha inchi nutshell extract might be a potential lipid lowering agent which can be used as a supplement for treatment of hypercholesterolemia.

Conclusion

In conclusion, Sacha inchi nutshell extract showed the highest antioxidant activity and total phenolic content. It might be able to reduce blood cholesterol level through the uncompetitive HMG-CoA reductase inhibition, and cholesterol esterase inhibition. As oxidative stress and hyperlipidemia are contributed to CVDs development, consumption of Sacha inchi nutshell which contain high amount of antioxidant might prevent CVDs. However, more investigation in an *in vivo* model could further confirm the potential of Sacha inchi nutshell extract in treating hypercholesterolemia.

Conflict of interest

There are no conflicts of interest associated with this publication.

Acknowledgments

We would like to thank the Faculty of Associated Medical Sciences for the financial support. We thank Oil Star Tak limited partnership for providing Sacha inchi plant and oil extract.

References

[1] Reddy KS, Yusuff S. Emerging epidemic of cardiovascular disease in developing countries. Circulation 1998; 97: 596-601.

[2] Ohira T, Iso H. Cardiovascular disease epidemiology in Asia: an overview. Circ J 2013; 77(7): 1646-52.

[3] Kilkenny MF, Dunstan L, Busingye D, Purvis T, Reyneke M, Orgill M, *et al*. Knowledge of risk factors for diabetes or cardiovascular disease (CVD) is poor among individuals with risk factors for CVD. PloS one 2017; 12(2): e0172941-e.

[4] Maliszewska K, Adamska-Patruno E, Kretowski A. The interplay between muscle mass decline, obesity, and type 2 diabetes. Pol Arch Intern Med 2019; 129(11): 809-816. doi: 10.20452/pamw.15025.

[5] Combes A, Franchineau G. Fine particle environmental pollution and cardiovascular diseases. Metabolism 2019; 100S: 153944. doi: 10.1016/j.metabol.2019.07.008.

[6] Bellosta S, Corsini A. Statin drug interactions and related adverse reactions: an update. Expert Opin Drug Saf 2018; 17(1): 25-37.

[7] Salvamani S, Gunasekaran B, Shaharuddin NA, Ahmad SA, Shukor MY. Antiartherosclerotic effects of plant flavonoids. Biomed Res Int 2014; 2014: 480258. doi: 10.1155/2014/480258.

[8] Krause BR, Sliskovic DR, Anderson M, Homan R. Lipid-lowering effects of WAY-121,898, an inhibitor of pancreatic cholesteryl ester hydrolase. Lipids 1998; 33: 489-98.

[9] Bailey JM, Gallo LL, Gillespie J. Inhibition of dietary cholesterol ester absorption by 3-BCP, a suicide inhibitor of cholesterol-esterase. Biochem Soc Trans 1995; 23: 408S.

[10] Jeon SM, Kim HS, Lee TG, Ryu SH, Suh PG, Byun SJ, *et al*. Lower absorption of cholesteryl oleate in rats supplemented with *Areca catechu* L. extract. Ann Nutr Metab 2000; 44: 170–6.

[11] Wang S, Zhu F, Kakuda Y. Sacha inchi (*Plukenetia volubilis* L.): Nutritional composition, biological activity, and uses. Food Chem 2018; 265: 316-28.

[12] Vicente J, de Carvalho MG, Garcia-Rojas EE. Fatty acids profile of Sacha Inchi oil and blends by ^{1}H NMR and GC-FID. Food Chem 2015; 181: 215-21.

[13] Chirinos R, Zuloeta G, Pedreschi R, Mignolet E, Larondelle Y, Campos D. Sacha inchi (*Plukenetia volubilis*): a seed source of polyunsaturated fatty acids, tocopherols, phytosterols, phenolic compounds and antioxidant capacity. Food Chem 2013; 141(3): 1732-9.

[14] Garmendia F, Pando R, Ronceros G. Effect of sacha inchi oil (*Plukenetia volúbilis* L.) on the lipid profile of patients with hyperlipoproteinemia. Rev Peru Med Exp Salud Publica 2011; 28(4): 628-32.

[15] Bueno-Borges LB, Sartim MA, Gil CC, Sampaio SV, Rodrigues PHV, Regitano-d'Arce MAB. Sacha inchi seeds from sub-tropical cultivation: effects of roasting on antinutrients, antioxidant capacity and oxidative stability. J Food Sci Technol 2018; 55(10): 4159-66.

[16] Tian W, Xiao N, Yang Y, Xiao J, Zeng R, Xie L, *et al*. Structure, antioxidant and immunomodulatory activity of a polysaccharide extracted from Sacha inchi seeds. Int J Biol Macromol 2020; 162:116-126.

[17] Dewanto V, Wu X, Adom KK, Liu RH. Thermal processing enhances the nutritional value of tomatoes by increasing total antioxidant activity. J Agric Food Chem 2002; 50(10): 3010-4.

[18] Kokina M, Salević A, Kalušević A, Lević S, Pantić M, Pljevljakušić D, *et al*. Characterization, antioxidant and antibacterial activity of essential Oils and their encapsulation into biodegradable material followed by freeze drying. Food Technol Biotechnol 2019; 57(2): 282-9.

[19] Hajlaoui H, Arraouadi S, Mighri H, Chaaibia M, Gharsallah N, Ros G, *et al*. Phytochemical constituents and antioxidant activity of *Oudneya Africana* L. leaves extracts: evaluation effects on fatty acids and proteins oxidation of beef burger during refrigerated storage. Antioxidants (Basel) 2019; 8(10): 442. doi: 10.3390/antiox8100442.

[20] Asmaa BH, Ream N. *In vitro* screening of the pancreatic cholesterol esterase inhibitory activity of some medicinal plants grown in Syria. Int J Pharmacognosy and Phytochem Res 2016; 8(8); 1432-36.

[21] Lopes RHO, Macorini LFB, Antunes KA, Espindola PPT, Alfredo TM, Rocha PS, *et al*. Antioxidant and hypolipidemic activity of the hydroethanolic extract of *Curatella americana* L. leaves. Oxid Med Cell Longev 2016; 2016: 9681425.

[22] Sirtori CR. The pharmacology of statins. Pharmacol Res 2014; 88: 3-11.

[23] Thompson PD, Panza G, Zaleski A, Taylor B. Statin-associated side effects. J Am Coll Cardiol 2016; 67(20): 2395-2410.

[24] Gunasekaran B, Shukor MY. HMG-CoA reductase as target for drug development. Methods Mol Biol 2020; 2089: 245-250.

[25] Gholamhoseinian A, Shahouzehi B, F S-F. Inhibitory activity of some plant methanol extracts on 3-hydroxy-3-methylglutaryl coenzyme a reductase. Int J Pharmacol 2010; 6(5): 705-11.

[26] Baskaran G, Salvamani S, Ahmad SA, Shaharuddin NA, Pattiram PD, Shukor MY. HMG-CoA reductase inhibitory activity and phytocomponent investigation of *Basella alba* leaf extract as a treatment for hypercholesterolemia. Drug Des Devel Ther 2015; 9: 509-17.

[27] Salvamani S, Gunasekaran B, Shukor MY, Shaharuddin NA, Sabullah MK, Ahmad SA. Anti-HMG-CoA reductase, antioxidant, and anti-Inflammatory activities of *Amaranthus viridis* leaf extract as a potential treatment for hypercholesterolemia. Evid Based Complement Alternat Med 2016; 2016: 8090841. doi: 10.1155/2016/8090841.

[28] Iqbal D, Khan MS, Khan MS, Ahmad S, Hussain MS, Ali M. Bioactivity guided fractionation and hypolipidemic property of a novel HMG-CoA reductase inhibitor from *Ficus virens* Ait. Lipids Health Dis 2015; 14: 15. doi: 10.1186/s12944-015-0013-6.

[29] da Costa RF, Freire VN, Bezerra EM, Cavada BS, Caetano EW, de Lima Filho JL, *et al*. Explaining statin inhibition effectiveness of HMG-CoA reductase by quantum biochemistry computations. Phys Chem Chem Phys 2012; 14(4): 1389-98.

[30] Kato E, Tsuji H, Kawabata J. Selective purification of intestinal maltase complex by affinity chromatography employing an uncompetitive inhibitor as the ligand. Tetrahedron 2015; 71(9): 1419–24.

[31] Gonzales GF, Gonzales C. A randomized, double-blind placebo-controlled study on acceptability, safety and efficacy of oral administration of sacha inchi oil (*Plukenetia volubilis* L.) in adult human subjects. Food Chem Toxicol 2014; 65: 168–76.

Journal of Associated Medical Sciences 2021; 54 (3): 27-31

JAMS
Journal of Associated Medical Sciences

Thai-Journal Citation Index Centre (TCI) & ASEAN Citation Index (ACI)

Journal of Associated Medical Sciences

Journal homepage: https://www.tci-thaijo.org/index.php/bulletinAMS/index

Calculation of absorbed doses from computed tomography in pelvic phantom using Monte Carlo Simulation

Janejirarak Ritpanja[1,4] **Phiphat Phruksarojanakun**[2] **Waraporn Sudjai**[3] **Chayanit Jumpee**[4*]

[1]*Department of Diagnostic Radiology, Lampang Cancer Hospital, Lampang Province, Thailand*
[2]*Office of Atoms for Peace, Ministry of Higher Education, Science, Research and Innovation, Bangkok, Thailand*
[3]*Thailand Institute of Nuclear Technology (Public Organization), Nakorn Nayok Province, Thailand*
[4]*Department of Radiologic Technology, Faculty of Associated Medical Science, Chiang Mai University, Chiang Mai Province, Thailand*

ARTICLE INFO

Article history:
Received 5 March 2021
Accepted as revised 28 May 2021
Available online 28 May 2021

Keywords:
Computed tomography (CT), absorbed dose, MCNP, Monte Carlo, OSL nanodot

ABSTRACT

Background: Computed Tomography (CT) is an effective diagnosis method which deposits high absorbed doses on internal organs; therefore, it is necessary to understand dosimetry nature of this method.

Objectives: To improve CT absorbed dose estimation by using a more appropriate phantom representing a human body and a Monte Carlo transport code.

Materials and methods: The Monte Carlo N-Particle transport code Version 5 or MCNP5 is used in this study to simulate a Rando phantom representing pelvic section of a patient in a CT procedure. Absorbed doses of various internal organs from MCNP5 are compared with standard experimental measurements based on the InLight nanoDot dosimeters.

Results: CT absorbed dose between MCNP5 simulation and standard experiment measurement are mostly in reasonable agreements within 10-percent discrepancy except those at skin positions.

Conclusion: Further study is recommended for calculating absorbed doses at skin positions, MCNP5 is practically reliable for estimating absorbed doses in a number of internal organs. The MCNP5 simulation is one of alternative method to evaluate patient radiation dose which helps radiology team manage diagnosis and treatment planning.

Introduction

In recent years, computed tomography (CT) is one of the most important image modalities for medical diagnosis since its image outputs can provide a physician thorough understanding of internal organ that cannot be achieved through a traditional 2-D imaging method. However, this practice inevitably comes at the expense of high-level X-ray exposure from many different radiation angles. Effective doses resulting from CT scan can vary from 2 to 16 mSv, depending on organ range examination.[1] As an alternative measurement of effective dose on a particular organ, an absorbed dose has recently been used to assess a radiation risk on a patient.[2] Traditionally, CT dose index (CTDI) is employed to calculate CT absorbed doses. However, CTDI is limited by its physical geometry as it only contains two cylindrical objects made of homogeneous polymethyl methacrylate (PMMA) phantom (CTDI phantom) representing head and trunk. This study aimed to improve CT absorbed dose estimation by using a more appropriate phantom representing a human body and a Monte Carlo transport code.

* **Corresponding author.**
Author's Address: *Department of Radiologic Technology, Faculty of Associated Medical Science, Chiang Mai University, Chiang Mai province, Thailand.*
** **E-mail address:** chayanit.j@cmu.ac.th
doi: 10.14456/jams.2021.20
E-ISSN: 2539-6056

Materials and methods

Absorbed Dose Measurement in Rando phantom

The InLight nanoDot dosimeters which is a crystal of Al2O3:C compound of Optically Stimulated Luminescence Dosimeter (OSL nanoDot) were positioned inside the Pelvic-Rando phantom (10 slices, 2.54 cm/slice) to represent 19 position of internal organs (Table 1). Rando phantom is modelled after anatomical characteristics of the reference man and consists of a real human skeleton embedded in soft tissue equivalent material. Figure 1 shows all slabs of pelvic Rando phantom (Left) and dosimeter holder together with OSL nanoDot (Right). The duplicate 19 OSL nanoDot were irradiated using 64 slices CT scanner of the Aquilion64 (Toshiba) from the department of Radiologic Technology, faculty of Associated Medical Sciences, Chiang Mai University, Thailand. The scanning protocol is shown in Table 2. Subsequently, all OSL nanoDot samples were evaluated by Thailand Institute of Nuclear Technology (Public Organization), Nakorn Nayok, Thailand and reported in an organ absorbed dose that expressed in unit of centigray (cGy).

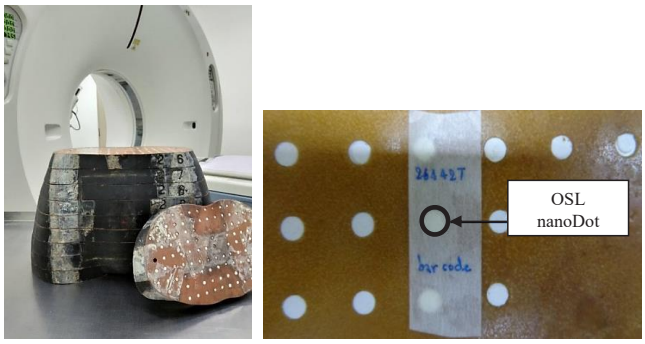

Figure 1. *Pelvic Rando phantom.*

Table 1 Sociodemographic data of stroke participants.

Equivalent organ	Number of OSL	Coordination (X,Y,Z)* [cm]
Rt. Ovary	1	(-6,0,15.24)
Lt. Ovary	1	(6,0,15.24)
Bladder	6	(-3,4.50,15.24), (3,4.50,15.24), (-3,4.50,17.78), (3,4.50,17.78), (-3,0,20.32), (3,0,20.32)
Uterus	1	(0,2,12.70)
Prostate	2	(-1.50,-1,22.86), (1.50,-1,22.86)
Skin	8	Outside (anterior, posterior, right, left) Z = 8.39, 13.97
Total	19	

Note: *Coordinate of Rando phantom center is X=0, Y=0 and Z=12.70, cm: centimeter*

Table 2 CT scan protocol for irradiations of the Rando phantom.

Parameter	Value
kVp	120
mA	tube current modulation mode
rotation time	0.5 sec
slice thickness	0.5x64 cm.
scan length	20 m.

MCNP Simulation

The Monte Carlo N-Particle transport code Version 5 (MCNP5) with F6 tally that is deposition energy (MeV/g. photon) in each cell was used to simulate a set of direct measurements based on 19 OSL nanoDot dosimeters in pelvic RANDO phantom including X-ray source structure of CT scanner (Figure 2). The 120 kVp X-ray source with energy spectrum shown in Figure 3 was located on 36 positions on circumference of 50 cm CT gantry. As shown in Figure 4, each position was equally spaced out as its radial line made a 10-degree angle to another adjacent radial line. This source placement was an attempt to model a spiral continuous movement of X-ray tube rotation about CT gantry. The collimator was also included in model to collimate a cone beam from X-ray source into a fan-shaped beam with an angle of 49.2 degree and 1-cm thickness. The results of F6 tally, which is energy deposition averaged over a cell in unit of MeV/g, are normalized per a simulated photon particle. In order to obtain absorbed dose to current, it was necessary to multiply the MCNP5 results, a source strength which is given in a unit of a number of photons per current-time (photon/mAs). In this study, source strength was chosen as 1.75E+11 photon/mAs from preliminary study that was calculated from equation (1) according to G Jarry *et.al*.[3]

$$\text{Source strength} = \left[\frac{\text{Air kerma}_{\text{measured}}}{\text{Air kerma}_{\text{MCNP5}}}\right]/\text{mAs} \qquad (1)$$

$\text{Air kerma}_{\text{measured}}$ is absorbed dose measured in air using ionization chamber detector at the isocenter of CT scanner and $\text{Air kerma}_{\text{MCNP5}}$ is absorbed dose simulated using MCNP5 transport code at under the same condition of experimental measurement.

To ensure that whole pelvic section of the Rando phantom was accounted, absorbed doses covering 20-cm scan length were calculated by MCNP5 and reported in unit of cGy. The number of histories for all simulations, were appropriately adjusted to ensure that relative errors of the results were always less than 5 percent.[4] In this study, only MCNP5 results that were within 10-percent discrepancy with OSL nanoDot measurements were acceptable.

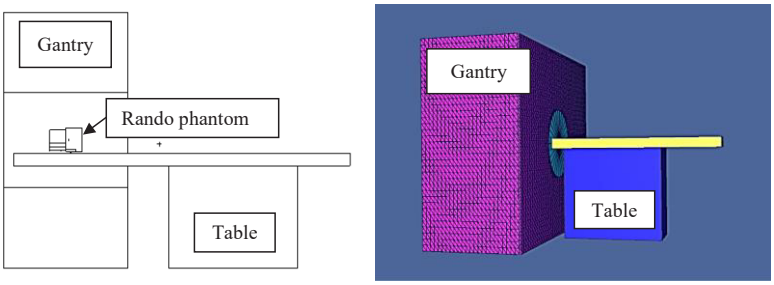

Figure 2. *2D (left) and 3D (right) MCNP5 simulation geometry of radiation measurement in Rando phantom.*

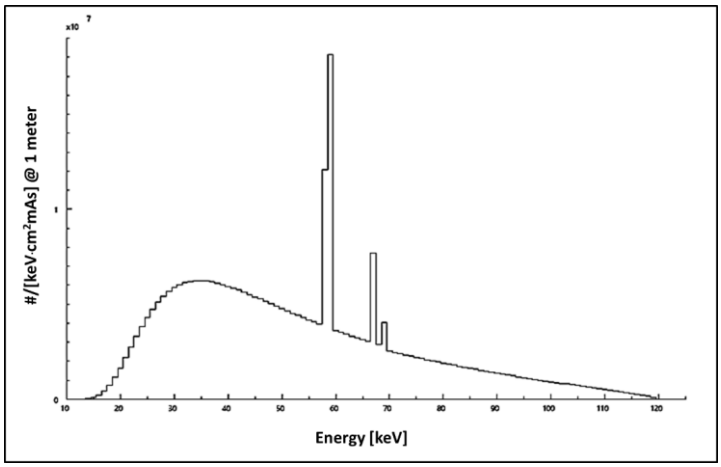

Figure 2. *120 kVp X-ray source spectrum (SpekCalc program).*

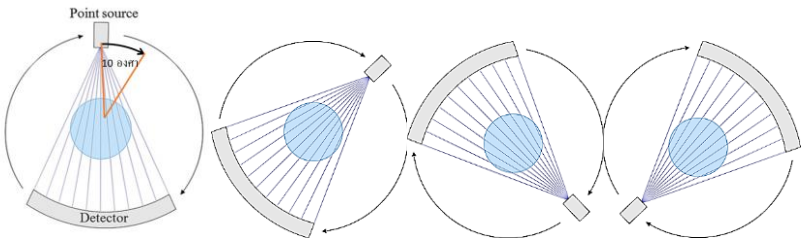

Figure 4. *Movement simulation of X-ray source from CT scanner.*

$$\% \text{ Difference} = [(D_{MCNP5} - D_{OSL}) / D_{OSL}] \times 100 \quad (2)$$

Results

Absorbed doses from MCNP5 calculation (D_{mcnp5}) and OSL nanoDot (D_{OSL}) measurement are compared then % difference of them were calculated following the equation (2) which exhibited in Table 3. Eleven absorbed doses of internal organs (No. 1 to 11) are in good agreements with less than 10 percent differences. However, eight absorbed doses from skin areas (No. 12 to 19) are observed with higher than 10 percent differences, especially in cases of left and right side (No. 14, 15, 18 and 19). It is believed that a shorter distance between a radiation source and a detector contributes to large discrepancies observed as illustrated in Figure 5. Similar discrepancies have also been observed by several studies performed by Thomas M. *et al*.[5] and Kara U[6] as shown in Table 4. Uncertainties of OSL nanoDot measurements caused by angular dependence also significantly impact on both efficient measurement and results, especially at the position of 90° and 270° (i.e., right and left side of skin).[7] In addition, Kazuki Takegami *et.al*.[8] indicated that there were a great deal of uncertainties with roughly 30% when using OSL nanoDot for patient entrance surface dose (ESD) measurement. Therefore, radiation doses recorded by OSL nanoDot might be lower than the actual values.

Table 3 Absorbed dose of equivalent organs and percentage difference.

No.	Equivalent organ	Absorbed dose (cGy)		%Difference
		MCNP5	OSL nanoDot	
1	Uterus	3.31±0.25	3.48±0.14	-5.06
2	Bladder1	4.36±0.45	4.47±0.23	-2.43
3	Bladder2	4.63±0.38	4.39±0.35	5.52
4	Bladder3	3.86±0.73	4.20±0.44	-8.11
5	Bladder4	4.37±0.73	4.05±0.32	7.72
6	Bladder5	2.20±0.19	2.37±0.10	-7.23
7	Bladder6	2.20±0.09	2.43±0.44	-9.65
8	Prostate gland1	1.98±0.12	2.02±0.06	-2.21
9	Prostate gland2	1.99±0.09	2.14±0.07	-7.12
10	Right ovary	3.03±0.57	3.01±0.33	0.87
11	Left ovary	3.23±0.43	3.08±0.24	5.03
12	Skin ($Z_{8.89}$, anterior)	8.54±0.59	4.42±0.41	93.27
13	Skin ($Z_{8.89}$, posterior)	7.03±2.14	3.68±0.78	91.17
14	Skin ($Z_{8.89}$, right)	7.42±0.34	3.50±0.21	112.24
15	Skin ($Z_{8.89}$, left)	17.94±8.60	3.23±0.23	455.39
16	Skin ($Z_{13.97}$, anterior)	9.04±1.16	5.26±0.81	71.75
17	Skin ($Z_{13.97}$, posterior)	4.66±0.42	3.96±0.29	17.66
18	Skin ($Z_{13.97}$, right)	10.65±3.55	3.58±0.85	197.08
19	Skin ($Z_{13.97}$, left)	17.82±8.34	3.82±0.81	366.90

Note: *Coordinate of Rando phantom center is X=0, Y=0 and Z=12.70, cm: centimeter.*

Table 4 Absorbed dose ratio of skin to ovary (skin/ovary) .

Condition	This study	Thomas M. *et.al* [9]	Kara U. *et.al* [10]
Absorbed dose ratio (skin/ovary)	48.88-469.33%	47.47%	58.33%
Measurement method	MCNP	OSL + post-mortem	MCNP
CT model	Aquilion64, Toshiba	Aquilion ONE, Toshiba	Lightspeed, GE

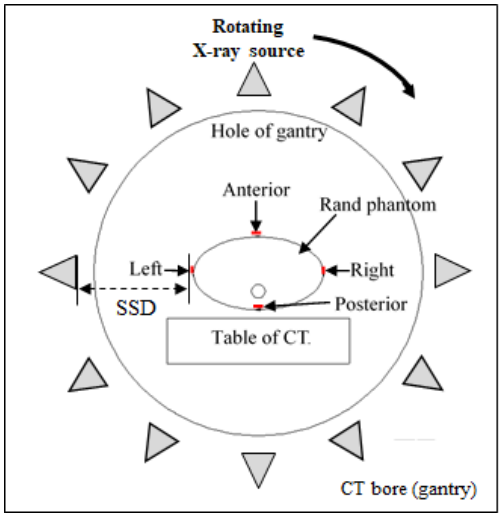

Figure 4. *Simulated setup for radiation measurement at Rando phantom surface (skin dose). The dosimeters were placed at surface of Rando phantom (4 red dots).*

Conclusion

The MCNP5 model can be used to estimate absorbed doses on internal organ from CT scanning. MCNP5 results would be normalized by machine-specific normalization factor to obtain appropriate absorbed doses. It is conceivable to provide efficient and safe CT procedure for both a radiation physicist and a physician in radiation diagnosis plan for the patients. However, the significance of difference of absorbed doses between MCNP5 calculation and OSL nanoDot measurement for skin positions should be further investigated to verify that MCNP5 calculation is reliable for predicting absorbed doses on skins or near-surface organs. More number of OSL nanoDot measurements should be contacted for statistical reliability.

Acknowledgments

The authors would like to express my sincere gratitude to the Department of Radiologic Technology, Faculty of Associated Medical Sciences Chiang Mai University, for all supporting facilities. The authors also gratefully acknowledge the financial support from Department of Diagnostic Radiology, Lampang Cancer Hospital.

References

[1] McNitt-Gray MF. AAPM/RSNA Physics Tutorial for Residents: Topics in CT. Radiation dose in CT. Radiographics. 2002; 22(6): 1541-53.

[2] Moore BM, Brady SL, Mirro AE, Kaufman RA. Size-specific dose estimate (SSDE) provides a simple method to calculate organ dose for pediatric CT examinations. Medical physics. 2014; 41(7): 071917.

[3] Jarry G, DeMarco JJ, Beifuss U, Cagnon CH, McNitt-Gray MF. A Monte Carlo-based method to estimate radiation dose from spiral CT: from phantom testing to patient-specific models. Physics in Medicine and Biology. 2003; 48(16): 2645-63.

[4] Booth TE, Hughes HG, Zukaitis A, Brown FB, Mosteller RD, Boggs M, et al. Estimated Relative Errors in MCNP. In: Girard SM, editor. MCNP — A General Monte Carlo N-Particle Transport Code, Version 5 Volume I: Overview and Theory. 1. CA, USA: Los Alamos National Laboratory, 2003. p. 113-5.

[5] Griglock TM, Sinclair L, Mench A, Cormack B, Bidari S, Rill L, et al. Determining Organ Doses from CT with Direct Measurements in Postmortem Subjects: Part 1—Methodology and Validation. 2015; 277(2): 463-70.

[6] Kara U, Tekin HO. Estımatıon of Absorbed Dose Dıstrıbutıon in Dıfferent Organs durıng the CT Scan: Monte Carlo Study. Austin Journal of Radiology. 2017; 4(1): 1063.

[7] Okazaki T, Hayashi H, Takegami K, Okino H, Kimoto N, Maehata I, et al. Fundamental Study of nanoDot OSL Dosimeters for Entrance Skin Dose Measurement in Diagnostic X-ray Examinations. J Radiat Prot Res. 2016; 41(3): 229-36.

[8] Takegami K, Hayashi H, Yamada K, Mihara Y, Kimoto N, Kanazawa Y, et al. Entrance surface dose measurements using a small OSL dosimeter with a computed tomography scanner having 320 rows of detectors. Radiol Phys Technol. 2017; 10(1): 49-59.

[9] Thomas MG, Lindsay S, Anna M, Brian C, Sharatchandra B, Lynn R, et al. Determining organ doses from CT with direct measurements in postmortem subjects. Radiology. 2015; 277: 463-70.

[10] Kara U, Tekin H. Estimation of absorbed dose distribution in different organs during the CT scan: Monte Carlo study. Austin J Radiol. 2017; 4: 01-3.

Journal of Associated Medical Sciences 2021; 54 (3): 32-42

JAMS
Journal of Associated Medical Sciences

Thai-Journal Citation Index Centre (TCI) & ASEAN Citation Index (ACI)

Journal of Associated Medical Sciences

Journal homepage: https://www.tci-thaijo.org/index.php/bulletinAMS/index

Validation of the 6 MV TrueBeam linear accelerator model for out-of-field radiation dose calculation using PHITS Monte Carlo code

Pattarakan Suwanbut[1] Thiansin Liamsuwan[1*] Danupon Nantajit[1] Wilai Masa-nga[2] Chirapha Tannanonta[2]

[1]Faculty of Medicine and Public Health, HRH Princess Chulabhorn College of Medical Science, Chulabhorn Royal Academy, Bangkok, Thailand
[2]Radiation Oncology Department, Chulabhorn Hospital, Chulabhorn Royal Academy, Bangkok, Thailand

ARTICLE INFO

Article history:
Received 2 March 2021
Accepted as revised 28 May 2021
Available online 28 May 2021

Keywords:
6 MV X-rays, out-of-field dose, Monte Carlo simulation, TrueBeam, PHITS

ABSTRACT

Background: Radiotherapy treatment planning usually concerns in-field radiation dose to produce a high therapeutic ratio with high dose to the target and minimum normal tissue complication. However, out-of-field radiation dose should also be considered because it causes additional radiation exposure to the patient, resulting in an increased risk for developing secondary cancer in the patient and health consequences in the fetus if the patient is pregnant. Monte Carlo simulation is useful for estimating out-of-field dose. The American Association of Physicists in Medicine Task Group 158 (AAPM TG 158) recommends that Monte Carlo simulation for calculation of out-of-field radiation dose should be validated in terms of percentage depth dose, lateral beam profile, dose near the phantom surface and peripheral dose.

Objectives: To validate the 6 MV TrueBeam linear accelerator model developed using Particle and Heavy Ion Transport code System (PHITS) Monte Carlo code for out-of-field dose calculation for the field sizes of 10x10, 10x20 and 40x40 cm^2.

Materials and methods: The Monte Carlo simulation was validated against experimental data at the same conditions. Percentage depth dose, lateral beam profile and dose near the phantom surface were measured at 10x10, 10x20, and 40x40 cm^2 field sizes, while peripheral doses were measured using 10x10 cm^2 field size at 0, 5, 10 and 15 cm distances from the field edge and at 5 and 10 cm depths in a water phantom. The 6 MV radiation fields were delivered using Varian TrueBeam linear accelerator. For the Monte Carlo simulation, phase space data above the jaws were provided by the vendor. PHITS code version 3.20 was used for modeling the treatment head downstream of the phase space surface and the measurement set-up. The gamma evaluation method was used to compare between the calculation and the measurement.

Results: The experimental data and the Monte Carlo simulation were in good agreement. The gamma passing rates with 3%/3mm criteria were 100% for percentage depth dose, 95% for lateral beam profile, 50% for dose near the phantom surface and 81% for peripheral dose.

Conclusion: The 6 MV TrueBeam linear accelerator model developed using PHITS Monte Carlo code was validated according to the AAPM TG 158's recommendation. The simulation results showed good agreement with the experimental data. Therefore, this Monte Carlo model can be used for out-of-field dose calculation.

* **Corresponding author.**
Author's Address: *Faculty of Medicine and Public Health, HRH Princess Chulabhorn College of Medical Science, Chulabhorn Royal Academy, Bangkok, Thailand.*
** **E-mail address:** thiansin.lia@pccms.ac.th
doi: 10.14456/jams.2021.21
E-ISSN: 2539-6056

Introduction

Radiotherapy treatment planning systems focus on in-field radiation dose for determination of treatment plans. The aim is to have a high therapeutic ratio with high dose to the target and minimum dose to healthy tissues to minimize any normal tissue complications. However, out-of-field radiation dose should also be considered because it may cause unwanted radiation exposure to the patient, increasing risk for developing secondary cancer and health consequences in the fetus of a pregnant patient. Therefore, accurate determination of out-of-field dose is important for assessment of secondary cancer risks as well as fetal dose and its consequences.[1-3]

Out-of-field dose in radiotherapy using linear accelerators arises from head leakage, collimator scatter and patient scatter. Out-of-field dose was found to be dependent on the distance from the central axis and the field size, but nearly independent on the depth. Similarly, dose near the surface of the patient is dependent on the field size and also on the photon energy.[4] The contributions from patient scatter and collimator scatter give rise to the dependence of out-of-filed dose on the field size and the distance near the field edge, while head leakage affects out-of-field dose at distances far away from the field edge.[5-10]

Out-of-field dose cannot be estimated using treatment planning systems. A comparison of measured doses with those calculated by a treatment planning system showed that the difference of dose could exceed 30% even at 3 cm distance from the field edge and the discrepancy increases with increased distance from the field edge.[4]

Measurement of out-of-field dose is subject to large errors if the detector was calibrated for in-field measurement because of different energy spectra between in-field and out-of-field radiations. The average energy of scattered photons contributed to out-of-field dose was found to be lower than in-field photon energy, being 0.2 and 1.5 MeV for a 6 MV photon beam, respectively.[4] The difference in energy spectra will cause different detector responses.[4] To overcome the limitation in the measurement, Monte Carlo simulation is another method of choice for out-of-field dose determination.[4]

Monte Carlo simulations have been used for determination of out-of-field dose for various treatment techniques and linear accelerator models.[4, 11] Testing accuracy of radiation dose calculated by a Monte Carlo simulation should be done by comparing experimental data obtained from reliable measurements with simulated results from the Monte Carlo simulation. For in-field dose calculations, calculated percentage depth dose (beyond the depth of the maximum dose, D_{max}) and lateral beam profile should be validated against their corresponding measurements. In addition, for out-of-field dose calculations, the American Association of Physicists in Medicine Task Group 158 (AAPM TG 158) recommends that Monte Carlo Simulation should also be validated in terms of dose near the phantom surface and peripheral dose. Dose near the phantom surface (in the build-up region) corresponds to dose at depths shallower than the depth of the maximum dose (D_{max}), taking into account electron dose near the surface that might affect the accuracy of out-of-field dose calculation. Peripheral dose is dose outside the field edge, directly representing out-of-field radiation dose.

In this work, the 6 MV TrueBeam linear accelerator (Varian Medical System. Inc., Palo Alto, CA, USA) was modeled using the Particle and Heavy Ion Transport code System (PHITS) Monte Carlo code for the purpose of out-of-field dose calculation to be used in the evaluation of fetal dose during breast cancer radiotherapy. The field sizes of interest included 10x10, 10x20 and 40x40 cm^2. Percentage depth dose, lateral beam profile, dose near the phantom surface and peripheral dose calculated by the Monte Carlo simulation were validated against the measurements at the same conditions.

Materials and methods

Measurement set-up

Percentage depth dose, lateral beam profile and peripheral dose were measured in Wellhofer Scanditronix Blue water phantom (IBA Dosimetry, Schwarzenbruck, Germany). Dose near the phantom surface was measured in WP1D water phantom (IBA Dosimetry, Schwarzenbruck, Germany) with 100 MU. Irradiation of 6 MV X-rays was achieved using Varian TrueBeam linear accelerator at 100 cm source-surface distance (SSD) and dose rate of 400 MU/min. The measured data were analyzed with Omni-pro program (IBA Dosimetry, Schwarzenbruck, Germany) and presented in term of dose relative to D_{max} for percentage depth dose (PDD) and dose near the phantom surface (DNS) as shown in equation 1, as well as dose relative to the central axis dose for lateral beam profile (LP) and peripheral dose (PD) as shown in equation 2.

$$\text{PDD and DNS} = D(z)/D_{max} \times 100 \quad (1)$$

$$\text{LP and PD} = D(r)/D(0) \times 100 \quad (2)$$

where D is dose at a specified depth z or lateral distance r (in-plane or cross-plane), D_{max} is the maximum dose of the depth dose curve and D(0) is dose at the central axis.

CC13 ionization chamber (IBA dosimetry, Schwarzenbruck, Germany) was used for measuring percentage depth dose, lateral beam profile and peripheral dose. However, for the measurement of dose near the phantom surface, which needed a higher spatial resolution, PP05 parallel plate ionization chamber (IBA dosimetry, Schwarzenbruck, Germany) was used instead. CC13 has the active volume of 0.13 cm^3 with the inner diameter of the outer electrode of 6.0 mm, while PP05 has the active volume of 0.05 cm^3 and the small collecting volume of 0.6 mm plate spacing. Therefore, PP05 offers a higher spatial resolution of dose measurement and is a more suitable detector than CC13 for dose determination in the region with high dose gradient such as that near the phantom surface.

Most of the measurements were done for the field sizes of 10x10, 10x20 and 40x40 cm^2, except for the measurement of the peripheral dose that was done only for 10x10 cm^2 field size. Percentage depth dose was measured in 1 mm step from 0.09 to 27.49 cm depth. Dose near the phantom surface was measured also in 1 mm step from 0.00 to 19.50 cm depth. The measurement of lateral beam profile was done at 5 and 10 cm depths with a step of 1 mm. Peripheral dose was measured at the distances of 0, 5, 10,

15 cm from the field edge (10x10 cm^2 field size), corresponding to ±5, ±10, ±15, and ±20 cm distances from the central axis, respectively.

Monte Carlo simulation

Monte Carlo simulation required the information of the treatment head in terms of dimension, elemental composition and density. To model the treatment head, TrueBeam Monte Carlo Data Package was used.[12] This data package provides phase space files of photons and electrons just above the movable upper jaws at the distance of 73.3 cm from the isocenter with 100 cm SSD as well as the detailed information (dimension, material type and material density) of the treatment head components downstream of the phase space surface. Twenty-five phase space files were converted with PSFC4PHITS to dump files readable by PHITS[13], corresponding to the number of converted particles of about 1.2×10^9. The lower part of the treatment head was simulated in detail, consisting of X and Y Jaws with the characteristics as described in the TrueBeam Monte Carlo Data Package and shown in Figure 1.

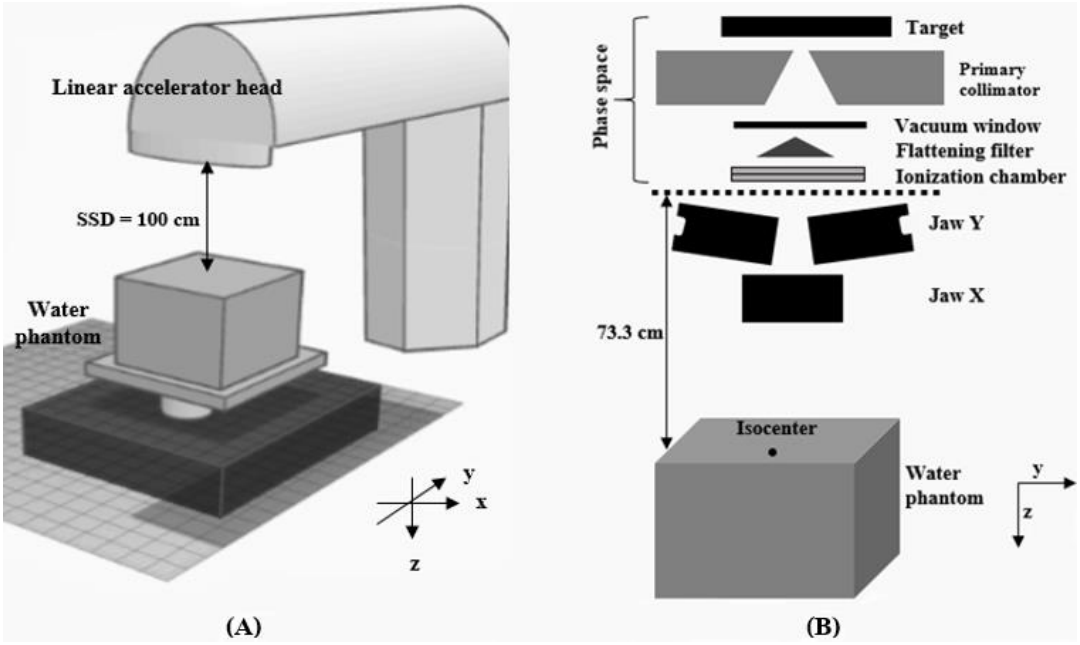

Figure 1. *Set-up of the TrueBeam linear accelerator and the water phantom: (A) Measurement set-up and (B) Monte Carlo model. Dashed line in figure (B) indicates the phase space surface for the Monte Carlo simulation.*

PHITS (Particle and Heavy Ion Transport code System) is a general purpose Monte Carlo particle transport simulation code that can simulate all particles and electromagnetic radiation over wide energy ranges. PHITS can be used to study a variety of topics, for example, accelerator technology, radiation protection and radiotherapy.[14] PHITS version 3.20 was used in this work for modeling the treatment head and for calculation of radiation dose. EGS5 mode of PHITS was used for electron and photon transport. The number of simulated particles at the phase space surface was in the range of 10^9 to produce reasonable standard deviations of the simulated results. The dose was calculated in the water phantom (50 cm x 50 cm x 50 cm) for 100 cm SSD.

Percentage depth dose and dose near the phantom surface was calculated in cylindrical voxels with 0.5 cm radius and 0.1 cm step ranging from 0.05 to 27.50 cm depth in the water phantom. Standard deviations of the results were not exceeding 3.3%. For the calculation of lateral beam profile and peripheral dose, dose was tallied in rectangular voxels with the dimensions of 2x0.1x2 cm^3 and 0.1x2x2 cm^3 for in-plane and cross-plane dose, respectively. The standard deviations of the calculated lateral beam profiles were less than 1.2% at the central region. The simulations were done on a high-performance computing (HPC) server using 16 cores of Intel Xeon E5-2600 v4 at 3.2 GHz with the simulation time of about 5.5 h for each simulated field size.

Comparison between the experimental data and the Monte Carlo simulation of percentage depth dose, lateral beam profile, dose near the phantom surface and peripheral dose was done using gamma evaluation method[15] with 3% dose difference at 3 mm distance-to-agreement (3%/3mm). In addition, for the lateral beam profile, point-by-point comparison of dose was done at the central region (plateau region) and the comparison of penumbra width (80%-20%) was done at the penumbra region. In this study, the central regions were defined between ±4.9 cm, ±9.9 cm and ±19.9 cm distances from the central axis for the field sizes of 10x10 cm^2, 10x20 cm^2 (in-plane or cross-plane) and 40x40 cm^2, respectively. In this work, the Monte Carlo simulated results for lateral beam profile and peripheral dose are presented as dose relative to average dose at the central regions.

Results

The experimental data and the Monte Carlo simulated results of percentage depth dose are shown in Figure 2A, Figure 3A and Figure 4A for the field sizes of 10x10 cm^2, 10x20 cm^2 and 40x40 cm^2, respectively. The experimental data and the Monte Carlo simulated results of dose near the phantom surface are shown in Figure 2B, Figure 3B and Figure 4B for the respective field sizes. D_{max} in the measured percentage depth dose curves were 1.55, 1.55 and 1.35 cm, while D_{max} in the measured doses near the phantom surface were 1.45, 1.45 and 1.15 cm, for the respective field sizes. In comparison, D_{max} obtained from the Monte Carlo simulation were 1.65, 1.45 and 1.55 cm, respectively. The maximum standard deviations of the measured doses near the phantom surface were 0.3%, 0.2% and 0.3% for the respective field sizes, and the maximum standard deviations of the Monte Carlo simulated results were 3.3%, 3.1% and 2.6%, respectively. For percentage depth dose and dose near the phantom surface, the average differences between the calculated and measured doses for all investigated field sizes were 2.7% and 8.6%, respectively. Moreover, the gamma passing rates (3%/3mm) of percentage depth dose and dose near the phantom surface were at least 100% and 50%, respectively, as shown in Table 1.

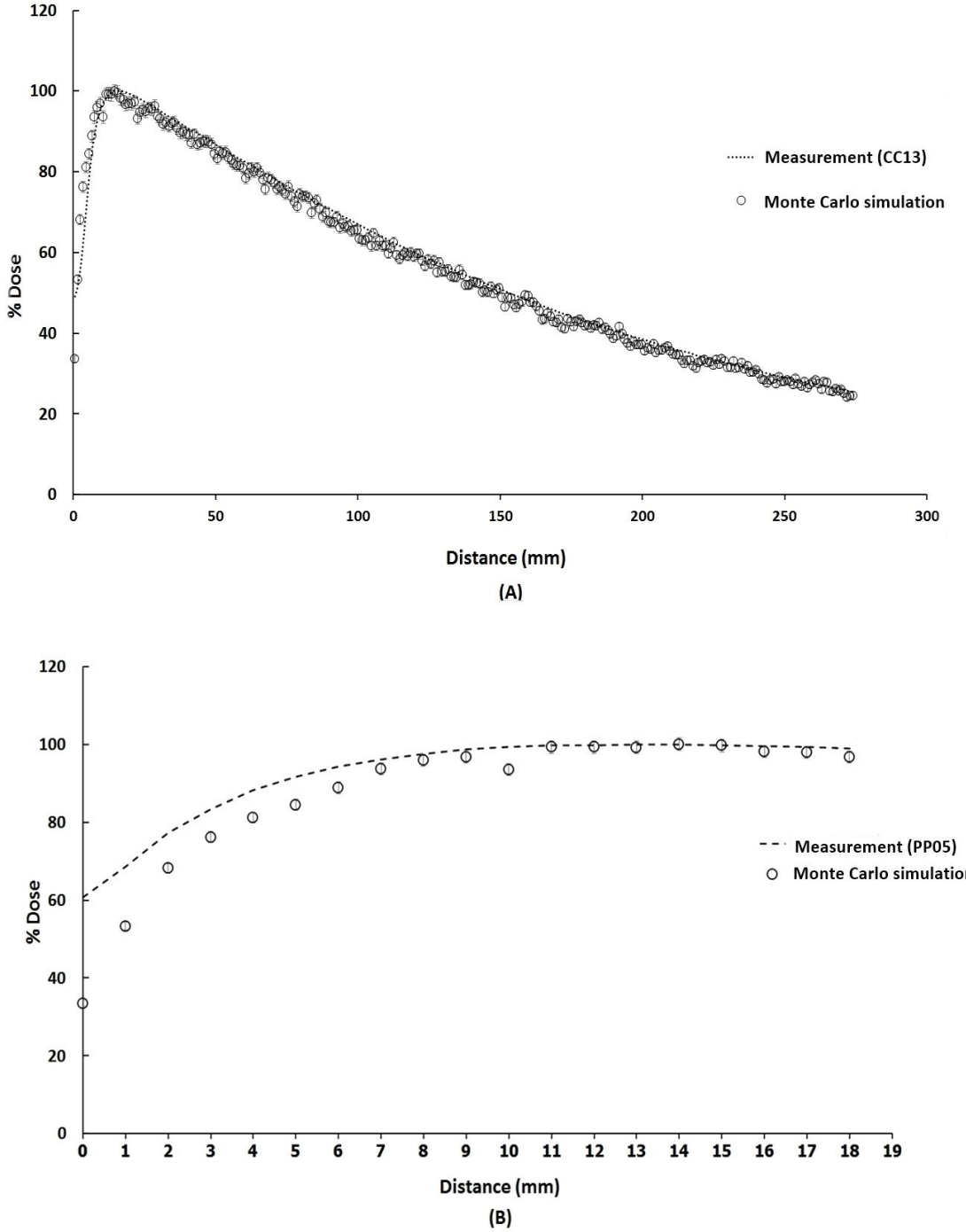

Figure 2. *Percentage depth dose and dose near the phantom surface for 10x10 cm^2 field size. A: percentage depth dose, B: dose near the phantom surface, symbols are Monte Carlo simulated results and lines are experimental data.*

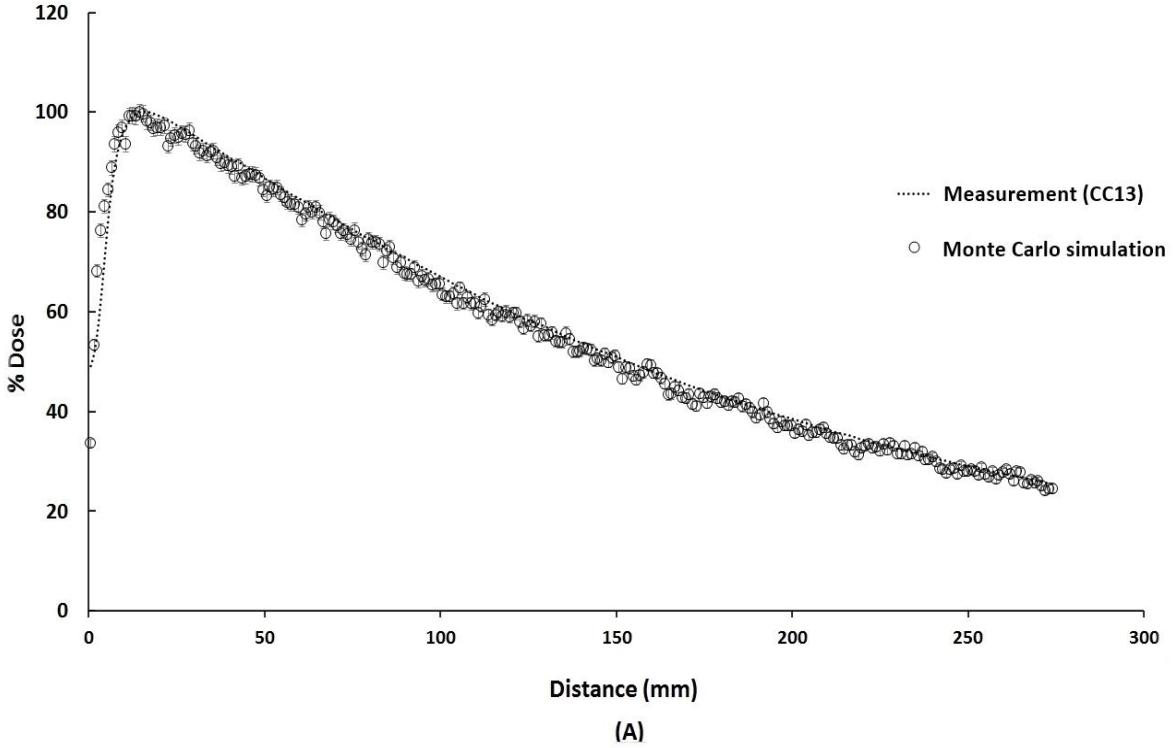

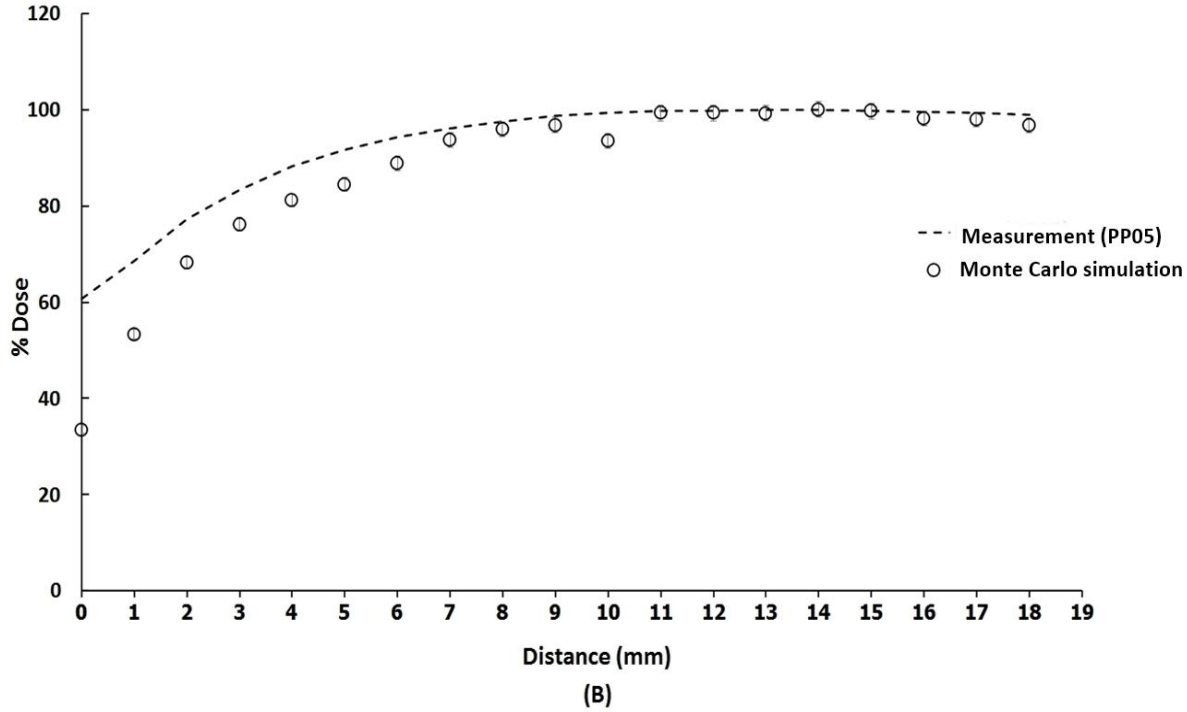

Figure 3. *Percentage depth dose and dose near the phantom surface for 10x20 cm^2 field size. A: percentage depth dose, B: dose near the phantom surface, symbols are Monte Carlo simulated results and lines are experimental data.*

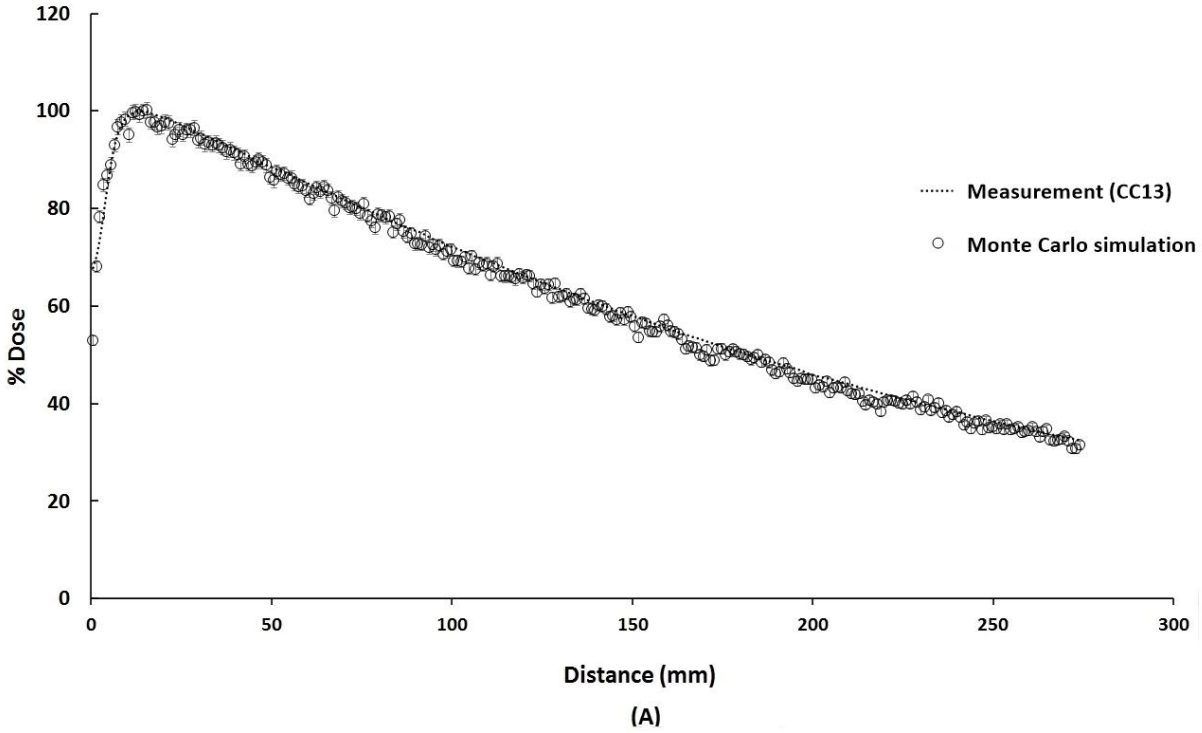

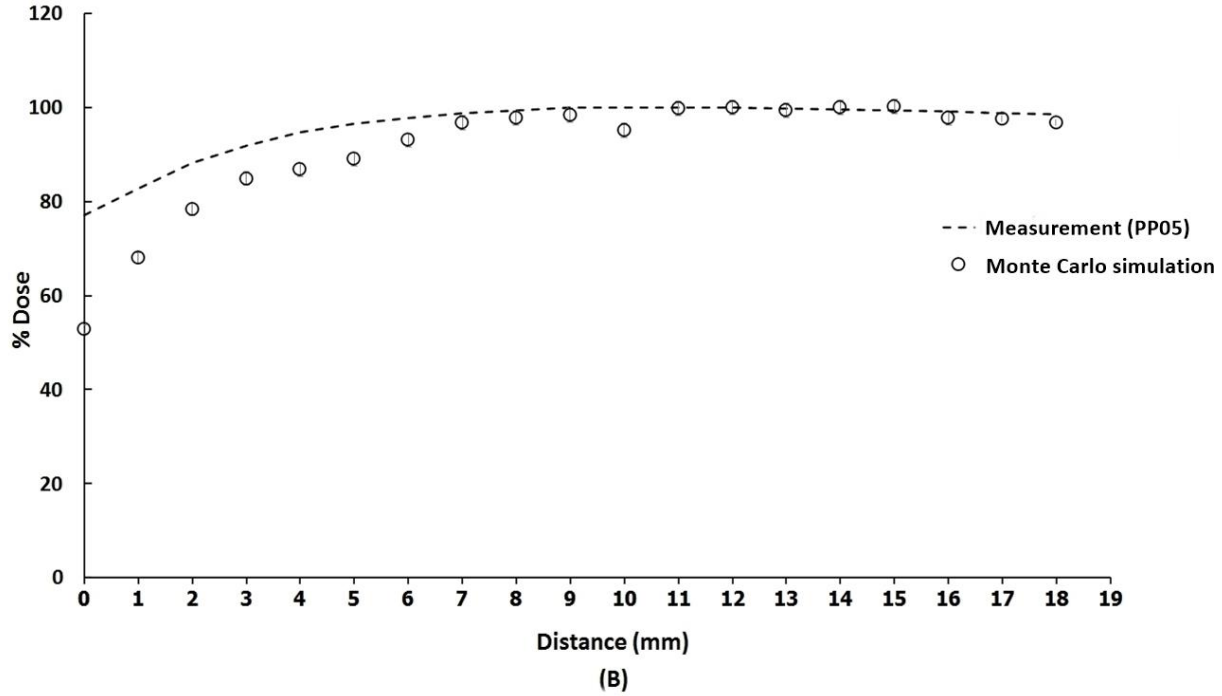

Figure 4. *Percentage depth dose and dose near the phantom surface for 40x40 cm² field size: A: percentage depth dose, B: dose near the phantom surface, symbols are Monte Carlo simulated results and lines are experimental data.*

Table 1 Summary of gamma passing rates with 3%/3mm criteria of percentage depth dose and dose near the phantom surface.

Field size	Gamma passing rates (%)	
	Percentage depth dose	Dose near the phantom surface
10x10 cm^2	100.0	75.0
10x20 cm^2	100.0	73.3
40x40 cm^2	100.0	50.0

The experimental data and Monte Carlo simulated results of lateral beam profile, including in-plane and cross-plane doses, at 5 and 10 cm depths are shown in Figure 5, Figure 6 and Figure 7 for the field sizes of 10x10, 10x20 and 40x40 cm^2, respectively. The maximum standard deviations of the Monte Carlo simulated results were 1.2%, 1.1% and 0.9%, for the respective field sizes. The differences of the simulated and measured doses at the central regions did not exceed 3% and the differences of the penumbra widths were at maximum 3 mm for all investigated field sizes.

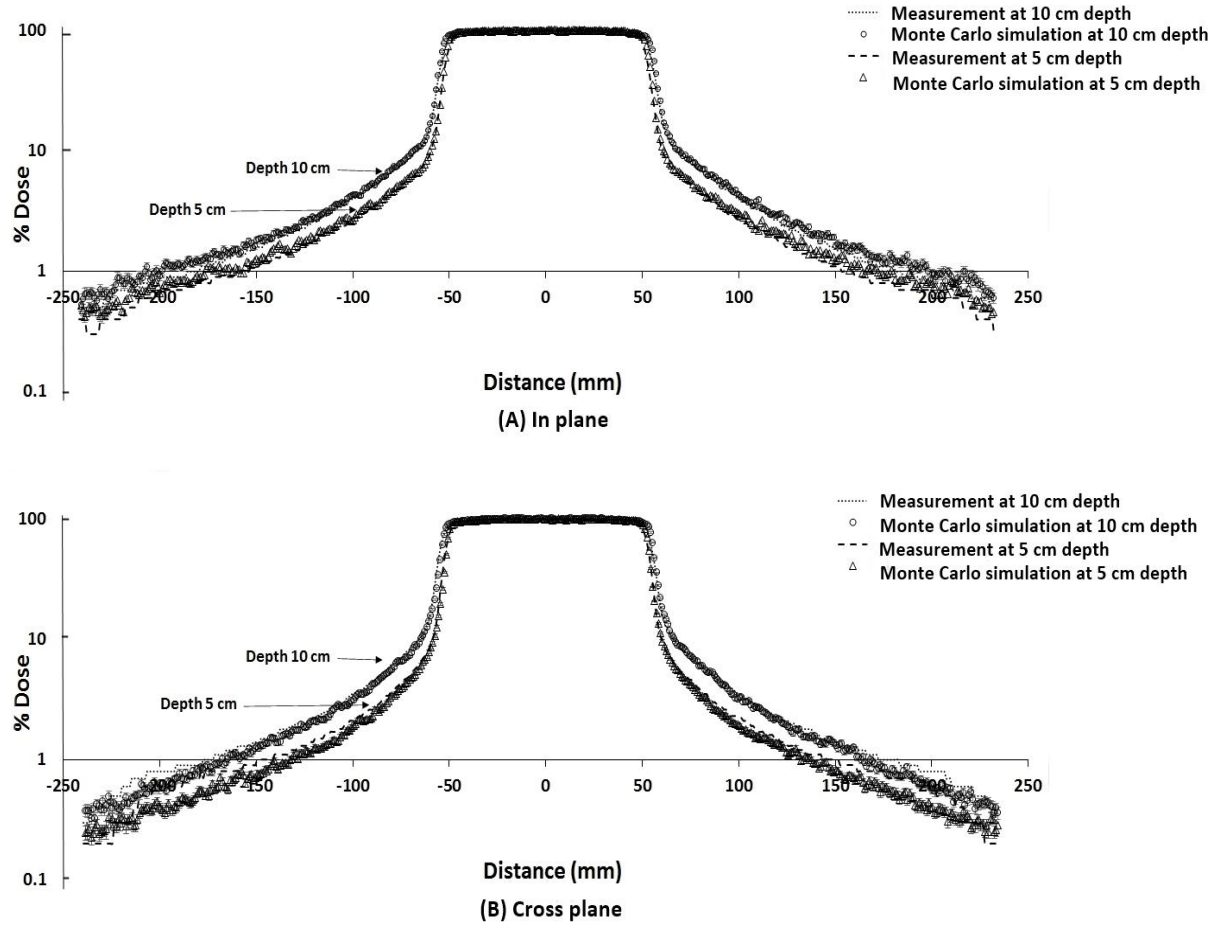

Figure 5. *Lateral beam profiles for the field sizes of 10x10 cm^2 at 5 and 10 cm depth. A: in-plane, B: cross-plane doses, symbols are Monte Carlo simulated results and lines are experimental data.*

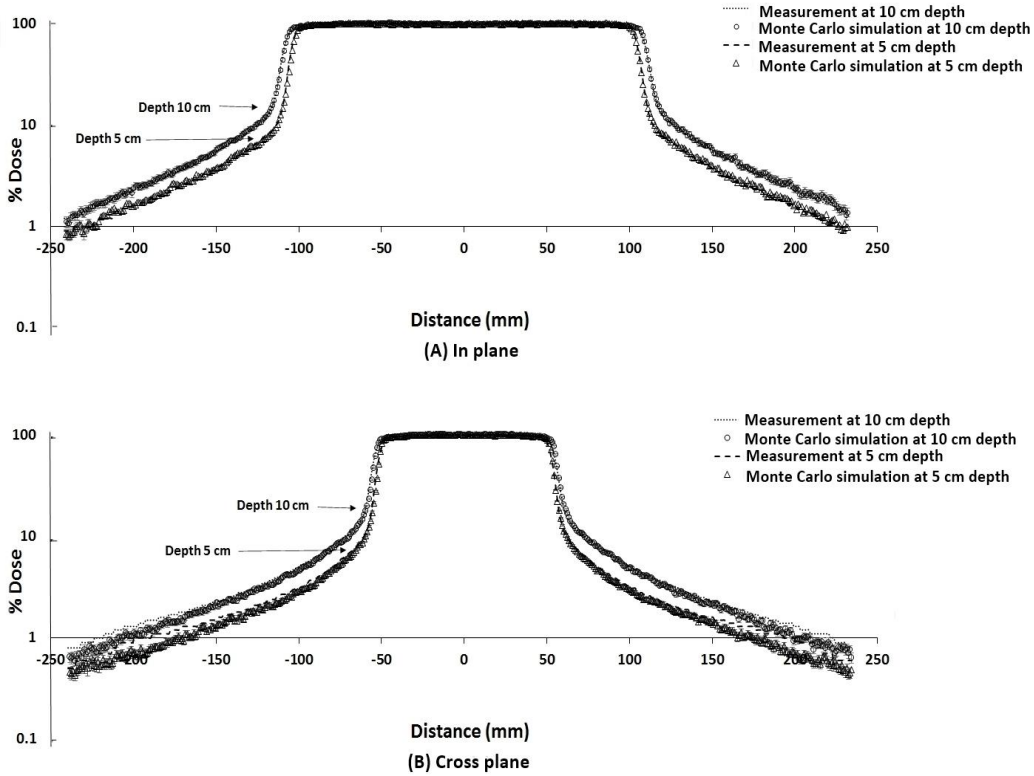

Figure 6. *Lateral beam profiles for the field sizes of 10x20 cm² at 5 and 10 cm depth. A: in-plane, B: cross-plane doses, symbols are Monte Carlo simulated results and lines are experimental data.*

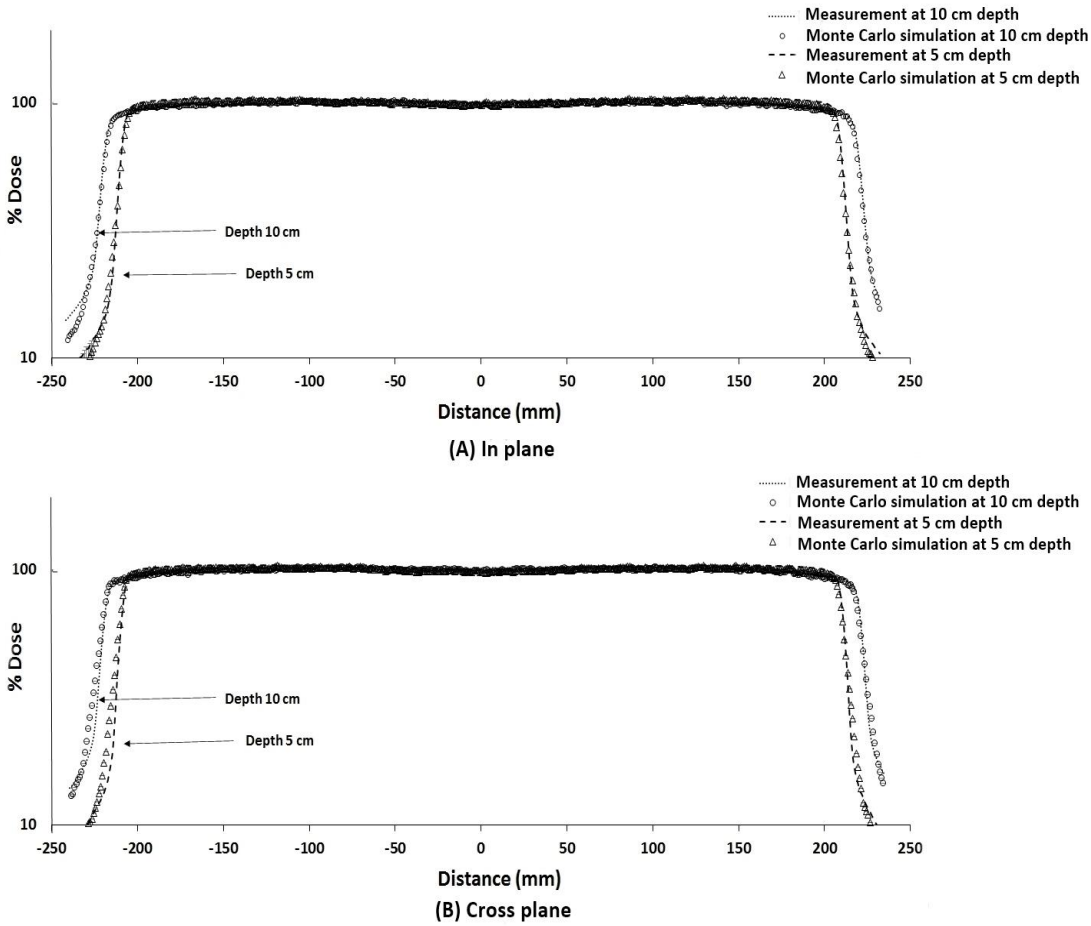

Figure 7. *Lateral beam profiles for the field sizes of 40x40 cm² at 5 and 10 cm depth. A: in-plane, B: cross-plane doses, symbols are Monte Carlo simulated results and lines are experimental data.*

Table 2 Summary of gamma passing rates with 3%/3mm criteria of lateral beam profile.

Field size	Lateral beam profile at 5 cm depth						Lateral beam profile at 10 cm depth					
	central region		Penumbra region		All regions		central region		Penumbra region		All regions	
	In plane	Cross plane	In plane	Cross plane	In plane	Cross plane	In plane	Cross plane	In plane	Cross plane	In plane	Cross plane
10x10 cm^2	95.0	96.9	100.0	100.0	95.0	95.8	97.0	97.9	100.0	100.0	96.3	96.2
10x20 cm^2	99.4	96.0	100.0	100.0	95.1	95.1	100.0	97.9	100.0	100.0	97.6	95.1
40x40 cm^2	95.0	97.0	100.0	100.0	96.2	96.3	96.0	98.0	100.0	100.0	98.9	98.7

Table 3 Summary of peripheral doses.

Distance from the central axis (cm)	Peripheral dose at 5 cm depth				Peripheral dose at 10 cm depth			
	In plane		Cross plane		In plane		Cross plane	
	Exp	MC	Exp	MC	Exp	MC	Exp	MC
-20 cm	0.70	0.67±0.10	0.60	0.40±0.09	0.90	0.90±0.09	0.80	0.60±0.07
-15 cm	1.10	1.21±0.07	0.95	0.73±0.07	1.60	1.76±0.06	1.40	1.25±0.05
-10 cm	2.68	2.63±0.04	2.10	1.86±0.05	3.98	4.22±0.03	3.55	3.10±0.04
-5 cm	73.10	84.73±0.01	73.80	76.18±0.01	85.60	93.40±0.01	89.60	90.70±0.01
5 cm	80.00	90.00±0.01	84.80	90.79±0.01	89.60	92.40±0.01	90.60	93.99±0.01
10 cm	2.70	3.20±0.04	2.30	1.93±0.04	4.00	4.38±0.03	3.55	3.24±0.03
15 cm	1.10	1.20±0.06	1.00	0.80±0.06	1.50	1.60±0.05	1.40	1.35±0.06
20 cm	0.60	0.78±0.09	0.60	0.40±0.08	0.80	0.94±0.08	0.80	0.57±0.07
Gamma passing rate	83.0%		84.0%		85.0%		81.0%	

Note: *Exp: experimental data, MC: Monte Carlo simulation, % relative to average dose in the central region and gamma passing rates with 3%/3mm criteria.*

Discussion

In this study, the 6 MV TrueBeam linear accelerator model for out-of-field dose calculation was developed using PHITS Monte Carlo code for the field sizes of 10x10, 10x20 and 40x40 cm^2. The Monte Carlo model was validated against experimental data according to the recommendation of AAPM TG 158.[4]

In terms of percentage depth dose and dose near the phantom surface, the comparisons of the calculated and measured doses gave the gamma passing rates (3%/3mm) of 100% and at least 50% for all investigated field sizes, respectively. In general, the gamma passing rates of dose near the phantom surface is expected to be lower than those of percentage depth dose due to a steep dose gradient near the phantom surface. As recommended by a previous study[16], the comparison of experimental data and Monte Carlo calculated doses near the phantom surface should not exceed 15%. When analyzing the present results following that recommendation, it was found that all parts of doses near the phantom surface passed this criterion except at the surface. As shown in previous studies, differences of doses at the phantom surface obtained from measurements and Monte Carlo simulations were as large as 40%.[10,17,18] In term of field size dependence, the calculated doses near the phantom surface obtained in this work exhibited a field size dependence, in accordance with previous studies.[9,10,19] The larger field size was associated with the larger dose due to a higher degree of electron contamination.[10,19]

For the validation of lateral beam profile, the gamma passing rates were at least 95% for all investigated field sizes and depths. The point-by-point differences of doses at the central region did not exceed 3% and the differences of the penumbra widths were less than 3 mm for all investigated field sizes and depths. The differences of doses at the central region and penumbra widths should not exceed 3% and 3 mm, respectively.[16] Thus, the simulation and the measurement carried out in this work were considered to be in good agreement.

For the validation of peripheral dose, the gamma passing rates were larger than 81% for all investigated depths. In this work, the measured peripheral doses were in relatively

good agreement with the Monte Carlo simulated results at close distances from the field edge. However, the differences of the calculated and measured doses at 15 cm distance from the field edge (20 cm distance from the central axis) were as large as 33%. Such large discrepancies have also been observed in the previous studies,[5,6,20] which may arise from statistical uncertainties of the simulation (up to 10% in this work) and the uncertainty of dose measurement[4].

It should be mentioned that using phase space files obtained from the vendor allowed fewer opportunities to improve the Monte Carlo model. For example, the treatment head model upstream from the jaws needed to be treated as a black box that could not be adjusted to give a better agreement to the experimental data. Nevertheless, from the validation carried out in this work, the agreement between the measured and calculated doses suggested that the developed Monte Carlo model of the 6 MV TrueBeam linear accelerator can be used for out-of-field dose calculation.

Conclusion

In this work, the 6 MV TrueBeam linear accelerator model developed using PHITS Monte Carlo code for out-of-field dose calculation was validated against experimental data based on the recommendation of AAPM TG 158. The field sizes of interest included 10x10, 10x20 and 40x40 cm^2. Percentage depth dose, lateral beam profile, dose near the phantom surface and peripheral dose calculated by the Monte Carlo simulation were validated against the measurements at the same conditions. The comparison showed good agreement between the experimental data and the Monte Carlo simulation for all investigated field sizes with the gamma passing rates (3%/3mm) of at least 100% for percentage depth dose, 95% for lateral beam profile, 50% for dose near the phantom surface and 81% for peripheral dose at 5 and 10 cm depth. The results suggested that the developed Monte Carlo model can be used for calculation of out-of-field dose, for example, for determination fetal dose during radiotherapy for a pregnant patient.

Conflict of interest

The authors declare that there is no conflict of interest.

References

[1] Mazonakis M, Damilakis J. Estimation and reduction of the radiation dose to the fetus from external-beam radiotherapy. Phys Med. 2017; 43: 148-52. doi: 10.1016/j.ejmp.2017.09.130.

[2] D'Arienzo M, Masciullo SG, Sanctis VD, Osti MF, Chiacchiararelli L, Enrici RM. Integral dose and radiation-induced secondary malignancies: comparison between stereotactic body radiation therapy and three-dimensional conformal radiotherapy. Int J Environ Res Public health. 2012; 9(11): 4223-40. doi: 10.3390/ijerph9114223.

[3] Taylor ML, Kron T. Consideration of the radiation dose delivered away from the treatment field to patients in radiotherapy. J Med Phys. 2011; 36(2): 59. doi: 10.4103/0971-6203.79686.

[4] Kry SF, Bednarz B, Howell RM, Dauer L, Followill D, Klein E, et al. AAPM TG 158: measurement and calculation of doses outside the treated volume from external-beam radiation therapy. Med Phys. 2017; 44(10): e391-e429. doi: 10.1002/mp.12462.

[5] Bednarz B, Xu XG. Monte Carlo modeling of a 6 and 18 MV Varian Clinac medical accelerator for in-field and out-of-field dose calculations: development and validation. Phys Med Biol. 2009; 54(4): N43. doi: 10.1088/0031-9155/54/4/N01.

[6] Kry SF, Titt U, Pönisch F, Followill D, Vassiliev ON, Allen White R, et al. A Monte Carlo model for calculating out-of-field dose from a Varian beam. Med Phys. 2006; 33(11): 4405-13. doi: 10.1118/1.2360013.

[7] Wijesooriya K, Liyanage NK, Kaluarachchi M, Sawkey D. Part II: Verification of the TrueBeam head shielding model in Varian VirtuaLinac via out-of-field doses. Med Phys. 2019; 46(2): 877-84. doi: 10.1002/mp.13263.

[8] Siji C, Mustafa M, Ganapati R. Out-of-field photon dosimetry study between 3-D conformal and intensity modulated radiation therapy in the management of prostate cancer. J Radiat Res. 2015; 13(2): 127-34. doi: 10.7508/ijrr.2015.02.002.

[9] Starkschall G, St. George F, Zellmer D. Surface dose for megavoltage photon beams outside the treatment field. Med Phys. 1983; 10(6): 906-10. doi: 10.1118/1.595362.

[10] Apipunyasopon L, Srisatit S, Phaisangittisakul N. An investigation of the depth dose in the build-up region, and surface dose for a 6-MV therapeutic photon beam: Monte Carlo simulation and measurements. J Radiat Res. 2013; 54(2): 374-82. doi: 10.1093/jrr/rrs097.

[11] Kry SF, Salehpour M, Titt U, White RA, Stovall M, Followill D. Monte Carlo study shows no significant difference in second cancer risk between 6-and 18-MV intensity-modulated radiation therapy. Radiother Oncol. 2009; 91(1): 132-7. doi: 10.1016/j.radonc.2008.11.020.

[12] Varian Medical System. TrueBeam Monte Carlo Data Package version 1.1. Palo Alto, CA: Varian Medical system; 2014.

[13] Furuta T, Hashimoto S, Sato T. Medical Applications of the PHITS Code (3): User Assistance Program for Medical Physics Computation. Igaku Butsuri. 2016; 36(1): 50-4. doi: 10.11323/jjmp.36.1_50.

[14] Sato T, Iwamoto Y, Hashimoto S, Ogawa T, Furuta T, Abe S-i, et al. Features of particle and heavy ion transport code system (PHITS) version 3.02. J Nucl Sci Technol. 2018; 55(6): 684-90. doi: 10.1080/00223131.2017.1419890.

[15] Low DA, Harms WB, Mutic S, Purdy JA. A technique for the quantitative evaluation of dose distributions. Med Phys. 1998; 25(5): 656-61. doi: 10.1118/1.598248.

[16] Venselaar J, Welleweerd H, Mijnheer B. Tolerances for the accuracy of photon beam dose calculations of treatment planning systems. Radiother Oncol. 2001 Aug 1; 60(2): 191-201. doi: 10.1016/s0167-8140(01)00377-2.

[17] Chetty IJ, Curran B, Cygler JE, DeMarco JJ, Ezzell G, Faddegon BA, Kawrakow I, Keall PJ, Liu H, Ma CM, Rogers DW. AAPM Task Group Report No. 105;"Issues associated with clinical implementation of Monte Carlo-based photon and electron external beam treatment planning,". Med Phys. 2007; 34: 4818-52. doi: 10.1118/1.2795842.

[18] Shende R, Gupta G, Patel G, Kumar S. Commissioning of TrueBeam TM medical linear accelerator: quantitative and qualitative dosimetric analysis and comparison of flattening filter (FF) and flattening filter free (FFF) beam. Int'l J. of Medical Physics, Clinical Eng. and Radiation Oncology. 2016; 5(01): 51.

[19] Klein EE, Esthappan J, Li Z. Surface and buildup dose characteristics for 6, 10, and 18 MV photons from an Elekta Precise linear accelerator. J App Clin Med Phys. 2003; 4(1): 1-7. doi: 10.1120/jacmp.v4i1.2537.

[20] Kry SF, Titt U, Followill D, Pönisch F, Vassiliev ON, White RA, et al. A Monte Carlo model for out-of-field dose calculation from high-energy photon therapy. Med Phys. 2007; 34(9): 3489-99. doi: 10.1118/1.2756940.

Journal of Associated Medical Sciences 2021; 54 (3): 43-47

JAMS
Journal of Associated Medical Sciences

Thai-Journal Citation Index Centre (TCI) & ASEAN Citation Index (ACI)

Journal of Associated Medical Sciences

Journal homepage: https://www.tci-thaijo.org/index.php/bulletinAMS/index

Evaluation of efficiency of artificial intelligence for chest radiograph interpretation for pulmonary tuberculosis screening in mobile x-ray vehicle

Khemipa Sanklaa

Department of Radiological Technology, Faculty of Allied Health Sciences, Thammasat University, Pathum Thani Province, Thailand

ARTICLE INFO

Article history:
Received 20 January 2021
Accepted as revised 31 May 2021
Available online 31 May 2021

Keywords:
Pulmonary tuberculosis, artificial intelligence, chest radiograph, quality control, portable x-ray

ABSTRACT

Background: Tuberculosis (TB) is one of the major global health threats. The chest radiograph (CXR) is one of the primary tools for detecting TB, especially pulmonary TB. Artificial Intelligence (AI) is increasingly used with radiological technology by developing AI software for health screening by CXR.

Objectives: To compare the pulmonary TB screening results between the radiologist and AI software from the mobile x-ray screening vehicle of the Faculty of Allied Health Sciences, Thammasat University.

Materials and methods: 449 patients (408 normal, 41 abnormal) were exposed for chest radiograph at the mobile x-ray screening vehicle of Faculty of Allied Health Sciences, Thammasat University. The retrospective data was randomly collected between 2016 and 2018. The methods were divided into three steps: quality control for the x-ray machine, transferring the radiograph from digital radiography to PACS and AI, and displaying the results on the monitor with the StatPlus program.

Results: The mobile x-ray machine has passed the quality control test. In addition, the TB interpretation by AI showed Area Under Curve of 0.859 and the study demonstrated high specificity of 0.995 but low sensitivity of 0.722. The positive predictive value (PPV) was 0.951, which was less than the Negative Predictive Value of 0.963.

Conclusion: Artificial intelligence is becoming a healthcare supporter to help radiologists analyze and interpret chest radiographs and provide a fast diagnosis.

Introduction

Tuberculosis (TB) is a major global health threat, and the World Health Organization (WHO) estimates that Thailand is one of the 14 countries in the world with a TB prevalence in 2018.[1] The chest radiograph (CXR) is one of the primary tools for detecting TB, especially pulmonary TB because CXR has a high sensitivity for pulmonary TB. However, CXR has poor specificity.[2] Therefore, TB screening should always be made on TB diagnosis on bacteriological confirmation (sputum-smear microscopy or a molecular test). During the check-up, a chest radiograph in the posteroanterior view is usually taken. The patient is breast-attached with a cassette and the hand is on the patient's hip to separate the scapular from the lung. To reconstruct a chest radiograph, the patient needs to take a deep breath and hold it during the x-rays to reduce motion. The right technique should be good exposure, no rotation of the patient, and ensure patients are at the right marker. Airways should be without any deviation, centrally located in the radiograph and the angle at the carina should be less than 90 degrees. Bones and soft tissue have the ability to count the number of ribs (10 ribs posteriorly and 6 ribs anteriorly) and check the bone's lucency, bone opacity, and vertebral bodies. Cardiac size should not be more than half the size of the thorax. We should check the diaphragm to see if the left side is higher than the right side, the availability of air below the diaphragm, any gastric

* **Corresponding author.**
Author's Address: *Department of Radiological Technology, Faculty of Allied Health Sciences, Thammasat University, Pathum Thani Province, Thailand.*
** **E-mail address:** w_biu@hotmail.com
doi: 10.14456/jams.2021.22
E-ISSN: 2539-6056

bubble, and the Costophrenic and Cardiophrenic angles. Lung fields should be uniform or have some opacities or lucencies. Appearance of pulmonary tuberculosis on the radiograph contains small opaque spots throughout the lungs and enlargement of a hilar region in early stages or regions of calcification with cavitations which is frequently in the area of upper lobes and apices with upward retraction of hila.

Artificial intelligence (AI) often instantiated as software programs is a branch of computer science that attempts to understand and build intelligent entities. The subset of AI is Machine learning (ML) and the subset of ML is Deep learning (DL). AI in clinical practice can be used for interpreting patient genomes, treatment selection, automated surgery, and disease diagnosis.[3] Nowadays, Artificial Intelligence is increasingly employed with radiological technology by developing AI software for health screening by CXR. Most of the x-ray machine vendors have launched the AI section in x-ray machines such as FDR AQRO mini mobile system from FujiFilm,[4] Ysio X.pree from Siemens,[5] ALND from Samsung for lung nodule detection, etc. [6]

The purpose of this study is to compare the pulmonary TB screening results between the radiologist and AI software from the mobile x-ray screening vehicle of the Faculty of Allied Health Sciences, Thammasat University.

Materials and methods

This research is based on a retrospective descriptive study. 449 patients (408 normal, 41 abnormal) were exposed by x-ray for chest radiograph at the mobile x-ray screening vehicle of the Faculty of Allied Health Sciences, Thammasat University. This research recording was approved by the ethical review sub-committee board for human research involving sciences, Thammasat University, No.3 and the approval code is COA No.017/2563. The retrospective data was randomly collected between 2016 and 2018. The methods were divided into 3 steps, namely quality control for the x-ray machine, transferring radiograph from digital radiography to Picture Archiving and Communication System (PACS) and AI, displaying results on a monitor.

The X-ray machine in the mobile vehicle (GEMSS, TITAN 2000, No.793291105153, Korea) was subjected to quality control, which includes general checklist, the general condition of medical and electrical components, motion and lock check, target to film distance indicator check, field size indication, congruence of light and radiation fields, cross hair centering, focal spot size, exposure consistency, timer accuracy, mA or mAs linearity, kVp linearity, and automatic exposure control.[7]

The image was obtained from a modality, which is a digital radiography system. Then, the image was sent to PACS and AI engine (Manage AI, Internet Thailand Public Company Limited, Thailand) to analyze the results as shown in Figure 1 and the percent below the red box is the accuracy of AI for this radiograph. This program was tested for tuberculosis detection which obtained an accuracy, sensitivity, and specificity of 96, 96, and 95 percent, respectively. The system has detected and characterized the exam for suspected tuberculosis. The result displayed an alert message from the AI engine to PACS with the information, identification, and graphics highlighting abnormalities. The TB cases, which were detected by AI, will be flagged and prioritized for expedited reading in the worklist within 10 seconds. Then, the chest x-ray results from the radiologists (2 and 10 years of clinical experience) and AI program results were compared. The data was analyzed by StatPlus (Build 7.3.3/Core v7.3.32, AnalystSoft Inc., USA). The tuberculosis detection performance was assessed using Receiver Operating Characteristics (ROC) analysis and area under the curve (AUC). The data was validated by calculating the specificity, sensitivity, and positive predictive value (PPV).

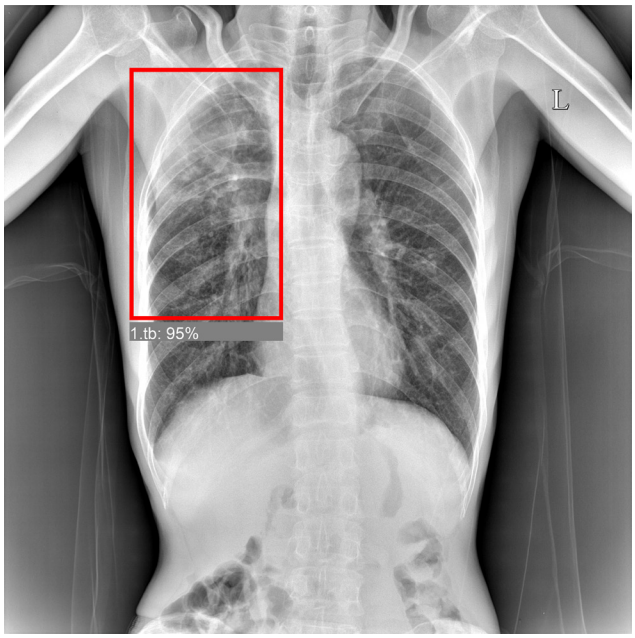

Figure 1. *Result of AI interpretation.*

Results

Quality control of mobile x-ray machines was composed of the following sections. First, the physical test of the machine was passed. The congruence of Source to Image Distance (SID) between the set value and measurement was correlated. The movement and lock system were tested. It can only move up and down and can lock automatically. The light intensity from the x-ray tube was less than 100 lux in every area. Exposure reproducibility was passed because the coefficient of variation (CV) was 0.035 which was within 0.05 limit. Time reproducibility was 0.004% of CV that was within the limit of 5%. Also, time accuracy was passed (within the limit of 10% error).[7] The kVp reproducibility was passed because it is very precise and had no deviation. The kVp accuracy and mAs linearity are still within the limit.

Image quality was passed that included central beam alignment, dynamic range, special resolution, contrast resolution, homogeneity as demonstrated in Figure 2. The misalignment of the light and x-ray field is acceptable (within 2% of SID). When the x-ray machine is checked by testing, it can be used for the examination accurately.

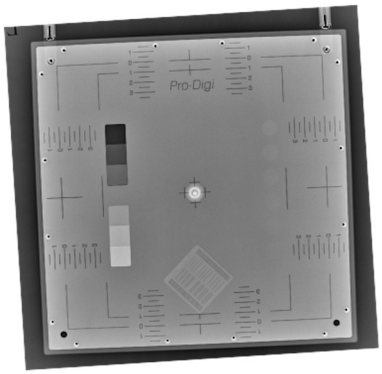

Figure 2. *Image quality of x-ray machine using Pro-Digi, Raysafe.*

The final step was to analyze the data set using the StatPlus program, and the result showed that the AUC was 0.859, as shown in Figure 3. Also, the study demonstrates that the TB interpretation by AI was high specificity (0.995) but low sensitivity (0.722) because the number of tuberculosis cases was small as demonstrated in table 1. Table 2 showed that the Positive predictive value (PPV) was 0.951, which was less than the Negative predictive value (0.963). Therefore, the TB diagnosis by AI is accurate and precise as the gold standard is the radiologist's interpretation.

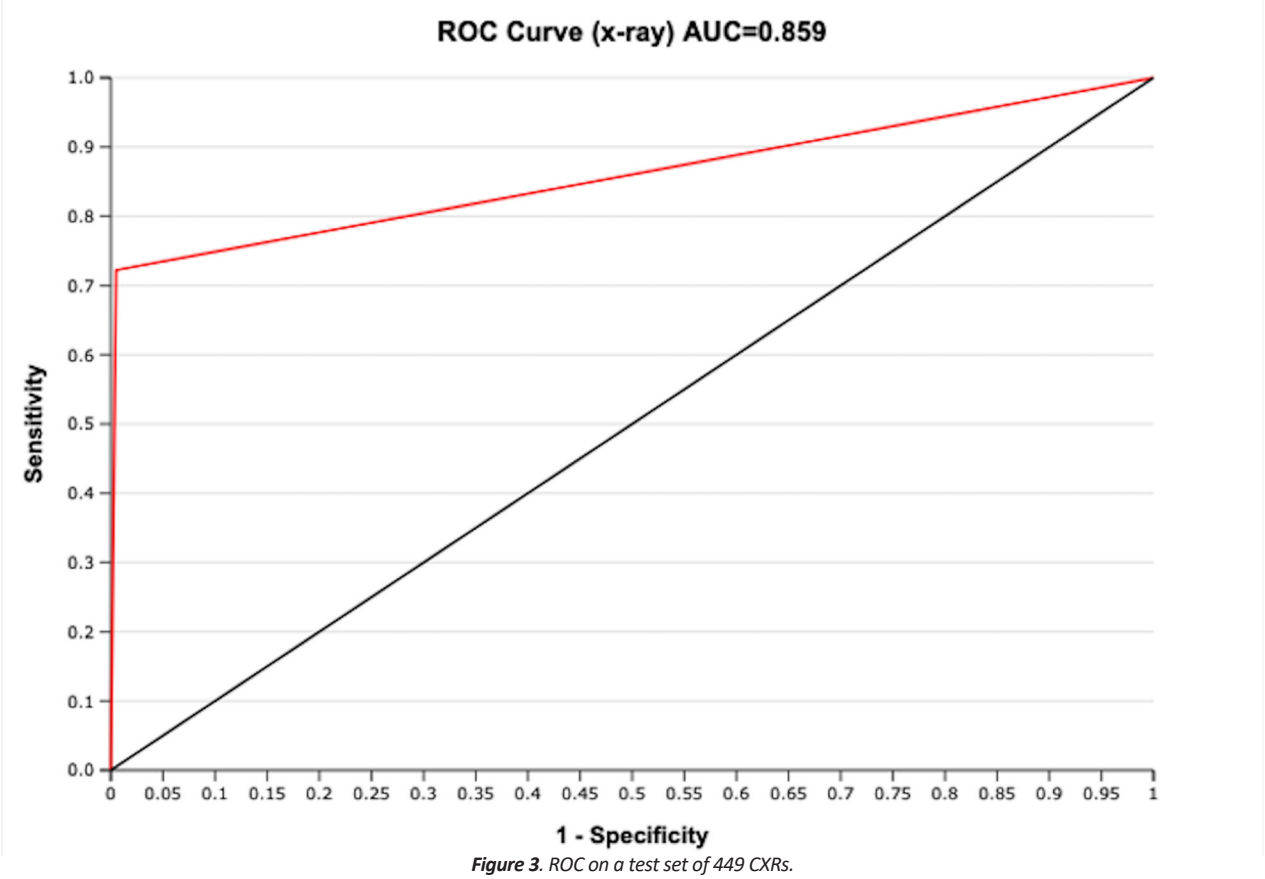

Figure 3. *ROC on a test set of 449 CXRs.*

Table 1 Number of cases in this study.

Result	Number of TB cases	Number of normal cases	Total patient
Radiologist	41 (9.13%)	408 (90.87%)	449
Artificial Intelligence	54 (12.03%)	395 (87.97%)	

Table 2 Performance indices from this study.

	Performance indices
Sensitivity	0.7222
Specificity	0.9949
Accuracy	0.9621
Positive predictive value	0.9512
Negative predictive value	0.9632
True positive	39
True negative	393
False-positive	2
False-negative	15
Positive Likelihood Ratio	142.64
Negative Likelihood Ratio	0.28

Discussion

The radiologists who interpreted chest radiographs have approximately 6 years of experience. From this study, the sensitivity of the AI program was 0.722 and specificity was 0.995. The specificity was higher than sensitivity. Therefore, TB patients will be detected correctly. Area under the curve was 0.859, which is more than the computed aid detection (CAD) (AUC=0.71-0.75).[8] While in other research, Hwang., et al.[9] found that tuberculosis can be detected (AUC=0.988) by using the 450 Korean data sets (300 normal, 150 tuberculosis). The result was excellent because of the validation by a group of thoracic radiologists and a variety of sample sizes. Moreover, Muyoyeta M., et al.[10] found that tuberculosis detection by deep learning (AUC=0.82) was a better result than Computer Aid Detection (AUC=0.71-0.75). In the research of El-Solh A. et al.,[11] an artificial neural network (ANN) was developed using clinical and radiographic information to predict active pulmonary TB and found that the accuracy of the model was 0.923±0.056 from 119 patients formed the validation set. Lakhani P. et al.,[12] studied in AI for Pulmonary Tuberculosis diagnosis from CXR using AlexNet and GoogLeNet. They found that AUC was 0.99 had 97.3% sensitivity, and 100% of specificity. Rapurkar P. et al.,[13] used Deep Learning (CheXNeXt) for atelectasis detection (AUC=0.862), and radiologists' AUC was 0.808. The radiologist spent more time for interpretation. Moreover, Steiner A. et al.,[14] found that software CAD4TB can evaluate chest radiographs from an asymptomatic prison population (AUC=0.75) on the superset of 1321 radiographs in a short time. The finding in this research suggests that radiologist interpretation is still the first choice for accurate chest x-ray diagnosis, but AI can be supported as well as it can interpret chest x-ray faster.

The major limitation of this study is that instead of using mycobacterial culture, we have used the chest x-ray result from a radiologist which we do not know whether the patients have Tuberculosis or not. Also, the artifact in the chest radiograph can lead to AI misinterpretation such as the screen shirt or button which are usually found in the patient's body at the check-up center as shown in Figure 4. Moreover, the number of tuberculosis cases is small, which affects the sensitivity in this study.

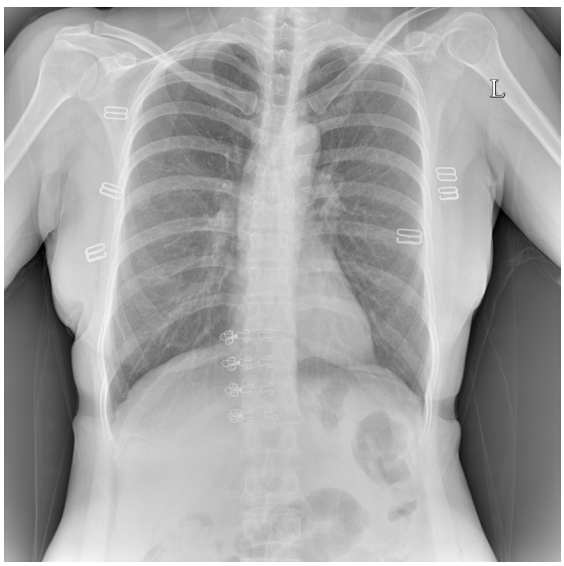

Figure 4*. Chest radiograph with artifacts.*

Conclusion

Artificial intelligence is becoming a healthcare supporter to help radiologists quickly interpret chest radiographs and provide a fast diagnosis. However, some artifacts in the film such as metal artifacts can make AI give misleading results. Therefore, patients should change their dress to a hospital gown and remove the accessories before having a chest x-ray. However, AI is good for TB screening and there are many publications for Covid-19 primary screening but the gold standard is still the swap test and CT scan. AI has many benefits for medical diagnosis, but we still have to do a second check to validate the results.

Conflict of interest

The author declare no conflicts of interest.

Acknowledgments

I would like to thank the faculty's staff for the kind support and health care service center, Faculty of Allied Health Sciences, Thammasat University for making this research a success.

References

[1] World Health Organization. Global tuberculosis report 2020. Geneva: World Health Organization; 2021.

[2] Department of disease control. National tuberculosis control programme guidelines, Thailand, 2018. [in Thai]. Bangkok: 2018; 50-57.

[3] Yu K, Beam A, Kohane I. Artificial intelligence in healthcare. Nat Biomed Eng 2018 October; 2: 719-31. doi: 10.1038/s41551-018-0305-z.

[4] Staff news brief. FUJIFILM showcases AI for digital radiology [Internet]. 2019 Dec [cited 2020 Nov 11]. Available from: https://www.appliedradiology.com/articles/fujifilm-showcases-ai-for-digital radiography

[5] Michelfeit F. Siemens healthineers uses artificial intelligence to take x-ray diagnostics to a new level [Internet]. 2020 Jun [cited 2020 Nov 15]. Available from: https://www.siemens-healthineers.com/press-room/press-releases/ysioxpree-ai-chest.html

[6] Samsung brings together medical imaging and AI for radiologists at RSNA 2018 [Internet]. 2018 Nov [cited 2020 Nov 15]. Available from: https://news.samsung.com/global/samsung-brings-together-medical-imaging-and-ai-for-radiologists-at-rsna-2018

[7] Department of medical sciences, Ministry of public health. Quality standard of diagnostic x-ray systems. 1st ed. Bangkok: The agricultural cooperative federation of Thailand limited; 2015.

[8] Maduskar P, Muyoyeta M, Ayles H, Hogeweg L, Peters L, Ginneken B. Detection of tuberculosis using digital chest radiography: automated reading vs. interpretation by clinical officers. Int J Tuberc Lung Dis 2013; 17: 1613-20.

[9] Hwang S, Kim H, Jeong J, Kim H. A novel approach for tuberculosis screening based on deep convolutional neural networks. Medical imaging 2016: computer-aided diagnosis 2016 Mar; 9785. doi: 10.1117/12.2216198.

[10] Muyoyeta M, Maduskar P, Moyo M, Kasese N, Milimo D, Spooner R, et al. The sensitivity and specificity of using a computer aided diagnosis program for automatically scoring chest X-rays of presumptive TB patients compared with Xpert MTB/RIF in Lusaka Zambia. PLOS ONE 2014 Apr; 9(4): e93757. doi: 10.1371/journal.pone.0093757.

[11] El-Solh A, Goodnough S, Serghani J, Brydon B. Predicting active pulmonary tuberculosis using an artificial neural network. Clinical investigations; chest. 1999 May; 116: 968-73.

[12] Lakhani P, Sundaram B. Deep learning at chest radiography: automated classification of pulmonary tuberculosis by using convolutional neural networks. Radiology. 2017 Aug; 284(2): 574–82. doi: 10.1148/radiol.2017162326.

[13] Rajpurkar P, Irvin J, Ball R, Zhu K, Yang B, Mehta H, et al. Deep learning for chest radiograph diagnosis: A retrospective comparison of the CheXNeXt algorithm to practicing radiologists. PLoS Med. 2018 Nov; 15(11):e1002686. doi: 10.1371/journal.pmed.1002686.

[14] Steiner A, Mangu C, Hombergh J, Deutekom H, Ginneken B, Clowes P, et al. Screening for pulmonary tuberculosis in a Tanzanian prison and computer-aided interpretation of chest X-rays. Public Health Action 2015 Dec; 5(4): 249-54. doi: 10.5588/pha.15.0037.

Journal of Associated Medical Sciences 2021; 54 (3): 48-56

JAMS
Journal of Associated Medical Sciences

Thai-Journal Citation Index Centre (TCI) & ASEAN Citation Index (ACI)

Journal of Associated Medical Sciences

Journal homepage: https://www.tci-thaijo.org/index.php/bulletinAMS/index

Measurement of the distribution of neutrons produced by a 15 MV linear accelerator in a solid water phantom using CR-39 detectors

Kasama Homkhaow[1] Thiansin Liamsuwan[1*] Sawanee Suntiwong[2] Natch Rattanarungruangchai[3] Waraporn Sudchai[3]

[1]Faculty of Medicine and Public Health, HRH Princess Chulabhorn College of Medical Science, Chulabhorn Royal Academy, Bangkok, Thailand
[2]Radiation Oncology Department, Chulabhorn Hospital, Chulabhorn Royal Academy, Bangkok, Thailand
[3]Nuclear Technology Service Center, Thailand Institute of Nuclear Technology (Public Organization), Nakorn Nayok Province, Thailand

ARTICLE INFO

Article history:
Received 2 April 2021
Accepted as revised 27 June 2021
Available online 27 June 2021

Keywords:
CR-39 detector, neutron dosimetry, nuclear track density, high energy photon therapy

ABSTRACT

Background: In high energy photon therapy with >10 MV x-rays, neutrons are produced from photonuclear reactions between high energy photons and high atomic number materials in the treatment head. Although neutron dose is expected to be relatively small compared to the primary photon dose to the target, neutrons have high quality factors that are associated with the increased secondary cancer risk of the treated patient. Due to the attenuation of neutrons by the patient's body, the distribution of neutron doses at different positions in the patient should be determined for the assessment of organ-specific secondary cancer risks.

Objectives: To determine the distribution of neutrons from a 15 MV linear accelerator at different lateral distances from the isocenter and at different depths in a solid water phantom, as a mimic for the patient body.

Materials and methods: The distribution of neutrons was measured with BARYOTRAK CR-39 detectors in term of nuclear track densities in the CR-39 detectors. A half of the detector's surface area was covered with a boron converter and a polyethylene radiator for thermal and fast neutron measurement, while the other half had no boron converter making it only sensitive to fast neutrons. The detectors were placed in a solid water phantom at 0, 5, 10 and 15 cm lateral distances from the isocenter and at 0, 3, 7, 11, 15 and 18 cm depths from the phantom surface. The detectors were irradiated with 15 MV photon beams at 0° gantry angle for the field size of 20x20 cm^2.

Results: The nuclear track density initially increased with depth, reached a maximum at 3 cm depth and decreased with depth beyond the depth of the maximum. The contributions from fast and thermal neutrons at shallow depths were competitive while at large depths most of neutrons became thermalized. The lateral distribution of the track density had a maximum at the central axis. Thermal neutrons were responsible for this behavior. In contrast, nuclear track densities generated by fast neutrons were nearly constant with the off-axis distance.

Conclusion: Nuclear track densities generated by neutrons varied with the depth and the lateral distance from the isocenter. The conversion coefficients from nuclear track density to dose should consider the energy spectrum of neutrons especially at shallow depths.

* **Corresponding author.**
Author's Address: *Faculty of Medicine and Public Health, HRH Princess Chulabhorn College of Medical Science, Chulabhorn Royal Academy, Bangkok, Thailand.*
** **E-mail address:** thiansin.lia@pccms.ac.th
doi: 10.14456/jams.2021.23
E-ISSN: 2539-6056

Introduction

In radiotherapy with high energy photons of >10 MV nominal energy, neutrons are produced from photonuclear reactions between high energy photons and high atomic number materials in the treatment head including primary collimator, target, flattening filter, jaws and shielding materials.[1, 2] Neutron production in the treatment head results in unnecessary radiation exposure to the patient. Although neutron dose is expected to be relatively small compared to the primary dose to the target, neutrons have high quality factors[3] and the exposure of neutrons increases the risk of developing secondary malignancies in the patient.[4] Therefore, neutrons produced by medical linear accelerators operated at energies larger than 10 MV should not be neglected in the radiation protection consideration for radiotherapy patients. Moreover, to determine organ-specific secondary cancer risks, the distribution of neutron doses at different positions in the patient is required.[5]

Previous measurements of photoneutrons from linear accelerators were mostly done in air,[6, 7] on the surface of the patient[8] or on the treatment couch.[9, 10] However, using in-air or surface neutron dose for estimating neutron dose in an organ leads to incorrect dose values because the average neutron energy in air or at the surface could be about 71.4%. different from that found *in vivo*.[11, 12]

In vivo measurements of neutrons are difficult to perform as they are invasive. Therefore, determination of neutron doses in patients receiving radiation therapy are limited to Monte Carlo simulations and in-phantom measurements. In general, the Monte Carlo simulation is considered to be accurate but needs realistic machine modelling and relatively long computational time to produce reasonable results.[13] The machine geometry is sometimes too complex to be modelled with simple mathematical expressions. In that case, the uncertainty related to machine modelling and geometry accuracy effect is not avoidable.[13] Moreover, for events that have relatively low probabilities, for example, neutron generation in photon treatment rooms, a large number of initial particles or radiations need to be simulated to produce dose with acceptable statistical uncertainties. In contrast, in-phantom measurement is easier to perform and mimics the measurement in a patient.

Several groups have performed in-phantom neutron dose measurements. For example, Awotwi-Pratt and Spyrou[14] reported measured neutron dose equivalent as a function of depth and distance from the field edge for 5x5 cm^2, 10x10 cm^2 and 20x20 cm^2 field sizes from a Varian Clinac 2100C linear accelerator operated at 15 MV using bubble detectors. For all field sizes, the neutron dose equivalent was found to maximize at 1 cm depth in a water phantom and at 0 cm distance from field edge, in agreement with d'Errico *et al*.'s experiment performed with an 18 MV linear accelerator at 10x10 cm^2 field size.[15] Yücel *et al*.[16] measured neutron fluxes from an 18 MV Varian Clinac DHX dual energy linear accelerator at 0, 5 and 10 cm depths in a solid water phantom for the field size of 20x20 cm^2 using the foil activation method. The neutron flux was found to maximize at 5 cm depth, providing the maximum neutron dose of about 0.64±0.04 mSv per Gy of photon prescribed dose. Dawn *et al*.[17] measured in-field photoneutron fluences at difference depths in a tissue equivalent phantom irradiated by 15 MV photons from TrueBeam and Novalis Tx linear accelerators for the field size of 30x30 cm^2 using polyallyl diglycol carbonate (PADC) or CR-39 detectors. The fast neutron fluence from both accelerator models had a maximum at the phantom surface and decreased with the depth in the phantom, while the thermal neutron dose peaked at 3 and 6 cm depths for TrueBeam and Novalis Tx, respectively.

Since each neutron detector has different responses to different neutron energy spectra, detector selection should be done appropriately.[18] CR-39 detectors are particularly useful for neutron dose determination in high energy x-ray therapy because they are insensitive to photons, require no electronic equipment, have non-fading signals and are tissue equivalent.[19] When neutrons collide with the polymeric structure of the CR-39 detector, proton and carbon recoils are generated from elastic scattering, inducing latent damage regions.[18] In addition, CR-39 detectors can be modified to detect thermal neutrons by using a converter made of boron (^{10}B) or lithium (^{6}Li) placed on top of the detectors.[20, 21] Neutron dose is converted from nuclear track density obtained by CR-39 measurement using an appropriate calibration coefficient. Since CR-39 detectors have been used for personal dose monitoring for many years[22-24], the calibration of these detectors are usually based on standard neutron sources such as $^{241}Am/Be$ and ^{252}Cf.[25] However, it is not clear whether a calibration coefficient obtained from a standard source is also valid for neutron measurement in a radiation field generated by high energy linear accelerator such as the Varian TrueBeam linear accelerator (Varian Medical System, Palo Alto, CA, USA). This is because a standard source produces a different neutron spectrum than that produced in the treatment room. Thus, converting the nuclear track density generated in the detector to dose by using the calibration coefficient obtained from a measurement with a standard source may provide incorrect neutron dose.

The objective of this work was to determine the distribution of neutrons, in term of nuclear track densities in CR-39 detectors, in a solid water phantom mimicking a patient receiving 15 MV X-rays from the TrueBeam linear accelerator (Varian Medical System, Palo Alto, CA, USA), to be used for determination of location-specific calibration coefficients in conjunction with Monte Carlo simulation (more detail in Discussion). The detectors were placed at different distances from the isocenter and at different depths in the solid water phantom. The relationship between the nuclear track density and the measurement position as well as the distribution of fast and thermal neutrons are presented in this paper.

Materials and methods

CR-39 detectors

The CR-39 detectors used in this study were BARYOTRAK neutron detectors (Nagase Landauer, Ltd., Japan). BARYOTRAK consists of a CR-39 plastic sheet with the dimension of 15.50 mm x 9.34 mm x 0.86 mm. The CR-39 sheet was put into a plastic holder with a half of the surface area covered with a boron converter (Teflon® doped with boron-10) and a polyethylene radiator and the other half with only a polyethylene radiator, as shown in Figure 1. Fast neutrons are detected in both areas covered by the polyethylene radiator through neutron-proton elastic scattering that converts fast neutrons to recoil protons. Since thermal neutrons have relatively low probability of elastic scattering but relatively high probability of neutron capture reaction, the boron converter is used to induce $^{10}B(n,\alpha)^{7}Li$ reaction for thermal neutron detection. Following these interactions, recoil protons and alpha particles produce latent damages in CR-39 sheets that are associated with fast neutrons and thermal neutrons, respectively. Figure 2 shows the conceptual design of the Baryotrak neutron detector.

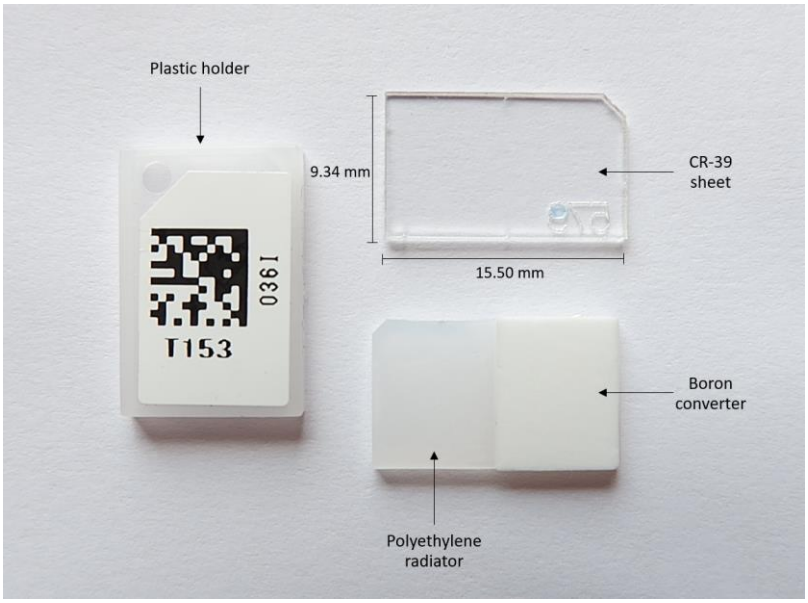

Figure 1. *BARYOTRAK neutron detectors (Nagase Landauer, Ltd., Japan).*

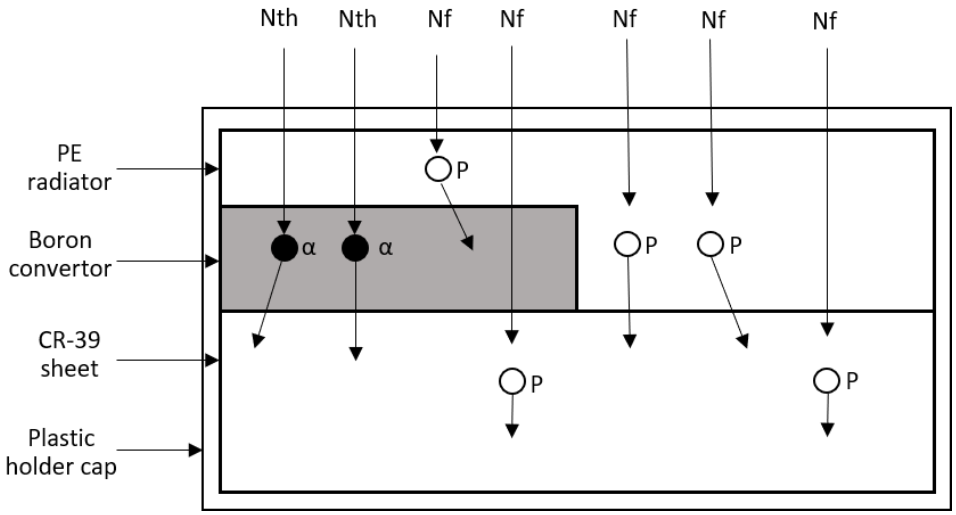

Figure 2. *Neutron detection by BARYOTRAK neutron detectors (side view). Nth: a thermal neutron and Nf: a fast neutron, PE: polyethylene.*

Irradiated CR-39 detectors were etched in a chemical solution of 5.26 M NaOH at a temperature of 72±1 °C for 15 hours and 30 minutes. After the chemical process, tracks produced by the collision of secondary alpha particles or recoil protons on the CR-39 sheets became visible under a microscope. The tracks were discriminated in term of neutron energy (tracks from thermal and fast neutrons) and counted manually using a light microscope (Euromex Microoscopen, Arnhem, Netherland) in an area of 4.5x3 mm^2 of each half of the surface area at a magnification of 400x. The illustration of track counting on the CR-39 detectors can be seen in Figure 3. The number of tracks per square centimeter corresponds to the nuclear track density (tracks/cm^2).

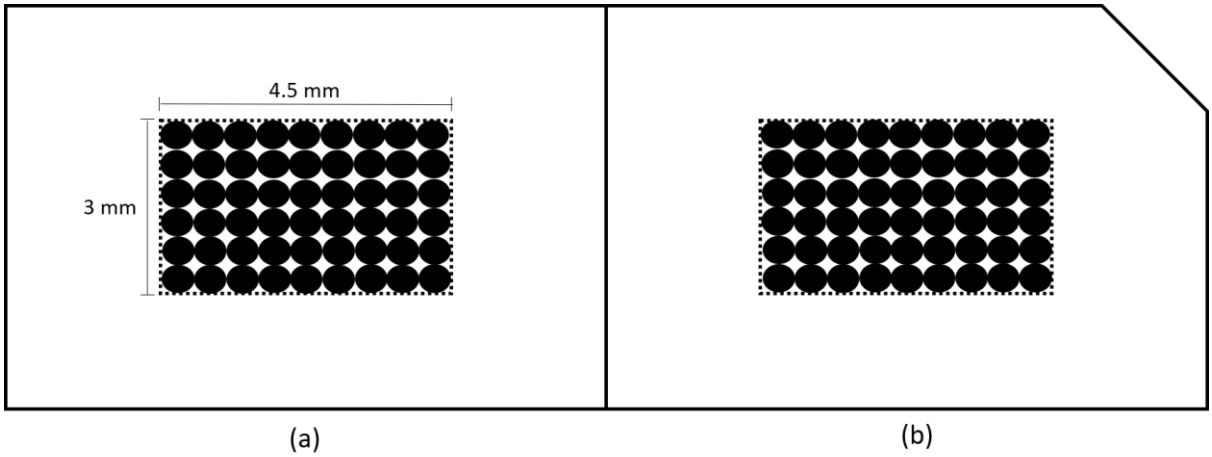

Figure 3. *Illustration of areas used for counting tracks in the CR-39 detectors. The shaded regions are the counting areas, (a): a half of the surface area covered with a boron converter and a polyethylene radiator, (b): the other half of the surface area covered only with a polyethylene radiator.*

Measurement set-up

The CR-39 detectors were placed in a 30x30x22 cm^2 GAMMEX solid water phantom (RMI®, Middleton, WI, U.S.A) at 0, 5, 10 and 15 cm lateral distances from the isocenter in the transverse plane parallel to the treatment couch top and at 0, 3, 7, 11, 15 and 18 cm depths from the phantom surface, as shown in Figure 4. The detectors were sandwiched between boluses, which were used to reduce air gaps between the solid water phantom slabs.

The CR-39 detectors were exposed to the secondary neutron field generated by 15 MV photon beams from the Varian TrueBeam linear accelerator (Varian Medical System, Palo Alto, CA, USA). The irradiation was done at 219.5 MU (2Gy prescribed dose at the isocenter) and the source-to-axis distance (SAD) was 100 cm. The photon beam was delivered to the solid water phantom in one direction (0° gantry angle) with the field size of 20x20 cm^2 at the isocenter. The isocenter was at 11 cm depth from the phantom surface, mimicking the depth representing the average uterine position of patients.[26] The measurement was repeated for 3 times.

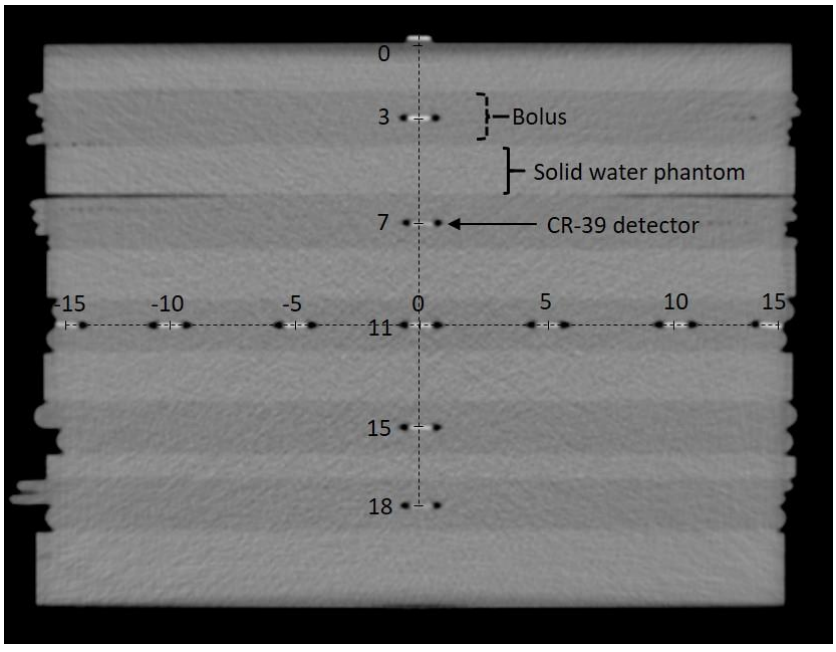

Figure 4. *Placement of CR-39 detectors and boluses (dark grey) in the solid water phantom (light grey) (side view). The scales are in centimeter (cm).*

Results

The microscopic images of tracks in one of the CR-39 detectors after etching are shown in Figure 5. Nuclear tracks generated by thermal neutrons in the detector area covered with the boron converter were larger in size than those produced by fast neutron tracks because thermal neutrons were converted to alpha particles that are heavier than recoil protons converted from fast neutrons. In most cases, tracks were nearly spherically symmetric. However, when a neutron hit the CR-39 detector in the direction that was not perpendicular to the CR-39 detector, a tail of the track could be seen in the microscopic image, as shown in Figure 5c.

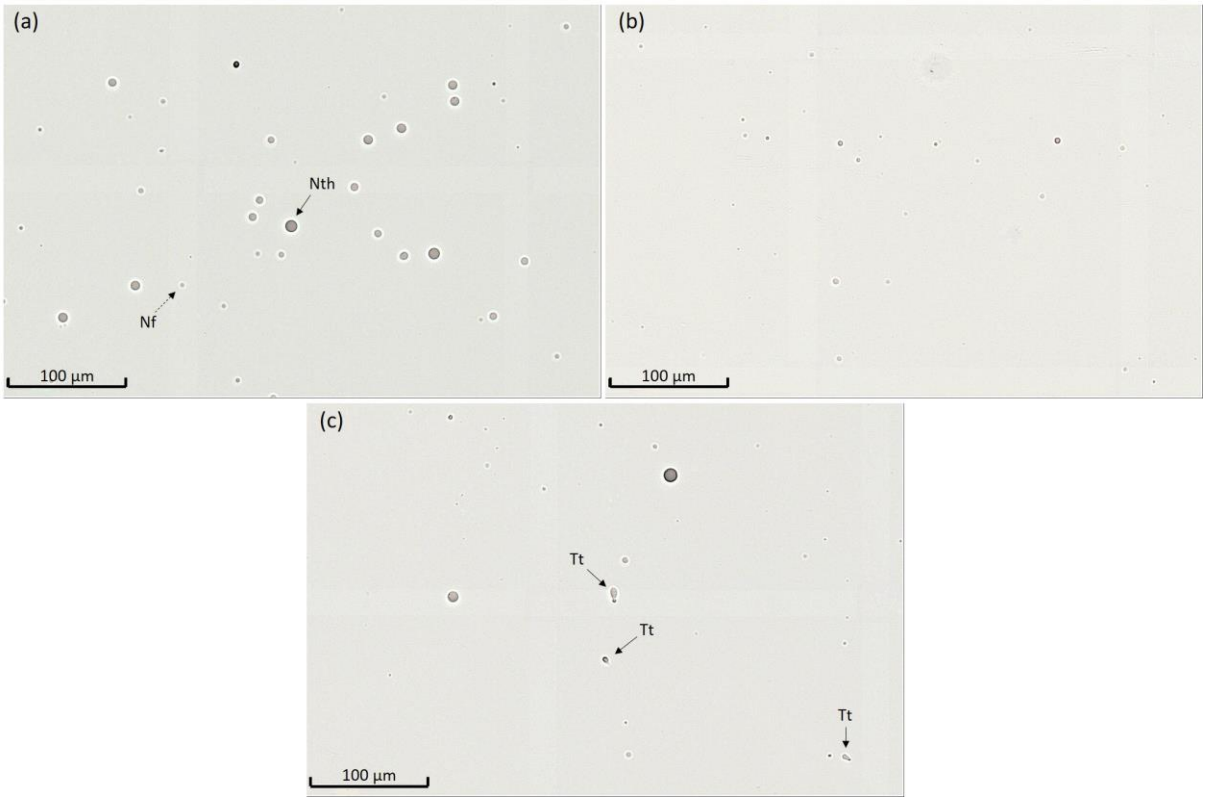

Figure 5*. Microscopic images of tracks obtained from CR-39 measurement. (a): detector area covered with boron converter, (b): other area without boron converter, (c): tracks produced when neutrons hit the CR-39 detector in the directions that were not perpendicular to CR-39 detector, Nth: tracks from thermal neutrons, Nf: tracks from fast neutrons, Tt: track from a neutron hitting the CR-39 detector in the direction that was not perpendicular to CR-39 detector.*

Figure 6 shows the nuclear track density as a function of depth in the solid water. For each measurement, the nuclear track density increased with depth until it reached a maximum at 3 cm depth in the solid water phantom. Beyond the depth of the maximum, track density decreased with depth and was similar to the percentage depth dose of photons. Figure 6 also shows the nuclear track densities induced by thermal neutrons and fast neutrons as functions of depth in solid water phantom. Nuclear track densities induced by fast neutrons maximized at the surface and decreased with the depth in solid water phantom. In contrast, the track densities induced by thermal neutrons, first, increased with the depth until it reached a maximum at a 3 cm depth in solid water phantom. Beyond the depth of the maximum, track densities from thermal neutrons decreased with the depth

Figure 7 shows the lateral distribution of track densities at different distances from the isocenter (at 11 cm depth). The maximum values of track densities were at the center of the radiation field (0 cm distance from isocenter), and the track density decreased when the distance from the isocenter was increased. Moreover, it was found that the track density induced by thermal neutrons maximized at the central axis of the photon beam and rapidly decreased when the distance from the isocenter was increased. In contrast, the track densities from fast neutrons were relatively constant with the distance away from the isocenter.

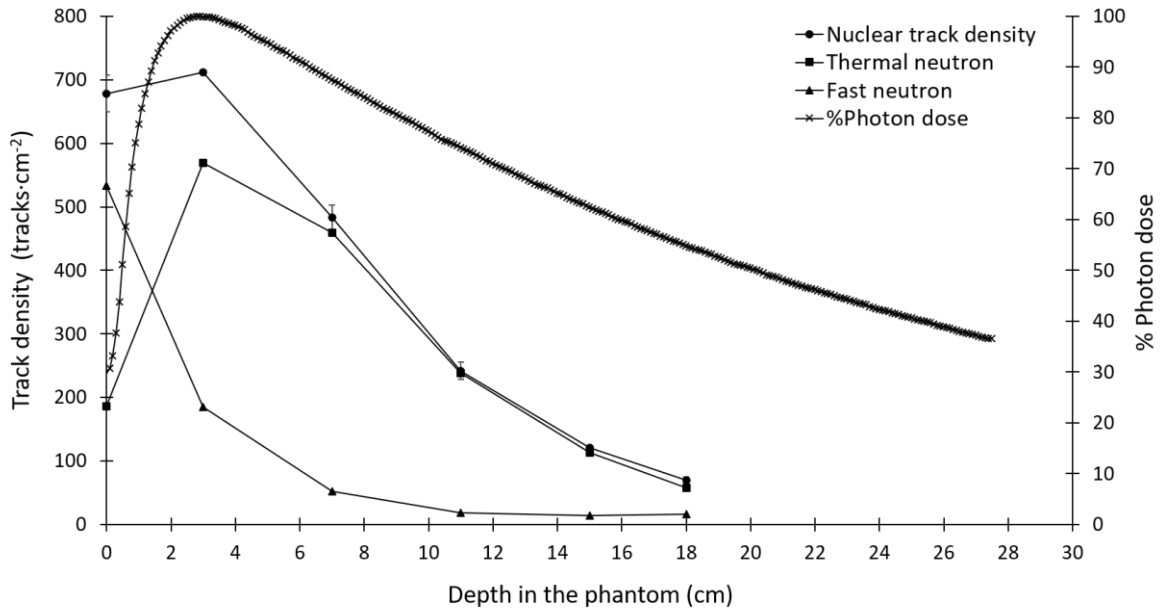

Figure 6. *Nuclear track density as a function of depth in solid water phantom (left ordinate) compared to the photon depth dose distribution (right ordinate).*

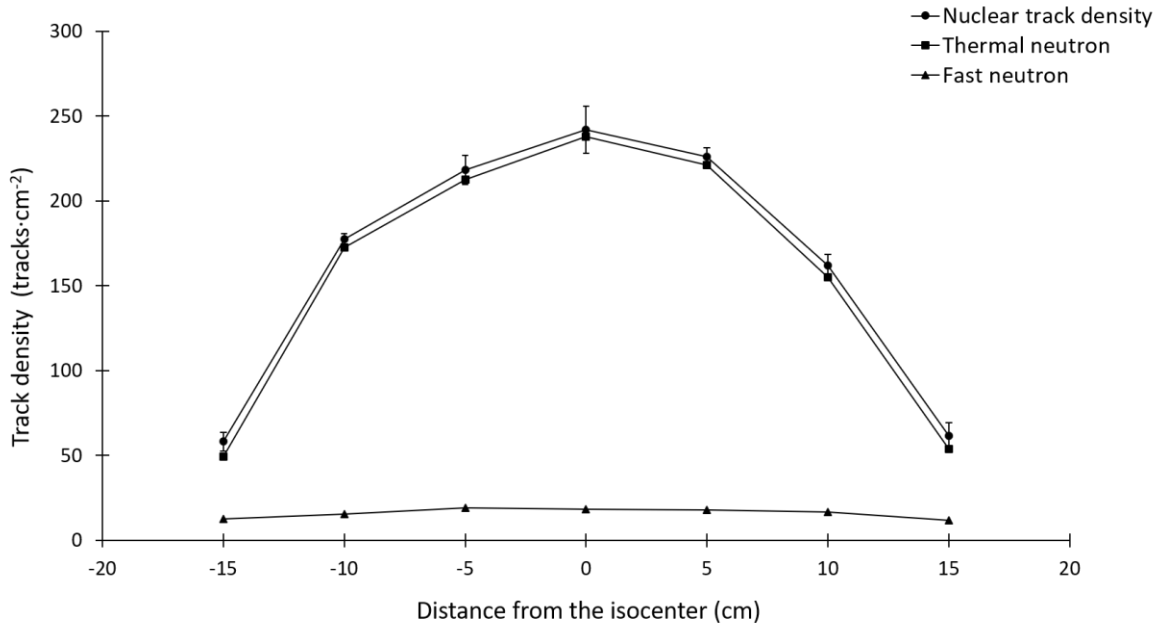

Figure 7. *Lateral distribution of track densities at the isocenter depth (11 cm depth).*

Discussion

In this work, nuclear track densities in CR-39 neutron detectors were measured in a solid water phantom irradiated with 15 MV photon beams from the TrueBeam linear accelerator for the field size of 20x20 cm^2. The nuclear track density is proportional to the number of neutrons hitting the detector per unit area.

From the measurement, it was found that the track density initially increased with depth, reached a maximum at 3 cm depth and decreased with depth beyond the depth of the maximum, in agreement with previous reports.[12, 27, 28] The buildup of the track density arose from the competitive processes between the moderation of fast neutrons from the accelerator head by elastic scattering with hydrogen atoms and the absorption of thermal neutrons.

The nuclear track density as a function of lateral distance from the isocenter showed a maximum at the central axis. The track density induced by thermal neutrons maximized at the central axis and decreased with the distance away from the isocenter while the track density induced by fast neutrons was relatively constant with the off-axis distance. The maximum track density at the central axis indicated that the forward-directed neutrons originated by the highest energy photons were likely to be produced along the central beam axis. Similar observations have been reported by Awotwi-Pratt and Spyrou[14] and Brkić *et al*.[29]

Evaluation of neutron dose from the CR-39 measurement, the track density needs to be converted to neutron dose by using an appropriate conversion coefficient obtained from the measurement in a neutron standard field similar to that present during the detector usage due to the energy dependence of the neutron detectors.[11] The detectors used in this study have been calibrated for personal dose monitoring purposes in term of $H_p(10)$ in standard neutron fields of a bare ^{252}Cf source, a D_2O moderated ^{252}Cf source, an $^{241}Am/Be$ source and a graphite pile moderated ^{252}Cf source (thermal neutrons). However, it is not clear whether $H_p(10)$ measured in the standard sources is valid for neutron measurement in a radiation field generated by the high energy linear accelerator. This is because a standard source produces a different neutron spectrum than that produced in the treatment room. Since standard neutron fields similar to those present in the phantom are not available,[25] neutron dose obtained from a Monte Carlo simulation can be used as the reference dose to evaluate position-specific neutron track density-to-dose conversion coefficients of the CR-39 detector. In the future work, we will perform a Monte Carlo simulation to evaluate the neutron spectra at different positions in the solid water phantom to determine the nuclear track density-to-dose conversion coefficients at different depths and off-axis distances in the phantom.

Conclusion

In the present study, CR-39 detectors were used to measure the distribution of neutrons inside a solid water phantom at different depths and at different lateral distances from the isocenter. The results are presented in term of nuclear track densities, which are related to neutron fluence and neutron doses. It was found that the nuclear track density initially increased with depth and reached a maximum at 3 cm depth in the solid water phantom, beyond the depth of the maximum the nuclear track density decreased with depth. The lateral distribution of nuclear track densities in the isocenter plane (at 11 cm depth) showed a maximum at the central axis and decreased with the off-axis distance. Thermal neutrons were responsible for this behavior. In contrast, nuclear track densities induced by fast neutrons were relatively constant with the off-axis distance. The current study indicated that the contribution of fast and thermal neutrons to total neutron dose varied with the depth in the phantom but only the contribution of thermal neutrons varied with the off-axis distance from the isocenter. The conversion coefficients from nuclear track density to dose should consider the different neutron spectra inside the phantom for the accurate evaluation of neutron doses. The result of this work can be used together with the Monte Carlo simulation to estimate position-specific neutron track density-to-dose conversion coefficients of the CR-39 detector. Such conversion coefficients can be directly used with the CR-39 detector to determine neutron dose in patients or in phantoms with a higher accuracy compared to using conversion coefficients typically obtained from standard measurements.

Conflict of interest

The authors declare that there is no conflict of interest.

References

[1] Kry SF, Bednarz B, Howell RM, Dauer L, Followill D, Klein E, et al. AAPM TG 158: measurement and calculation of doses outside the treated volume from external-beam radiation therapy. Med Phys 2017; 44(10): 391-429. doi: 10.1002/mp.12462.

[2] Biltekin F, Yeginer M, Ozyigit G. Investigating in-field and out-of-field neutron contamination in high-energy medical linear accelerators based on the treatment factors of field size, depth, beam modifiers, and beam type. Phys Med 2015; 31(5): 517-23. doi: 10.1016/j.ejmp.2015.03.015.

[3] Nuclear Regulatory Commission and Department of Veterans Affairs. Neutron quality factor. United States: Oak Ridge Inst. for Science and Education; 1995.

[4] Takam R, Bezak E, Marcu L, Yeoh E. Out-of-field neutron and leakage photon exposures and the associated risk of second cancers in high-energy photon radiotherapy: current status. Radiat Res 2011; 176(4): 508-20. doi: 10.1667/rr2606.1.

[5] Schneider U, Zwahlen D, Ross D, Kaser-Hotz B. Estimation of radiation-induced cancer from three-dimensional dose distributions: Concept of organ equivalent dose. Int J of Radiation Oncology* Biol Phys 2005; 61(5): 1510-5. doi: 10.1016/j.ijrobp.2004.12.040.

[6] Chu W, Lan J, Chao T, Lee C, Tung C. Neutron spectrometry and dosimetry around 15 MV linac. Radiat Meas 2011; 46(12): 1741-4. doi: 10.1016/j.radmeas.2011.06.029.

[7] Montgomery L, Evans M, Liang L, Maglieri R, Kildea J. The effect of the flattening filter on photoneutron production at 10 MV in the Varian TrueBeam linear accelerator. Med Phys 2018; 45(10): 4711-9. doi: 10.1002/mp.13148.

[8] Reft CS, Runkel-Muller R, Myrianthopoulos L. In vivo and phantom measurements of the secondary photon and neutron doses for prostate patients undergoing 18 MV IMRT. Med Phys 2006; 33(10): 3734-42. doi: 10.1118/1.2349699.

[9] Alem-Bezoubiri A, Bezoubiri F, Badreddine A, Mazrou H, Lounis-Mokrani Z. Monte Carlo estimation of photoneutrons spectra and dose equivalent around an 18 MV medical linear accelerator. Radiat Phys Chem 2014; 97: 381-92. doi: 10.1016/j.radphyschem.2013.07.013.

[10] Ipe NE, Roesler S, Jiang S, Ma C, editors. Neutron measurements for intensity Modulated Radiation therapy. Proceedings of the 22nd Annual International Conference of the IEEE Engineering in Medicine and Biology Society (Cat No 00CH37143); 2000: IEEE.

[11] Hälg RA, Besserer J, Boschung M, Mayer S, Clasie B, Kry SF, et al. Field calibration of PADC track etch detectors for local neutron dosimetry in man using different radiation qualities. Nucl Instrum Methods Phys Res, A 2012; 694: 205-10. doi: 10.1016/j.nima.2012.08.021.

[12] Kry SF, Howell RM, Salehpour M, Followill DS. Neutron spectra and dose equivalents calculated in tissue for high-energy radiation therapy. Med Phys 2009; 36(4): 1244-50. doi: 10.1118/1.3089810.

[13] Seco J, Verhaegen F., editors. Monte Carlo techniques in radiation therapy. Florida: CRC press; 2013.

[14] Awotwi-Pratt J, Spyrou N. Measurement of photoneutrons in the output of 15 MV varian clinac 2100C LINAC using bubble detectors. J Radioanal Nucl Chem 2007; 271(3): 679-84. doi: 10.1007/s10967-007-0325-8.

[15] d'Errico F, Nath R, Tana L, Curzio G, Alberts WG. In-phantom dosimetry and spectrometry of photoneutrons from an 18 MV linear accelerator. Med Phys 1998; 25(9): 1717-24. doi: 10.1118/1.598352.

[16] Yücel H, Çobanbaş İ, Kolbaşı A, Yüksel AÖ, Kaya V. Measurement of photo-neutron dose from an 18-MV medical linac using a foil activation method in view of radiation protection of patients. Nucl Eng Technol 2016; 48(2): 525-32. doi: 10.1016/j.net.2015.11.003.

[17] Dawn S, Pal R, Bakshi A, Kinhikar R, Joshi K, Jamema S, et al. Evaluation of in-field neutron production for medical LINACs with and without flattening filter for various beam parameters-Experiment and Monte Carlo simulation. Radiat Meas 2018; 118: 98-107. doi: 10.1016/j.radmeas.2018.04.005.

[18] Farhood B, Ghorbani M, Goushbolagh NA, Najafi M, Geraily G. Different methods of measuring neutron dose/fluence generated during radiation therapy with megavoltage beams. Health Phys 2020; 118(1): 65-74. doi: 10.1097/HP.0000000000001130.

[19] Kumar V, Sonkawade R, Dhaliwal A. Optimization of CR-39 as neutron dosimeter. Indian J Pure Appl Phys 2010; 48(7): 466-9.

[20] Oda K, Miyake H, Michijima M. CR39-BN detector for thermal neutron dosimetry. Nucl Sci Tech 1987; 24(2): 129-34. doi: 0.3327/jnst.24.129

[21] Mameli A, Greco F, Fidanzio A, Fusco V, Cilla S, D'Onofrio G, et al. CR-39 detector based thermal neutron flux measurements, in the photo neutron project. Nucl Instrum Methods Phys Res Section B: Beam Interactions with Materials and Atoms 2008; 266(16): 3656-60. doi: 10.1016/j.nimb.2008.05.122.

[22] García M, Amgarou K, Domingo C, Fernández F. Neutron response study of two CR-39 personal dosemeters with air and Nylon converters. Radiat Meas 2005; 40(2-6): 607-11. doi: 10.1016/j.radmeas.2005.04.017.

[23] Pal R, Nadkarni VS, Naik D, Beck M, Bakshi AK, Chougaonkar MP, et al. Development and dosimetric characterization of indigenous PADC for personnel neutron dosimetry. Nucl Technol Radiat Prot 2015; 30(3): 175-87. doi: 10.2298/NTRP1503175P.

[24] Romero-Expósito M, Martínez-Rovira I, Domingo C, Bedogni R, Pietropaolo A, Pola A, et al. Calibration of a Poly Allyl Diglycol Carbonate (PADC) based track-etched dosimeter in thermal neutron fields. Radiat Meas 2018; 119: 204-8. doi: 10.1016/j.radmeas.2018.11.007.

[25] Thomas D, Bedogni R, Méndez R, Thompson A, Zimbal A. Revision of ISO 8529—reference neutron radiations. Radiat Prot Dosim 2018; 180(1-4): 21-4. doi: 10.1093/rpd/ncx176.

[26] Oonsiri P, Vannavijit C, Wimolnoch M, Suriyapee S, Saksornchai K. Estimated radiation doses to ovarian and uterine organs in breast cancer irradiation using radio-photoluminescent glass dosimeters (RPLDs). J Med Radiat Sci 2020; 68: 167-174. doi: 10.1002/jmrs.445.

[27] Rezaian A, Nedaie HA, Banaee N. Measurement of neutron dose in the compensator IMRT treatment. Appl Radiat Isot 2017; 128: 136-41. doi: 10.1016/j.apradiso.2017.06.013.

[28] Martinez-Ovalle S, Barquero R, Gomez-Ros J, Lallena A. Neutron dose equivalent and neutron spectra in tissue for clinical linacs operating at 15, 18 and 20 MV. Radiat Prot Dosim 2011; 147(4): 498-511. doi: 10.1093/rpd/ncq501.

[29] Brkić H, Ivković A, Kasabašić M, Sovilj MP, Jurković S, Štimac D, et al. The influence of field size and off-axis distance on photoneutron spectra of the 18 MV Siemens Oncor linear accelerator beam. Radiat Meas 2016; 93: 28-34. doi: 10.1016/j.radmeas.2016.07.002

Journal of Associated Medical Sciences 2021; 54 (3): 57-65

JAMS
Journal of Associated Medical Sciences

Thai-Journal Citation Index Centre (TCI) & ASEAN Citation Index (ACI)

Journal of Associated Medical Sciences

Journal homepage: https://www.tci-thaijo.org/index.php/bulletinAMS/index

Effect of Thai traditional play protocol on working memory and inhibitory control in children with attention-deficit/hyperactivity disorder

Krongporn Chinchai **Sarinya Sriphetcharawut***

Occupational Therapy Department, Faculty of Associated Medical Sciences, Chiang Mai University, Chiang Mai Province, Thailand

ARTICLE INFO

Article history:
Received 9 June 2021
Accepted as revised 23 June 2021
Available online 29 June 2021

Keywords:
Executive functions, working memory, inhibitory control, school-aged children with ADHD, and Thai traditional play

ABSTRACT

Background: Children with attention-deficit/hyperactivity disorder (ADHD) commonly have problems with executive functions (EFs), especially working memory and inhibitory control. There are a growing number of appropriate EF interventions for children with ADHD. Since all aspects of occupational functioning can be affected, occupational therapists have much to offer in providing interventions for school-aged children with ADHD to improve their executive function skills.

Objectives: The aim of this research was to examine the effects of Thai traditional play protocol on working memory and inhibitory control in children with ADHD.

Materials and methods: The study was conducted with a one group-pretest-posttest research design. Seven school-aged children with ADHD, aged between 8 and 9 years with T-scores ≥ 65 on the Behavioral Rating Inventory of Executive Function (BRIEF), Parent Form: Thai version, participated in this study. The Thai traditional play protocol was designed and developed by researchers. Twenty Thai traditional play activities that had cognitive challenges focusing on working memory and inhibitory control skills were selected and analyzed. Self-regulatory strategies, heavy work activities, and parent education were also implemented. Children with ADHD participated in a 24-session protocol, across 8 weeks with 3 sessions per week, lasting 60 minutes per session. An outcome measure was the Stroop Color and Word Test (SCWT): Children Edition. Data was analyzed using descriptive and non-parametric statistics.

Results: By using the Wilcoxon Signed-Rank Test, a comparison of SCWT scores between before and after receiving a protocol showed a statistical difference of $p<0.05$ in working memory, whereas no statistically significant difference was found in inhibitory control ($p>0.05$).

Conclusion: The findings demonstrated the positive effect of Thai traditional play protocol on working memory in children with ADHD. Occupational therapists can apply this protocol as a prototype for planning intervention focusing on working memory for school-aged children with ADHD.

* **Corresponding author.**
Author's Address: *Occupational Therapy Department, Faculty of Associated Medical Sciences, Chiang Mai University, Chiang mai Province, Thailand.*
** **E-mail address:** sarinya.sri@cmu.ac.th
doi: 10.14456/jams.2021.24
E-ISSN: 2539-6056

Introduction

Attention-Deficit/Hyperactivity Disorder (ADHD) is one of the most common neurodevelopmental disorders found in children, with its main symptoms being attention deficit, hyperactivity, and impulsiveness that can potentially affect emotional, behavioral, educational, and social development.[1] Moreover, it has been found that ADHD often causes deprivation of group activities and separation from friends.[2] Therefore, ADHD may cause children to struggle with school, social, and home activities. Additionally, ADHD is associated with executive function deficits, especially impaired working memory and inhibitory control.[3-4] According to Diamond[5], executive functions are a higher brain function that can help control emotions and behaviors. Working memory, inhibitory control and cognitive flexibility are the basis of EFs that underpin goal-directed behaviors, and lead to the development of metacognitive ability.[3,5]

Working memory is the ability to process and remember information and it is necessary for a number of everyday functions as well as for academic performance.[6-7] Children with working memory problems may not be able to complete a task with multiple steps and are often reported as being easily distracted and forgetful, often missing details about instructions or forgetting instructions, and they lose their belongings easily.[3,5,8] Inhibitory control is the ability of a child to withhold and think before acting and being able to regulate emotions and behaviors in appropriate and/or effective ways, as well. Children with ADHD who have deficient inhibitory control often have difficulties in controlling themselves, so they are often reported as being unaware that they are bothering others.[9-10] These types of children have difficulty controlling emotions such as sadness, frustration, and regret are often prone to display outbursts due to these emotional triggers.[10]

Because of their poor executive functions, school-aged children with ADHD face more difficulties with daily activities than typically developed children of the same age.[10] Furthermore, EFs in childhood can predict adult health and well-being outcomes, such as physical health, substance dependency, wealth, and criminality independent of intelligence level and social class.[11] Furthermore, both working memory and inhibitory control skills are crucial for children with ADHD to effectively perform and participate in everyday tasks as well as academic performance. Thus, the appropriate assistances needed to allow these skills to emerge must be provided and it is necessary to ensure that children will have the opportunities to transfer and generalize these skills to their real-world contexts.[12] Research shows that there is efficacy of positive outcomes of specific interventions, such as computerized training, non-computerized games, aerobics, martial arts, yoga, mindfulness, and certain school curricula, that can help children with executive function deficits to gain better performance skills.[13-15] An occupational therapist is one member of a multidisciplinary team who can help children with ADHD improve certain skills, such as the ability to do daily occupations,[16] motor coordination,[17] self-regulation,[18] and executive function abilities.[19] For executive function interventions, an occupational therapist will help to identify the specific EF skills that a child has challenges with and can enhance the relevant skills required for executive functioning in the performance of daily life activities.

It has been suggested that participating in physical activities such as aerobic exercise and yoga; organized sports activities such as soccer; and traditional marital arts such as Tae Kwon Do with repeated practice and constantly challenging executive functions are crucial for EFs.[14-15,20] It is quite clear that the significant effects of using physical activities, organized sport activities, and martial arts with cognitive challenges on EFs are substantiated. Once these challenges are embraced, the children's attention span, working memory, perseverance, flexibility, creativity, emotional, and behavioral control are improved.[13,21-22] This emerging data is promising for school-aged children with ADHD, as these activities require children to practice by the rules, regulate their own emotions and behaviors, adapt and display flexibility toward peers' behaviors and actions, and must monitor their own performance. However, not all of them are feasible or appropriate for some children with ADHD. Furthermore, EFs can be fostered or hindered by many factors, such as a child's stress levels, family structure, and educational opportunities.[23]

As Thai traditional play activities involve body movement and cognitive training, they can be used to practice both cognitive and physical skills. Thai traditional play refers to traditional games for children and adults that are played for enjoyment, including games with or without rules, and games with songs and without songs.[24] Furthermore, Thai traditional play has been manifested as a group game that requires players to interact in groups and to develop social skills. While playing, children are allowed to learn to control themselves both emotionally and behaviorally.[25] Recent evidence has shown that inhibitory control based on Thai traditional game training program in elementary school students was effective in enhancing inhibitory control among elementary school students.[26] These findings suggest that Thai traditional play could be beneficial to enhance EFs in school-aged children. Therefore, Thai traditional play activities that employed working memory and inhibitory control were selected, analyzed, and applied in the present study.

Educating parents and teachers about the symptoms of ADHD, understanding of the deficits, and learning how to deal with disruptive behaviors is also a key in helping children with ADHD.[27] Previous studies of executive function training for children with ADHD revealed the significant outcomes of parental involvement in interventions on the improvement of working memory, inhibitory control, and planning and organizing skills in children.[28-29]

Children with ADHD frequently fail in proper self-regulation. Therefore, teachers and parents often reported that children are inattentive, hyperactive, and impulsive. Learning new skills that require working memory and inhibitory control skills became problematic because children with ADHD cannot control themselves enough to focus at length on the task at hand.[30] Students with ADHD are often described by teachers as getting easily distracted by peers, being fidgety, or calling out answers and commenting without permission.[31]

Children with ADHD have diminished self-awareness and have less self-monitoring skills than children without ADHD.[32] Since the self-regulatory shortfalls in children with ADHD can impact occupational functioning, it is important to help them possess optimal levels of arousal as well as demonstrate well-organized behaviors, when engaging in daily tasks. Self-regulatory strategies and sensory-based activities, such as heavy work activities[33] are commonly used in helping children with ADHD to be calm and focused.[34] Occupational therapists use self-regulatory strategies by starting to teach a child to identify his or her own arousal level and then guiding the child to choose appropriate sensory strategies to adjust arousal level to meet environmental demands.[35] Heavy work activity refers to a type of sensory-based activity that typically involves pushing, pulling, squeezing, carrying, and lifting heavy objects or items.[35] The research found that heavy work activities can help children to regulate their sensory needs and to adapt their arousal to an optimal level. For instance, they can learn to stay still and sit in a chair for longer durations[36-37] and display improved selective attention.[34]

Based on a review of previous studies, we proposed to develop and use Thai traditional play protocol (targeting physical activities, cognitive challenges focusing on working memory and inhibitory control training, self-regulation strategies, heavy work activity and parent education) as an intervention to improve working memory and inhibitory control for Thai school-aged children with ADHD. Thus, the objective of this study was to examine the effectiveness of Thai traditional play protocol on working memory and inhibitory control in school-aged children with ADHD. In this sense, it was hoped that examining its effect on children with ADHD may lead to an evidence-based intervention that helps broaden the treatment options for this population

Materials and methods

Study design

This study was a single group, pretest-posttest research design with an aim to examine the effectiveness of Thai traditional play protocol on working memory and inhibitory control in school-aged children with ADHD.

Participants

Seven children with ADHD who were studying during the 2020 academic year at Ban Rim Tai School, Mae Rim District, Chiangmai Province, Thailand, were selected using purposive sampling. Their caregivers were also asked to participate in this study. The inclusion criteria for children were as follows: 1) being able to communicate with fluent Thai, 2) being diagnosed with ADHD by a pediatrician and/or a child and adolescent psychiatrist, 3) having no other developmental problems such as intellectual disability, autistic spectrum disorder, or cerebral palsy, 4) having T-scores of ≥ 65 on the Behavioral Rating Inventory of Executive Function (BRIEF), Parent Form: Thai version that presented EFs deficit, and 5) having obtained informed signed by their parents before participating in the study. All caregivers were required to meet the following inclusion criteria: 1) being able to communicate with fluent Thai, 2) haven taken care of children for more than 6 months, and 3) providing informed signed consent before participating in the study. Ethical approval for the study was obtained from the Ethical Review Committee for Research in Humans, Faculty of Associated Medical Sciences, Chiang Mai University (Ref. no AMSEC-62FB-003).

Measurements

Two instruments were used in data collection, including the Behavioral Rating Inventory of Executive Function (BRIEF), Parent Form: Thai version and the Stroop Color and Word Test (SCWT): Children Edition.

The BRIEF is a rating scale for parents and teachers of school-aged children (aged between 5-18 years) to assess everyday behaviors associated with executive functions in the home and school settings. There are two forms, including the Parent Form and Teacher Form. Each form contains a total of 86 questions, and it takes about 10-15 minutes to complete. The BRIEF has sound psychometric properties, with high test–retest reliability (r=0.82 for parents and r=0.88 for teachers), and internal consistency score of 0.80-0.98.[38] This tool has proven to be sensitive to EF impairment in ADHD, oppositional defiant disorder (ODD) and autism spectrum disorders.[38-40] In this study, the Behavioral Rating Inventory of Executive Function (BRIEF), Parent Form: Thai version was used to screen whether a child had executive function problems. A cutoff T-score of ≥65 was used as the threshold for impairment in executive functioning.[38]

The SCWT: Children Edition was developed and designed by Golden *et al*.[41] to assess flexibility, inhibitory control, and working memory for children aged 5-14 years. The assessment tool includes 3 subtests: Word Test (W), Color Test (C), and Color-Word Test (CW). During testing, the participants are asked to read the names of colors printed in black ink for testing their abilities in Word Test (W), name different colored patches for evaluating their abilities in Color Test (C) and read the names of colors printed in various colors for the Color-Word Test (CW). Each word was printed inconsistently in colored ink, for instance, the word "red" was printed in green ink. When testing, the evaluator observes how quickly and accurately the subject responded, and how many words and colors the children could read in 5 minutes. The CW score shows ability in flexibility and working memory. An increased CW score shows higher working memory and flexibility performance, and the interference score shows the ability of inhibitory control. A decreased interference score shows higher inhibitory control performance. Psychometric property of the SCWT has shown excellent test- retest reliability (r=0.86 for Word Test, r=0.82 for Color Test, and r=0.83 for Color-Word Test).[41]

Intervention

The Thai traditional play protocol on working memory and inhibitory control in children with ADHD was developed by the researchers. The protocol was comprised of two main parts: (1) indirect intervention, in which caregivers of children with ADHD participated in a one-hour session of parent education with the aim to enhance caregivers' knowledge and understanding of the executive functions of school-aged children, especially in

working memory and inhibitory control. Caregivers were also required to acquire and gain knowledge about the symptoms of ADHD, its impacts, and behavioral management strategies; and (2) direct intervention, in which two occupational therapy graduate students, including the first author led twenty-four sessions, 60 minutes per session, three sessions a week for 8 consecutive weeks for children with ADHD (2 adults, 7 students). Duration and frequency of intervention were designed based on the outcomes of previous studies of Thai traditional play activity and heavy work activity[29,42] and in conjunction with the recommendations of Diamond *et al*. [13] in which the appropriate frequency in improving executive function must be more than two times per week for group therapy.

Direct intervention included three parts: self-regulatory strategies, heavy work activities, and Thai Traditional play activities.

In this study, self-regulatory strategies were developed by applying sensory integration knowledge[33] and were implemented before children began to engage in Thai traditional play activities. At first, children were asked to look at the self-regulation visual tool which contained a set of 3 pictures, including a sloth that appeared slow and inactive, a man appearing calm and productive, and a running tiger that was fast and hyper-energetic. Each picture represented a different state of arousal and feeling. Children chose one picture at the beginning of the session and stuck it on the board next to their names. After they finished playing Thai traditional play activities, they chose a picture again to indicate their arousal levels as well as feelings. Each child was asked to explain how he felt in relation to a picture he chose, and then was provided feedback regarding his performance during play.

Heavy work activities such as animal walks, jumping on a trampoline, weightlifting with a ball, and deep pressure activity were used in each intervention session to calm and organize children's behaviors.[34, 43] As a good sensory strategy that can provide proprioceptive input to calm and organize the brain,[36] children with ADHD in this study became involved with heavy work activities throughout the session,[34,44] especially prior to Thai traditional play activities. It was hoped that these activities could lead to organized behaviors and optimal learning.

Thai traditional play activities were chosen and analyzed by using the principle of executive function training as suggested by Diamond,[18] with the purpose to promote working memory and inhibitory control. Since there were many children activities that were categorized as Thai traditional games, key selection criteria were set. The researchers chose activities that presented actions and movements, had poems, lyrics, and songs that required children to memorize and act, be playful, had rules to follow and respond, allowed to play in a group/ team, and required repeated practice for skill acquisition. Furthermore, they must be age-appropriate, safe, and fun. For example, when children played "Ngoo Kin Hang or Tail-Eating Snake", they would play in a group. Two players were signified as a mother snake and a father snake. The rest of children acted as baby snakes. The aim of this game was for a mother snake to protect her baby snakes from being outwitted by a father snake. Baby snakes lined up behind a mother snake and tried to walk or run as quickly as possible to avoid being seized by a father snake. Children were expected to memorize lyrics, planned their actions according to their roles. In order to help children to understand the rules as well as how to play games, they had a chance to try out in advance of real games. Being able to memorize lyrics, sing, and perform movements accurately and appropriately demonstrated the ability of working memory, meanwhile inhibitory control abilities were observed in being able to follow the rules and to control their attention and behaviors, such as not running away from a mother snake and other baby snakes, staying in the playing area, waiting until a whistle signal was sounded.

After receiving feedback and recommendations from the thesis advisor (the second author), the content validity was examined. In this process, the Thai traditional play activities were examined by three experts including, one occupational therapy lecturer with more than 5 years of teaching experience in pediatric occupational therapy, one occupational therapist with professional experience in using sensory integration, and one university lecturer with research experience in using Thai traditional play to enhance executive function in school-aged children. Consequently, 20 activities were selected with the average index of item-objective congruence (IOC) at 0.91 which indicates a very good content validity.[45]

Data collection schedule

For the indirect intervention, the first author provided a one-hour session of parent education to caregivers. Apart from knowledge and understanding of the executive functions of school-aged children and ADHD symptoms and its impact, the Thai traditional play protocol was also introduced and explained in terms of how this protocol was implemented and its expected benefits. This was conducted one week before the pre-test at Ban Rim Tai School, Chiangmai Province.

After the completion of parent education, caregivers were asked to fill out the BRIEF. Data obtained from the BRIEF was interpreted by an occupational therapy graduate student who was formally trained in the proper administration of this battery. This graduate student did not get involved in providing the intervention protocol. Seven children who had T-scores of ≥65 on the BRIEF indicating having executive function deficits were chosen to receive the direct intervention from two occupational therapy graduate students, including the first author. These two graduate students worked together to understand the protocol, plan the intervention sessions, administrate the direct intervention to children with ADHD, record children's performance and behaviors, and review progress. They provided the protocol to seven children with ADHD at Ban Rim Tai School for a period of 8 weeks, three times per week, one hour each time.

Pre- and post-test data was collected within a 1-day timeframe immediately before and immediately after the study by a clinical psychologist who was trained in the proper administration of the SCWT. The Color-Word (CW) score and the Interference score were recorded and then interpreted. In order to certify the accuracy of reporting

and scoring, both researchers checked and reviewed all data obtained from every step of the data collection process.

Statistical analysis

Demographic characteristics of children with ADHD were calculated using descriptive statistics. The comparisons of the SCWT scores at pre- and post-intervention were analyzed using the Wilcoxon Signed Ranks Test. The level of statistical significance was set at 0.05. All statistical analyses were conducted using SPSS statistical package.

Results

All children completed the study successfully and they were eligible for data analysis. As shown in Table 1, all of them were boys and most of them studied in Grade 2.

Table 1 Demographic data of children with ADHD (n=7).

Demographic data	Variables	Numbers (%)
Gender	Boy	7 (100)
	Girl	0 (0)
Age (years)	8-9	7 (100)
Class level	Grade 1	1 (14.30)
	Grade 2	5 (71.40)
	Grade 3	1 (14.30)

Since the Color-Word Test scores reflected the ability of working memory and the Interference Test scores represented the ability of inhibitory control, the results also showed that participants' working memory and inhibitory control scores increased after receiving the protocol, as shown in Table 2.

Table 2 Median, quartile deviation (Q.D.), minimum and maximum scores of working memory and inhibitory control, before and after receiving the intervention protocol (n=7).

Variables	Pre-test				Post-test			
	Median	Q.D	Min	Max	Median	Q.D	Min	Max
Working memory (Color Word Test)	21	3	17	21	25	3.5	22	31
Inhibitory control (Interference Test)	-14	5	-24	-5	-18	4	-26	-1

As displayed in Table 3, it was found that children's level of performance in working memory after receiving the protocol had changed. There was an increased number of children in the average (A) in the post-test category. It was also impressive that there was one child identified in the high average (HA) level in the post-test category that was not labeled as such before intervention.

Table 3 Comparison of performance level in working memory and inhibitory control, before and after receiving the intervention protocol (n=7).

Variables	Level of performance							
	Pre-test Numbers (percentage)				Post-test Numbers (percentage)			
	HA	A	BA	SI	HA	A	BA	SI
Working memory (Color Word Test)	0 (0)	2 (28.57)	4 (57.14)	1 (14.28)	1 (14.28)	5 (71.42)	1 (14.28)	0 (0)
Inhibitory control (Interference Test)	1 (14.28)	6 (85.71)	0 (0)	0 (0)	1 (14.28)	6 (85.71)	0 (0)	0 (0)

Note: HA: high average, A: average, BA: below average, SI: severely impaired

The results showed that scores of working memory at post-intervention were significantly higher than those at pre-test ($p<0.05$) and no statistically significant difference was found in inhibitory control ($p>0.05$), as shown in Table 4.

Table 4 Comparison of working memory and inhibitory control in children with ADHD, before and after receiving the intervention protocol (n=7).

Variables	Mean Rank	Z	Asymp. Sig. (2-tailed)
Working Memory (Color Word Test)	4.0	-2.366	0.018*
Inhibitory Control (Interference Test)	3.0	-0.318	0.750

*$p<0.05$

Discussion

Working memory and inhibitory control in this study were measured by the Color-Word Test and Interference Test of the SCWT, respectively. Results showed that working memory of children with ADHD increased significantly from pre-intervnetion to post-intervention ($p<0.05$). However, scores in inhibitory control of these children between pre-intervnetion and post-intervention was not significantly different ($p>0.05$). Additionally, as displayed in Table 3, it was found that children's level of performance in working memory after receiving the protocol had changed. There were an increasing number of children in the average (A). It was also notable that there was one child identified in the high average (HA) level after receiving the protocol.

The results from this study indicated that the Thai traditional play protocol has potential as a promising intervention for school-aged children with ADHD who had difficulties in executive functioning on working memory. Thai traditional play activities were properly designed to target working memory for children with ADHD. As Baddeley pointed out, short-term memory normally disappears quickly, with the exception of when being repeatedly memorized.[46-47] This process that is a complex operation performed by the central executive is the core of working memory.[47-48] As explained earlier in terms of how the protocol was designed in the intervention section, children were allowed to practice poems, songs, and rhymes at least 3-4 times until they could sing along, and then they were taught to remember movements that were required for each activity. The fundamental gestures for each part of the songs were demonstrated by the researcher (the first author) and her assistant. Both songs and movements were considered as task-relevant information for children. Furthermore, the opportunities to perform repetition on practice were provided. Therefore, it was clear that both effects worked significantly on working memory abilities of children with ADHD in this study. For instance, after being taught the lyrics and gestures of the "Tap Tap Tap" game, children practiced their dances along with singing. Each child had to put his hands together and move them like a fish in water when their friends sang the lyrics "the little mermaid is floating". Children were provided the proper time to play again and again during the intervention hour under close attention of researchers. Children were challenged by playing the same game later on during a few sessions that included a full version of lyrics and more complex movements. Before more complex movements were demonstrated, they had the opportunities to recall and repeat the previous game songs and gestures once again. Subsequently, it was found that they could learn new movements and memorize additional lyrics quickly. In addition, recent research showed that structured game activities with music or poems were found to help children improve their working memory in children with ADHD.[49] Also, there is evidence that aerobic dancing with music can improve working memory and executive function.[50]

It has conclusively been shown that executive function can be developed by choosing the right activity to meet specific EF skills that a child has challenges with.[18] All intervention sessions were also implemented in a motivating and playful atmosphere as well as in a small group setting. Moreover, in order to promote EF skills, the appropriate frequency in improving executive function must be more than two times per week for group therapy.[13,18] Likewise, a study by Tamm *et al*.[51] which sought to study the effect of executive function training in young children with ADHD has confirmed that by giving a 60-minute session, 3-4 sessions per week, for 8 weeks, flexibility and working memory abilities were improved. Such appropriate duration and frequency of intervention was applied effectively in this study, as well.

It was evident that prior to the intervention, children with ADHD in this study were more likely to have high levels of arousal. Disorganized behaviors, such as hyperactivity, impulsivity, and being easily distracted were observed. They often rocked their bodies, stomped their feet, and jumped around which indicated they had problems in regulating themselves.[52-53] However, after self-regulatory strategies and heavy work activities were employed, children displayed more organized behaviors, such as calming down, sitting still for a longer period, staying focused on tasks, listening intently to instructions and rules, and being able to follow commands. Consequently, children could memorize lyrics and gestures much better. Adults' warnings and reminders were gradually decreased, as well. According to sensory integration theory, if children can adapt their level of arousal appropriately, they can control their behaviors better.[45,54] It has been suggested that heavy work activities can assist children to regulate their sensory needs and to adjust their level of arousal to optimal learning states. For instance, children can sit still on chair for longer durations of time[36-37] and have improved selective attention.[34] Meanwhile, Horowitz *et al*.[22] found that sensory-motor activity can help children to adapt their optimal arousal and promote selective attention, and children with good selective attention make progress in working memory.[5,34]

Furthermore, all intervention sessions were also

implemented in a motivating and playful atmosphere as well as in a small group setting. The design of the protocol was based on Diamond's and Kaufman's suggestions,[18,55] in which the intervention program that will successfully improve EFs are those that give children playfulness and a sense of belonging that helps them feel included.[18,55] Moreover, as this protocol was designed to provide children with ADHD a chance to play in a group, it was found that playing with peers in a group game format can help increase the opportunities for children in this study to learn to work together, listen to each other, and respect other people's opinions. It was congruent with a research study by Clark *et al*.[56] which found that playing with friends helped increased social skills and adaptive behaviors, which connects to executive function ability in working memory, inhibitory control, and flexibility.

In contrast to a recent study conducted by Somsri *et al*.,[26] our study found no difference in inhibitory control scores after children with ADHD completely participated in the intervention protocol. This may be due to how the Thai traditional play protocol was designed for children with ADHD in the current study. We aimed to target two executive function skills in children with ADHD, including working memory and inhibitory control. Therefore, children had to practice both skills in each activity. As a result, the findings demonstrated the positive effect of the Thai traditional play protocol on working memory in children with ADHD. However, these results could imply that improving inhibitory control in these children required more time and practice for these skills to be developed and generalized. It will be very interesting for future research to increase the number of Thai traditional play activities that provide inhibitory control skills in the Thai traditional play protocol. As is already known, inhibitory control helps children to change and choose how to behave and react. Without inhibitory control, children will respond or behave based on their old habits and/or stimuli in the environment or external temptations.[18] Children must be taught to learn and practice to have the ability to exercise inhibitory control and be able to apply and transfer these skills to be use on a daily basis.[55] Even though Thai traditional play activities were designed and analyzed to ensure that inhibitory control skills would emerge, we found that our protocol targeting inhibitory control skills was in need of revision in order to add more opportunities for children to use these skills at home as well as in classrooms. Moreover, the physical environment itself may be a barrier to treatment.[55] Regardless, the overall surroundings appeared to work perfectly for these interventions as the large-open space in the basement hall was sufficient for children to move, since most of Thai traditional play activities are often played outdoors or in open spaces. However, during intervention sessions, it was noticeable that children with ADHD were frequently distracted by noises and people walking by. Even though researchers had adjusted the environment by roping in the area and using shades to reduce other stimuli, it was evident that children with ADHD were still distracted by school announcements and noises from activities taking place around the area. An environment for inhibitory control training should be adapted or arranged by eliminating anything that disrupts or bothers the children.[55,57] For that reason, a good environment can help children to focus more on their activities, which leads to selective attention ability and appropriate response to stimuli.[5]

Limitations and Future Research

There are some limitations of this study. Since the present study was a one-group pre-test and post-test research design, there was no control group of children with ADHD to compare the outcome variables. The use of one geographic location and the small numbers of the participants also limits the generalizability of this study. An important future research goal must be to increase the collaboration process with homeroom teachers in the intervention protocol.

Conclusion

This study examined the effectiveness of the Thai traditional play protocol on working memory and inhibitory control in children with ADHD at Ban Rim Tai School, Mae Rim District, Chiangmai Province, Thailand. The results showed that working memory of children with ADHD increased significantly from pre-intervention to post-intervention ($p<0.05$). Scores in inhibitory control of these children between pre-intervention and post-intervention was not significantly different ($p>0.05$). On the basis of the current findings, the study results proved that the Thai traditional play protocol has potential as a promising intervention for school-aged children with ADHD who had difficulties in executive functioning on working memory.

Conflict of interest

The authors declare no competing interests in this research.

Acknowledgement

This study was funded by the Faculty of Associated Medical Sciences, Chiang Mai University, Chiangmai, Thailand. Special appreciation goes to all participants for their willingness to participate in this study. The authors thank teachers at Ban Rim Tai School, Mae Rim District, Thailand for their supports.

References

[1] Kotkin RA, Fine AH. Chapter 1 - attention deficit hyperactivity disorder and learning disabilities: An overview for practitioners. In: Fine AH, Kotkin RA, editors. Therapist's guide to learning and attention disorders. San Diego: Academic Press; 2003. p. 1-42.

[2] Biederman J, Faraone S, Milberger S, Guite J, Mick E, Chen L, *et al*. A prospective 4-year follow-up study of attention-deficit hyperactivity and related disorders. Arch Gen Psychiatry. 1996; 53(5): 437-46.

[3] Barkley RA: Behavioral inhibition, sustained attention, and executive functions: constructing a unifying theory of ADHD. Psychol. Bull. 1997; 121(1): 65.

[4] Willcutt EG, Doyle AE, Nigg JT, Faraone SV, Pennington BF: Validity of the executive function theory of attention-decit/hyperactivity disorder: a metaanalytic review. Biol. Psychiatry. 2005, 57(11): 1336-1346.

[5] Diamond A. Executive Functions. Annu. Rev. Psychol. 2013; 64(1): 135-68.

[6] Meltzer L. Executive function in education: From theory to practice: Guilford Publications; 2018.

[7] Spencer-Smith M, Klingberg T. Benefits of a working memory training program for inattention in daily life: A systematic review and meta-analysis. PLoS One 2015; 10(3): e0119522.

[8] Alloway TP, Alloway RG. Investigating the predictive roles of working memory and IQ in academic attainment. J Exp Child Psychol. 2010; 106(1): 20-9.

[9] Sonuga-Barke EJ, Dalen L, Daley D, Remington B. Are planning, working memory, and inhibition associated with individual differences in preschool ADHD symptoms? Dev Neuropsychol. 2002; 21(3): 255-72.

[10] McBurnett K, Pfiffner L. Attention deficit hyperactivity disorder: Concepts, controversies, new directions: CRC Press; 2007.

[11] Moffitt TE, Arseneault L, Belsky D, Dickson N, Hancox RJ, Harrington H, *et al*. A gradient of childhood self control predicts health, wealth, and public safety. Proc Natl Acad Sci U S A 2011; 108: 2693 8. doi: 10.1073/pnas.1010076108.

[12] Diamond A, Barnett WS, Thomas J, Munro S. Preschool program improves cognitive control. Science. 2007; 318(5855): 1387-8

[13] Diamond A, Lee K. Interventions shown to aid executive function development in children 4 to 12 years old. Science. 2011; 333(6045): 959-64.

[14] Hillman CH, Castelli DM, Buck SM. Aerobic Fitness and Neurocognitive Function in Healthy Preadolescent Children. Med. Sci. Sports Exerc. 2005; 37(11): 1967-74.

[15] Diamond A, Ling DS. Aerobic-Exercise and resistance-training interventions have been among the least effective ways to improve executive functions of any method tried thus far. Dev. Cogn. Neurosci. 2019; 37: 100572.

[16] Roley SS, Bissell J, Clark GF. Providing occupational therapy using sensory integration theory and methods in school-based practice. Am J Occup Ther. 2009; 63(6): 823-42.

[17] Yang C-Y, Howe T-H. Motor performance of children with attention deficit hyperactivity disorder in fourth to sixth grades: Differences among subtypes. Am J Occup Ther. 2017; 71(4 Supp1): 7111505094 p1-p1.

[18] Bodison SC, Parham LD. Specific sensory techniques and sensory environmental modifications for children and youth with sensory integration difficulties: A systematic review. Am J Occup Ther. 2017; 72(1): 7201190040 p1-p11.

[19] Kim MJ, Park HY, Yoo EY, Kim JR. Effects of a cognitive-functional intervention method on improving executive function and self-directed learning in school-aged children with attention deficit hyperactivity disorder: A single-subject design study. Occup Ther Int. 2020; 2020: 1250801.

[20] Diamond A, Ling DS. Conclusions about interventions, programs, and approaches for improving executive functions that appear justified and those that, despite much hype, do not. Dev. Cogn. Neurosci. 2016; 18: 34-48.

[21] Landreth GL. Play therapy the art of the relationship. 3rd Ed. New York: Routledge; 2012

[22] Lakes K, Hoyt W. Promoting self-regulation through school-based martial arts training. J. Appl. Dev. Psychol. 2004; 25: 283-302.

[23] Johanna Calderon. Executive function in children why it matters and how to help [internet]. Cambridge: Hardvard Health Publishing; 2020 Dec - [cited 2021 June 5]. Available from: https://www.health.harvard.edu/blog/executive-function-in-children-why-it-matters-and-how-to-help-2020121621583.

[24] Plookpedia. khwāmmāi khǭng kham wākān la lē nakha 'ong Thai [internet]. Bangkok: TruePlookpanya; 2017 April – [cited 2021 June 5]. Available from: https://www.trueplookpanya.com/blog/content/58006.

[25] Department of Physical Education. kānlalēn phūnbān Thai. Bangkok: S off graphic design; 2557.

[26] Somsri T, Haenjohn J, Supwirapakorn W. A development of inhibitory control based on Thai traditional game training program in elementary school students [internet]. 2019 June - [cited 2021 June 5]; 21(2): 222-30. Available from: https://he01.tci-thaijo.org.

[27] Chu S, Reynolds F. Occupational therapy for children with attention deficit hyperactivity disorder (ADHD), part 2: A multicentre evaluation of an assessment and treatment package. Br J Occup Ther. 2007; 70(10): 439-48.

[28] Shuai L, Daley D, Wang YF, Zhang JS, Kong YT, Tan X, *et al*. Executive function training for children with attention deficit hyperactivity disorder. Chin Med J (Engl). 2017; 130(5): 549-58.

[29] Chaimaha N, Sriphetcharawut S, Lersilp S, Chinchai S. Effectiveness of therapeutic programs for students with ADHD with executive function deficits. J Occup Ther Sch Early Interv. 2017; 10(4): 436-56.

[30] Lane SJ. Sensory modulation functions and disorders. In: Anita C. Bundy SJL, editor. Sensory integration theory and practice United States of America: F. A. Davis Company; 2020. p. 151-80.

[31] DuPaul GJ, Stoner G. ADHD in the schools: Assessment and intervention strategies. 2nd Ed. New York: The Guilford Press; 2003.

[32] Pfiffner LJ, Barkley RA. Treatment of ADHD in school settings. In: Barkley RA editor. Attention-deficit hyperactivity disorder—a handbook for diagnosis and treatment. 2nd Ed. New York: The Guilford Press; 1998. P 458-90.

[33] Ayres AJ. Treatment of sensory integrative dysfunction. Aust. Occup. Ther. J. 1972; 19(2): 88.

[34] Horowitz LJ & Röst C. Helping hyperactive kids? A sensory integration approach: Techniques and tips for parents and professionals. Canada: Hunter House; 2007.

[35] Williams MS, Shellenberger S. How does your engine run? . Albuquerque NM USA: Therapy Works; 1994.

[36] Wells AM, Chasnoff IJ, Schmidt CA, Telford E, Schwartz LD. Neurocognitive habilitation therapy for children with fetal alcohol spectrum disorders: an adaptation of the Alert Program®. Am J Occup Ther. 2012; 66(1): 24-34.

[37] Wilbarger J, Wilbarger P. The Wilbarger approach to treating sensory defensiveness. In A. C. Bundy, & S. J. Lane, editors. Sensory integration theory and practice. United States of America, USA: F. A. Davis Company; 1991. p. 426-32.

[38] Gioia GA, Isquith PK, Kenworthy L, Barton RM. Profiles of everyday executive function in acquired and developmental disorders. Child Neuropsychol. 2002; 8(2): 121-37.

[39] McCandless S, L OL. The clinical utility of the behavior rating inventory of executive function (BRIEF) in the diagnosis of ADHD. J Atten Disord. 2007;10(4): 381-9.

[40] Smithson PE, Kenworthy L, Wills MC, Jarrett M, Atmore K, Yerys BE. Real world executive control impairments in preschoolers with autism spectrum disorders. J Autism Dev Disord. 2013; 43: 1967-75.

[41] Golden CJ, Freshwater SM, Zarebeth G, Nova Southeastern University. Stroop color and word test children's version for ages 5-14: A manual for clinical and experimental uses. Wood Dale, Ill: Stoelting; 2003.

[42] Madteh F. Effect of traditional games training on early childhood development [dissertation]. Pattani: Prince of Songkla University; 2014.

[43] Bundy AC, Lane SJ, Murray EA. Sensory integration theory and practice. 2nd Ed. Philadelphia: F.A. Davis Company; 2002.

[44] Williams MS, Shellenberger S. How does your engine run?: A leader's guide to the alert program for self-regulation. Albuquerque NM USA: Therapy Works; 1996.

[45] Turner RC, Carlson L. Indexes of item-objective congruence for multidimensional items. Int. J. Test. 2003; 3(2): 163-71.

[46] Baddeley A. Working memory. Current Biology. 2010; 20(4): R136-R40.

[47] Baddeley A. Working Memory: Theories, models, and controversies. Annu. Rev. Psychol. 2012; 63(1): 1-29.

[48] Baddeley A, Gathercole S, Papagno C. The phonological loop as a language learning device. Psychol Rev. 1998; 105(1): 158-73.

[49] Khalili KF, Mohammadi MR, Yadegari F, Haresabadi F, Sadeghi SM. Working memory training in the form of structured games in children with attention deficit hyperactivity disorder. Iran J Psychiatry. 2016; 11(4): 224-33.

[50] Guiney H, Machado L. Benefits of regular aerobic exercise for executive functioning in healthy populations. Psychon Bull Rev. 2013; 20(1): 73-86.

[51] Tamm L, Nakonezny PA, Hughes CW. An open trial of a metacognitive executive function training for young children with ADHD. J Atten Disord. 2014; 18(6): 551-9.

[52] Reynolds S, Lane SJ. Sensory overresponsivity and anxiety in children with ADHD. Am. J. Occup. Ther. 2009; 63(4): 433-40.

[53] Dunn W. The impact of sensory processing abilities on the daily lives of young children and their families: A conceptual model. Infants & Young Children. 1997; 9(4): 23-35.

[54] Karamali ES, Shafaroodi N, Hassani MA, Parand A, Zarei M, Akbari ZS. Effect of play-based therapy on meta-cognitive and behavioral aspects of executive function: A randomized, controlled, clinical trial on the students with learning disabilities. Basic Clin Neurosci. 2017; 8(3): 203-12.

[55] Kaufman C. Executive function in the classroom: Practical strategies for improving performance and enhancing skills for all students. Michigan: Paul H. Brookes Publishing Co.,Inc; 2010. p. 79-94.

[56] Clark C, Prior M, Kinsella G. The relationship between executive function abilities, adaptive behaviour, and academic achievement in children with externalising behaviour problems. J Child Psychol Psychiatry. 2002; 43(6): 785-96.

[57] Dawson P, Guare R. Executive skills in children and adolescent: a practical guide to assessment and intervention. 2nd Ed. New York, NY: The Guilford Press; 2010.

Journal of Associated Medical Sciences 2021; 54 (3): 66-72

JAMS
Journal of Associated Medical Sciences

Thai-Journal Citation Index Centre (TCI) & ASEAN Citation Index (ACI)

Journal of Associated Medical Sciences

Journal homepage: https://www.tci-thaijo.org/index.php/bulletinAMS/index

Evaluation of scatter radiation dose to eye lens and thyroid gland from digital mammography

Patamaporn Molee[1] **Panatsada Awikunprasert**[1*] **Naruporn Marukatat**[2] **Vithit Pungkun**[3]

[1]*Department of Radiological Technology, Faculty of Medicine Vajira Hospital, Navamindradhiraj University, Bangkok, Thailand*
[2]*Department of Radiology, Faculty of Medicine Vajira Hospital, Navamindradhiraj University, Bangkok, Thailand*
[3]*Ionizing Radiation Metrology Group, Office of Atoms for Peace, Bangkok, Thailand*

ARTICLE INFO

Article history:
Received 20 April 2021
Accepted as revised 10 July 2021
Available online 10 July 2021

Keywords:
Scatter radiation dose, absorbed doses, eye lens, thyroid gland, digital mammography

ABSTRACT

Background: Digital mammography is a well-established screening examination for breast cancer due to its high sensitivity and specificity. However, digital mammography uses X-ray which is an ionizing radiation that can cause injury to all types of cells. In the patient positioning for mammography, the radiosensitive organs such as eye lens and thyroid gland are close to the radiation beam. Therefore, it is necessary to measure the scattered radiation dose to monitor and control the exposure within the standard limit.

Objectives: To study the scatter radiation dose of eye lens and thyroid gland and absorbed doses of breasts in patients undergoing digital mammography at Vajira Hospital, Bangkok, Thailand.

Materials and methods: Optically Stimulated Luminescent (OSL) dosimeters were taped to the patient's skin over the right and left lateral canthal angles, right and left thyroid lobes of 60 women (age range, 40–70 years) to measure the scattered radiation dose at each location in two routine mammographic projections; the cranial–caudal and the mediolateral oblique projections. The accumulated OSL dosimeters from patients were analyzed on a dosimeter reader. Breast compression thickness, compression force, average entrance skin dose, and glandular dose displayed on the mammography unit were recorded for each projection.

Results: The average scatter radiation dose to the skin overlying the right and left lateral canthal angles were 0.082 and 0.076 mGy, the right and left thyroid lobes were 0.929 and 0.883 mGy respectively. We found that the average scatter radiation doses were not exceed the radiation protection standards. On average, patients receive a glandular dose (AGD) of about 2.64 mGy. AGD was not exceed the dose limit recommended by the ACR where AGD of an ACR accreditation phantom shall not exceed 3 mGy. The average absorbed dose of breasts in digital mammography at Vajira Hospital was within the standard level. Meanwhile, the mean entrance skin dose was 9.96 mGy closer to the limit set by the IAEA, which was specified not to exceed 10 mGy for breasts of thickness between 4 and 6 cm.

Conclusion: The scatter radiation dose and absorbed doses determined through our study were within the standard level. Maximum visibility, especially for the signs of pathology, was achieved by imaging protocols that optimize the procedure and balance the quality requirements with the radiation dose to the patient. Monitoring of radiation dose in mammography reduces the risk of ionizing radiation and promotes the quality of public health services.

* **Corresponding author.**
Author's Address: *Department of Radiological Technology, Faculty of Medicine Vajira Hospital, Navamindradhiraj University, Bangkok, Thailand.*
** **E-mail address:** panatsada@nmu.ac.th
doi: 10.14456/jams.2021.25
E-ISSN: 2539-6056

Introduction

Breast cancer is the most common cancer in women worldwide. Since 2000, cancer has been the leading cause of death in Thailand.[1] In women, breast cancer is rapidly increasing with over 19,452 new cases expected in 2025.[1] The American Cancer Society recommends that women undergo regular screening mammography for early detection and to reduce the number of deaths from breast cancer. Digital mammography is a well-established screening examination for breast cancer due to its high sensitivity (67.8%) and specificity (70%).[2] Although, breast cancer screening with mammography alone is not perfect, but it has been one of the worldwide health strategies to reduce breast cancer mortality.[3] The goal of routine mammographic positioning is to screen the entire breast adequately. In most cases, the two standard mammographic projections, cranial-caudal (CC) view and mediolateral oblique (MLO) view, provide the best coverage of the breast tissue.[4] In addition, 3D Digital Breast Tomosynthesis (DBT) can be examined by taking images of the breast tissue as thin slices, one slice at a time, where each slice is 1 mm thick. At an angle of 15-50 degrees in tomosynthesis, approximately 50 slices of images are produced each time, where images were taken for a total of 4 times (2 times per side). Therefore, 200 images, each with 1 mm apart, will be obtained in the examination. This enables the observation of breast tissue that was previously stacked more clearly, despite the breast being dense, which includes patients with breast augmentation. Thus, lesions and abnormalities can be accurately identified, resulting in less images to be taken. The advantages of DBT have been confirmed by various studies[5-7] which includes faster detection of primary cancers and better visualization that enhances the observation of abnormalities in the breast.

However, both conventional and tomosynthesis modes of mammography are performed using X-ray which is an ionizing radiation that can cause injury to all types of cells. This adverse effect depends on the amount and energy of the exposed X-ray along with type and age of the cells. Excessive doses of X-ray can cause both short- and long-term cell damage and injury, where the risk of radiation exposure does not only depend on the energy, amount and type of radiation, but also on the organ being examined, size of the patient, as well as the examination techniques. In the posture adjustment of the patient for breast X-ray, it was found that the organs close to the radiation beam were the eye lens and thyroid gland.[8] Radiation exposure measurement to monitor and control within the limit requires a personal dose measuring device such as the Optically Stimulated Luminescence (OSL) dosimeter which can also be used to measure low-dose radiation from diagnostic radiology.[9] As OSL dosimeter can be molded into various aspects, making it small, easy to use with high sensitivity to radiation, can reanalyze the radiation dose, and is radiolucent which does not affect imaging diagnosis of diseases. For instance, the use of a nanoDot™ OSL dosimeter that has a wide range of radiation energy response (approximately 5 keV – 20 MeV) in diagnostic radiology can be employed to measure the amount of scattered and absorbed radiation on the skin near the organ of interest[10] or radiation sensitive areas such as eye lens and thyroid gland.

This study aims to determine the average glandular dose and entrance skin dose and use nanoDot™ OSL dosimeters to measure the scatter radiation dose received at anatomical locations like eyes and thyroid gland from digital mammography in representative patient population in order to monitor and control the radiation dose within the prescribed radiation safety standard.

Materials and methods

The study was approved by the Research Ethics Committee of the Faculty of Medicine Vajira Hospital, Navamindradhiraj University, Bangkok, Thailand (COA 160/2563). Informed written consent was sought and documented. The subjects in this study consisted of 60 women (age range of 40–70 years) who received screening mammography were invited to participate in the study. The inclusion criteria is women aged 40–70 years have a screening mammogram as recommended by U.S. Preventive Services Task Force (USPSTF) and the American College of Obstetricians and Gynecologists (ACOG) recommendations.[11] However, we excluded the women age younger than 40 years old or older than 70 years old, pregnant women, women with breast implantation or augmentation, women with breast abnormalities, women with mastectomy or history of breast cancer.

The characteristic of nanoDot™ OSL dosimeter is shown in Table 1. These dosimeters are well appropriated for scatter radiation measurements because minimal angular dependence and sensitive to energies from 5 keV to 20 MeV. The accuracy is ±10% according to the manufacturer's specifications. The lower limit of detection (LLD) of the OSL dosimetry system was 0.0335 mGy, as stated on the manufacturer's calibration certificate. Front of nanoDot™ carried alphanumeric sensitivity code with serial number, for instance, the alphanumeric sensitivity code is DN082 refers to the sensitivity of 0.82. Each OSL dosimeter has different sensitivity which will be included in an algorithm of OSL reader software to calculate the radiation dose.

In this study, the correction factor for the 80 kVp to 44 kVp was not included for the calculation. We do concern for this factor, however, the value of conversion factor is very small.[12, 13] We expected that it would not have much impact on the results.

Table 1 Characteristic of nanoDot™ OSL dosimeter.

Type of radiation measured	X and gamma rays, beta
Useful energy range	From 5 keV to 20 MeV
Detector	nanoDot™ OSL (Optically Stimulated Luminescence)
Technology	Aluminium oxide doped with carbon, Al_2O_3:C
Dot	10 mm x 10 mm
Thickness	2 mm
Angular dependence	Minimal angular or energy dependence: Ideal for measuring skin dose at a point of interest

Note: Results expressed in absorbed dose

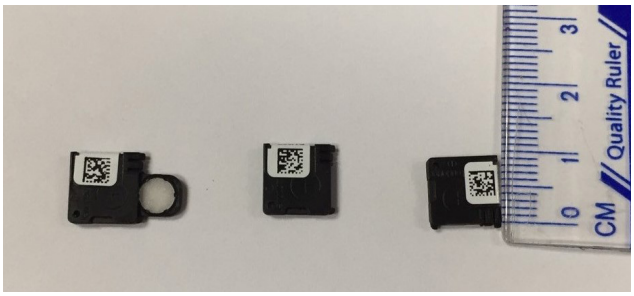

Figure 1. *Photograph showing Optically Stimulated Luminescence dosimeter (nanoDot™), which is 1 × 1 cm noninvasive radiation detector.*

Before the mammographic examination, four nanoDot™ OSL dosimeters (Figure 1) were taped to the patient's skin over the right and left lateral canthal angles of eyes, right thyroid lobe and left thyroid lobe (Figure 2). During mammography, the nanoDot™ OSL dosimeters measured the skin entrance scattered radiation doses at each location in two routine mammography projections, the conventional cranial-caudal (CC) view and both conventional and tomosynthesis mediolateral oblique (MLO) projections following the routine protocol of Vajira Hospital. Each nanoDot™ OSL dosimeter was read and erased before using with the next patient.

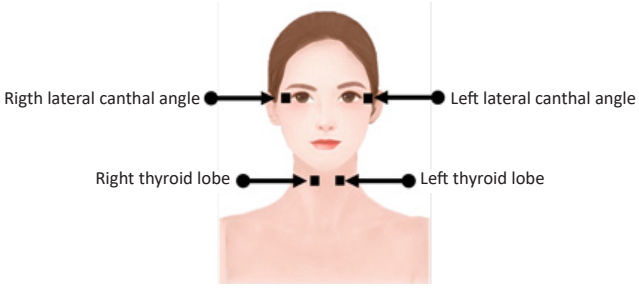

Figure 2. *Placement of nanoDot™ OSL dosimeters.*

All mammograms were obtained with the same mammography unit (MAMMOMAT Revelation; Siemens Medical Solutions Inc., Erlangen, Germany) installed in the year 2020 at Vajira Hospital, Faculty of Medicine Vajira Hospital, Navamindradhiraj University, Bangkok, Thailand (Figure 3). The mammographic unit was checked and certificated by Department of Medical Sciences Ministry of Public Health, Thailand according to quality standards of medical diagnostic X-ray machines. Mammography unit operated in standard automatic exposure control mode. Tube potential (peak kilovoltage) and tube current–time product (milliampere seconds), target-filter combination (W/Rh), and patient age were recorded. For each mammographic projection, breast compression thickness, compression force, average entrance skin dose, and glandular dose displayed on the mammography unit were recorded. Image quality of all mammograms was verified by radiological technologists and accepted by radiologist.

nanoDot™ OSL dosimeters were removed and stored with a control dosimeter until readout. The accumulated nanoDot™ OSL dosimeters from patients were analyzed on a dosimeter reader (MicroStar Dosimetry Reader, Landauer) (Figure 4). The exposed dosimeters were readout the next day after irradiation to prevent signal loss and addition of background radiations. Each nanoDot™ OSL was repeatedly read three times. The average readings were calculated. Results were also adjusted for background radiation based on control dosimeter readings. These nanoDot™ OSL dosimeters results represented dose at the skin external to the eye lens and thyroid gland.

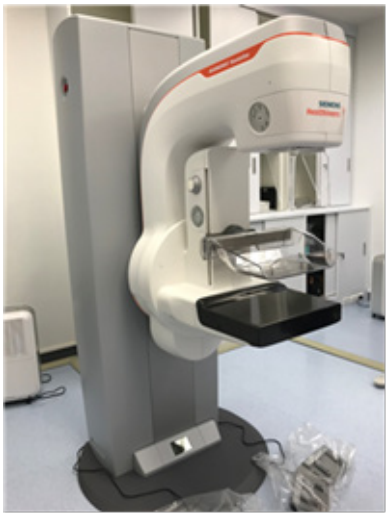

Figure 3. *A digital mammographic unit (MAMMOMAT Revelation; Siemens Medical Solutions Inc., Erlangen, Germany) installed in the year 2020 at Vajira Hospital, has been used to perform 2D conventional mammography and 3D breast tomosynthesis.*

Figure 4. *Photographs show MicroStar dosimetry reader for reading OSL dosimeters with MicroStar reader software for interpreting results.*

Results

The average age of subjects in this study was 56 years (range of 40-70 years). The average tube potential in this study was 43.95 kVp. The average tube current–time product was 220.23 mAs, and the mean compression force was 64.4 N (Table 2).

Scatter radiation dose measurements

The average scatter radiation dose, maximum dose, and minimum dose to the skin overlying the thyroid gland and lateral canthal angles of eyes are shown in Table 2. Distribution of each value from each location is shown in Figure 5.

Table 2 Scatter radiation dose of skin near organs of interest.

Organ	Average dose (mGy)	Maximum dose (mGy)	Minimum dose (mGy)	SD (mGy)
Right eye	0.082	0.323	<0.0335	0.063
Left eye	0.076	0.207	<0.0335	0.046
Right thyroid	0.929	2.276	0.188	0.497
Left thyroid	0.883	2.050	0.276	0.428

Right and left eyes

nanoDot™ OSL dosimeters placed near the right and left lateral canthal angles were used to estimate scatter radiation received by the eye lens. One measurement for the right and left eyes from one patient was below the LLD of the dosimeters. Other individual entrance skin measurements for the eye lens were above LLD of the dosimeters. The average scatter radiation dose to the skin at the right and left lateral canthal angles were 0.082 and 0.076 mGy respectively.

Thyroid gland

nanoDot™ OSL dosimeters taped above both thyroid lobes were used to estimate exposure of the thyroid gland. All individual skin measurements for the thyroid glands were over LLD of the dosimeters. The average scatter radiation doses to the skin above the right and left thyroid lobes were 0.929 and 0.883 mGy respectively.

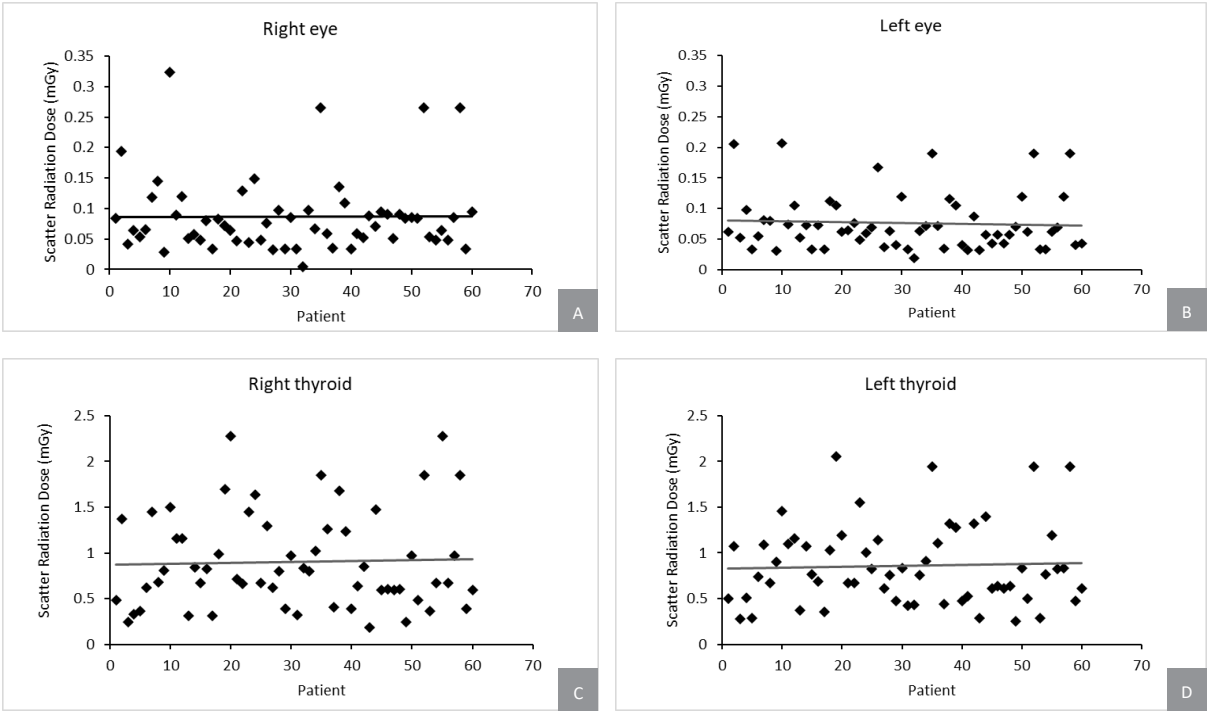

Figure 5. *Scatterplots show entrance skin doses for right (A) and left (B) lateral canthal angles, right (C) and left lobes of thyroid gland (D).*

Average Glandular dose and Entrance skin dose

Regarding the absorbed doses and correlated parameters in sixty mammographic examination participants in our study at Vajira Hospital, Faculty of Medicine Vajira Hospital, Navamindradhiraj University, it was found that the average glandular dose, which is a system-displayed average value was 1.33 mGy and 1.46 mGy for right cranial–caudal (RCC) and left cranial–caudal (LCC), and 4.08 mGy and 3.70 mGy for right mediolateral oblique (RMLO) and left mediolateral oblique (LMLO), respectively. The average glandular dose which is a system-displayed average value for all mammographic views was 2.64 mGy. The average glandular dose in the craniocaudal view was less than that in the mediolateral oblique view. The mean entrance skin dose was 5.06 mGy and 4.7 mGy for RCC and LCC, and 14.87 mGy and 15.2 mGy for RMLO and LMLO, respectively. The mean entrance skin dose which is a system-displayed average value for all mammographic views was 9.96 mGy. The mean entrance skin dose in the craniocaudal view was less than that in the mediolateral oblique view (Table 3).

Breast Compression Thickness

The average breast compression thickness was 55.47 mm and 54.09 mm for RCC and LCC, and 58.79 mm and 58.53 mm for RMLO and LMLO, respectively. The average breast compression thickness in our study was 56.72 mm for all views (Table 3). Average glandular dose increased with increasing breast compression thickness. Figure 6 shows the average glandular doses as a function of breast compression thickness for RCC (A), LCC (B) views in conventional mode and RMLO (C), LMLO (D) views in conventional and tomosynthesis mode (Figure 6).

Table 3 Parameters measured for each mammographic view.

Projection	kVp	mA	Compression Thickness (mm)	Compression Force (N)	Average Glandular dose (mGy)	Average Entrance skin dose (mGy)
Right craniocaudal (RCC)	29.11 (26, 32)	116.92 (50.4, 279.1)	55.47 (28, 84)	56.64 (28, 111)	1.33 (0.65, 3.6)	5.06 (0.91, 14.6)
Left craniocaudal (LCC)	28.98 (26, 32)	109.85 (47.1, 222.6)	54.09 (24, 79)	53.89 (29, 95)	1.46 (0.6, 10.4)	4.70 (0.82, 12.4)
Right mediolateral oblique (RMLO)	58.79 (54, 64)	332.53 (163.8, 740)	58.79 (33, 85)	74.15 (34, 131)	4.08 (2.12, 18.16)	14.87 (2.25,42.3)
Left mediolateral oblique (LMLO)	58.91 (54, 64)	321.64 (161.3, 621.2)	58.53 (34, 85)	72.92 (31,127)	3.70 (1.92, 10)	15.20 (2.45,32.4)

Note: Values are averages with minimum and maximum, MLO projections consist of conventional and tomosynthesis modes.

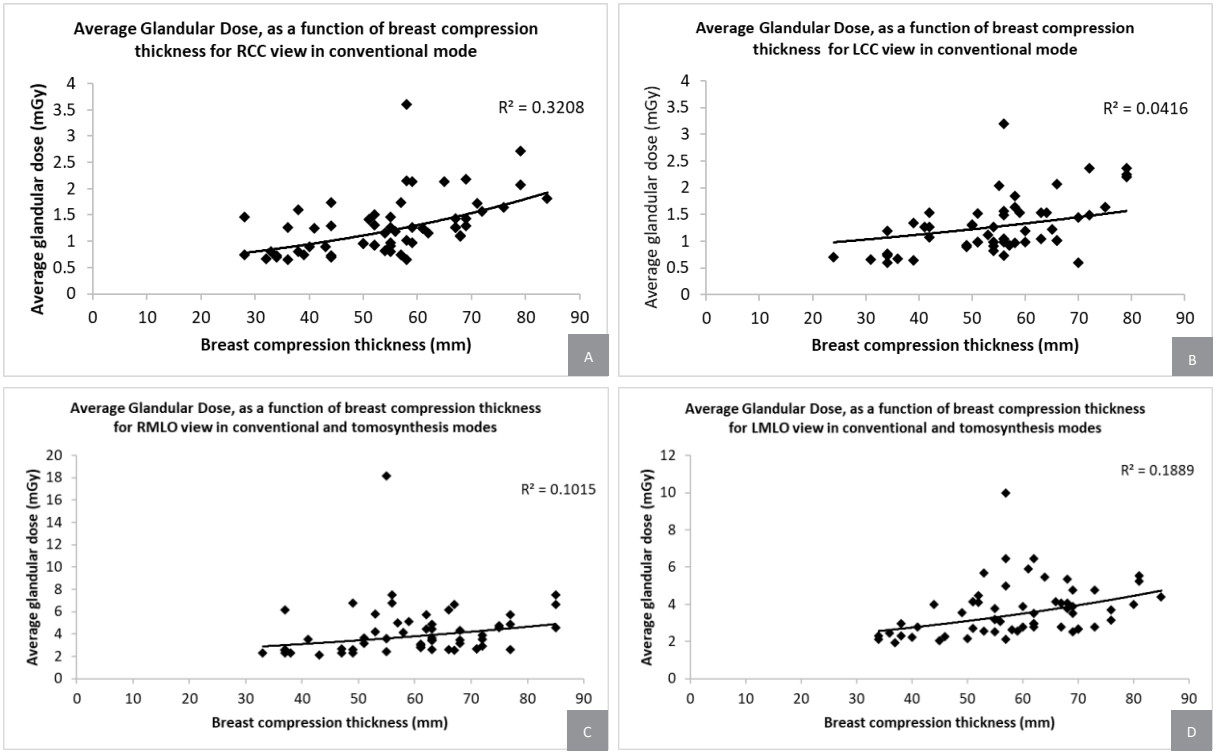

Figure 6. *Average glandular doses, as a function of breast compression thickness for RCC (A), LCC (B) views in conventional mode and RMLO (C), LMLO (D) views in conventional and tomosynthesis modes.*

Discussion

In this study, we measured the scatter radiation dose by using nanoDot™ OSL dosimeters placed on the skin of a representative population of women. We focused on tissues that have greater susceptibility to radiation effects, including the eye lens and thyroid gland.[14, 15] During positioning, a relaxed posture allows the breasts to naturally fall forward and loosen the skin and muscles of the chest.[4] Chest wall is brought closer to the image receptor by turning the patient's head to the contralateral side, and bringing it forward around the face shield. This results in visualization of more medial, superior, and posterior tissue of the breast. Just turning the head to the side is contrary to the positioning process.[4]

In this study, we placed nanoDot™ OSL dosimeters on the skin overlying the lateral canthal angles of the eyes which turned the patient's head to the contralateral side. The placement of this research is consistent with the suggestion of Chusin T *et al*. that eyes close to the imaged side received a higher dose whereas the contralateral eye received a negligible dose, implying that nanoDot™ OSL dosimeters should be pasted on eyes that are close to imaged tissue for improving accuracy of measurement.[16] The positions of nanoDot™ OSL dosimeters at thyroid gland in the study by Chetlen *et al*. are comparable to those employed by us.[8]

Sixty female patients were studied using a digital mammography facility at Vajira Hospital, Faculty of Medicine Vajira Hospital. Chetlen *et al*. reported that the average

scatter radiation dose to the skin overlying the eye lens and thyroid gland from digital screening mammography in 207 female subjects were 0.025 and 0.245 mGy respectively.[8] In this study, we found that the average scatter radiation dose to the skin overlying the lateral canthal angles of eyes were 0.082 and 0.076 mGy, the right and left thyroid lobes were 0.929 and 0.883 mGy, respectively. The average scatter radiation dose of eyes and thyroid gland in our study was higher than Chetlen *et al*.'s study because we performed MLO projections with both conventional and tomosynthesis modes according to routine protocol of Vajira Hospital while Chetlen *et al*. performed MLO projections with only conventional mode. Nonetheless, the average scatter radiation doses of eyes were not higher than the ocular-radiation protection standards formulated by the National Council on Radiation Protection and Measurements (NCRP) and the International Commission Radiological Protection (ICRP). It was all predicated on the assumption that radiation cataracts are deterministic and only appear when a threshold dose is exceeded. For detectable opacities, this value is currently 0.5–2 Gy for acute exposures and 5 Gy for chronic exposures.[17] Although, average scatter radiation doses of thyroid gland measured in our study was relatively high, Yuan *et al*. reported that patients who had been exposed to radiation from mammography did not have significantly higher risk of development of thyroid and hematologic cancers.[18] Further, the thyroid gland is considered less radiosensitive compared to the eye lens.

On average, patients receive a glandular dose (Mean AGD) of about 1.39 mGy in cranio-caudal view and 3.89 mGy in mediolateral oblique view. The AGD of 1.39 mGy for cranio-caudal view in our study was similar to those reported by Chetlen *et al*. and Theerakul K and Krisanachinda A as 1.36 mGy and 1.65 mGy respectively.[8, 19] The AGD of 3.89 mGy for mediolateral oblique view in our study was similar to Raed M K M Ali *et al*.'s study reported as 3.6 mGy.[20] Moreover, we found that when breast compression thickness increases, increasing the average glandular dose preformed with both conventional and tomosynthesis modes in all views comparable to other studies.[8, 19]

Mean AGD of cranio-caudal view was not exceed the dose limit recommended by the American College of Radiology (ACR) that AGD delivered during a single cranio-caudal view of an FDA-accepted phantom simulating a standard breast shall not exceed 3.0 mGy (0.3 rad) per exposure. Dose from a mode that combines a 2D view with a DBT view is not subject to the 3.0 mGy performance criteria. Each view within the mode should be compared separately against the performance criteria.[21] The average absorbed dose of breasts in digital mammography at Vajira Hospital was within the standard level. Meanwhile, the mean entrance skin dose displayed on the mammography unit was 9.96 mGy closer to the limit set by the International Atomic Energy Agency (IAEA) which specified not to exceed 10 mGy for breasts of thickness between 4 and 6 cm.[22] The mean entrance skin dose in our study was close to 10 mGy because the average breast compression thickness in our study was close to 6 cm. Radiation protection as low as reasonably achievable principle can be applied to patients to prevent any radiation incident.

Conclusion

Scatter radiation dose and absorbed doses determined through our study were within the standard level. Selection of a proper technique (technique factors, image processing, etc.) is what makes mammography the examination that requires the highest image quality for diagnosis. Maximum visibility, especially of the signs of pathology, is achieved by using state-of-the-art equipment and imaging protocols that optimize the procedure and balance the quality requirements with the radiation dose to the patient. Monitoring of radiation dose in mammography reduces the risk of ionizing radiation and promotes the quality of public health services. As a result, the hospital uses a quality mammography unit by maintaining the image quality that can be diagnosed following the standard for the patients effectively.

Acknowledgement

This work has been supported by a grant from the Navamindradhiraj University Research Fund (Project code: 132/63).

References

[1] Insamran W, Sangrajrang S. National Cancer Control Program of Thailand. Asian Pacific Journal of Cancer Prevention. 2020; 21(3): 577-82.

[2] Aekplakorn W. Breast Cancer Screening. Journal of Health Science. 2016; 25(4): 2.

[3] Coldman A, Phillips N, Wilson C, Decker K, Chiarelli AM, Brisson J, et al. Pan-Canadian Study of Mammography Screening and Mortality from Breast Cancer. JNCI: Journal of the National Cancer Institute. 2014; 106(11).

[4] Andolina V, Lillé S. Mammographic Imaging: A Practical Guide: Wolters Kluwer/Lippincott Williams & Wilkins Health; 2011.

[5] Ciatto S, Houssami N, Bernardi D, Caumo F, Pellegrini M, Brunelli S, et al. Integration of 3D digital mammography with tomosynthesis for population breast-cancer screening (STORM): a prospective comparison study. The Lancet Oncology. 2013; 14(7): 583-9.

[6] Houssami N, Skaane P. Overview of the evidence on digital breast tomosynthesis in breast cancer detection. The Breast. 2013; 22(2): 101-8.

[7] Carbonaro LA, Di Leo G, Clauser P, Trimboli RM, Verardi N, Fedeli MP, et al. Impact on the recall rate of digital breast tomosynthesis as an adjunct to digital mammography in the screening setting. A double reading experience and review of the literature. European Journal of Radiology. 2016; 85(4): 808-14.

[8] Chetlen AL, Brown KL, King SH, Kasales CJ, Schetter SE, Mack JA, et al. Journal Club: Scatter Radiation Dose From Digital Screening Mammography Measured in a Representative Patient Population. American Journal of Roentgenology. 2016; 206(2): 359-64; quiz 65.

[9] Lim CS, Lee SB, Jin GH. Performance of optically stimulated luminescence Al2O3 dosimeter for low doses of diagnostic energy X-rays. Applied Radiation and Isotopes. 2011; 69(10): 1486-9.

[10] Okazaki T, Hayashi H, Takegami K, Okino H, Kimoto N, Maehata I, et al. Fundamental Study of nanoDot OSL Dosimeters for Entrance Skin Dose Measurement in Diagnostic X-ray Examinations. Journal of Radiation Protection and Research. 2016; 41(3): 229-36.

[11] Siu AL. Screening for Breast Cancer: U.S. Preventive Services Task Force Recommendation Statement. Annals of Internal Medicine. 2016; 164(4): 279-96.

[12] Awikunprasert P, Chandaeng T, Kuepitak K, Pungkun V, Kianprasit J. Radiation Dose and Dose Distribution from Fluoroscopy: Phantom Study. Srinagarind Medical Journal. 2019; 34(6): 565-73.

[13] Kawaguchi A, Matsunaga Y, Suzuki S, Chida K. Energy dependence and angular dependence of an optically stimulated luminescence dosimeter in the mammography energy range. Journal of Applied Clinical Medical Physics. 2017; 18(2): 191-6.

[14] Mettler FA. Medical effects and risks of exposure to ionising radiation. Journal of Radiological Protection. 2012; 32(1): N9-n13.

[15] The 2007 Recommendations of the International Commission on Radiological Protection. ICRP publication 103. Annals of the ICRP. 2007; 37(2-4): 1-332.

[16] Chusin T, Matsubara K, Takemura A, Okubo R, Ogawa Y. Assessment of scatter radiation dose and absorbed doses in eye lens and thyroid gland during digital breast tomosynthesis. Journal of Applied Clinical Medical Physics. 2019; 20(1): 340-7.

[17] Stewart FA, Akleyev AV, Hauer-Jensen M, Hendry JH, Kleiman NJ, Macvittie TJ, et al. ICRP publication 118: ICRP statement on tissue reactions and early and late effects of radiation in normal tissues and organs--threshold doses for tissue reactions in a radiation protection context. Annals of the ICRP. 2012; 41(1-2): 1-322.

[18] Yuan MK, Chang SC, Hsu LC, Pan PJ, Huang CC, Leu HB. Mammography and the risk of thyroid and hematological cancers: a nationwide population-based study.The Breast Journal. 2014; 20(5): 496-501.

[19] Theerakul K, Krisanachinda A. Radiation dose from digital breast tomosynthesis system. Chulalongkorn Medical Journal. 2014; 58(3): 235-45.

[20] RMK MA, England A, Tootell AK, Hogg P. Radiation dose from digital breast tomosynthesis screening - A comparison with full field digital mammography. J Med Imaging Radiat Sci. 2020; 51(4): 599-603.

[21] Berns EA, Pfeiffer DE, Butler PF, Adent C, Baird R, Baker JA, et al. Digital Mammography Quality Control Manual. 2nd ed. Reston, Va: American College of Radiology; 2018.

[22] Optimization of the Radiological Protection of Patients: Image Quality and Dose in Mammography (Coordinated Research in Europe). Vienna: International Atomic Energy Agency; 2005.

Journal of Associated Medical Sciences 2021; 54 (3): 73-77

JAMS
Journal of Associated Medical Sciences

Thai-Journal Citation Index Centre (TCI) & ASEAN Citation Index (ACI)

Journal of Associated Medical Sciences

Journal homepage: https://www.tci-thaijo.org/index.php/bulletinAMS/index

Radiation emitted from patients undergoing nuclear medicine examination at Udonthani Cancer Hospital

Chaisunthorn Wisetnan[1] **Panatsada Awikunprasert**[2*] **Thayada Kaewsombat**[1] **Patamaporn Molee**[2]

[1]*Division of Nuclear Medicine, Department of Diagnostic Radiology and Nuclear Medicine, Udonthani Cancer Hospital, Udon Thani Province, Thailand*

[2]*Department of Radiological Technology, Faculty of Medicine Vajira Hospital, Navamindradhiraj University, Bangkok, Thailand*

ARTICLE INFO

Article history:
Received 16 June 2021
Accepted as revised 13 July 2021
Available online 13 July 2021

Keywords:
Nuclear medicine, radiopharmaceutical, radiation protection

ABSTRACT

Background: Diagnostic nuclear medicine involves intravenous injection of radiopharmaceutical substances into the patient, after which they still possess the substance within their bodies and depict mobile radiation sources. Although the amount of radiation emitted is little and harmless to others, practitioners in and outside the Division of Nuclear Medicine along with related personnel and relatives of the patient are anxious about radiation exposure from a patient undergoing nuclear medicine examination.

Objectives: This study aimed to measure radiation doses from the patients at different times and distances.

Materials and methods: The radiation dose was measured from 66 patients (19-79 years) undergoing bone scan, MUGA scan, and thyroid scan. The data were collected at different times intervals and different distances from the patients.

Results: The results showed that the radiation dose from patients after a bone scan and MUGA scan at a distance less than 0.50 meter was higher than 10 µSv/hr, which is the radiation exposure limit of the practitioner.

Conclusion: Results of this study are helpful in operation planning such as increasing the distance and reducing the time of close contact, which can ease anxiety of concerned personnel, while radiation practitioner training as well as educating patients and relatives must be carried out to encourage better understanding.

Introduction

Udonthani Cancer Hospital began providing diagnostic nuclear medicine services with a single photon emission computed tomography (SPECT) in December 2019. In the year 2020, there were a total of 1,248 patients which were 1,137 cases of bone scan, 50 cases of multi -gated acquisition scan (MUGA scan), 47 thyroid scans, and 14 parathyroid scans. Nuclear medicine examination is a diagnostic test that uses a radioactive unsealed radionuclide source labeled with a pharmaceutical compound called radiopharmaceuticals which is administered into the patient intravenously. Selection of the radiopharmaceuticals is based on the diagnostic techniques such as ^{99m}Tc-methylene diphosphonate (MDP) for bone scan, ^{99m}Tc-phytate for gastrointestinal (GI) study or solid gastric emptying scintigraphy, and ^{99m}Tc-pertechnetate for cardiac and thyroid scans. Radiation emitted from the patient is measured and utilized to create images to diagnose function of the organs of interest. After the examination, patients still contain the radioactive substance within their bodies and depict mobile radiation sources, although the amount of radiation emitted by the patient's body is small and harmless to others,[1-3] which does not exceed the radiation exposure limit; below 1 millisievert per year (mSv/y) for

* **Corresponding author.**
Author's Address: *Department of Radiological Technology, Faculty of Medicine Vajira Hospital, Navamindradhiraj University, Bangkok, Thailand.*
** **E-mail address:** panatsada@nmu.ac.th
doi: 10.14456/jams.2021.26
E-ISSN: 2539-6056

general public, and below 20 mSv/y (or 10 µSv/hr) for technical practitioners. Generally, the radiation dose emitted from the patient decreases with increasing period of time.[4] Therefore, increasing the distance between the patient and other persons[1] along with the use of radiation shielding devices to reduce the radiation dose are recommended. Several studies have observed the radiation dose to occupational radiation workers (i.e. technician, radiologist, nurses in nuclear medicine services)[5] and non-occupational radiation workers (accompanying nurses, relatives, other staffs and patient)[6-8] from nuclear medical procedures. The results indicated that there is no need to quarantine patients for the radioactive decays. Except in some circumstances, such as being away from children and pregnant woman or traveling long distances by public transport.[7, 8] However, practitioners, both in and outside the Division of Nuclear Medicine along with accompanying persons and relatives of the patient are anxious about radiation exposure from a patient undergoing nuclear medicine examination. This is because after nuclear medicine examination, some patients may be required to proceed with other diagnosis such as ultrasound, electrocardiogram or other laboratory tests, as well as commuting by public transport or private vehicle where the patients can radiate radioactivity towards relatives or people in the surroundings.

The Division of Nuclear Medicine, Department of Diagnostic Radiology and Nuclear Medicine, Udonthani Cancer Hospital has never recorded and conducted the study of the radiation dose emitted by the patients before. Therefore, this study aims to measure the radiological radiation dose from patients undergoing nuclear medicine examination at different periods of time and varied distances from the patients. The results of this study shall determine the radiation dose from the patient emitted into the environment, and notify the operating practitioners, as well as inform the patients along with their relatives in order to encourage the awareness of preventive measures and avoid radiation exposure.[3]

Materials and methods

This is a surveillance study that measured radiation dose emitted from the patients which has been approved by the Human Research Ethics Committee under project number UCH-CT 12/2563. Dose rate measurements were recorded from 66 patients. The patients had a range of age (19-79 years), weight (34-79 kg) and body mass index (BMI) [17-28 kg/m^2]. The data were collected from patients undergoing bone scan (n=56), MUGA scan (n=8), and thyroid scan (n=2) over a period of 2 months, from 1 November 2020 to 31 December 2020 (Ethic approval from Human Research Ethics Committee under project number UCH-CT 12/2563).

Using a calibrated survey meter with pancake GM probe, Ludlum model 3000 (Ludlum Measurements, Inc., Sweetwater, Texas). Radiation dose rate was measured from the external surface of abdominal region of the patients at varied distances of 0.25 m, 0.50 m, 1.00 m, and 2.00 m for each interval (Figure 1).

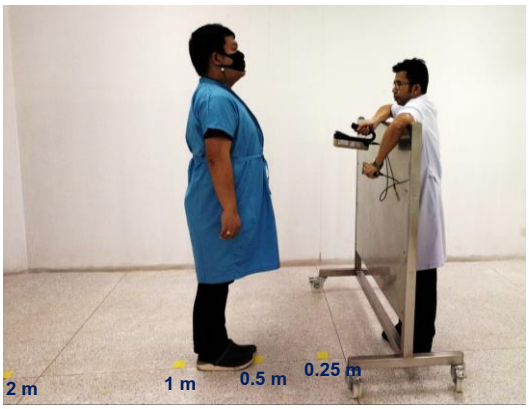

A

B

Figure 1. *Radiation dose measurement at varied distances (A) 0.50 m (B) 1.00 m.*

Since, all three scans use different protocols, the waiting time to radiation measurement are not the same as shown in Table 1. Patients undergoing bone scan would receive 20 mCi of ^{99m}Tc-MDP and wait for 3 hrs to allow accumulation of the radiopharmaceutical around the bone before undergoing a SPECT scan. During the 3 hrs waiting time, radiation dose measurement was measured from the patients at three intervals after injection of the radiopharmaceuticals; immediate (0 hr), 1 hr, 2 hrs, and 3 hrs.

MUGA scan using modified in-vivo (^{99m}Tc-pertechnetate) technique. Patients were injected stannous 1.5-2.0 ml intravenously. After 20 minutes, patients were intravenously administered with 20 mCi ^{99m}Tc-pertechnetate. Patients undergoing MUGA scan have to wait for 20 minutes to allow accumulation of the radiopharmaceutical around the cardiac muscle. Radiation dose rate was measured from the patients immediately (0 hr) after the injection. Then the patients underwent SPECT scanning for about 15-20 minutes. After imaging, the patients were asked to wait for another 20 minutes in the waiting room for the dose rate measurement at 1 hr after injection.

Patients undergoing thyroid scan would receive 3 mCi of ^{99m}Tc- pertechnetate and radiation dose measurement was measured immediately after injection. Then after 15 minutes waiting for radiotracer accumulation in thyroid, patients would undergo a SPECT scan.

Table 1 Time of radiation dose measurement from patients undergoing nuclear medicine examination.

Examination	Radioactivity	Waiting time for SPECT scan (minutes)	Time of measurement after radiotracer injection (hrs)			
			0	1	2	3
Bone Scan (^{99m}Tc-MDP)	20 mCi	180 min	/	/	/	/
MUGA (^{99m}Tc-pertechnetate)	20 mCi	20 min	/	/	N/A	N/A
Thyroid scan (^{99m}Tc-pertechnetate)	3 mCi	15 min	/	N/A	N/A	N/A

N/A: not available

Results

During the data collection period of 2 months in the Division of Nuclear Medicine, Udonthani Cancer Hospital, a total of 66 patients aged between 19-79 years old underwent nuclear medicine examination; 56 cases of bone scan, 8 cases of MUGA scan, and 2 cases of thyroid scan. Table 2 shows the radiation dose emitted from patients undergoing nuclear medicine examination at various distances and times of measurement.

Results of the radiometric measurements from patients undergoing bone scan showed that after the injection of ^{99m}Tc-MDP by a mean dose of 20.2 mCi was administered, we found the maximum radiation dose of 58.8±9.0 µSv/hr at a distance of 0.25 meters and it decreased to 5.0±0.5 µSv/hr at 2.00 meters distance. It was found that the radiation dose was higher than 10 µSv/hr when the distance from the patient was less than 1.00 meters. Also, the radiation dose was still higher than 10 µSv/hr when measured 3 hrs after the injection of radiopharmaceuticals was administered at the distance less than 0.50 m (Figure 2).

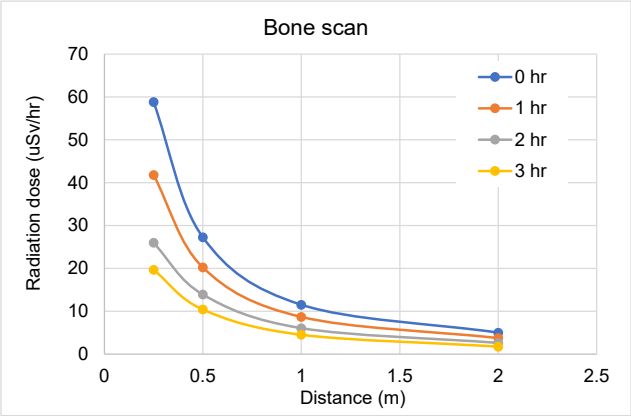

Figure 2. *Radiation dose of bone scan patients at different distances immediately and every 1 hr after injection of the radiopharmaceuticals.*

The radiation dose emitted from patients undergoing MUGA scan showed the maximum radiation dose of 57.1±9.8 µSv/hr after the injection of a mean dose of 20.1 mCi was administered. ^{99m}Tc- pertechnetate measured at a distance of 0.25 meters, which decreased to 5.1±0.5 µSv/hr at 2.00 meters distance. It was found that the radiation dose emitted from the patient decreased to below 10 µSv/hr when measured 1 hr after the injection at more than 1.00 meters distance (Figure 3).

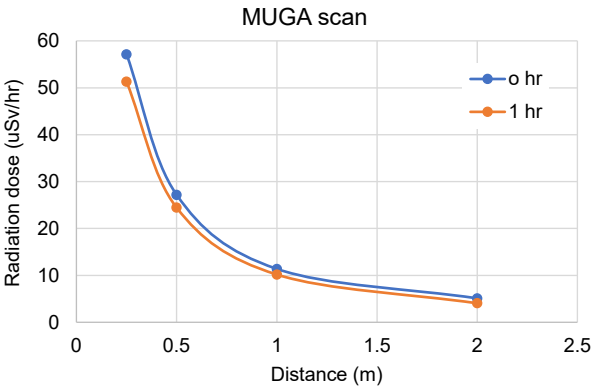

Figure 3. *Radiation dose of MUGA scan patients at different distances immediately and every 1 hr after injection of the radiopharmaceuticals.*

The radiation dose emitted from patients undergoing thyroid scan showed the maximum radiation dose of 10.0±0.2 µSv/hr after the injection of a mean dose of 3.4 mCi was administered. ^{99m}Tc- pertechnetate measured at a distance of 0.25 meter and decreased to 0.9±0.1 µSv/hr at 2.00 meter distance (Figure 4).

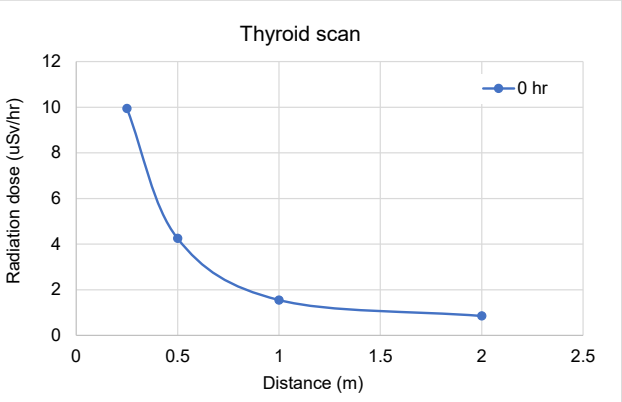

Figure 4. *Radiation dose of thyroid scan patients at different distances immediately after injection of the radiopharmaceuticals.*

Table 2 Radiation dose measured in µSv/hr immediately after injection of the radiopharmaceuticals was administered at different distances.

Examination	N	Radioactivity (mCi)	µSv/hr (mean±SD)			
			0.25 m	0.50 m	1.00 m	2.00 m
Bone Scan (^{99m}Tc-MDP)	56	20.2	58.8±9.0	27.3±4.3	11.5±1.5	5.0±0.5
MUGA (^{99m}Tc-pertechnetate)	8	20.1	57.1±9.8	27.2±3.7	11.4±1.1	5.1±0.5
Thyroid scan (^{99m}Tc-pertechnetate)	2	3.4	10.0±0.2	4.3±0.1	1.6±0.1	0.9±0.1

Discussion

In this study, the radiation doses were measured from patients undergoing nuclear medicine examination to diagnose various diseases. Different diagnostic protocols use different radiopharmaceuticals with different radiation strengths, where high-intensity protocols increase the radiation dose emitted from the patients when measured at different times and distances. In clinical, the radiation did not meet the inverse square law. The relevant factors such as biological distribution, bone metastases, and urinary excretion.[4] Results from this study are consistent with the previous works[1, 3] and the radiation protection principles. The reduction of exposure time, the increase of distance, and the use of shielding devices when exposed to the source of radiation. These can be applied as a protection against radiation hazards for nuclear medicine practitioners. The findings from this study are helpful for the assessment and planning of operations in the Division of Nuclear Medicine. Radiation dose emitted from patients should be regularly monitored to provide a database that can be used to assist protection planning against radiation hazards. In addition, training of practitioners on radiation hazard prevention as well as the importance of the radioprotection principle "As Low As Reasonably Achievable (ALARA)" is mandatory to promote a work culture that concerns radiation hazards.

Provision of information and operational guidelines can reduce the anxiety of related staff of other departments in the hospital who require close contact with patients undergoing bone and MUGA scans. There should be a minimum distance of 0.50-1.00 meter from the patients while waiting for services along with the close contact time as short as possible in order to maintain a safe radiation exposure limit within 10 µSv/hr. On the other hand, the radiation dose emitted from patients undergoing thyroid scans is within the safe limits for operational practitioners due to lower radiation strength with decreasing physical and biological half-lives. Hence, practitioners of other departments can perform their duties with the patient safely. Radiological technician or staffs who are responsible for patient positioning at a distance less than 0.50 meter should spend as little time as possible to minimize radiation exposure.

Meanwhile, patients undergoing bone and MUGA scans should be informed about radiation emission from their bodies that may be harmful to those around them, because the emission of radiation dose immediately after injection of radiopharmaceuticals is high. Therefore, patients should sit and wait in the provided area or isolated room to reduce radiation exposure to others, which includes providing information on practices for patients after the examination. Since the radiation dose at a distance less than 0.50 meter is still higher than 10 µSv/hr, the patient must have at least 0.50 meter distance from others and avoid holding or being close to children because they are more susceptible to radiation hazards.

Moreover, relatives of close care for the patients undergoing nuclear medicine examination should keep a distance from the patient and use telephones to communicate with the patient to reduce radiation exposure. In case of unavoidable circumstances such as a journey in the same vehicle or use of public transportation, the patient may be allowed to wait for another 1-2 hrs before departure so as to let the radioactivity to decay.

Conclusion

The radiation dose from the patient after a bone scan and MUGA scan at a distance less than 0.50 meter is still higher than the radiation exposure limit of the practitioner. Hence practitioners, relatives, and the patient themselves should be informed and aware of this emission in order to prevent harmful radiation. The findings derived from this real-world data can be used to develop the standard operating procedure which is suitable for our center. As a result, it would strengthen the radiation safety management for the hospital accreditation. This could be practiced by increasing the distance and reducing the time of close contact, while training and educating practitioners on radiation dose will enhance better understanding and reduce anxiety at work.

Acknowledgement

The authors thankfully acknowledge Udonthani Cancer Hospital for the support of facilities and helps. Special thanks of the ethical writing guidance to Research Publishing and Academic Support, Udonthani Cancer Hospital.

Conflict of interest

There are no conflicts of interest to disclose.

Ethic approval

Human Research Ethics Committee under project number UCH-CT 12/2563

References

[1] Bayram T, Yilmaz AH, Demir M, Sonmez B. Radiation dose to technologists per nuclear medicine examination and estimation of annual dose. J Nucl Med Technol. 2011; 39(1): 55-9.

[2] Gomez-Palacios M, Terrón JA, Domínguez P, Vera DR, Osuna RF. Radiation doses in the surroundings of patients undergoing nuclear medicine diagnostic studies. Health Phys. 2005; 89(2 Suppl): S27-34.

[3] Stenstad L-I, Pedersen G, Landmark A, Brattheim B. Nuclear radiation dose to the surroundings from patients who are undergoing nuclear medicine examinations. Radiograph Open. 2014; 1: 11-8.

[4] Castronovo FP. Time Dependent Radiation Exposures Surrounding Technetium-99m MDP Patients. J Nucl Med Technol 1991; 19(3): 182-4.

[5] Chiesa C, De Sanctis V, Crippa F, Schiavini M, Fraigola CE, Bogni A, et al. Radiation dose to technicians per nuclear medicine procedure: comparison between technetium-99m, gallium-67, and iodine-131 radiotracers and fluorine-18 fluorodeoxyglucose. Eur J Nucl Med. 1997; 24(11): 1380-9.

[6] Amaral A, Cabral G, Campos L, Guimarães MI. Exposure of persons accompanying patients in nuclear medicine departments. Cell Mol Biol 2002; 48(5): 505-9.

[7] Harding LK, Bossuyt A, Pellet S, Reiners C, Talbot J. Radiation doses to those accompanying nuclear medicine department patients: a waiting room survey. EANM Task Group Explaining Risks. European Association of Nuclear Medicine. Eur J Nucl Med. 1994; 21(11): 1223-6.

[8] Harding LK, Harding NJ, Warren H, Mills A, Thomson WH. The radiation dose to accompanying nurses, relatives and other patients in a nuclear medicine department waiting room. Nucl Med Commun. 1990; 11(1): 17-22.

Journal of Associated Medical Sciences 2021; 54 (3): 78-83

JAMS
Journal of Associated Medical Sciences

Thai-Journal Citation Index Centre (TCI) & ASEAN Citation Index (ACI)

Journal of Associated Medical Sciences

Journal homepage: https://www.tci-thaijo.org/index.php/bulletinAMS/index

Effect of acquisition time on image quality and lesion detectability with ^{131}I SPECT: A phantom study

Supakiet Piasanthia[1] Putthiporn Charoenphun[1] Wirinya Saengthamchai[1] Krisanat Chuamsaamarkkee[1*]

[1]Department of Diagnostic and Therapeutic Radiology, Faculty of Medicine Ramathibodi Hospital, Mahidol University, Bangkok, Thailand

ARTICLE INFO

Article history:
Received 30 June 2021
Accepted as revised 18 August 2021
Available online 18 August 2021

Keywords:
^{131}I SPECT, lesion detectability, contrast, contrast-to-noise ratio, acquisition time

ABSTRACT

Background: One important parameter in single-photon emission computed tomography (SPECT) is the acquisition time. Longer acquisition time can reduce noise, improving image quality while patient motion might be presented.

Objectives: This study intended to examine the effect of acquisition time on qualitative and quantitative analysis of ^{131}I (Iodine-131) SPECT.

Materials and methods: A National Electrical Manufacturers Association/International Electrotechnical Commission (NEMA/IEC) phantom with a set of fillable spheres was filled with ^{131}I solution to generate two conditions: (a) hot lesion with no background and (b) hot lesion with a warm background at a ratio of 10:1. SPECT images were acquired with acquisition times per frame of 20, 30, 40, and 90 second/frame (s/f).

Results: Qualitative assessment in the no background condition showed that all spheres were visible at all acquisition settings, while the smallest sphere in the images in hot lesion with a warm background at a ratio of 10:1 was not visible even at the longest acquisition time of 90 s/f. Quantitative analysis revealed that the contrast and contrast-to-noise ratio (CNR) increased upon extending the acquisition time in both conditions. Interestingly, the statistical results indicated that the mean CNRs acquired at 20 or 30 s/f were not significantly different when compared with 40 s/f for no background. However, for the warm background, the mean CNRs at 20 s/f were significantly different than those at 40 s/f, while they were not significantly different at 30 s/f.

Conclusion: The acquisition time for no background condition can be optimized, while the image quality is still clinically acceptable. For the warm background, the acquisition time can be shortened; however, the time selection must be carefully considered.

Introduction

Radioiodine (^{131}I) has been used for the diagnosis and treatment of thyroid diseases for over 80 years. The beta emissions offer a therapeutic property whereas the discrete gamma photons can be imaged with nuclear medicine imaging techniques to provide clinical information such as tumour size, treatment efficiency, sites of metastasis, and dosimetry calculations.[1, 2]

For many decades, the whole-body planar imaging of ^{131}I was the standard method used to identify the thyroid remnant, metastases, or lesion. However, low resolution and lack of anatomical localization make interpretation of ^{131}I planar imaging challenging. Several recent studies suggested that ^{131}I SPECT provides superior clinical results compared to ^{131}I planar imaging.[3-5] Nonetheless, undesirable

* **Corresponding author.**
Author's Address: *Department of Diagnostic and Therapeutic Radiology, Faculty of Medicine Ramathibodi Hospital, Mahidol University, Bangkok, Thailand.*
** **E-mail address:** krisanat.chu@mahidol.ac.th
doi: 10.14456/jams.2021.27
E-ISSN: 2539-6056

image quality with ^{131}I could compromise the accuracy and detectability limit.[6, 7] One important parameter in SPECT is the acquisition time, which refers to the time per stop in the imaging parameter. Unquestionably, longer acquisition time has the advantages of higher counts, noise reduction, as well as better contrast and resolution. On the other hand, longer acquisition time can be associated with patient agitation that can further result in artefacts and image degradation.[8, 9]

Although several studies have attempted to study the clinical impact of acquisition time reduction using resolution recovery software in bone and parathyroid SPECT with Technetium-99m.[10, 11] Nevertheless, fewer studies have attempted to study with ^{131}I SPECT due to the complexity of its emission spectrum. Therefore, this study intended to examine the effect of acquisition time on image quality and aimed to qualitatively assess this effect on lesion detectability with ^{131}I SPECT using NEMA/IEC (National Electrical Manufacturers Association/International Electrotechnical Commission) body phantom.

Materials and methods

Phantom preparation

The NEMA/IEC body phantom (Data Spectrum Corp., Chapel Hill, North Carolina, USA) with a set of fillable hollow spheres was used in this study. The volume and inner diameter (ID) of the fillable hollow spheres were 26.52 mL (ID 37 mm), 11.49 mL (ID 28 mm), 5.58 mL (ID 22 mm), 2.57 mL (ID 17 mm), 1.15 mL (ID 13 mm), and 0.52 mL (ID 10 mm). However, the 5.58 mL sphere was excluded from the experiment due to a defect. The spheres were filled with an aqueous solution of ^{131}I-sodium iodide (NaI) with an activity concentration of 740 kBq.mL^{-1} to simulate a hot lesion. The background activity was filled with deionized water and ^{131}I-NaI with an activity concentration of 74 kBq.mL^{-1} to simulate no background and the hot lesion to warm background ratio of 10:1, respectively. The selected concentration was based on ^{131}I clinical images from previously published studies.[12-14]

SPECT scanner and acquisitions

All SPECT images were acquired using a dual-head gamma camera (Infinia Hawkeye-4, General Electric Medical Systems, Milwaukee, Wisconsin, USA) equipped with a high-energy general purpose (HEGP) collimator and crystal thickness of 25.4 mm. The projection data were acquired for 60 views with 360° camera rotation in the orbit mode. The main photo peak was set at 364 keV and 20% energy window. The acquisition time per frame was varied from 20, 30, 40, and 90 s/f. Additional CT images were also acquired for localization of the hot spheres.

Image reconstruction

All SPECT data were reconstructed with the ordered subsets expectation maximization (OSEM) method (2 iterations and 10 subsets per series) and a Hann filter, as recommended by the manufacturer. Image size was 128 × 128 and the slice thickness was 4 mm. The attenuation correction was performed with Chang's method. The scatter correction was also carried out using the dual-energy window method with a lower scatter window set at 297 keV with 20% energy window).

Qualitative analysis

To perform qualitative analysis, all SPECT images were analysed by a consensus between three nuclear medicine physicians (each with at least 3 years of experience). The subsequent images were blindly graded by each observer; "S" was given when the sphere was observed, and "NS" was given when the sphere was not observed. The final qualitative evaluation for each sphere was based on a consensus between at least 2 out of the 3 observers.[15] Cohen's kappa (k) statistic was used to assess agreement between the observers.[16]

Quantitative analysis

For quantitative analysis, we calculated contrast and contrast-to-noise ratio (CNR) for each sphere using equations 1 and 2.[14]

$$contrast = \frac{|C - C_B|}{C_B} \quad (1)$$

$$CNR = \frac{|C - C_B|}{\sigma_B} \quad (2)$$

where C is the mean pixel value in the sphere region of interest (ROI), C_B is the mean voxel value in the background ROI, and σ_B is the standard deviation (SD) in the background ROI. Then, ROIs were created and positioned on the co-registered CT image with the size being about 50% of each sphere. The background ROI was delineated at the center of the phantom. To eliminate inconsistency, the ROIs were repeatedly drawn on three separate occasions. The mean CNRs and SDs were calculated (mean±SD) and plotted. A two-tailed, paired student t-test was used to determine statistical significance by setting the probability (p=0.05, 95% confidence interval).

Results

Based on our experiments, Figure 1 shows the sample of selected transverse (axial) images of the NEMA IEC body phantom for different acquisition times per frame of the hot lesion with no background (row A) and the hot lesion with a warm background at a ratio of 10:1 (row B).

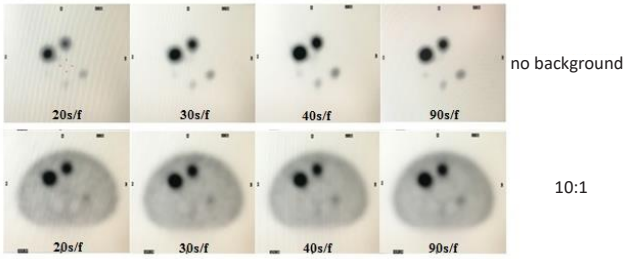

Figure 1. *Examples of selected transverse (axial) images of the NEMA/IEC (National Electrical Manufacturers Association/International Electrotechnical Commission) body phantom with (a) hot lesion with no background and (b) hot lesion with warm background at a ratio of 10:1, with acquisition times at 20, 30, 40, and 90 s/f.*

The qualitative results after consensus from three experienced nuclear medicine physicians are tabulated in Table 1. For hot lesions with no background, all spheres were observed at every acquisition time. In contrast, the smallest sphere (0.52 mL, ID 10 mm) was not seen even with the longest acquisition of 90 s/f for hot lesions with a warm background at a ratio of 10:1.

Table 1 Qualitative result (consensus from 2 out of 3 observers).

	Acquisition time (time per frame)							
	20 s		30 s		40 s		90 s	
Volume (mL)	NB[a]	10:1[b]	NB[a]	10:1[b]	NB[a]	10:1[b]	NB[a]	10:1[b]
26.52	S	S	S	S	S	S	S	S
11.49	S	S	S	S	S	S	S	S
2.57	S	S	S	S	S	S	S	S
1.15	S	S	S	S	S	S	S	S
0.52	S	NS	S	NS	S	NS	S	NS

[a]*NB: hot lesion with no background,* [b]*10:1: hot lesion with a warm background at a ratio of 10:1.*

For quantitative analysis, effects of acquisition time on image contrast (mean±SD) for each sphere are presented in Figure 2. The contrast decreased as the acquisition time shortened. The highest contrast was observed when setting the acquisition time 90 s/f and the larger sphere presented with greater contrast as expected. For hot lesions with no background, the image contrast for small spheres (0.52 mL, 1.15 mL, and 2.57 mL) of 30 and 40 s/f acquisitions were oscillated, which is further discussed in the following section. The image contrast for lesion to background ratio 10:1 for all spheres were as anticipated.

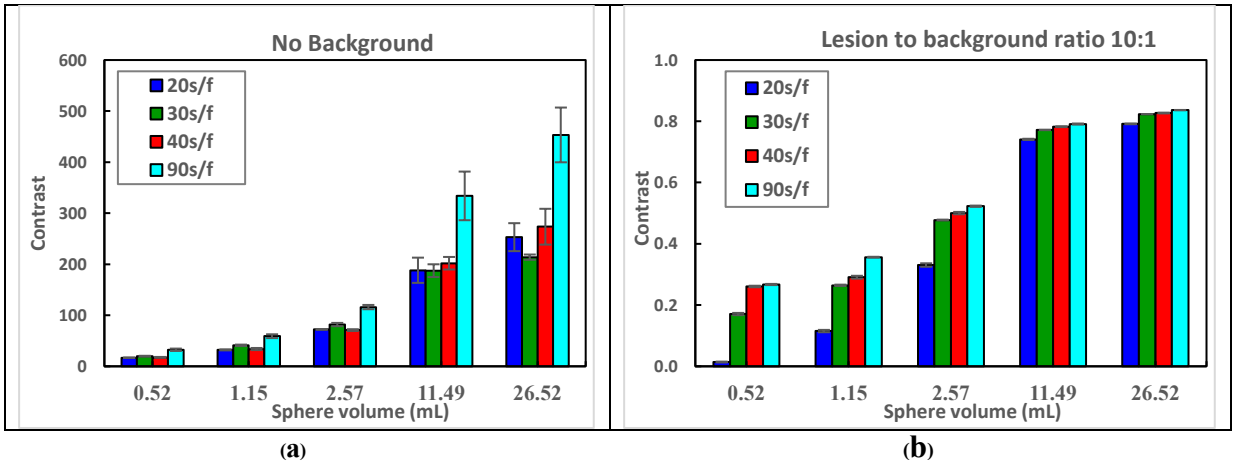

Figure 2. *Image contrast (mean±SD) plot with sphere sizes. The blue, green, red, and light blue represent acquisition times at 20, 30, 40, and 90 s/f. (a): hot lesion with o background, (b): hot lesion with a warm background at a ratio of 10:1.*

The plot of CNR (mean±SD) for each sphere volume as a function of acquisition time per frame is shown in Figure 3. As expected, the highest CNR was found when scanning with 90 s/f for both conditions. For the hot lesion with no background, the CNRs increased when acquisition time was prolonged, especially in large spheres (sizes of 11.49 and 26.52 mL). For the hot lesion with a warm background at a ratio of 10:1, the mean CNRs also increased when acquisition time was increased; interestingly, these longer acquisition times had a greater effect on CNR compared with the hot lesion with no background.

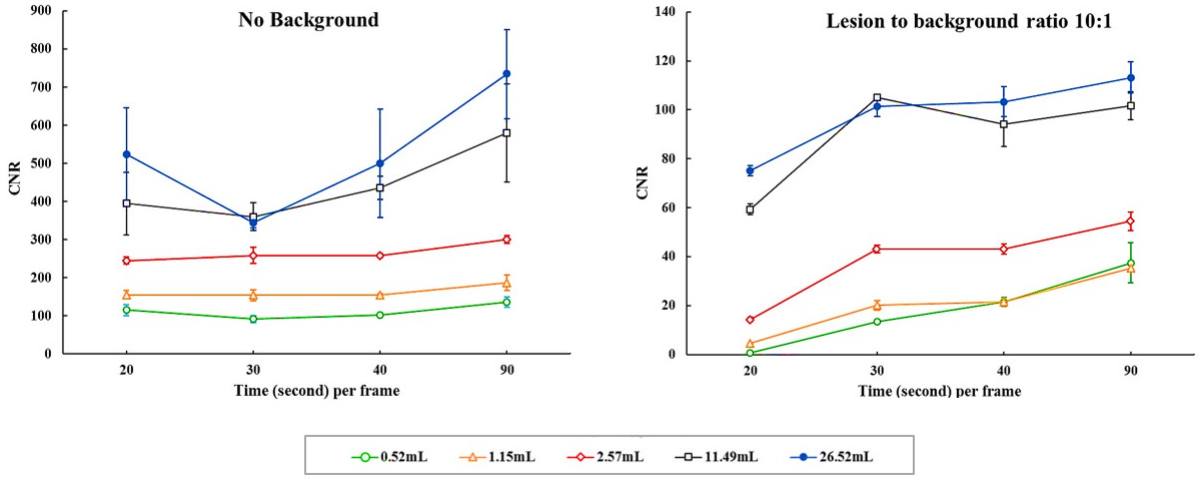

Figure 3. *Quantitative contrast-to-noise ratio (CNR) analysis (mean±SD) plot with acquisition time (time per frame). (a) hot lesion with no background and (b) hot lesion with a warm background at a ratio of 10:1.*

Additionally, the statistical results of ^{131}I quantification are presented in Table 2. Here, the mean CNR of acquisition time at 40 s/f (our clinical setting) was used as a standard to compare with other data sets. The data were considered statistically significant when $p<0.5$.

Table 2 Statistical results of ^{131}I quantitative evaluation.

	Statistical Results (time per frame)[a]					
	20 second		30 second		90 second	
Volume (mL)	NoBkg	10:1	NoBkg	10:1	NoBkg	10:1
26.52	Y	X(p=0.0173)	Y	Y	Y	Y
11.49	Y	X(p=0.0242)	Y	Y	Y	Y
2.57	Y	X(p=0.0020)	Y	Y	X(p=0.0067)	X(p=0.0194)
1.15	Y	X(p=0.0060)	Y	Y	Y	X(p=0.0004)
0.52	Y	X(p=0.0025)	Y	X(p=0.0178)	Y	Y

[a]*X: significant differences (p<0.05), Y: not significantly different.*

The statistical results for the hot lesion with no background indicate that mean CNRs for acquisition times at 20 and 30 s/f were similar to that at 40 s/f. Meanwhile, the CNR for the 2.5-mL sphere was statistically different at 90 s/f (p=0.0067). For the hot lesion with a warm background at a ratio of 10:1, the mean CNRs for all spheres acquired at 20 s/f were statistically different from those at 40 s/f. Significant results were also found in the smallest sphere (0.52 mL) at 30 s/f, and in the 1.15- and 2.57-mL spheres at 90 s/f.

Discussion

The qualitative performance of SPECT imaging was evaluated by three experienced nuclear medicine physicians. For infinite contrast (no background), all volume sizes of the spheres (0.52 to 26.52 mL) were detected at all acquisition times (20, 30, 40, and 90 s/f). This agrees well with the published work by Erdi, who also reported the detectability limit of radioiodine with SPECT at a tumour diameter of about 1 cm (volume about 0.53 mL).[17]

For hot lesion with a warm background at a ratio of 10:1, this ratio was typically found in clinical studies such as ^{131}I-metaiodobenzylguanidine (mIBG) for tumour imaging.[12] Our qualitative results indicate that the nuclear medicine physicians could not detect the smallest sphere of 0.52 mL. As the consensus result was used to evaluate the same set of SPECT images, consequently, the inter-observer and Kappa agreement were also analysed (as tabulated in Table 3).

Table3 Kappa analysis for inter-observer agreement.

Observer[a]	Percentage Observed Agreement	Kappa Agreement (K)	Interpretation [b]
Observer 1 vs. Observer 2	100.00	1.000	Perfect Agreement
Observer 1 vs. Observer 3	87.50	0.479	Moderate Agreement
Observer 2 vs. Observer 3	87.50	0.479	

[a]*observer 1, observer 2, and observer 3 have work experience of 7, 6, and 4 years, respectively,* [b]*Interpretation of kappa is based on published work by Viera AJ and Garrett JM.*

Based on Table 3, the agreement between observers 1 and 2 (K=1.000) was higher than that between observers 1 and 3 (K=0.479), and that between observers 2 and 3 (K=0.479). Despite having at least 3 years of experience, the differences between their years of experience have been clearly demonstrated in this study as the agreement was higher and more consistent for the more experienced observer. Hence, this can be noted as one of the limitations of this study.

In this study, the effect of acquisition time on quantitative detectability was examined using contrast and CNR. Contrast is related to diameter of sphere, uptake ratio, and resolution of imaging system. The measured contrast decreased when the acquisition time was shortened. Additionally, the contrast detail was inferior in the small spheres. This might have resulted from the partial volume effect (PVE), which is related to poor resolution of imaging systems and usually results in underestimating the activity. Many published works suggest that the object size must be larger than 2 times the system's full-width at half maximum (FWHM) to avoid PVEs.[18-20] The Medical Internal Radiation Dose (MIRD) pamphlet no.24: *Guidelines for quantitative ^{131}I SPECT in dosimetry applications* recommended that PVEs due to poor resolution of ^{131}I SPECT can be observed for any volumes that are smaller than approximately 8 mL (about 25 mm diameter).[21] Hence, according to the IEC phantom specification, only the 26.52 mL-spheres (37 mm diameter) and 11.49 mL-spheres (28 mm diameter) did not suffer from PVEs.

Imaging performance in terms of contrast and CNR was investigated in this work. As a rule of thumb, contrast increases with longer acquisition times due to higher count levels. Additionally, contrast in larger spheres is greater than that in smaller spheres, which also result in a loss in count signal from the PVE as described above. However, it

would be more representative to consider the noise component based on CNR, rather than only raw contrast signal. For the phantom with hot lesion without activity in the background, the mean CNRs improved with increased acquisition times. This result agreed well with those presented by M Elschot *et al*., who remarked that the CNR in hot spots was related to the number of counts in the region.[22] Furthermore, a recent study by M Brambilla *et al*. also demonstrated that contrast or CNR is associated with the number of counts in the data set.[23] Their result indicated that low counts lead to higher levels of deviation and non-Poisson statistics, which may reduce the CNR and quantitative accuracy. This is evident by the relatively high standard deviation of the analysed contrast and CNR as shown in Figure 2 and 3 in the short acquisition time.

Regarding the effects of sphere size, larger spheres were found to have higher CNRs compared to smaller spheres. This also resulted from a loss in count signal for objects with diameters that are small or similar in size to the resolution of the system. For the condition of lesion to background ratio of 10:1, the mean CNRs for each sphere were decreased compared to those with no background conditions. In this study, the ROI was fixed with the size of about half of the diameter of each sphere, using CT data as a guide for the ROI location. This helped to minimize the counts from background activity. However, the decrease in CNR also resulted from elevated background radiation from the scattered ^{131}I photons.

From the two-tailed, paired student t-test statistical analysis as tabulated in Table 2, there was no statistical significance between mean CNRs when acquired at 20 and 30 s/f for all sphere sizes compared to our clinical practice (40 s/f) when no background activity was present. Nevertheless, mean CNR of 2.57-mL sphere acquired with 90 s/f was statistically significant (p=0.0067), while larger and smaller spheres were not statistically different in the no background condition. However, these results included a large SD from drawing ROIs in the background region. This could be due to the scattered photons as we observed that background noises were higher in the no background condition than that of hot lesion with a warm background at a ratio of 10:1. On the other hand, for the hot lesion with a warm background at a ratio of 10:1, mean CNRs acquired at 20 s/f were significantly different from our current clinical practice for all sphere sizes. In addition, the statistical result indicates that only the mean CNR of the smallest sphere (0.52 mL) significantly differed when acquired at 30 s/f, while the other spheres presented no difference. This indicates that the acquisition time per frame must be carefully considered when the lesions are small and background activity is present. At 90 s/f, the results were undersigned as the mean CNRs of the 1.15 mL- and 2.57-mL spheres were not statistically significant while the other spheres (0.52, 11.49, and 26.52 mL) presented no difference. This error might explain the experimental error of CNR at 90 s/f. Hence, repeating this experiment is required for further study.

Furthermore, the main limitation of this work is that the data were only generated from a phantom, which is not sufficient for an actual clinical situation in terms of exact organ shape, non-uniform distribution, and the activity concentration in the organ. For the latter factor, the simulated concentration of 740 kBq/mL in our study did not cover all ^{131}I concentrations in clinical practice. However, the data may provide an idea of the method to determine the effects of acquisition time and lesion detectability. Additionally, this work was studied on a 25.4 mm (1 inch) thick crystal SPECT system. Data obtained with a standard 9.5 mm (3/8 inch) thick crystal could have resulted in lower efficiency. However, the clinical impact of this study has demonstrated that it is possible to reduce the total scanning time and the image quality is still clinically acceptable. This can reduce motion artefacts due to long scanning times. Moreover, this work has provided a study model to extend this qualitative and quantitative analysis to optimize other related factors, such as reconstruction parameters and other scatter modelling methods for lesion detectability with ^{131}I SPECT.

Conclusion

The effect of acquisition time on image quality and lesion detectability of 131I SPECT was quantitatively and qualitatively analysed using NEMA/IEC phantom. The clinical impact of this study could be shortening total scan time by determining the lesion size and background activity from the whole-body image prior to SPECT. For no background condition, the acquisition time could be set at 20 or 30 s/f (instead of 40 s/f), which led to reducing 5 to 10 minutes of total acquisition time. Based on our results, there was no statistically significant difference in terms of CNR when compared with 40 s/f, as well as with qualitative assessment by experienced observers. For the lesion with a warm background at a ratio of 10:1, the reduction is possible. However, the size of the lesion should be considered, especially when the lesions are small.

Conflict of interest

The authors declare that they have no conflicts of interest.

Ethic approval

This article does not contain any studies performed with human participants and animals.

References

[1] Xue Y-L, Qiu Z-L, Perotti G, Salvatori M, Luo Q-Y. 131I SPECT/CT: a one-station imaging modality in the management of differentiated thyroid cancer. Clin Transl Imaging. 2013; 1(3): 163-73.

[2] Salvatori M, Perotti G, Villani MF, Mazza R, Maussier ML, Indovina L, et al. Determining the appropriate time of execution of an I-131 post-therapy whole-body scan: comparison between early and late imaging. Nucl Med Commun. 2013; 34(9): 900-8.

[3] Beijst C, Kist JW, Elschot M, Viergever MA, Hoekstra OS, de Keizer B, et al. Quantitative Comparison of 124I PET/CT and 131I SPECT/CT Detectability. J Nucl Med. 2016; 57(1): 103-8.

[4] Kenneth FK, Anastasia Y, Yuni KD. Recovery of total I-131 activity within focal volumes using SPECT and 3D OSEM. Phys Med Biol. 2007;52(3): 777.

[5] Rault E, Vandenberghe S, Van Holen R, De Beenhouwer J, Staelens S, Lemahieu I. Comparison of image quality of different iodine isotopes (I-123, I-124, and I-131). Cancer Biother Radiopharm. 2007; 22(3): 423-30.

[6] Oh JR, Byun BH, Hong SP, Chong A, Kim J, Yoo SW, et al. Comparison of (1)(3)(1)I whole-body imaging, (1)(3)(1)I SPECT/CT, and (1)(8)F-FDG PET/CT in the detection of metastatic thyroid cancer. Eur J Nucl Med Mol Imaging. 2011; 38(8): 1459-68.

[7] Radioiodine Scintigraphy with SPECT/CT: an Important diagnostic tool for thyroid cancer staging and risk stratification. J Nucl Med. 2012;53(5): 754-64.

[8] He B, Frey EC. Effects of shortened acquisition time on accuracy and precision of quantitative estimates of organ activity. Med phys. 2010; 37(4): 1807-15.

[9] Bar R, Przewloka K, Karry R, Frenkel A, Golz A, Keidar Z. Half-time SPECT acquisition with resolution recovery for Tc-MIBI SPECT imaging in the assessment of hyperparathyroidism. Mol Imaging Biol. 2012; 14(5): 647-51.

[10] Aldridge MD, Waddington WW, Dickson JC, Prakash V, Ell PJ, Bomanji JB. Clinical evaluation of reducing acquisition time on single-photon emission computed tomography image quality using proprietary resolution recovery software. Nucl Med Commun. 2013; 34(11): 1116-23.

[11] Thientunyakit T, Taerakul T, Chaudakshetrin P, Ubolnuch K, Sirithongjak K. A comparison of the diagnostic performance of half-time SPECT and multiplanar pelvic bone scan in patients with significant bladder artifacts. Nucl Med Commun communications. 2013; 34(3): 233-9.

[12] Tan HK, Wassenaar RW, Zeng W. Collimator selection, acquisition speed, and visual assessment of 131I-tositumomab biodistribution in a phantom model. J Nucl Med Technol. 2006; 34(4): 224-7.

[13] Pereira JM, Stabin MG, Lima FRA, Guimarães M, Forrester JW. Image quantification for radiation dose calculations – limitations and uncertainties. Health phy. 2010; 99(5): 688-701.

[14] Van Gils CA, Beijst C, Van Rooij R, De Jong HW. Impact of reconstruction parameters on quantitative I-131 SPECT. Phys Med Biol. 2016; 61(14): 5166-82.

[15] Trägårdh E, Johansson L, Olofsson C, Valind S, Edenbrandt L. Nuclear medicine technologists are able to accurately determine when a myocardial perfusion rest study is necessary. BMC Med Inform Decis Mak. 2012; 12(1): 97.

[16] Viera AJ, Garrett JM. Understanding interobserver agreement: the kappa statistic. Fam Med. 2005; 37(5): 360-3.

[17] Erdi YE. Limits of tumor detectability in nuclear medicine and PET. Mol Imaging Radionucl Ther. 2012; 21(1): 23.

[18] Kessler RM, Ellis JR, Jr., Eden M. Analysis of emission tomographic scan data: limitations imposed by resolution and background. J Comput Assist Tomogr. 1984; 8(3): 514-22.

[19] Zaidi H. Quantitative Analysis in Nuclear Medicine Imaging: Springer US; 2006.

[20] Burg S, Dupas A, Stute S, Dieudonné A, Huet P, Guludec DL, et al. Partial volume effect estimation and correction in the aortic vascular wall in PET imaging. Phys Med Biol. 2013; 58(21): 7527.

[21] Dewaraja YK, Ljungberg M, Green AJ, Zanzonico PB, Frey EC, Bolch WE, et al. MIRD pamphlet No. 24: Guidelines for quantitative 131I SPECT in dosimetry applications. J Nucl Med. 2013; 54(12): 2182-8.

[22] Elschot M, Vermolen BJ, Lam MG, de Keizer B, van den Bosch MA, de Jong HW. Quantitative comparison of PET and Bremsstrahlung SPECT for imaging the in vivo yttrium-90 microsphere distribution after liver radioembolization. PLoS One. 2013; 8(2): e55742.

[23] Brambilla M. Performance evaluation of hardware and software for spect cardiac imaging. Physica Medica. 2016; 32, Supplement 3: 179.

Journal of Associated Medical Sciences 2021; 54 (3): 84-91

JAMS
Journal of Associated Medical Sciences

Thai-Journal Citation Index Centre (TCI) & ASEAN Citation Index (ACI)

Journal of Associated Medical Sciences

Journal homepage: https://www.tci-thaijo.org/index.php/bulletinAMS/index

Quality of life outcomes following 1 year encouragement of pelvic floor muscle exercise among urinary incontinence women living in the community

Jitapa Chawawisuttikool Thanyaluck Sriboonreung Araya Yankai Arisa Parameyong *

Department of Physical Therapy, Faculty of Associated Medical Sciences, Chiang Mai University, Chiang Mai Province, Thailand

ARTICLE INFO

Article history:
Received 25 April 2021
Accepted as revised 16 August 2021
Available online 16 August 2021

Keywords:
Urinary incontinence, pelvic floor muscles exercise, quality of life, long-term effect.

ABSTRACT

Background: Urinary incontinence (UI) is a silent problem affecting women's health. This problem causes lower self-confidence to participate in various activities. Pelvic floor muscle exercise (PFE) is the first recommended for treatment of UI. Adherence to PEF is the key to success in maintaining continence. However, no studies have supported the effect of sustaining PFE continually on the symptoms of UI and the quality of life (QoL) in the long term.

Objectives: This study aimed to investigate the effect of the 1-year encouragement of PFE on UI symptoms and the quality of life among incontinence women living in the community.

Materials and methods: Thirty-four women with UI aged between 50-70 years were invited in this study. The women were interviewed for the UI variables including the ability to hold urine, the frequency and amount of UI, feeling urgency to urinate, the frequency of urination during the daytime and nighttime. Additionally, the King's health questionnaire (KHQ- Thai version) was used to measure the quality of life. The UI variables and KHQ were measured at baseline, 3rd, 6th, 9th and 12th months of the intervention. PFE program was provided to participants after baseline measurement and encouraged to perform continually and consistency for 1 year. Descriptive statistics, one-way repeated ANOVA and Friedman test were used to analyze the data.

Results: At the end of program, 24 women (92.3%) had no problems with urinary control. In part of the frequency and the amount of stress UI, all of them were completely improves (100%). In terms of the symptoms associated with urged UI such as the feeling urgency to urinate, most of them had no hustle during urination (80.8%). The frequency of urination was reduced, all of them had less than 5 times urination during the day. The severity of symptoms associated with UI was significantly different compared to baseline. In addition, the KHQ score for all items was lower, indicating a higher QoL when compared to baseline.

Conclusion: Longterm promoting of PFE was effective for the improvement of UI and significantly increased the QoL among incontinence women living in communities.

* **Corresponding author.**
Author's Address: *Department of Physical Therapy, Faculty of Associated Medical Sciences, Chiang Mai University, Chiang Mai Province, Thailand.*
** **E-mail address:** arisa.p@cmu.ac.th
doi: 10.14456/jams.2021.28
E-ISSN: 2539-6056

Introduction

Urinary incontinence (UI) is defined as involuntary leakage of urine. UI is divided into 3 types: stress urinary incontinence (SUI), urge urinary incontinence (UUI) and mixed urinary incontinence (MUI).[1-3] SUI is involuntary leakage of urine during an effort or physical exertion (e.g. sporting activities), or on sneezing or coughing. SUI is the most common form of UI which is caused by poor urethral support by pelvic floor muscle during an increased abdominal pressure pushes down on the bladder. UUI is the involuntary urine loss associated with sudden and strong desire to urinate. UUI is commonly known as overactive bladder which usually caused by involuntary contractions of the detrusor muscle of the bladder wall at improper times. MUI is the symptoms that include both stress and urge UI. UI is a silent health problem affecting many community-dwelling, especially in women more than men. The prevalence of the UI is estimated that 22-48 % in women and increased with age significantly every year.[4] This problem causes a lower quality of life (QoL) in various aspects such as physical and mental health, hygiene, economy, career, social, family and even sexual relations. Regarding psychosocial health, UI causes stress, depression, annoyance, anxiety, embarrassment, lack of confidence, refusal to participate in various activities outdoor and even withdrawal from social.[5]

Pelvic floor muscle exercise (PFE) is the conservative interventions recommended as the first-line treatment of UI.[6] This type of exercise is very easy and does not take too much time. The exercise consists of fast and slow contraction of pelvic floor muscles 30 times a day. Beginning with rapid and maximal contraction about 5-10 times, followed by squeeze and hold about 5-10 seconds, 5-10 times, with a variety of starting positions (lying, sitting and standing).[7] The effectiveness of the PFE in the management of UI has been shown by several studies.[3, 7-8] Additionally, the systemic reviews had demonstrated that PFE significantly improves QoL.[9] PFE is beneficial in women with SUI. However, PFE sometimes also recommends for UUI and MUI. There was a systematic review indicated that PFE can improve symptoms of SUI and all other types of UI.[10] The Guideline of UI, National Institute for Health and Care Excellence (NICE) and International Continence Society (ICS) recommend that PFE program should be continued for at least 3 months to achieve the improvements.[1, 11] Nevertheless, the improvements are not always sustained over the long term. The effectiveness will lessen with time if there is no continuity of exercise.[12] Poor exercise adherence is the main obstacle in the management of UI. The factor related to reduction in frequency of exercise including not having enough time, forgetting to do exercise and boredom with the exercise.[13] A possible way to maintain continence and quality of life is to sustain the adherence of PFE in everyday life. Venegas et al.[14] indicated that the patient-related factor is the strongest influence on long term adherence to PFE. They suggested that strategies involving reminders to perform the exercise may be useful for long term adherence. The strategies may include personalized written form and progress visits every 3-6 months to encourage and motivate a woman with UI to perform the exercise. It would be helpful to apply this strategy among UI women living in the community. However, there is no studies have supported the effect of sustaining PFE continually on the symptoms of UI and the quality of life for the long term. Therefore, this study aimed to investigate the effect of 1-year encouragement of PFE on UI symptoms and quality of life among incontinence women living in the community.

Materials and methods

Study design and participants

This was a community-based study conducted in the Sri Bua Ban Subdistrict, Lamphun Province, Thailand. Forty women who acknowledged having UI were invited by community health agents to participate in this study by screening with the two standard questions “Do you leak urine during physical activities such as coughing, running or sneezing?” and “Does urine leak when you rush to the toilet? These two questions were used to determine the women's eligibility in this study. The women who reported at least one time of involuntary loss of urine in the last one week were considered having UI. The inclusion criteria include incontinence women aged between 50-70 years who capable of reading, writing and agreed to participate in this study. The exclusion criteria were as follows: women suffering from neurological conditions, pregnant women or presented of the symptoms of urinary tract infection. The participants were withdrawn if they are unable to continue the PFE program (lacking more than 2 times of meeting) or request to stop participating in the program. There were thirty-four participants who met-the inclusion criteria. All participants gave their informed and written consent before the commencement of the study. The study was approved by the research ethics committee for research in humans, Faculty of Associated Medical Science, Chiang Mai University (Project code AMSEC-60EX-016).

Measurements

The outcome measured included the symptoms and severity of UI variables (the ability to hold urine, the leakage of urine while coughing or sneezing, the frequency and the amount of leakage etc.) and the KHQ Thai-version to measure the quality of life. Outcomes were measured at baseline, 3rd, 6th, 9th and 12th months of the intervention. The details of outcomes measurements are described below.

The incontinence urinary variables questionnaire

The participants were interviewed individually regarding the symptoms related to UI. There are seven aspects of questions including the ability to hold urine, the frequency of urine leakage while coughing or sneezing, the urgent feeling to urinate, the frequency and the amount of leakage and the frequency of urination during daytime and nigh time. The question was modified from international consultation on incontinence questionnaire-female lower urinary tract symptoms (ICIQ-FLUTS) Thai-version.[15] The participants were asked to rate the severity of symptoms from zero to four, less number indicating the less severity and the high number indicating severe problem. For example,

the aspect of frequency of leakage, 1= none, 2= once a week or very little, 3= once a day or moderate problem and 4= several times a day or many problems. The detail of other aspects are described in the Table 2.

King's health questionnaire

KHQ is the most commonly used questionnaire for measuring the quality of life that is specific for people with urinary incontinence. This questionnaire was translated to Thai-version with a good reliability.[16] Originally, it is a self-administered questionnaire without needing an interviewer. However, some question is needed to clarify in elderly women especially women in community dwelling. Thus, the procedure for answering in this study performed in conference room and divided into equal groups, with four physical therapists present in each group to explain the question if they need. As well as helping to read the questionnaire in those who cannot see the letters clearly. Therefore, participants answered the questionnaires themselves. KHQ has two parts consisting of twenty-one items and separated in nine domains. Part one considers general health perception and incontinence impact on life. Part two consists with the limitations, relationships, emotion and the incontinence severity. In part of KHQ, each domain is scaled from 0; best to 100; worst. The lower KHQ scores is an indication of a better quality of life.[17]

Pelvic floor muscle exercise program

The intervention program was conducted in the community by a physical therapist with more than 5 years of experience teaching in UI women. After the confirmation about incontinence symptoms, participants were educated about the structure and function of the pelvic floor and the associated factor of the UI. Then, the researcher educated the participants on how to perform a correct pelvic floor muscle contraction by practicing as a group and examining individually. The program consists of the strong and fast contraction of pelvic floor muscles (contract/relax) for 5-10 times and followed by sustained pelvic floor muscle contraction holding for 5-10 seconds. The time holding the contraction of pelvic floor muscle gradually increase depending on each participant. This program was counted as 1 set, making a total of 30 sets per day at least 3-4 days a week.[18]

Participants were asked to fill out in the self-daily report after they do this program. In addition, participants were followed up by monthly phone calls to tracking and encourage the consistency in the training program. Moreover, the researcher organizes a meeting every 3 months during the trial to monitor consistency and adherence to the training program. Including collecting and checking the logbook daily report from participants and receiving new book until reaching 1 year.

Data analysis

Descriptive statistics were used to describe demographic data and UI variables. Friedman and Wilcoxon Signed Ranks Test were used to compare the UI variables from baseline and in 3, 6, 9 and 12 months after treatment. All of the variables of KHQ showed normal distribution. Therefore, one-way repeated measure ANOVA was used to compare the quality of life measured by KHQ scores before (baseline), and at 3rd, 6th, 9th and 12th months after treatment. The level of significance was set at $p<0.05$. The statistical analyses were performed using SPSS for windows version 20.

Results

There were thirty-four women participated in this study. However, at the 3rd months of intervention, there was 1 drop off because of moving to another province. Between the 6th to 9th month we had two participants requested to leave due to illness, one for taking care of the newly born nephew and there were four drop out without answering the phone. Finally, only twenty-six participants finished the program. The mean age of participants was 57.85±4.4. The most prevalent type of UI was SUI (65.4%); followed by MUI (26.9%) and UUI (7.7%). The level of education of all participants is a primary school. Their characteristics of participants are presented in Table 1. The descriptive data for UI variables presented in Table 2. At baseline, 18 of them (69.2%) was answering that they had a little problem in the ability to hold the urine, 5 (19.2%) had a moderate problem and 3 (11.5%) had many problems to control the urine. During the intervention from 3rd to 12th months, the UI variables showed gradually improves. At the end of the program 24 of them (92.3%), found that they had no problems with urinary control and 2 (7.7%) saying that there was only a little problem. In part of the frequency of urine leak while having activity (such as coughing, sneezing), all of them (100%) had no urine leakage while coughing, sneezing and during the general day. In addition, the frequency of UI and the amount of UI during the general day was also completely improved. In terms of the symptoms associated with UUI such as the feeling urgency to urinate results showed that 21 of them (80.8%) had no hustle, 3 (11.5%) had infrequent urgency and 2 (7.7%) had hurry sometimes. The frequency of urination was reducing both during the daytime and nighttime. During the daytime, we found 100% participants had less than 5 times urination during the day considered it as normal status. For the night-time, 11 of them (42.3%) did not have urination, 15 (57.7 %) had once to twice times urination during the nighttime.

The severity of the UI variables was analyzed and presented in Table 3, the results showed that the severity of the UI variables is significant change from 3rd, 6th, 9th and 12th of intervention when compared to baseline. Considering each period, all UI variables significant change after three months of intervention when compared to baseline except the frequency of urination during day-time. For the QoL, all 9 items of the KHQ was found gradually reducing score from 3rd to 12th months. All items of the QoL is significantly different when compared to baseline (p=0.001). In part of personal relationships, emotions, sleep/energy and incontinence severity after the ending of the program, the score is reduced to zero which indicated that a better of QoL (Table 4).

Table 1 Characteristics of participants (n=26).

Data	Mean±SD
Age (years)	57.85±4.4
Weight (kg)	57.42±7.1
Height (cm)	153.35±5.1
BMI (kg/m^2)	24.35±3.2
Type of Urinary incontinence*	
- Stress	17 (65.4%)
- Urge	2 (7.7%)
- Mixed	7 (26.9%)
Mode of delivery*	
- Vaginal	25 (96.2%)
- Cesarean	1 (3.8%)
Number of deliveries*	
- No	1 (3.8%)
- 1 time	7 (26.9%
- 2 times	16 (61.5%)
- 3 times	2 (7.7%)

**Data presents as number (%)*

Table 2 Percentage distribution of participants according to symptoms and severity of urinary incontinence.

Urinary incontinence variables	Number (%)				
	baseline	3 months	6 months	9 months	12 months
The ability to hold urine					
no problem		8 (30.8%)	16 (61.5%)	8 (30.8%)	24 (92.3%)
a little problem	18 (69.2%)	13 (50.0%)	8 (30.8%)	11 (42.3%)	2 (7.7%)
moderate problem	5 (19.2%)	4 (15.4%)	1 (3.8%)	7 (26.9%)	-
many problem	3 (11.5%)	1 (3.8%)	1 (3.8%)	-	-
Stress incontinence while coughing or sneezing					
no problem	2 (7.7%)	2 (7.7%)	5 (19.2%)	8 (30.8%)	26 (100%)
a little problem	8 (30.8%)	13 (50%)	17(65.4%)	13 (50.0%)	-
moderate problem	7 (26.9%)	8 (30.8%)	3 (11.5%)	5 (19.2%)	-
many problem	9 (34.6%)	3 (11.5%)	1 (3.8%)	-	-
Frequency of leakage					
none		7 (26.9%)	14 (53.8%)	12 (46.2%)	26 (100%)
once a week or very little	17 (65.4%)	16 (61.5%)	9 (34.6%)	14 (53.8%)	-
2-3 times a day	4 (15.4%)	-	2 (7.7%)	-	-
several times a day	5 (19.2%)	3 (11.5%)	1 (3.8%)	-	-
The amount of protection use					
none	4 (15.4%)	7 (26.9%)	5 (19.2%)	13 (50.0%)	26 (100%)
permeate underwear	13 (50.0%)	14 (53.8%)	16 (61.5%)	12 (46.2%)	-
change underwear	6 (23.1%)	4 (15.4%)	4 (15.4%)	1 (3.8%)	-
change the pant	3 (11.5%)	1 (3.8%)	1 (3.8%)	-	-

Table 2 Percentage distribution of participants according to symptoms and severity of urinary incontinence. (continues)

Urinary incontinence variables	Number (%)				
	baseline	3 months	6 months	9 months	12 months
Feeling urgency to urinate					
don't hurry		2 (7.7%)	5 (19.2%)	13 (50.0%)	21 (80.8%)
infrequency		7 (26.9%)	14 (53.8%)	8 (30.8%)	3 (11.5%)
sometimes	9 (34.6%)	11 (42.3%)	6 (233.1%)	4 (15.4%)	2 (7.7%)
every time	17 (65.4%)	6 (23.1%)	1 (3.8%)	1 (3.8%)	-
Frequency of urination during daytime					
less than 5 times	19 (73.1%)	22 (84.6%)	25 (96.2%)	26 (100%)	26 (100%)
5-6 times per day	6 (23.1%)	4 (15.4%)	1 (3.8%)	-	-
6-7 times per day	1 (3.8%)	-	-	-	-
every hour per day	-	-	-	-	-
Frequency of urination at night					
none	5 (19.2%)	5 (19.2%)	5 (19.2%)	8 (30.8%)	11 (42.3%)
1-2 time	6 (23.1%)	17 (65.4%)	18 (69.2%)	11 (42.3%)	15 (57.7%)
3-4 times	9 (34.6%)	4 (15.4%)	3 (11.5%)	7 (26.9%)	-
More than 4	6 (23.1%)	-	-	-	-

Table 3 Comparison of the severity of symptoms associated with urinary incontinence before and after intervention.

Urinary incontinence variables	baseline	3 months	6 months	9 months	12 months	*p* value
The ability to hold urine	2.42 ± 0.70	1.92 ± 0.80 [a]	1.50 ± 0.76 [a,b]	1.96 ± 0.77 [a,c]	1.08 ± 0.27 [a,b,c,d]	0.001
The leakage of urine while coughing or sneezing	2.88 ± 1.00	2.46 ± 0.81[a]	2.00 ± 0.69 [a.b]	1.88 ± 0.71 [a,b]	1.00 ± 0.00 [a,b,c,d]	0.001
Frequency of leakage	2.46 ± 0.91	1.96 ± 0.87 [a]	1.2 ± 0.80 [a,b]	1.54 ± 0.51 [a,b]	1.00 ± 0.00 [a,b,c,d]	0.001
The amount of leakage	2.31 ± 0.88	1.96 ± 0.77 [a]	2.04 ± 0.72	1.54 ± 0.58 [a,b,c]	1.00 ± 0.00 [a,b,c,d]	0.001
Feeling urgency to urinate	3.65 ± 0.50	2.81 ± 0.90 [a]	2.12 ± 0.80 [a,b]	1.73 ± 0.90 [a,b]	1.31 ± 0.62 [a,b,c,d]	0.001
Frequency of urination during daytime	1.31 ± 0.55	1.15 ± 0.37	1.04 ± 0.20 [a]	1.00 ± 0.00 [a,b]	1.00 ± 0.00 [a,b]	0.001
Frequency of urination at night	2.62 ± 1.06	1.96 ± 0.60 [a]	1.92 ± 0.56 [a]	1.96 ± 0.77 [a]	1.58 ± 0.50 [a,b,c,d]	0.001

[a]Statistically significant differences when compared with baseline (p<0.05), [b]Statistically significant differences when compared with 3 months (p<0.05), [c]Statistically significant differences when compared with 6 months (p<0.05), [d]Statistically significant differences when compared with 9 months (p<0.05).

Table 4 Comparison of the KHQ score before and after intervention.

KHQ domains	baseline	3 months	6 months	9 months	12 months	*p* value
General health perceptions	41.35±12.13	33.62±14.04 [a]	22.12±14.71[a,b]	18.27±15.10 [a,b]	7.69±11.77 [a,b,c,d]	0.001
Impact on life	76.93±15.69	55.13±26.57 [a]	25.64±28.76 [a,b]	15.38±23.53 [a,b,c]	7.69±14.32 [a,b,c]	0.001
Role limitations	66.67±18.26	37.82±30.75 [a]	18.59±26.38 [a,b]	6.41±12.54 [a,b,c]	6.41±11.62 [a,b,c]	0.001
Physical limitations	69.23±11.25	33.33±30.91[a]	14.74±26.39 [a,b]	3.85±7.16 [a,b,c]	3.85±7.16 [a,b,c]	0.001
Social limitations	48.72±17.52	26.07±23.72 [a]	12.39±22.73 [a,b]	2.14±6.30 [a,b,c]	0.00±0.00 [a,b,c]	0.001
Personal relationship	17.31±28.47	6.41±15.69 [a]	3.85±9.78 [a]	0.00±0.00 [a,b,c]	0.00±0.00 [a,b,c]	0.001
Emotions	32.48±15.37	18.80±18.80 [a]	6.84±10.92 [a,b]	3.85±6.99 [a,b]	0.00±0.00 [a,b,c,d]	0.001
Sleep/energy	35.90±19.83	21.80±21.48 [a]	10.26±16.38 [a,b]	5.13±10.29 [a,b]	0.00±0.00 [a,b,c,d]	0.001
Incontinence severity	32.05±17.90	19.23±16.63 [a]	13.78±15.63 [a,b]	8.97±10.78 [a,b,c]	0.00±0.00 [a,b,c,d]	0.001

[a]Statistically significant differences when compared with baseline (p<0.05), [b]Statistically significant differences when compared with 3 months (p<0.05), [c]Statistically significant differences when compared with 6 months (p<0.05), [d]Statistically significant differences when compared with 9 months (p<0.05.

Discussion

UI is a common problem found in women, especially in middle-aged and elderly women. This problem is affecting both physical and psychological health. This is a silent problem that has less help-seeking behavior and tended to delay treatment particularly in an urban community.[19] Therefore, healthcare providers should be targeted for health education and intervention regarding this problem. The PFE is the first choice recommended as means of preventing and treating UI.[1, 3, 6] Systemic reviews have addressed the positive effect of PFE on the QoL of women with UI.[9] The underlying mechanism of PFE is an increase in muscle strength and endurance of pelvic floor muscle which is urethral support. The result of this study is consistent with previous studies that an improvement in UI symptoms occur after continuously PFEs for 3 months.[20-24] In addition, PFE not only decreased the UI symptoms but also significantly improves the QoL of women with UI.[9] PFE is a non-invasive treatment that provides an effective treatment as combined with or without another treatment method such as combined with vaginal cone,[25] Bladder training[22] and pessary therapy.[26] Moreover, this exercise can performed with various training positions without affecting performance.[7] PFE is very simple and suitable to educate in UI women living in the community. This study demonstrated the effectiveness of PFE throughout 1-year encouragement emphasized on the patient-related factor include the personalized self-daily report, phone calls every month, progress visits every 3 months and remind to perform the exercise via sticker note. This strategy is very useful for long term adherence. This study found that PFE causes improve UI symptoms and QoL after 3 months and throughout the program. Additionally, the present study found that between the 6th to the 9th month after starting the program, showing relatively stable results or a tendency to worsen compared to the previous period such as the ability to control urine and QoL but when compared to the baseline, all clinically relevant in symptoms and condition related to QoL were report the good improvement. An explanation for these results may be the exercise consistency was reduced, this finding related to the self-daily report which found during the 6th to the 9th month most of the participants decreased their exercise frequency. Six months after starting the interventions is the focus point for promoting and encouraging the exercise. In this study, a professional physical therapist provided the program with intensive exercise tracking. Including calling every month and provide meetings every 3 months for 1 year to encourage, stimulate and maintain exercise consistency.

Actually, PFE is commonly recommended for SUI. According to the present study, 100 % of participants had no urine leakage while coughing, sneezing and during the general day at the end of the program. PFE used to strengthen the pelvic floor muscle and enhances the function of urethral sphincter. A research showed that PFE result in hypertrophy of the urethral sphincter and reduces bladder neck motion during coughing.[27] However, PFE sometimes also recommends for UUI and MUI.[10] The-long term of PFE in this study demonstrated the reduction of urinary frequency during the day and night time. Hersh and Salzman[28] explained that voluntary contraction of pelvic floor and relaxation reduces the incontinence by producing urethral closure and decreasing the stimulation of the central nervous system to the detrusor muscle and thus reduces the UUI. However, the cause of UI especially UUI are multifactorial, and the success of treatment might include lifestyle modification such as appropriate fluid intake, reduction of caffeine or weight loss if a patient is overweight or obese.[29] The most important key success is the exercise compliance with treatment because the pelvic floor muscle strength depends heavily on continuous training.

Besides, the QoL measured by KHQ showed a significant difference in all domains compared to baseline. Five domains showed decreasing values to zero at ending the training program which indicates a very good quality of life. This present study supports that PFE improves the quality of life as reported by other studies.[30-31] Although UI is not a life-threatening condition, it is related to restriction in personal and social life. Improvement of UI symptoms significant impact on QoL by increase self-confidence and promote social gathering which has impact on their social interaction. The decrease of urinary frequency and feeling urgency especially during the nighttime might has a positive on the quality of sleep[32] and decrease on the risk of falls, which may lead to fractures and other morbidities in the elderly.[33]

This study focuses intensively on encouraging, stimulating and following participants. Creating the motivation, adjust attitudes, and reach out to volunteers to listen, talk, and adjust individual treatment plans that do not affect work and their daily life to maintain adherence to the treatment. It would be helpful for the healthcare providers to recommend this methodology to women with UI to resolve the problem. Limitation of this study include there are a small number of participants due to request to leave and loss of follow up. Moreover, there was no control group in this study. Further study should add a control group to help strengthen the research. Although, the UI variables were modified from ICIQ-FLUTS Thai-version questionnaire, but some variables were added to clarify and cover the severity of symptoms. This questionnaire need to be validated for further study.

Conclusion

This study showed that continuous PFE is an effective treatment of UI and significantly increases the QoL among incontinence women living in communities. The motivation and encouragement on patient-related factors was effective for the improvement of UI and significantly increased QoL among incontinence women living in communities.

Conflict of interest

The authors declare that they have no conflict of interest.

Acknowledgements

This work was supported by a research grant from Faculty of Associated Medical Sciences, Chiang Mai University.

References

[1] Abrams P, Andersson K-E, Birder L, Brubaker L, Cardozo L, Chapple C, et al. Fourth International Consultation on Incontinence Recommendations of the International Scientific Committee: evaluation and treatment of urinary incontinence, pelvic organ prolapse, and fecal incontinence Neurourol Urodyn. 2010; 29(1): 213-40. doi: 10.1002/nau.20870.

[2] Haylen BT, de Ridder D, Freeman RM, Swift SE, Berghmans B, Lee J, et al. An International Urogynecological Association (IUGA)/International Continence Society (ICS) joint report on the terminology for female pelvic floor dysfunction. Int Urogynec J. 2010; 21(1): 5-26. doi: 10.1007/s00192-009-0976-9.

[3] McClurg D, Campbell P, Pollock A, Hagen S, Elders A, Hill D, et al. Conservative interventions for urinary incontinence in women: an overview of Cochrane systematic reviews. Physiotherapy. 2017; 103(1): e26-e7. doi: doi.org/10.1016/j.physio.2017.11.185.

[4] Komesu YM, Schrader RM, Ketai LH, Rogers RG, Dunivan GC. Epidemiology of mixed, stress, and urgency urinary incontinence in middle-aged/older women: the importance of incontinence history. Int Urogynec J. 2016; 27(5): 763-72. doi: 10.1007/s00192-015-2888-1.

[5] Krhut J, Gärtner M, Mokris J, Horcicka L, Svabik K, Zachoval R, et al. Effect of severity of urinary incontinence on quality of life in women. Neurourol Urodyn. 2018; 37(6): 1925-30. doi: 10.1002/nau.23568.

[6] Dumoulin C, Hunter KF, Moore K, Bradley CS, Burgio KL, Hagen S, et al. Conservative management for female urinary incontinence and pelvic organ prolapse review 2013: summary of the 5th International Consultation on Incontinence. Neurourol Urodyn. 2016; 35(1): 15-20. doi: 10.1002/nau.22677.

[7] Borello-France DF, Zyczynski HM, Downey PA, Rause CR, Wister JA. Effect of pelvic-floor muscle exercise position on continence and quality-of-life outcomes in women with stress urinary incontinence. Phys Ther. 2006; 86(7): 974-86. doi: 10.1093/ptj/86.7.974.

[8] Dumoulin C, Hay-Smith EJ, Mac Habée-Séguin G. Pelvic floor muscle training versus no treatment, or inactive control treatments, for urinary incontinence in women. Cochrane Database Syst Rev. 2014(5): CD005654. doi: 10.1002/14651858.CD005654.pub3.

[9] Radziminska A, Straczynska A, Weber-Rajek M, Styczynska H, Strojek K, Piekorz Z. The impact of pelvic floor muscle training on the quality of life of women with urinary incontinence: a systematic literature review. Clin Interv Aging. 2018; 13: 957-65. doi: 10.2147/CIA.S160057.

[10] Price N, Dawood R, Jackson SR. Pelvic floor exercise for urinary incontinence: a systematic literature review. Maturitas. 2010; 67(4): 309-15. doi:10.1016/j.maturitas.2010.08.004.tas.

[11] Syan R, Brucker BM. Guideline of guidelines: urinary incontinence. BJU Int. 2016; 117(1): 20-33. doi: 10.1111/bju.13187.

[12] Bø K, Hilde G. Does it work in the long term?—A systematic review on pelvic floor muscle training for female stress urinary incontinence. Neurourol Urodyn. 2013; 32(3): 215-23. doi: 10.1002/nau.22292.

[13] Holley RL, Varner RE, Kerns DJ, Mestecky PJ. Long-term failure of pelvic floor musculature exercises in treatment of genuine stress incontinence. South Med J. 1995; 88(5): 547-9. doi: 10.1097/00007611-199505000-00008.

[14] Venegas M, Carrasco B, Casas-Cordero R. Factors influencing long-term adherence to pelvic floor exercises in women with urinary incontinence. Neurourol Urodyn. 2018; 37(3): 1120-7. doi: 10.1002/nau.23432.

[15] Chattrakulchai K, Manonai J, Silpakit C, Wattanayingcharoenchai R. Validation of the Thai version of the International Consultation on Incontinence Questionnaire-Female Lower Urinary Tract Symptoms (ICIQ-FLUTS). Int Urogynecol J. 2020; 31(12): 2603-10. doi: 10.1007/s00192-020-04422-1.

[16] Kochakarn W, Pummangura N, Kijvikai K, Viseshsindh W, Sukying C, Lertsithichai P. Reliability of a Thai version of King's Health Questionnaire in Thai females with overactive bladder symptoms. J Med Assoc Thai. 2005; 88(11): 1526-34.

[17] Hebbar S, Pandey H, Chawla A. Understanding King's Health Questionnaire (KHQ) in assessment of female urinary incontinence. Int J Res Med Sci. 2015; 3: 531-8. doi:10.5455/2320-6012.ijrms20150301.

[18] Luginbuehl H, Baeyens J-P, Taeymans J, Maeder I-M, Kuhn A, Radlinger L. Pelvic floor muscle activation and strength components influencing female urinary continence and stress incontinence: a systematic review. Neurourol Urodyn. 2015; 34(6): 498-506. doi: 10.1002/nau.22612.

[19] Wu C, Sun T, Guan X, Wang K. Predicting delay to treatment of urinary incontinence among urban community-dwelling women in China. Int J Nur Sci. 2015; 2(1): 34-8. doi: 10.1016/j.ijnss.2015.01.015.

[20] Cacciari LP, Dumoulin C, Hay-Smith EJ. Pelvic floor muscle training versus no treatment, or inactive control treatments, for urinary incontinence in women: a Cochrane systematic review abridged republication. Braz J Phys Ther. 2019; 23(2): 93-107. doi: 10.1016/j.bjpt.2019.01.002.

[21] Dumoulin C, Hay-Smith J, Habée-Séguin GM, Mercier J. Pelvic floor muscle training versus no treatment, or inactive control treatments, for urinary incontinence in women: a short version Cochrane systematic review with meta-analysis. Neurourol Urodyn. 2015; 34(4): 300-8. doi: 10.1002/nau.22700.

[22] Sherburn M, Bird M, Carey M, Bø K, Galea MP. Incontinence improves in older women after intensive pelvic floor muscle training: an assessor-blinded randomized controlled trial. Neurourol Urodyn. 2011; 30(3): 317-24. doi: 10.1002/nau.20968.

[23] Sjöström M, Umefjord G, Stenlund H, Carlbring P, Andersson G, Samuelsson E. Internet-based treatment of stress urinary incontinence: 1- and 2-year results of a randomized controlled trial with a focus on pelvic floor muscle training. BJU Int. 2015; 116(6): 955-64. doi: 10.1111/bju.13091.

[24] Wein AJ. Re: Incontinence improves in older women after intensive pelvic foor muscle training: an assessor-blinded randomized controlled trial. J Urol. 2012; 188(4): 1232-9.

[25] Pereira VS, de Melo MV, Correia GN, Driusso P. Vaginal cone for postmenopausal women with stress urinary incontinence: randomized, controlled trial. Climacteric. 2012; 15(1): 45-51. doi: 10.3109/13697137.2011.593211.

[26] Kenton K, Barber M, Wang L, Hsu Y, Rahn D, Whitcomb E, et al. Pelvic floor symptoms improve similarly after pessary and behavioral treatment for stress incontinence. Female Pelvic Med Reconstr Surg. 2012; 18(2): 118-21. doi: 10.1097/SPV.0b013e31824a021d.

[27] McLean L, Varette K, Gentilcore-Saulnier E, Harvey MA, Baker K, Sauerbrei E. Pelvic floor muscle training in women with stress urinary incontinence causes hypertrophy of the urethral sphincters and reduces bladder neck mobility during coughing. Neurourol Urodyn. 2013; 32(8): 1096-102. doi: 10.1002/nau.22343.

[28] Hersh L, Salzman B. Clinical management of urinary incontinence in women. Am Fam Physician. 2013; 87(9): 634-40.

[29] Hu JS, Pierre EF. Urinary incontinence in women: evaluation and management. Am Fam Physician. 2019; 100(6): 339-48.

[30] Hensangvilai K, Pirunsan U, Snow WM. Effects of pelvic floor exercises on the quality of life in incontinent women. J Assoc Med Sci. 2017; 50(2): 209-16. doi: 10.14456/jams.2017.20.

[31] Paiva LL, Ferla L, Darski C, Catarino BM, Ramos JG. Pelvic floor muscle training in groups versus individual or home treatment of women with urinary incontinence: systematic review and meta-analysis. Int Urogynecol J. 2017; 28(3): 351-9. doi: 10.1007/s00192-016-3133-2.

[32] Mesas AE, LóPez-GarcíA E, RodríGuez-Artalejo F. Self-reported sleep duration and falls in older adults. J Sleep Res. 2011; 20(1 pt 1): 21-7. doi: 10.1111/j.1365-2869.2010.00867.x.

[33] Brown JS, Vittinghoff E, Wyman JF, Stone KL, Nevitt MC, Ensrud KE, et al. Urinary incontinence: does it increase risk for falls and fractures? Study of Osteoporotic Fractures Research Group. J Am Geriatr Soc. 2000; 48(7): 721-5. doi: 10.1111/j.1532-5415.2000.tb04744.x.

Journal of Associated Medical Sciences 2021; 54 (3): 92-101

JAMS
Journal of Associated Medical Sciences

Thai-Journal Citation Index Centre (TCI) & ASEAN Citation Index (ACI)

Journal of Associated Medical Sciences

Journal homepage: https://www.tci-thaijo.org/index.php/bulletinAMS/index

Effectiveness of family interventions on health outcomes of family and children with autism: An integrative review

Anh Thi Lan Mai[1*] Nujjaree Chaimongkol[2] Nguyen Manh Dung[1]

[1]Namdinh University of Nursing, Vietnam 257 Han Thuyen Street, Nam Dinh city, Nam Dinh, Vietnam.
[2]Faculty of Nursing, Burapha University 169 Longhard Bangsaen Road, Muang District, Chon Buri Province, Thailand.

ARTICLE INFO

Article history:
Received 18 April 2021
Accepted as revised 16 August 2021
Available online 16 August 2021

Keywords:
Autism, family, health outcomes, family/parent intervention, integrative review.

ABSTRACT

Background: Autism is a lifelong disability that affects a person's social interaction, both verbal and nonverbal communication, and is often characterized by restrictive and repetitive behaviors. Family of children with autism plays a critical role in child's ability to adapt and live daily life. From the extensive literature review, the research highlighted the importance of interventions for families and children with autism.

Objectives: To review and describe interventions for family and children with autism.

Materials and methods: The integrative review design adopted PRISMA protocol to select studies. This review searched within the healthcare journals with the experimental design or randomized control trial, full-text, and published from January 2013 to April 2020 using the keywords of "autism", "family", "family/parent interventions" and "health outcomes". The articles were searched in the databases of MEDLINE, PubMed, CINAHL and ScienceDirect.

Results: Nine articles were identified. The common interventions for family of children with autism were family education, psychological, and technology-related interventions. The family education intervention enhanced family quality of life, parent-child shared management, and decreased depressive symptoms. Psychological support intervention increased positive thinking and skills of the family. The technology-related intervention affected parents positively, increased confidence, and reduced parenting stress. However, some of these interventions were complicated and unstructured; therefore, the evaluation of their effectiveness remained unclear and possibly bias.

Discussion: The evidence of intervention for family of children with autism was limited. To improve health outcomes of family and children with autism, health care providers should pay more attention on developing and implementing an appropriate intervention to build strengthen of family of children with autism and improve their health outcomes.

Introduction

Autism is a lifelong disability that affects a person's social interaction, both verbal and nonverbal communication, and is often characterized by restrictive and repetitive behaviors. According to Center for Disease Control and Prevention, the prevalence rates of autism in the United States are estimated at approximately one in 54 children aged 8 years.[1] Currently, exactly possible causal factors and specific treatment for the disorder are unavailable. However, the early behavioral, educational, and pharmacological interventions have been proved to be effective in improving the skills of children with autism as well as building considerably family strengthen related to autism across lifespan.[2] Families are the most important for a child's development, especially, family of children with autism play a critical role in their child's ability to adapt and live daily life. Families present their roles in diagnosis process as they are the first

* **Corresponding author.**
Author's Address: *Namdinh University of Nursing, Vietnam 257 Han Thuyen Street, Nam Dinh city, Nam Dinh 420000, Vietnam.*
** **E-mail address:** lananh.ndun@gmail.com
doi: 10.14456/jams.2021.29
E-ISSN: 2539-6056

people to recognize the behavior problem, therefore, they support physician in receiving a right diagnosis. Additionally, in intervention process, family cooperates with health care providers in developing and implementing appropriate intervention for their child.[3] Family members typically are active partners in child's educational intervention at home and community setting to ensure the intervention process is working appropriately.[4] By simultaneously shouldering multiple roles and responsibilities, families of children with autism often feel challenged and perplexed in their children daily activities and improvement of behavioral problems in the children.

Research indicated that there were various interventions available to families of children with autism. Intervention programs depended on the autism child's developmental level, the characteristics of the health care systems and the education level of family members.[5-8] Study mentioned that education intervention is associated with an increased likelihood for the mental health related quality of life, family functioning and child outcomes as well.[5] Family education intervention should be offered especially to family of children with chronic health conditions who lack of adequate support. The intervention can help family members manage children's problems and behavior more effectively.[6] In addition, psychological interventions for parents of individuals with autism may lead to both decreased stress in parents, and improvements in child behavior.[7] And technology-based intervention has been proved that families of children with autism would receive sufficient support in dealing with geographical distance or a variety of other logistical difficulties with health care service systems.[8]

Although, these interventions have been developed, implemented and researched, most families are not able to implement the interventions because some of the interventions remained controversial of the effectiveness of the intervention on family and children outcomes. In addition, some interventions even healthcare workers and families were not aware of its availability. Others unsure effectively implement these interventions, due to the complex and unclear steps of the intervention process, some interventions without a follow-up period for evaluation of intervention sustainability.[9-12] Moreover, most studies have not assessed the effectiveness of the interventions on both family and children outcomes. Therefore, the purpose of this review was to examine the clear literature on the effectiveness of family interventions on individuals with autism and their families. The focused question that framed this review was: "What is the evidence for the effectiveness of interventions for family of individuals with autism and their families?" as indicated. The results were the integrated review as evidence about effectiveness of interventions for family of children with autism. The interventions and their effectiveness discussed in this integrated literature review may support healthcare providers to apply the appropriate intervention in promoting family effectively during the intervention for their better outcomes. They would also facilitate family role of being responsible, knowledgeable, and helpful caretakers for their children with autism. Additionally, the integrated review may support healthcare institutions in developing and implementing the policy related to interventions for children with autism not only focus on children but also their family.

Materials and methods

Search procedure and database

An integrative review approach was conducted and PRISMA were used to improve the rigorous. Search strategy: A priori search was conducted in Google Scholar and EBSCO to identify if there were any similar reviews that were in progress or already published. The results indicated that there were some systematic reviews however, no similar integrative review existed. The review included all healthcare and special education studies conducted using experimental designs that compared a group of families receiving a family intervention to a group of family with usual intervention. Then, the researchers conducted an extensive database search using MEDLINE, PubMed, CINAHL and ScienceDirect to search for relevant literature, using the keywords "autism", "family", "family/parent interventions" and "health outcomes".

Inclusion and exclusion criteria

The journal articles were defined by the following eligibility criteria: (1) population were family of children with autism; (2) interventions were interventions for family/ parents, the elements of a intervention were examined; (3) The outcomes were purposes of the interventions (e.g. children/ family quality of life, family functioning, parent-child interaction, children behaviors, social-communication skill, and learning ability); (4) The most appropriate study designs were randomized control trials. The journal articles with population of families and children with mental health and serious comorbidity were excluded in the study.

Screening process

Two authors examined articles that utilized family intervention as a focus, however, concentrated on articles dealing with the population of family of children with autism. The peer-review journal articles published after 2013 were included in the study. Researcher then searching for studies cited in these collected studies. In addition, the researcher continued to examine of reference lists from key reviews to identify additional studies that had not been identified in the previous electronic search.

Data extraction

The two researchers performed the data extraction independently, based on certain criteria of differences in terms of variables such as study characteristics, population characteristics, intervention characteristics, study results and effectiveness.

Data analysis

From the included articles, we performed content analysis to find the themes regarding to interventions for family of children with autism.

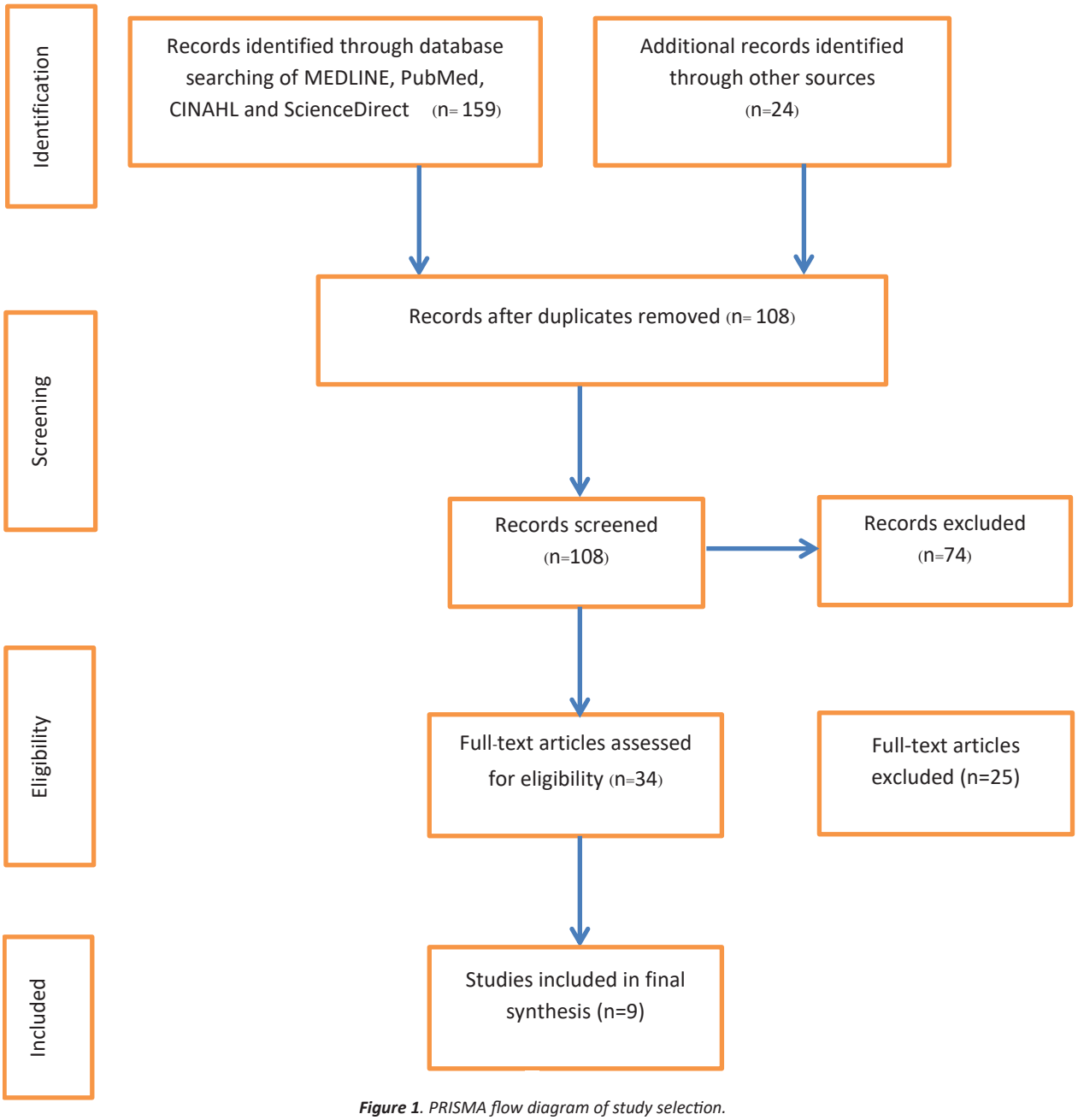

Figure 1. *PRISMA flow diagram of study selection.*

Results

During the search process by the database originally had 159 articles potentially relevant was found, and then adding 24 articles potentially relevant from reference lists of the original articles have been selected for review. After eliminating the duplication in excel, 108 potentially relevant articles were identified for inclusion in the evaluation. After conducting screening of the title and abstract of the articles, 34 articles were selected to be read in full. Finally, there were 9 articles were identified that fully met the inclusion criteria. These articles were summarized in the Table 1. Four articles are related to family education intervention program. Two articles demonstrated effectiveness of psychosocial support intervention for family members compared with usual interventions. Three articles revealed the effectiveness of technology-based interventions on family members of children with autism. The findings found three interventions as the following,

Parent education intervention. Parent education is intervention that enhances or facilitates parents to support their children, with the ultimate goal of improving positive developmental outcomes on their children.[13-14] In the educational interventions, multidisciplinary educational intervention had a positive impact on improving the quality of life, family function, and coping styles of parents of children with autism.[5] The 8-week intervention program had group classes once a week, each session of about 90 minutes facilitated by a multidisciplinary team consisting of special educators, community nurses, psychologists and psychiatrist. In the 8-week classes, parents were provided with lectures, case reports, role-play and discussions related to autism and family knowledge such as autism, characteristics, and management

of the family problems while taking care of children in their everyday life. The results show that multidisciplinary education had a positive impact on caregiver's quality of life. Participants reported that they were highly satisfied with the multidisciplinary educational program and wished for more and longer intervention.[5] The results of the study recommend that nurses and other health care providers actively apply the intervention program in routine care for children with autism and their families.

A research on education and behavior management intervention program for parents of children with autism indicated that parent educational intervention had a positive impact on children ability to manage their own behavior and autism symptoms.6 The entire education intervention process took twenty weeks, ten group sessions of 90 minutes and ten individual sessions of 60 minutes. In addition to the educational support of therapists, the intervention program provided opportunity for videotapes of content review and intervention adherence by therapists. The intervention program with group and individual sessions gave parents the opportunity to discuss their response to receiving an autism diagnosis and to increase their knowledge of autism and its effects on their children. The program provided the parents how to manage difficult behaviors and supported the development of children's communication, social and plays skills. The individual sessions were with the participation of children to train skills and action orientation. Parents were provided with workbooks, videos, rehearsal, homework assignments and feedback. Researchers suggested that education and behavior management intervention program can help parents more effectively cope and manage their children's problems and behavior. The program showed a certain effect on families and children with autism. However, the educational programs developed were complex and unstructured. Therefore, the evaluation of the effectiveness of these programs was still unclear and biased.

Table 1 The interventions for family of children with autism.

Author, year	Participants, sample size, sampling methods	Measurements	Intervention program	Findings/ recommendations
Ho MH & Lin LY, 2020	24 dyad of children with autism and parents were randomly divided into the intervention group or the control group	- Functional Emotional Assessment Scale and the Vineland Adaptive Behavior Scales were used to assess Adaptive functioning - The Chinese version of Psychoeducational Profile-Third edition were used to measure the Parenting skills	The parent education intervention within 14 weeks: • Group parent training intervention • Individual training approach • Parent – occupational therapist discussion on challenges of the intervention	• Significant improvements in children's emotional development and parenting skills were found in participants attending the 14-week intervention. • The participants did not get improvement in other developments and adaptive functioning after participating in the intervention program. • Healthcare professionals should supplement a DIR-based home parent training program to support interventions for children with ASD and their families to enhance children' emotional development and parenting skills.
Bearss et al., 2015	180 pairs of children with autism (ages 3 to 7) and their parents participated in the study and were randomly assigned to training and education groups.	The instruments for data collection were including: • The parent-rated ABC-I • The per-item mean score on the parent-rated Home Situations Questionnaire–Autism Spectrum Disorder (HSQ-ASD) • The Improvement item of the clinician-rated CGI (CGI-I)	The parent education and training intervention program includes: • Parent training on disruptive behavior management strategies (11 main sessions, 2 optional sessions; 2 phone reinforcement; 2 home visits) • Parental education about autism but no behavior management strategy (12 main sessions, 1 home visit).	• Through the results of parent reports, the parent training intervention program on disruptive behavior management strategies indicated a superior effectiveness than the family education program on the managing of children's behavior. • Clinicians were more likely to appreciate the parent training intervention program than the family education program

Table 1 The interventions for family of children with autism. (continues)

Author, year	Participants, sample size, sampling methods	Measurements	Intervention program	Findings/ recommendations
Ji B, Sun M, Yi R, Tang S 2014	42 caregivers of children with ASD (randomly assigned to intervention and control group) A quasi-experimental study	• The Chinese version of the SF-36 • McMaster Family Assessment Device • Simplified Coping Style Questionnaire • Multidimensional Scale of Perceived Social Support • Caregiver Burden Index • Childhood Autism Rating Scale • The General Self-Efficacy Scale • Multidisciplinary Parent Education Evaluation Form	The multidisciplinary parent education intervention: The caregivers in the intervention group were provided the multidisciplinary parent education program, which included 8-week sessions	• The research findings indicated that there were significant improvements in the mental HRQOL, family functioning, self-efficacy and positive coping style among the caregivers who received the intervention. • The multidisciplinary parent education program had significant positive effects on caregivers' mental health-related quality of life, however, the findings had little effect on their physical health-related quality of life
Tonge B, Brereton A, Kiomall M, Mackinnon A, Rinehart NJ, 2014	100 parents of children with autism were randomly assigned into the intervention group (n=70) and control group (n=35)	• The Vineland Adaptive Behavior Scales • The Developmental Behavior Checklist • The Psychoeducational Profile–Revised	The twenty weekly sessions of parent education and behavior management: • The intervention was based on a variety of early intervention and cognitive behavioral techniques that assist in imparting effective coping skills to parents with a systematic and structure approach. The parent education and counselling: • The parents were provided a manual-based education program The intervention program with 20 weeks of implementing was quite long which was likely to result in completing and withdrawal from the program of parents of children with autism.	• The research findings showed that the participants who received the intervention of parent education and behavior management had higher scores of in adaptive behaviour and autism symptoms; and parent education and behavior management

Table 1 The interventions for family of children with autism. (continues)

Author, year	Participants, sample size, sampling methods	Measurements	Intervention program	Findings/ recommendations
Ridderinkhof A, de Bruin EI, Blom R, Bögels SM, 2018	45 dyad of children with autism and their parent were recruited in the study	• The 65-item Social Responsiveness Scale • The Achenbach System of Empirically Based Assessment • The 10-item Children's Acceptance and Mindfulness Measure • The 64-item SRS-Adult form • The Adult Self Report (ASR) of the ASEBA • The Parenting Stress Index • The Interpersonal Mindfulness in Parenting Scale	The MYmind intervention: • The MYmind program was a mindfulness-based program • The 9-week MYmind Child Program was developed based on the MYmind protocol for youth with ADHD and mindfulness-based therapy for adults with ASD • The 9-week MYmind Parent Program was developed based on the Mindful Parenting manual	• The children reported no significant change in mindful awareness, however, decreased social communication problems, and improved emotional and behavioral functioning after the intervention. • Parents reported all the improvements of their children immediately after the intervention and 1 year after the intervention. • Parents reported improved emotional and behavioral functioning, parenting, and mental awareness at all time points. • This study shows that children, and their parents can benefit from MYmind intervention program
Bekhet 2017	There were 73 caregivers participating in the study of which, finally, 64 participated in either an intervention or a control group	• Quantitative data collection tool: Positive Thinking Skills Scale (PTSS) includes 8 sections • Qualitative data collection tool is a caregiver's online weekly homework log	The positive thinking training intervention: • The intervention program included PowerPoint presentations • The researcher sent the video to the caregiver online once a week	• The intervention indicated the effectiveness in improving positive thinking skills among caregivers of children with autism. • The research findings provided evidence of effectiveness of positive thinking training intervention and the future further research of positive thinking training for the large scales to find the effectiveness of the intervention on caregivers' well-being
Ingersoll & Berger 2015	27 parents of children with autism participating in the study, randomly assigned to a self-directed or therapist-assisted version of ImPACT Online groups	The research instruments were • The modified version of the Computer-Email-Web Fluency Scale (CEWFS) • The Center for Epidemiological Studies-Depression Scale (CES-D) • The ImPACT Knowledge Quiz • Videotaped during a parent-child interaction • The ImPACT Online website's electronic tracking of user behavior	The telehealth-based parent-mediated intervention program: • The self-directed group accessed the program of adapted Project ImPACT, which contained 12 self-directed weekly lessons of 80 minutes and supplemental material • Therapist-Assisted Group access to the ImPACT Online website with 12 twice weekly sessions of 30-minute remote coaching via Skype video conferencing	• The study results revealed that parents of children with autism exhibited high interaction and satisfaction with ImPACT Online for both the self-directed and therapist assisted version of the programs. • Parents who received enough support better completing the program and improved outcomes in parents and children • The program increased parents' access to parent-mediated intervention for families of children with autism

Table 1 The interventions for family of children with autism. (continues)

Author, year	Participants, sample size, sampling methods	Measurements	Intervention program	Findings/ recommendations
Dai YG, Brennan L, Como A, Hughes-Lika J, Dumont-Mathieu T, Rathwell IC, Minxhozi O, Aliaj B, Fein DA, 2018	Thirty-eight children-parent dyads were randomly assigned to either the intervention or the control group.	• The treatment Evaluation Inventory Short Form • The 31-item parents quiz • The Early Intervention Parenting Self-efficacy Scale	The video program: parents were trained through six weekly DVD modules and six weekly chapters of written material: • The videos included illustrative clips of ABA-based interventions. • The Guidelines for teaching and evidence-based behavior management. • Parents can access the DVD at least a few times per week. • Therapist supported parents by the phone in carrying out the instructions in the modules	• The results indicated that the intervention was effective on the outcomes of parents and children with autism. Specifically, the intervention improved parent self-efficacy and teaching knowledge for their children with autism, therefore, improved their behavior problems • The health care providers should consider to provide intervention to the parents at their first concern of their child problems to enhance positive change in the parent outcomes
Ingersoll B, Shannon K, Berger N, Pickard K, Holtz B, 2017	Twenty parents of children with autism were randomly assigned to a self-directed or therapist-assisted group	• The Computer-Email-Web Fluency Scale • ImPACT Online's electronic tracking of user behavior • The ImPACT Knowledge Quiz • The Behavioral Intervention Rating Scale	The ImPACT Online program: • The intervention was adapted from Project ImPACT, to provide to parents within 12 weekly sessions of 75 minutes. • The parents were provided supplemental material including video library, forum and information resources. • Parents receive emails with tips for implementing the intervention.	• The intervention with incorporation of parent education and video library and various resources indicated the positive results on participants: • Parents who received the intervention program increased intervention knowledge • The parents who were in open access trial provided positive feedback on the program

Psychological support intervention. While studies focus greatly on the treatment and intervention for behavioral problems in children with autism, very rare studies have been done to develop and evaluate the effectiveness of interventions on the psychological problem of parents and families of children with. In fact, in health-care facilities, services to the psychological needs of the parents were rarely approached, if any, incomplete and inadequate interventions, which did not improve the psychological problem of parents with autism, especially, the first diagnosis of autism. A study indicated that positive thinking support caregivers in improving the positive thinking skills and in turn improving the behavior problems of their children with autism.[7] In the positive thinking training intervention program, parents were participated in six sessions, in which each session the researcher provided a PowerPoint presentation and videos related to knowledge and practice of positive thinking. At the end of each session, participants were assigned a group assignment, in which caregivers relied on the videos viewed to come up with a positive thinking training strategy to address their life situations. The purpose of the intervention program was to focus on developing eight positive thinking abilities to assist caregivers with autism in many aspects of their lives, especially their daily psychological problems. The researcher recommended that health care workers, especially psychological nurses should provide positive thinking interventions that improve positive thinking skills for caregivers of children with autism. However, to do this, the nurse needs training the intervention process for the effective outcomes. This intervention can also be done online for caregivers who do not have access to a live intervention program. However, the nurse should be in mind that, providing only PowerPoint presentation may not help the caregiver get detailed information, the researcher should provide additional printed or written materials as well as provide more specific examples. In addition, the researcher proposed a future study applying the intervention program on a web platform, which created forums for caregivers

to interact and discuss their life situations. Ridderinkhof and colleagues in their research on MYmind program for parents and children with autism indicated that mindfulness intervention improved their emotional and behavioral functioning, parenting, and mental awareness; and the intervention decreased social communication problems, and improved emotional and behavioral functioning in children with autism. Research suggested that mental health nurses can effectively implement MYmind intervention program to enhance autistic children and parents' outcomes.[15]

Technology-based intervention. Some researchers have attempted to address the limitations of traditional parent training programs. In order to make parent training more accessible, researchers have utilized technology to provide services to parents in remote locations. Ingersoll and Berger conducted a study on 27 pairs of parents and children with autism to compare the effectiveness of the self-directed or therapist-assisted ImPACT Online intervention programs.[16] The both groups of participants were provided ImPACT Online access, where the self-directed group was engaged in 12 self-directed weekly lessons with 80 minutes per week, the therapist-assisted group was coached via Skype video conferencing in 12 weeks, 2 lessons per week within 30 minutes. The study results revealed that parents of children with autism in both groups were satisfied with the ImPACT Online program and showed great interaction on these two programs. However, the therapist-assisted group had better completion of the program and improved outcomes of parents and children with autism. The author of the study recommended that health care providers should use the intervention program to strengthen parents' access to parent-mediated intervention for families of children with autism.

Dai and her colleagues conducted a study involving home training for parents of children with autism. Research indicated that parents using technology effectively enhanced their knowledge and confidence in their ability of providing care to their children with autism.[17] The technologies applied in the study included video program, mail feedback and telephone support under three conditions. In the first condition, parents were trained knowledge on evidence-based teaching and behavior management techniques. Accordingly, the parents applied the gained knowledge to behavior management for their children with autism. On the process, the parents provided their feedback on the valuable of the training material after each module by mail. Finally, parents were supported weekly by the treatment group using phone calls. The process lasted for 14 to 16 weeks, each parent being able to access the video twice a week. The mail feedback process was conducted uniquely regarding each parent's specific needs and issues. Researchers suggested that training program is comprehensible and valuable for parents of children with autism in low-resource settings.[17]

In addition, research suggested internet-based interventions to train parents in implement interventions at home in a feasible way.8 Another study used video feedback to confirm the effectiveness of technology-based interventions on parents of children with autism. Research indicated that through the intervention, parents of children with autism improved the knowledge of autism intervention and reduced parent depressive symptoms.[18] Technology-based interventions indicated their effectiveness in many studies, however, the approach is a new area of research, and more studies are needed to further evaluate the effectiveness of the interventions. Moreover, technology-based interventions collected data through video record multiple times during the intervention to compare the improvement of the parents and children over time. This makes the approach become a limitation of the intervention, especially, for families with technology difficulties.

Discussion

The research results indicated that there were thre kinds of interventions for family of children with autism, including, family education intervention, psychosocial support intervention and technology-based interventions. The evidence suggested that all these family interventions have in common the involvement of the family in the intervention. However, these interventions have their own strengths and limitations. Therefore, the education intervention programs should be simplified and structured with certain sessions, therefore family member would be able to follow their autistic children through all sessions. The psychological support intervention indicated their effectiveness on supporting the psychological needs of parents of individuals with autism; however, sessions with only PowerPoint presentation may not be enough for caregivers understanding all the contents, they should be provided more written material as well as concrete examples to improve caregiver's knowledge and skills. The technology- based intervention with videotaped data is reasonable strategy of characteristics' autistic children and their families. The technologies enable health care workers and researchers to observe or follow in detail the daily behaviors of autistic children and their families during the intervention. The thing is that the intervention program with collections of videotaped data over numerous sessions also becoming the limitation of the intervention. Therefore, programs developed need to be more structured and feasibility. These interventions need to provide enough follow-up support by simply technology method for the long-term effects of intervention programs. Researchers suggested that future studies should develop a family-management intervention with phone call support. The program would build the strengths of families in supporting for children with autism. The intervention could help improve the quality of life and burden for families with autistic children and in turn, improve outcomes in autistic children.

This integrative review included information about intervention studies for families of children with autism and its effectiveness on families and children outcomes. Family interventions and outcomes for families and autistic children are a broad area in which many disciplines implemented. Meanwhile, the results of only 9 studies were analyzed and synthesized made the weakness of the results. A future study with a systematic review design should be conducted to reflect the picture of interventions that have been implemented to improve problems in parents and children with autism.

Conclusion

In summary, this review intended to answer question "What is the evidence for the effectiveness of interventions for family of individuals with autism?". The results of this review suggested that the most common intervention programs utilized was education, psychology and technology. These are not common research that focuses on all family members, but parents, caregivers or fathers, mothers only. Considering these results, there is a clear need to validate the effectiveness of family intervention of children with autism, especially, family education intervention, which found the most effective on family and children with autism compared to psychological support and technology-based intervention. However, the education programs developed need to be structured and feasibility. These interventions should provide enough follow-up support for the long-term effects of education programs. Researchers are therefore interested in developing an education intervention that will develop the strengths of families in supporting for children with autism. Education intervention programs will be Internet based and videotape tools. The intervention could help improve the quality of life for families of children with autism and improve children outcome.

Conflict of interest

The authors declare that they have no conflict of interest.

Funding Statement

This study was funded by Vietnam Ministry of Education and Training, Nam Dinh University of Nursing, Vietnam and Graduate school, Burapha University, Thailand.

References

1] Matthew J, Kelly A, Baio J, Wiggins L, Christensen DL, Maenner MJ, et al. Prevalence of autism spectrum disorder among children aged 8 years - autism and developmental disabilities monitoring network, 11 sites, United States, 2016. MMWR Surveill Summ. 2020; 69(4): 1-12. doi.org/10.15585/mmwr .mm6916a4.

[2] Johnson NL, Burkett K, Reinhold J, Bultas MW. Translating Research to Practice for Children With Autism Spectrum Disorder: Part I: Definition, Associated Behaviors, Prevalence, Diagnostic Process, and Interventions. J Pediatr Health Care. 2016; 30(1): 15-26. doi: 10.1016/j. pedhc.2015.09.008. Epub 2015 Oct 31. PMID: 26530271.

[3] Bultas MW, Johnson NL, Burkett K, Reinhold J. Translating Research to Practice for Children With Autism Spectrum Disorder: Part 2: Behavior Management in Home and Health Care Settings. J Pediatr Health Care. 2016; 30(1): 27-37. doi: 10.1016/j.pedhc. 2015.09.009. Epub 2015 Oct 30. PMID: 26525946.

[4] Kang-Yi CD, Grinker RR, Mandell DS. Korean culture and autism spectrum disorders. J Autism Dev Disord. 2013; 43(3): 503-20. doi: 10.1007/s10803-012-1570-4. PMID: 22723126..

[5] Ji B, Sun M, Yi R, Tang S. Multidisciplinary parent education for caregivers of children with autism spectrum disorders. Arch Psychiatr Nurs. 2014; 28(5): 319-26. doi: 10.1016/j.apnu.2014.06.003. Epub 2014 Jul 11. PMID: 25439973.

[6] Tonge B, Brereton A, Kiomall M, Mackinnon A, Rinehart NJ. A randomised group comparison controlled trial of 'preschoolers with autism': a parent education and skills training intervention for young children with autistic disorder. Autism. 2014 Feb;18(2):166-77. doi: 10.1177/1362361312458186.

[7] Bekhet AK. Positive Thinking Training Intervention for Caregivers of Persons with Autism: Establishing Fidelity. Arch Psychiatr Nurs. 2017; 31(3): 306-10. doi: 10.1016/j.apnu.2017.02.006. Epub 2017 Feb 16. PMID: 28499573.

[8] Hedda M & Marcus ED. Internet-based intervention training for parents of young children with disabilities: a promising service-delivery model. Early Child Development and Care. 2015; 185: 1, 155-69, doi: 10.1080/03004430.2014.908866.

[9] Goepfert E, Mulé C, von Hahn E, Visco Z, Siegel M. Family System Interventions for Families of Children with Autism Spectrum Disorder. Child Adolesc Psychiatr Clin N Am. 2015; 24(3): 571-83. doi: 10.1016/j. chc.2015.02.009. PMID: 26092740.

[10] Tanner K, Hand BN, O'Toole G, Lane AE. Effectiveness of Interventions to Improve Social Participation, Play, Leisure, and Restricted and Repetitive Behaviors in People With Autism Spectrum Disorder: A Systematic Review. Am J Occup Ther. 2015; 69(5): 6905180010p1-12. doi: 10.5014/ajot.2015.017806. PMID: 26356653.

[11] Kuhaneck HM, Madonna S, Novak A, Pearson E. Effectiveness of Interventions for Children With Autism Spectrum Disorder and Their Parents: A Systematic Review of Family Outcomes. Am J Occup Ther. 2015; 69(5): 6905180040p1-14. doi: 10.5014/ajot. 2015.017855. PMID: 26356656.

[12] Kuravackel GM, Ruble LA, Reese RJ, Ables AP, Rodgers AD, Toland MD. COMPASS for Hope: Evaluating the Effectiveness of a Parent Training and Support Program for Children with ASD. J Autism Dev Disord. 2018; 48(2): 404-16. doi: 10.1007/s10803-017-3333-8. PMID: 29022130.

[13] Bearss K, Johnson C, Smith T, Lecavalier L, Swiezy N, Aman M, et al. Effect of parent training vs parent education on behavioral problems in children with autism spectrum disorder: a randomized clinical trial. JAMA. 2015; 313(15): 1524-33. doi: 10.1001/jama.2015.3150. Erratum in: JAMA. 2016 Jul 19; 316(3): 350. Erratum in: JAMA. 2016 Jul 19; 316(3): 350. PMID: 25898050.

[14] Ho MH & Lin LY. Efficacy of parent-training programs for preschool children with autism spectrum disorder: A randomized controlled trial. Research in Autism Spectrum Disorders. 2020; 71(2): 96-104. doi: 10.1016/j.rasd.2019.101495.

[15] Ridderinkhof A, de Bruin EI, Blom R, Bögels SM. Mindfulness-Based Program for Children with Autism Spectrum Disorder and Their Parents: Direct and Long-Term Improvements. Mindfulness (N Y). 2018; 9(3): 773-91. doi: 10.1007/s12671-017-0815-x. Epub 2017 Oct 6. PMID: 29875881; PMCID: PMC5968048.

[16] Ingersoll B, Berger NI. Parent Engagement With a Telehealth-Based Parent-Mediated Intervention Program for Children With Autism Spectrum Disorders: Predictors of Program Use and Parent Outcomes. J Med Internet Res. 20156; 17(10): e227. doi: 10.2196/jmir.4913. Erratum in: J Med Internet Res. 2015; 17(11): e239. Erratum in: J Med Internet Res. 2015; 17(11): e257. PMID: 26443557; PMCID: PMC 4642401.

[17] Dai YG, Brennan L, Como A, Hughes-Lika J, Dumont-Mathieu T, Rathwell IC, Minxhozi O, Aliaj B, Fein DA. A Video Parent-Training Program for Families of Children with Autism Spectrum Disorder in Albania. Res Autism Spectr Disord. 2018; 56: 36-49. doi: 10.1016/j.rasd.2018.08.008. Epub 2018 Sep 10. PMID: 31275428; PMCID: PMC6605780.

[18] Ingersoll B, Shannon K, Berger N, Pickard K, Holtz B. Self-Directed Telehealth Parent-Mediated Intervention for Children With Autism Spectrum Disorder: Examination of the Potential Reach and Utilization in Community Settings. J Med Internet Res. 2017; 19(7): e248. doi: 10.2196/jmir.7484. PMID: 28701294; PMCID: PMC5529736.

Journal of Associated Medical Sciences 2021; 54 (3): 102-106

JAMS
Journal of Associated Medical Sciences

Thai-Journal Citation Index Centre (TCI) & ASEAN Citation Index (ACI)

Journal of Associated Medical Sciences

Journal homepage: https://www.tci-thaijo.org/index.php/bulletinAMS/index

Evaluation of two beam-matched linear accelerators for volumetric modulated arc therapy

Tinnagorn Donmoon[1] **Kulachatr Rattanakunchai**[1] **Sumalee Yabsantia**[2]

[1]*Department of Radiotherapy, Mahavajiralongkorn Thanyaburi Hospital, Pathumtani Province, Thailand*
[2]*Department of Radiological Technology, Faculty of Allied Health Sciences, Naresuan University, Phitsanulok Province, Thailand*

ARTICLE INFO

Article history:
Received 13 August 2021
Accepted as revised 17 August 2021
Available online 17 August 2021

Keywords:
Beam-matching, Linear accelerator, Volumetric modulated arc therapy

ABSTRACT

Background: Currently, Mahavajiralongkorn Thanyaburi Hospital has two linear accelerators (LINACs) of identical models and brands with volumetric modulated arc therapy (VMAT) capability. Since two identical LINAC systems have been installed for two years, it is of great interest to determine beam-matching techniques in order to interchange ongoing irradiated patients between the two LINACs without re-planning if any malfunction of one machine occurs.

Objectives: This study aimed to verify the dosimetric accuracy of beam-matching using VMAT plans after completing the extended beam-matching.

Materials and methods: After completing the acceptance test and initial vendor-recommended beam-matching test, the extent of beam-matching was measured to evaluate the level of beam matching in both LINACs. The original LINAC (LINAC 1) photon beams were selected as the reference for beam tuning of the second LINAC (LINAC 2). Planar dose measurements of head and neck, thorax, and pelvis regions were collected from 30 retrospective cancer patients. The VMAT plans were generated in the Monaco Treatment Planning System (TPS) using a 6 MV photon beam model. TPS doses calculated by LINAC 1 were used as a reference for all measurements. The LINAC 1's verification plans were irradiated in both LINACs by doing the machine override option available in LINAC 2 consoles. All of the VMAT plans were measured using the Octavius^{4D} dosimetry system. The data of Octavius measurement were compared with the TPS calculated planar doses with gamma criteria of 3% dose difference, and 3 mm distance to agreement (3%/3mm). In addition, the statistically significant differences for gamma passing rates of Octavius measurements between two LINACs was analyzed using a paired sample t-test at a 95% confidence interval (CI).

Results: For all thirty cases, the gamma passing rates of Octavius measurements on two beam-matched LINACs were higher than 95% with 3%/3mm gamma criteria. The mean gamma passing rates of LINAC 1 and LINAC 2 were 96.2±0.8% and 96.3±0.8%, respectively. There was no statistical difference in the gamma passing rates between LINAC 1 and LINAC 2 (p-value = 0.094).

Conclusion: The beam-matched LINACs showed good agreement between measurements and TPS calculations for VMAT plans. Insignificant differences in gamma passing rates between two LINACs prove the viability of interchanging VMAT patients between two beam-matched LINACs without re-planning VMAT plans to manage the machine downtime.

* **Corresponding author.**
Author's Address: *Department of Radiotherapy, Mahavajiralongkorn Thanyaburi Hospital, Pathumtani Province, Thailand.*

** **E-mail address:** tinnagorn.armrt@gmail.com
doi: 10.14456/jams.2021.30
E-ISSN: 2539-6056

Introduction

Beam matching has been increasingly used in centers with two or more radiotherapy treatment machines from a similar manufacturer. Beam matching is helpful for interchanging the patients between machines in case of machine failure without re-planning, preserving patient's time to continue their treatment, and reducing staff workload. Most of the previous studies reported dosimetric data for evaluating the feasibility of machine matching such as depth dose, beam profile, and output factors[1–11]. In addition, some studies extended the validation of beam matching to clinical patient treatment plans.[5,7] However, few studies performed patient-specific quality assurance by measuring the actual dose using point dose and planar dose.[8–10]

Recently, two identical models and brands of linear accelerators (LINACs) systems with volumetric modulated arc therapy (VMAT) treatment capability were installed at Mahavajiralongkorn Thanyaburi Hospital. The first was installed in 2016, and the second was consecutively installed in 2018. As two identical LINACs are available in our center, it is a great opportunity to try using beam matching techniques. The final purpose of this study was to interchange ongoing irradiated patients between the two LINACs without re-planning when any malfunction of one machine might occur. In our institution, machine breakdown occurs approximately 6 times a year. Therefore, interchanging patient purposes is beneficial.

To best our knowledge, few studies performed the actual measurement. However, there was no study utilized the Octavius[4D] dosimetric system for evaluating the dose of the treatment machine. Therefore, this study aimed to verify the dosimetric accuracy of beam matching using the Octavius[4D] dosimetric system for VMAT plans in head and neck, chest and pelvis regions.

Materials and methods

Two identical linear accelerators of Elekta Infinity (Elekta AB, Stockholm, Sweden) with an agility head (80 MLC leaf pairs of 5 mm leaf width) were evaluated for beam matching in this study. Both linear accelerators are equipped with XVI cone-beam computed tomography (CBCT) and iView GTTM portal imaging. The desktop software is Integrity 3.2. Each LINAC has two-photon beams of nominal energies 6 and 10 MV and five electron beams with nominal energies of 6, 9, 12, 15, and 18 MeV. Figures 1a and 1b illustrate the linear accelerators used in this study.

Figure 1. *1a: Original LINAC (LINAC 1), 1b: The second LINAC (LINAC 2).*

A preliminary study of beam matching was performed in our previous study.[12] We reported the comparison dosimetric parameters according to the initial vendor-recommended beam-matching of the two LINACs available in our center. The summary of dosimetric parameters of 6 MV photon beam for LINAC 1 and LINAC 2, including depth dose, beam profile at 10 cm depth, and output factor, are illustrated in Table 1-3. In addition, the beam quality in terms of tissue phantom ratio at depth 20 cm and 10 cm ($TPR_{20,10}$) of LINAC 1 and 2 were 0.679 and 0.677, respectively. The difference of $TPR_{20,10}$ between two LINACs was -0.29%. In Table 2, a high value of flatness was found mainly in large field sizes. However, the criteria of the Elektra machine were 106% for field sizes between 10x10 cm^2 and 30x30 cm^2 and 110% for field sizes greater than 30x 30 cm^2 according to the IEC protocol recommended in the customer acceptance test. The acceptable criterion of this difference for flatness and symmetry between beam-matched LINACs should be within ±2%.[13]

Table 1 Comparison of depth dose parameters between 2 linear accelerators.

Parameters	LINAC 1	LINAC 2	Difference
R_{100} (FS 5x5 cm^2) (cm)	1.50	1.60	0.10
R_{100} (FS 10x10 cm^2) (cm)	1.50	1.60	0.10
R_{100} (FS 20x20 cm^2) (cm)	1.40	1.43	0.03
R_{100} (FS 30x30 cm^2) (cm)	1.30	1.39	0.09

R_{100} is a range of 100% depth dose

Table 2 Comparison of flatness and symmetry of beam profiles between 2 linear accelerators.

Field size (cm^2)	In-plane				Cross-plane			
	Flatness (%)		Symmetry (%)		Flatness (%)		Symmetry (%)	
	LINAC 1	LINAC 2	LINAC 1	LINAC 2	LINAC 1	LINAC 2	LINAC 1	LINAC 2
5x5	101.37	101.58	101.03	100.24	101.78	101.99	100.24	100.53
10x10	103.00	103.99	100.62	100.70	104.52	104.67	100.63	100.88
15x15	104.07	104.93	101.02	100.76	104.60	105.26	100.44	100.62
20x20	103.05	105.02	100.87	100.83	103.42	104.43	100.42	100.92
30x30	103.02	104.28	101.07	101.03	103.24	104.74	100.70	101.09

Flatness = (D_{max}/D_{min}) x 100, Symmetry = $[max(D_{left}, D_{right})/min(D_{left}, D_{right})]$ x 100

Table 3 Comparison of output factors between 2 linear accelerators.

Field size (cm^2)	LINAC 1	LINAC 2	% difference
2x2	0.810	0.809	-0.12
3x3	0.848	0.847	-0.12
4x4	0.879	0.877	-0.23
5x5	0.906	0.905	-0.11
10x10	1.000	1.000	0.00
15x15	1.058	1.060	0.19
20x20	1.097	1.098	0.09
30x30	1.143	1.146	0.26
40x40	1.161	1.167	0.52

Dose measurement for clinical VMAT cases

The clinical assessment of beam matching between LINAC 1 and 2 was conducted in thirty cancer patients by collecting regions of head and neck, thorax, and pelvis, with ten patients for each region in this retrospective study. VMAT treatment plans were created in the Monaco (version 5.11.02) Treatment Planning System (TPS) (Elekta Oncology Systems, Crawley, UK) using 6 MV photon beam models of LINAC 1 for all patients. The doses were calculated using the Monte Carlo algorithm with a calculation grid size of 0.3 cm with the prescribed dose and other parameters described in Table 4. Treatment doses calculated on LINAC 1 were taken as a reference for all measurements.

Table 4 Treatment planning parameters for cancer patients used in this study.

Parameters	Head and Neck		Thorax		Pelvis
	GBM	NPC	Lung cancer	Esophagus cancer	Prostate cancer
Photon energy (MV)	6	6	6	6	6
Prescribed dose (cGy)	5940	7000	6000	5040	7800
Number of fractions	33	33	30	28	39
Number of arcs	2	2	2	1	2
Number of patients	3	7	4	6	10

The planar dose measurements were conducted using the Octavius^{4D} dosimeter (PTW, Freiburg, Germany). It is a cylindrical unit of 32 cm diameter and 34 cm length. To keep the consistency of measurement, the measured plane of the detector array aligns with the center plane of the cylinder which can be rotated in synchrony with the LINACs gantry using input from the inclinometer. All measurements were performed using the Octavius detector 1500 with 1405 plane-parallel vented ionization chambers uniformly arranged in a 27x27 cm^2 area. Each ionization chamber has a dimension of 4.4 mm x 4.4 mm x 3 mm (0.06 cm^3). The VeriSoft® software (version 6.2) was used for the measurement and dose analysis.

LINAC 1's verification plans were applied to set the irradiation in LINAC 1 and LINAC 2 rooms using the machine override option available in LINAC 2 consoles. Then VMAT treatment plans were evaluated using Octavius^{4D} phantom with VeriSoft® verification software. Figure 2 illustrates the measurement set-up geometry for this study. The doses of Octavius measurement were compared with the TPS calculated planar doses using gamma comparison with criteria of 3% dose difference and 3 mm distance to agreement (3%/3mm). The gamma passing rate between LINAC 1 and LINAC 2 was compared as a percentage of difference, and a statistically

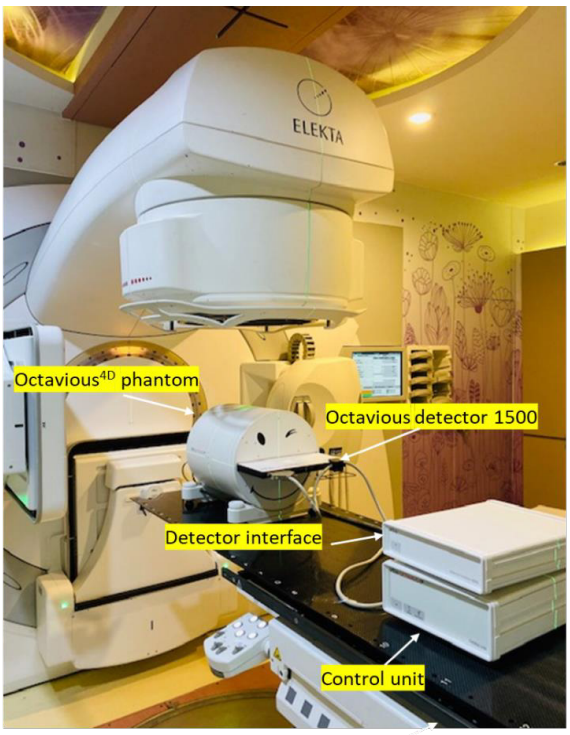

Figure 2. *Geometry of measurement.*

significant difference for gamma passing rates of Octavius measurements between LINAC 1 and LINAC 2 was analyzed using paired sample t-test at a 95% confidence interval (CI).

Results

Depth dose, beam profile, and output factors between LINAC 1 and LINAC 2 were comparable, as depicted in Table 1-3. More dosimetric parameters of photon and electron were reported in our previous study.[12] In this study, we extended the evaluation for clinical data of patients undergoing VMAT plans. In Figure 3, the gamma passing rates of Octavius measurements on two beam-matched LINACs were higher than 95% with 3%/3mm gamma criteria in all patients.

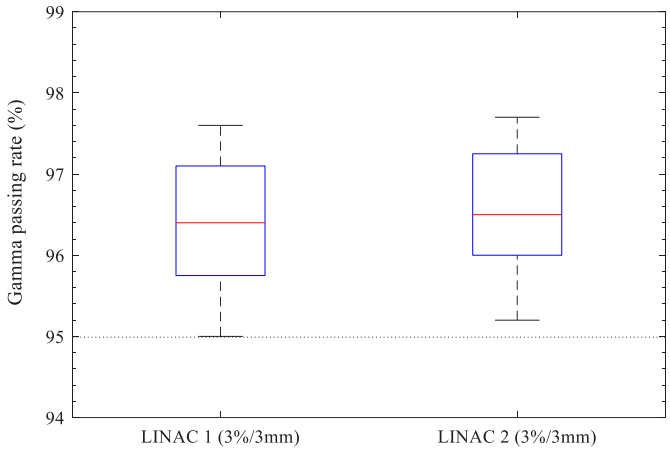

Figure 3. *Distributions of the average gamma passing rate of VMAT plans delivered on two beam matched LINACs.*

Percentage differences of gamma passing rate between LINAC 1 and LINAC 2 for thirty cases are demonstrated in Figure 4. The differences were within 1.1%. However, most of the gamma passing rates obtained from LINAC 2 were higher than those values obtained from LINAC 1, as illustrated by the positive percentage difference.

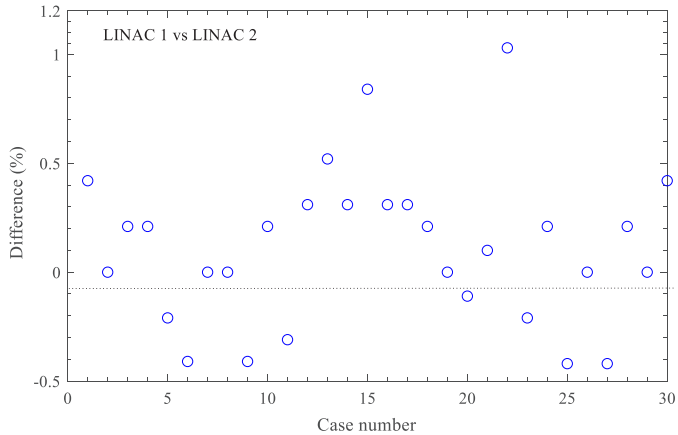

Figure 4. *Distributions of the percentage difference of gamma passing rate between 2 LINACS for thirty cases.*

Average gamma passing rates of LINAC 1 and LINAC 2 were 96.2±0.8% and 96.3±0.8%, respectively, as shown in Table 5. In addition, there was no statistically significant difference in the gamma passing rates between LINAC 1 and LINAC 2 (*p*-value = 0.094).

Table 5 Comparison of mean gamma passing rate and standard deviation (SD), and paired sample t-test analysis between LINAC 1 and LINAC 2.

Regions	Mean gamma passing rate (%) ± SD	
	LINAC 1	LINAC 2
Head and Neck (n=10)	96.6±0.9	96.6±0.9
Thorax (n=10)	96.0±0.8	96.2 ±0.8
Pelvis (n=10)	96.0±0.7	96.1±0.9
Total (n=30)	96.2±0.8	96.3±0.8
t-test (*p* value)	0.094	

Discussion

After beam matching, LINAC 1 and LINAC 2 in our center have similar beam energies for photon and electron beams.[12] For advanced techniques, the clinical implementation of beam matching should be more intensively considered for reducing the dosimetric error in patient dose delivery. The dosimetric analysis of the VMAT plan of head and neck, thorax, and pelvis swapped between two machines are well within clinical acceptable. In addition, the evaluation of beam matching with patient-specific quality assurance using Octavious dosimeter was a good agreement for all cases. Therefore, interchanging VMAT patients between two beam-matched LINACs without re-planning VMAT plans to manage the machine downtime could be acceptable. The mean gamma passing rate for each region was comparable between LINAC 1 and LINAC 2. The highest difference was found in case number 22 for the pelvic region, with a percentage difference of 1%, as shown in Figure 4.

In Table 5, mean gamma passing rate of LINAC 2 was slightly higher than LINAC 1. One of the reasons for these results might be affected by the time of beam tuning. Since the LINAC 2 was the newer machine tuned using the dosimetric data from LINAC 1, the commissioning data was transferred to a treatment planning system and used to model the VMAT plans in this study. Therefore, the newer machine might be closed to the treatment planning data, resulting in good agreement between TPS and measurement. However, the difference data might be due to the daily output variation of the machines. The clinical results in this study confirmed the finding from previous publications that beam-matched LINACS are undoubtedly possible.[8–10] However, regular quality assurance should be performed for evaluating the matched beam LINACS.

In this study, a quantitative evaluation of beam matching of two LINACs in terms of identical model and brand was performed for the Elekta machines. This methodology has advantages over our preliminary study of beam matching using dosimetric parameters such as depth doses, beam profiles, and output factors.[12] To improve the clinical workflow

and maintain high patient throughputs when interchange patients among beam-matched LINACs, the dosimetric accuracy of VMAT plans was evaluated based on 3%/3mm criteria according to the protocol used in our center. However, the difference in gamma passing rate criteria was not taken into account for the dosimetric accuracy evaluation. This was a limitation of this study. According to the update report published by AAPM TG-218, using γ3%/2mm is recommended for the appropriate criteria.[14] Therefore, the evaluation in other gamma passing rate criteria should be performed for further study.

Field sizes used in this study were limited from medium (5x5 cm^2) to large (30x30 cm^2) field sizes. Smaller field sizes (less than 5x5 cm^2) which are widely used in advanced techniques such as VMAT and stereotactic radiosurgery, were not included in the depth dose and beam profiles. In addition, output factors were conducted in field sizes larger than 2x2 cm^2. Munoz L *et al*. recently performed the small field dosimetry in beam-matched LINACS.[3] They found that the beams were matched for large field size and still matched down to field size 1x1 cm^2. For regular quality assurance for beam-matched LINACS, the assessment in a small field size should be incorporated. Moreover, treatment plan parameters comparison such as Planning Target Volume (PTV), body, and organ at risk (OAR) doses should be incorporated in order to confirm the clinical significance of beam matching in both LINACs.

Conclusion

Beam-matched LINACs show good agreement between measurements and TPS calculations for VMAT plans. In addition, slight differences in gamma passing rates between two LINACs prove the viability of interchanging VMAT patients between two beam-matched LINACs without re-planning VMAT plans to manage the machine downtime. However, these measurements should be frequently measured/re-checked and compared between LINAC systems in a part of hospital quality assurance programs, especially when interchange occurs.

Acknowledgements

All authors would like to sincerely thank senior medical physicist Mr. Paisarn Suwannakorn for his professional advice and contribution during beam measurements. We would like to thank Dr. Akarathan Jitnuyanont, director of Mahavajiralongkorn Thanyaburi hospital, for granting permission to use the laboratory facilities and support during the entirety of this work.

References

[1] Marshall MG. Matching the 6-MV photon beam characteristics of two dissimilar linear accelerators. Med Phys. 1993; 20: 1743-6.

[2] Watts RJ. Comparative measurements on a series of accelerators by the same vendor. Med Phys. 1999; 26: 2581-5.

[3] Muñoz L, Kron T, Petasecca M, Bucci J, Jackson M, Metcalfe P, et al. Consistency of small-field dosimetry, on and off axis, in beam-matched linacs used for stereotactic radiosurgery. J Appl Clin Med Phys. 2021; 22: 185-93.

[4] Hrbacek J, Depuydt T, Nulens A, Swinnen A, Van Den Heuvel F. Quantitative evaluation of a beam-matching procedure using one-dimensional gamma analysis. Med Phys. 2007; 34: 2917-27.

[5] Bhangle J, Sathiya Narayanan V, Kumar N, Vaitheeswaran R. Dosimetric analysis of beam-matching procedure of two similar linear accelerators. J Med Phys. 2011; 36: 176-80.

[6] Beyera GP. Commissioning measurements for photon beam data on three TrueBeam linear accelerators, and comparison with Trilogy and Clinac 2100 linear accelerators. J Appl Clin Med Phys. 2013; 14: 273-88.

[7] Krishnappan C, Radha CA, Subramani V, Gunasekaran MK. Is the dose distribution distorted in IMRT and RapidArc treatment when patient plans are swapped across beam-matched machines? J Appl Clin Med Phys. 2016; 17: 111-23.

[8] Ashokkumar S, Ganesh KM, Ramalingam K, Karthikeyan K, Jagadheeskumar N. Dosimetric validation of volumetric modulated arc therapy with three 6MV beam-matched linear accelerators. Asian Pacific J Cancer Prev. 2017; 18: 3439-44.

[9] Xu Z, Warrell G, Lee S, Colussi V, Zheng Y, Ellis R, et al. assessment of beam-matched linacs quality/accuracy for interchanging SBRT or SRT patient using VMAT without re-planning. J Appl Clin Med Phys. 2019; 20: 68-75.

[10] Rijken J, Schachenmayr H, Crowe S, Kairn T, Trapp J. Distributive quality assurance and delivery of stereotactic ablative radiotherapy treatments amongst beam matched linear accelerators: A feasibility study. J Appl Clin Med Phys. 2019; 20: 99-105.

[11] Ghazal M, Södergren L, Westermark M, Söderström J, Pommer T. Dosimetric and mechanical equivalency of Varian TrueBeam linear accelerators. J Appl Clin Med Phys. 2020; 21: 43-53.

[12] Donmoon T, Wattanachaiyasit S, Kaewboonperm U, Meennuch E, Klaitong C. Beam matching of two linear accelerators, identical model and brand. In: Journal of Physics: Conference Series. IOP Publishing; 2020.

[13] Precise treatment system. Customer acceptance test, part no. 4513370187004. Stockholm, Sweden: Elekta Oncology System limited, Elekta UK; 2003.

[14] Miften M, Olch A, Mihailidis D, Moran J, Pawlicki T, Molineu A, et al. Tolerance limits and methodologies for IMRT measurement-based verification QA: Recommendations of AAPM Task Group No. 218. Med Phys. 2018; 45: e53-83.

Journal of Associated Medical Sciences 2021; 54 (3): 107-124

JAMS
Journal of Associated Medical Sciences

Thai-Journal Citation Index Centre (TCI) & ASEAN Citation Index (ACI)

Journal of Associated Medical Sciences

Journal homepage: https://www.tci-thaijo.org/index.php/bulletinAMS/index

Transcriptomic change of human gingival cells during cultivation on gelatin composite hydroxyapatite and pig brain extract

Fahsai Kantawong[1*] Yasumin Chaiyasert[1] Nichanun Bungkhuan[1] Kanyamas Choocheep[1] Warunee Kumsaiyai[1] Penpitcha Wanachantararak[2] Thasaneeya Kuboki[3]

[1]Department of Medical Technology, Faculty of Associated Medical Sciences, Chiang Mai University, Chiang Mai Province, Thailand
[2]The Dental Research Center, Faculty of Dentistry, Chiang Mai University, Chiang Mai Province, Thailand
[3]Laboratory of Biomedical and Biophysical Chemistry, Institute for Materials Chemistry and Engineering, Kyushu University, Fukuoka, Japan

ARTICLE INFO

Article history:
Received 15 July 2021
Accepted as revised 18 August 2021
Available online 26 August 2021

Keywords:
Nano-hydroxyapatite, pig brain extract, pro-neuroinflammatory gene expression, transcriptome, ECM remodeling

ABSTRACT

Background: Biomaterials that contain mechanical and biochemical properties similar to neural tissue will provide the environment that support neuronal survival and development.

Objectives: This study assessed the effects of three gelatin-based biomaterials on gene expression of primary human gingival fibroblasts.

Materials and methods: Human gingival cells were cultured on 3 types of biomaterials; 10% gelatin, 10% gelatin with hydroxyapatite and 10% gelatin with hydroxyapatite and pig's brain extract. These biomaterials were used in cell culture to investigate that they could support long-term culture of adult somatic cells like human gingival cell or not.

Results: Human gingival cells were cultured on biomaterials for 21 days then, RNA sequencing showed up-regulation of 259 genes and down regulation of 210 gene in human gingiva cells cultured on Gel+HA+Brain compared to cells on tissue culture plates. RNA sequencing showed up-regulation of antioxidant genes, solute-carrier gene (*SLC*) superfamily, histone and cell cycle gene. Down-regulation of ECM and cytoskeletal protein were observed. The further study by reverse transcription real time – PCR was performed to confirm the result of *Klf4*, *Tuj1*, *OCN, ACAN* and *VCAN* gene expression in human gingival cells. Moreover, some neuronal related genes in human gingiva cells cultured on Gel+HA+Brain compared to cells on tissue culture plates were detected.

Conclusion: The biomaterials (Gel+HA+Brain) affected gene expression in many aspects at 21 days culture. It was possible that 10% gelatin with nano-hydroxyapatite and pig's brain extract could be used to support cell differentiation of the human gingival cells. In conclusion simple fabrication of the biomaterial from 10% gelatin with nano-hydroxyapatite and pig's brain extract could be used for modulation of gene expression in adult somatic cells.

* **Corresponding author.**
Author's Address: *Department of Medical Technology, Faculty of Associated Medical Sciences, Chiang Mai University, Chiang Mai Province, Thailand.*
** **E-mail address:** fahsai.k@cmu.ac.th
doi: 10.14456/jams.2021.31
E-ISSN: 2539-6056

Introduction

Clinically, gingival tissue is easy to collect by biopsy thus it is feasible to isolate cells from gingival tissue based on their highly proliferative nature.[1] The gingival tissues were containing mesenchymal stem cells (GMSCs). Around 90% of GMSCs are derived from cranial neural crest cells (CNCC) and 10% from the mesoderm.[1] GMSCs show remarkable tissue reparative and regenerative potential.[2] Human GMSCs showed the ability of differentiation into neuronal lineages make it a promising tissue construct for translational application. Recently, there has been an emergence of research groups offering new concepts focused on using human gingival cells to treat neurodegenerative disorders.[3] Moreover, human gingiva-derived mesenchymal stem cells (GMSC) have shown anti-inflammatory and immunomodulatory effects on modulating inflammatory monocytes/macrophages and alleviating atherosclerosis.[4] However, in the present study, there was no attempt to isolate stem cells because this study aimed to test the supportive role of the fabricated biomaterial before moving on to the bioinductive role in the future. Human gingival cells from healthy gingival tissue without inflammation were used in this study.

Biomaterials that contain mechanical and biochemical properties similar to neural tissue will provide the environment that support neuronal survival and development.[5] Previous studies by Kantawong *et al*. indicated that biomaterials produced from 10% gelatin, nano-hydroxyapatite and pig brain extract (Gel+Ha+Brain) enhanced increase expression of reprogramming factor *Klf4* and transcription factor (*Nfia*, *Nfib* and *Ptbp*) in NIH/3T3 at 9 days culture, which indicated the possibility of astrocytic phenotype.[6]

This study assessed the effects of three gelatin-based biomaterials on gene expression of primary human gingival fibroblasts. The biological evidence supporting the use of hydroxyapatite for neuronal differentiation was previously presented [6, 7] and the study of Lambrichts *et al.* also indicated that hydroxyapatite scaffolds containing peptide hydrogels enhanced blood vessel ingrowth.[8]

In the present study, human gingiva cells cultured on 10% gelatin with nano-hydroxyapatite and pig's brain extract were subjected for the further investigation by RNA sequencing (Next-Gen sequencing, Illumina) to observe change in global gene expression for predicting and validating roles of biomaterials in regulatory mechanisms underlying human gingival cell development.

Materials and methods

Brain extract

Brain extract preparation was modified from the previous study. [6] Pig brain was purchased from local market and preserved in frozen condition before use. Frozen pig brain was thawed at room temperature then 100 grams of pig brain was washed in sterile water before blending in a blender with 100 mL of sterile phosphate buffer saline (PBS) containing 1% Pen-Strep using liquidify mode for 1 min, then the liquidified brain was poured into 50 mL centrifuge tube and spun at 2,500 rpm for 10 min in the centrifuge (KUBOTA Model 5200). The supernatant was discarded and the white brain precipitant was kept at -20 °C until used.

Biomaterial preparation

Biomaterial preparation was modified from the previous study.[6] Gelatin (10% w/v) in distilled water was incubated in water bath 50 °C for 45 min until gelatin was dissolved. Then gelatin solution was stirred at 50 °C for 30 min. For Gel+HA, the gelatin solution was stirred for 15 min at room temperature before adding 100 mg of nano-hydroxyapatite and continued stirring for 30 min. For Gel+HA+Brain, add 1 mL of brain extract together with 100 mg HA then 25% glutaraldehyde 5-6 µL/mL was added and mixed with each type of gelatin solution before pouring into 6-well plate. The biomaterial was prepared well-by-well using 2 mL of solution per well. The solution was left overnight then polymerized gelatin was washed with sterile distilled water three times for 30 min each. After that polymerized gelatin was soaked in sterile distilled water overnight. Water was discarded and polymerized gelatin was then gently tapped on tissue paper to absorb the rest of water on surface of gelatin. Polymerized materials (Figure 1S) were frozen at -20 °C before freeze drying was performed in the lyophilizer (LYOLAB; LYOPHILIZATION SYSTEMS, INC, USA) at 9 mTorr with condenser temperature 84.1 °C for 24 hr.

Preconditioning of biomaterials

Biomaterials were immerged in 70% ethanol for 30 min. After 70% ethanol was discarded, biomaterials were immerged in sterile water for 30 min 3 times. Complete DMEM (3 mL) was added to each biomaterial and incubated in 5% CO_2 incubator at 37 °C for at least 24 hr. Then the biomaterials were ready for cell culture.

Human gingival cells culture

Ethical approval by the Ethics Committee of the Faculty of Dentistry, Chiang Mai University (21.1/2018), was obtained for the study of human gingival cells. Human gingiva tissue was rinsed in sterile phosphate-buffered saline and transferred to a Petri dish containing DMEM. The tissue was minced with a scalpel. The obtained suspension of tissue fragments and gingival cells were condensed by centrifugation (200 × g for 5 min). The resuspended pellet was placed in a tissue culture flask with culture medium (DMEM) containing 10% FCS penicillin/streptomycin. A monolayer culture was incubated at 37°C in an incubator containing 5% CO_2. The medium was renewed every 2 days. The human gingival cells were confluent after 5-7 days of culture. The human gingival cells were seeded onto each type of preconditioned biomaterials at the density $1x10^5$ cells per gel. The cells were cultured in an incubator with 5% CO_2 at 37 °C, medium was changed every 5-7 days until 3 weeks.

Sample preparation and RNA sequencing

Human gingival cells ($1x10^5$ cells per gel) were grown in tissue culture plate and Gel+HA+Brain for 21 days. Total RNAs were purified by NucleoSpin RNA isolation kit. The total RNA was collected from 42 gelatin biomaterials (7 plates of 6-well plate) and pooled together. The purity of the RNA preparations was qualified by nanodrops and gel electrophoresis as shown in supplementary data (Figure 2S). Transcriptome sequencing was performed using a service from Next Gen with the Illumina platform. Sequencing data processing. Reads are mapped to human reference genome.

Cell staining

Cell morphology was obtained by staining the cells with Alcian blue and Coomassie blue R. Briefly, the cells were fixed with 4% formaldehyde for 5-10 min and stained with 0.5% Alcian blue for 5 min. The stain was removed and the cells were rinsed with tap water before visualizing under an inverted microscope (Nikon ECLIPSE TS 100).

Real-time PCR

RNA extraction was performed using Nucleospin (MACHEREY-NAGEL) and cDNA synthesis was performed using ReverTra Ace cDNA synthesis kit (Toyobo) following the protocols of manufacturers. cDNA sample was diluted to the desired dilution, then 4.0 µL of the cDNA was mixed with SYBR Green Mastermix (Bioline) and the primer at a final concentration of 0.25 µM in the total volume of 10 µL. Real time-PCR was performed in LightCycler® 480. The PCR program contain 3 steps: (1) Pre-incubation step at 95 °C for 2 min (2) PCR step (denature at 95 °C, annealing at 60 °C and extension at 72 °C) for 40 cycles. (3) Melting curve analysis was performed at 95, 65 and 97 °C. The experiments were repeated at least 3 times. Target genes were normalized with reference genes *GAPDH* and *18s rRNA* using LightCyCler 4.0 software. Sequences of primers used in real-time PCR were shown in Table 1S.

Statistical analysis

For real-time PCR, three independent assays were performed. The fold change of gene expression in Gel+HA and Gel+HA+Brain was compared with Gel using independent t-test by SPSS 17.0 software. The statistical significance was determined at $p<0.05$.

Results

RNA sequencing

Differential gene expression found 259 genes up-regulation and 210 genes down-regulation in human gingival cells cultured on Gel+HA+Brain compared to those cultured on tissue culture plate (Figure 1).

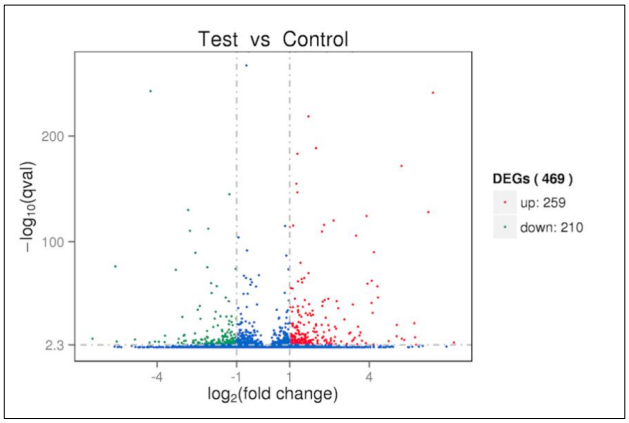

Figure 1. *Volcano plots showed differential gene expression between human gingival cells cultured on tissue culture plate (Control) and human gingival cells cultured on 10% gelatin with nano-hydroxyapatite and pig brain extract for 3 weeks (Test) with an adjusted P value of < 0.01. Genes with log 2-fold change ≥1 were highlighted in red while genes with log 2 fold-change ≤1 were highlighted in green.*

Table 1 Expression cytoskeletal proteins, ECM proteins and receptor-related proteins.

Genes	log2.Fold change*	Note
Collagen, type XII	-1.9662	A component of human skeletal muscle
Collagen, type XI	-2.1506	Broadly distributed in articular cartilage, testis, trachea, tendons, trabecular bone, skeletal muscle, placenta, lung, and the neoepithelium of the brain
Collagen, type XIV	-2.4678	Skin, tendon, cornea, and articular cartilage
Collagen, type IV	-2.7612	Found in the skin within the basement membrane zone
Collagen, type XV	-2.9963	Located in the basement membrane zones of microvessels and cardiac or skeletal myocytes
Collagen, type V	-3.0496	Bone matrix; corneal stroma; and the interstitial matrix of muscles, liver, lungs, and placenta
Laminin, alpha 1	-1.7556	Extracellular matrix glycoprotein
Fibulin 1	-2.8291	Elastic fiber–associated protein
Hyaluronan and proteoglycan link protein 1	-1.8867	A key molecule in the formation and control of hyaluronan-based condensed perineuronal matrix in the adult brain
Versican	-1.5414	Extracellular matrix (ECM) component
Biglycan	-1.8302	Extracellular space proteins
Podocan	-1.8867	Extracellular space proteins
Aggrecan	-2.1317	Major proteoglycan component of the extracellular matrix in the growth plate and articular cartilage
Fibronectin	-1.8995	Extracellular matrix glycoprotein
Tenascin C	-1.9473	Extracellular matrix glycoprotein

Table 1 Expression cytoskeletal proteins, ECM proteins and receptor-related proteins. (continues)

Genes	log2.Fold change*	Note
Nidogen 2	-1.0058	Basement membrane glycoprotein
Elastin	-3.2948	Extracellular matrix protein
Integrin, alpha 6	-1.0029	Transmembrane glycoproteins
Integrin, alpha 11	-1.5099	Transmembrane glycoproteins
Integrin, alpha 8	-1.7528	Transmembrane glycoproteins
Integrin, alpha 4	-1.9703	Transmembrane glycoproteins
Integrin, alpha 10	-2.9821	Transmembrane glycoproteins
Integrin, alpha 7	-3.6994	Transmembrane glycoproteins
Calponin 1	-1.0096	Actin-binding protein
Spectrin	-1.0127	Actin-bundling and membrane-anchoring proteins
Cadherin 13	-2.3413	Cell adhesion molecules
Tensin 1	-2.1974	Cytoplasmic phosphoprotein that localized to integrin-mediated focal adhesions
Matrix-remodeling associated 5	-1.3526	Secreted extracellular protein
Matrix metallopeptidase 10	-6.4405	Played roles in macrophage inflammation
Matrix metallopeptidase 14	1.2899	Transmembrane-type MMP, digests the triple helical portions of interstitial collagen types I, II, and III and other ECM components, including fibronectin, laminin, aggrecan, and gelatin
Matrix metallopeptidase 15	2.0475	Transmembrane-type MMP, digests fibronectin, tenascin, nidogen, aggrecan, perlecan, and laminin
Matrix metallopeptidase 3	2.4599	Progelatinase; involved in joint destruction in rheumatoid arthritis
Matrix metallopeptidase 7	5.768	Expressed in endothelial cells, cardiomyocytes, and macrophages
Nestin	-1.0175	Intermediate filament
Actin filament associated protein 1	-1.1859	Cytoskeletal associated protein
Actin, alpha 2	-1.7938	Cytoskeletal protein
Actin, gamma 2, smooth muscle	-3.934	Cytoskeletal protein
Myosin ID	-1.4094	Actin motor protein
Myosin X	-1.4293	Actin motor protein
Myosin, heavy chain 11	-5.524	Actin motor protein
Microtubule-associated protein 1B	-1.2792	Cytoskeletal associated protein
TPX2, microtubule-associated	-1.8495	Cytoskeletal protein
Anillin	-2.0966	Cctin binding protein
Kinesin family member 11	-2.0579	Motor proteins
Calponin 1	-1.0096	Calponin is an actin filament-associated regulatory protein
Lamin B2	-1.2096	Type V intermediate filaments
Syntrophin, beta 1	-1.1385	Role in cytoskeletal organization
Keratin 19	-2.6364	Low-molecular-weight cytoskeletal protein

Note: **adjusted p<0.001*

Table 2 Increased expression of antioxidant genes.

Antioxidant protein	log2.Fold change*	Gene expression
Thioredoxin reductase 1	1.1221	increased
Glutathione peroxidase 3	1.3424	increased
Thioredoxin	1.4955	increased
Microsomal glutathione S-transferase 1	1.9204	increased
Oxidative stress induced growth inhibitor family member 2	2.0575	increased
Heme oxygenase (decycling) 1	1.1758	increased

Note: **adjusted p<0.001*

Table 3 Increased expression of histone and cell cycle-related genes.

Histone	log2.Fold change*	Gene expression
H2A histone family, member Y2	1.2871	increased
Histone cluster 1, H2ac	1.8861	increased
Histone cluster 1, H2bk	1.9536	increased
Histone cluster 2, H2be	2.3063	increased
Histone cluster 1, H1c	2.4874	increased
Cyclin-dependent kinase inhibitor 1A (CDKN1A)	1.4043	increased
Cyclin L1	1.59	increased
Cyclin-dependent kinase inhibitor 2B (CDKN2B)	1.6196	increased
Cyclin D2	2.9397	increased
Regulator of cell cycle	1.2656	increased

Note: **adjusted p<0.001*

Table 4 Expression of genes related to neuronal function.

Gene	log2.Fold change*	Note
1. Neural proliferation and differentiation control protein-1 (NPDC-1)	1.0051	Control neural proliferation and differentiation [9-11]
2. Solute carrier family 6 (neurotransmitter transporter) (SLC6A8)	1.0865	GABA transporter [12, 13]
3. Leucine rich repeat neuronal 3 (LRRN3)	1.6603	Brain development [14] and the synaptic connection [15]
4. Neuromedin B (NMB)	1.7012	Neuropeptide found in the pituitary, gastrointestinal tract and the central nervous system [16]
5. CD44 molecule (CD44)	1.0214	Surface markers of neural lineage [17]
6. GABA(A) receptor-associated protein like 1 (GABARAPL1)	1.082	Maintaining normal autophagic flux [18, 19]
7. Amyloid beta (A4) precursor-like protein 1 (APLP1)	1.0749	Upregulated during postnatal development coinciding with synaptogenesis [20]
8. Semaphorin3C (SEMA3C)	1.2086	Growth of axon in dopamine neuron [21]
9. B-cell translocation gene 2 (Btg2)	2.5507	Played important roles in cholinergic neuronal differentiation of BMSCs [22]
10. Transmembrane protein 132A (TMEM132A)	2.3203	Considered as novel IG domain containing proteins of the CNS [23]
11. Transient receptor potential ankyrin 1 (TRAP1)	1.551	Played roles in matrix homeostasis and inflammation [24]
12. Activating transcription factor 3 (ATF3)	2.0147	CNS inflammatory responses [25]

Table 4 Expression of genes related to neuronal function. (continues)

Gene	log2.Fold change*	Note
13. Prostaglandin D2 synthase 21kDa (brain) (PTGDS)	4.093	Catalyzes the conversion of prostaglandin H2 (PGH2) to postaglandin D2 (PGD2). PGD2 functions as a neuromodulator as well as a trophic factor in the central nervous system [26]
14. Inhibitory synaptic factor 1 (INSYN1)	1.5057	Dampen neuronal activity through postsynaptic hyperpolarization [27]
15. Synuclein alpha (SNCA)	1.2324	Neuronal protein that plays several roles in synaptic activity such as regulation of synaptic vesicle trafficking and subsequent neurotransmitter release [28]
16. Neuronal pentraxin receptor (NPTXR)	1.0894	Synapse formation [29, 30]
17. Neuronal pentraxin 1 (NPTX1)	1.000	Synapse formation [29, 30]

Note: **adjusted p<0.001*

KEGG pathway & GO analysis

KEGG pathway analysis in human gingival cells cultured on Gel+HA+Brain compared to those on tissue culture plate were shown in Table 4S. The most significant KEGG pathway was lysosome (hsa04142) which might relate to ECM remodeling/degradation. Gene-ontology (GO) compared between human gingival cells cultured on Gel+HA+Brain and normal control was shown in Figure 2. No significant GO term was down-regulated and 11 GO terms was significantly up-regulated. The most significant GO terms were chemokine activity and chemokine receptor binding which related to up-regulation of increase expression of chemokines and cytokines was presented in Table 3S. Every biomaterial was carefully observed under the microscope and no microorganism infection was found. The researchers confidently believed that up regulation of all chemokines and cytokines (*CXCL1, CXCL5, CXCL14, CXCL10, CCL2, CXCL3, CXCL6, CX3CL1* and *CXCL2*) was the response of cells to biomaterials.

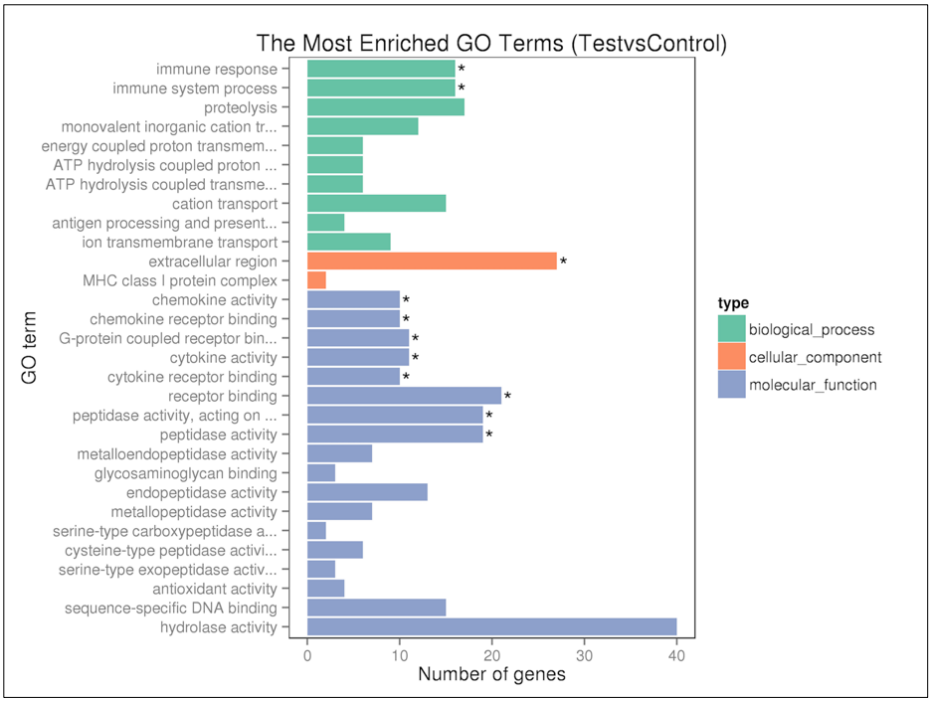

Figure 2. *GO enrichment of genes that were upregulated after cultivation on 10% gelatin with nano-hydroxyapatite and pig brain extract for 3 weeks. Vertical axis: GO terms, Horizontal axis: number of the differentially expressed genes annotated in the GO term. Total 11 GO terms were significantly up-regulated (p≤0.05). No GO term was significantly down-regulated.*

Cells staining

Human gingival cells were seeded on top of the biomaterials and penetrated into hydrogel. Human gingival cells appeared healthy and elongated on Gel+HA+Bain compared to cells cultured on tissue culture plate (Figure 3). Positive Alcian blue staining in human gingival cells was concordant with the differential gene expression that showed up-regulation of *lumican* (2.2299 folds) and *tsukushi* (1.6405 folds); small leucine rich proteoglycans. The images of human gingival cells indicated non-infection with any microorganism.

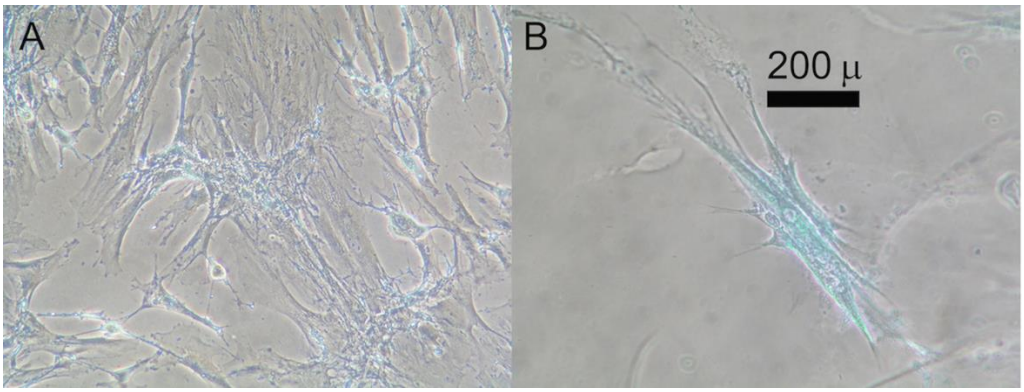

Figure 3. *Alcian blue staining. A: human gingival cells cultured on tissue culture plate for 3 weeks, B: human gingival cells cultured on 10% gelatin with nano-hydroxyapatite and pig brain extract for 3 weeks.*

Human gingival cells gene expression by real-time PCR

Figure 4 showed increased expression of *Klf4* gene and decreased expression of *βIII-tubulin* (*Tuj1*), *aggrecan (ACAN)*, *versican (VCAN)* and *osteocalcin (OCN)* using RT-PCR technique. The results of *Klf4*, *ACAN* and *VCAN* were correlated to the result from RNA sequencing that presented up-regulation of *Klf4* transcription factor and decreased ECM-cytoskeletal protein and proteoglycans.

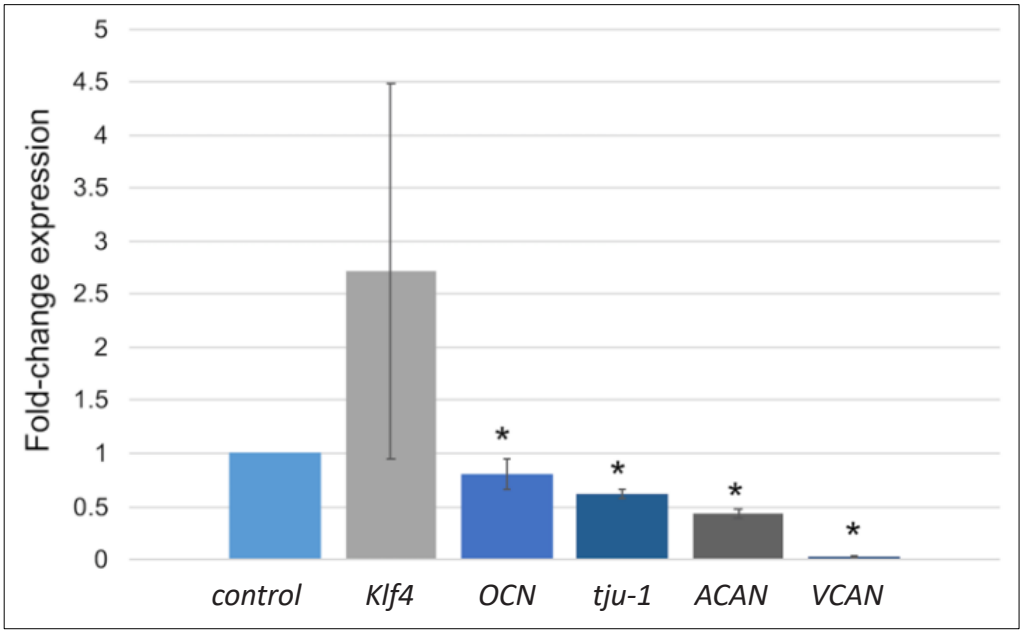

Figure 4. *Increased expression of Klf4 gene and decreased expression of βIII-tubulin (Tuj1), aggrecan (ACAN), versican (VCAN) and osteocalcin (OCN) when the expression of each gene in the control group was set as 1.*

Effect of nano-hydroxyapatite and pig brain extract

The comparison between each type of gelatin biomaterial was investigated to observe the effect of the addition of nano-hydroxyapatite and pig brain extract into gelatin. Since some neuronal related gene were detected in RNA sequencing so some neural-specific genes like *Glial fibrillary acidic protein (GFAP), Neurofilament light polypeptide (NFL), βIII-tubulin (Tuj1), Microtubule associated protein2 (MAP2)* and *CD44* were analyzed by real-time PCR. The expression of *MAP2* and *CD44* were changed. The level of *MAP2* gene expression in human gingival cells cultured in Gel+HA was 1.92 folds compared to plain 10% gelatin and not statistically significant (p=0.224587). The level of *MAP2* gene expression in human gingival cells cultured in Gel+HA+Brain was 10.7 folds compared to plain 10% gelatin and not statistically significant (p=0.136431) (Figure 5A). *CD44* gene expression was 1.57 folds and not significantly increased in human gingival cells cultured in Gel+HA compared to plain 10% gelatin (p=0.113239). The level of *CD44* gene expression in human gingival cells cultured in Gel+HA+Brain was 1.6 folds and not statistically significant compared to plain 10% gelatin (p=0.241992) (Figure 5B). The expression of *Tuj1* gene was decreased in human gingival cells cultured on Gel+HA+Brain without statistically significant (Figure 3S). The expression of *GFAP* and *NFL* genes were not detected.

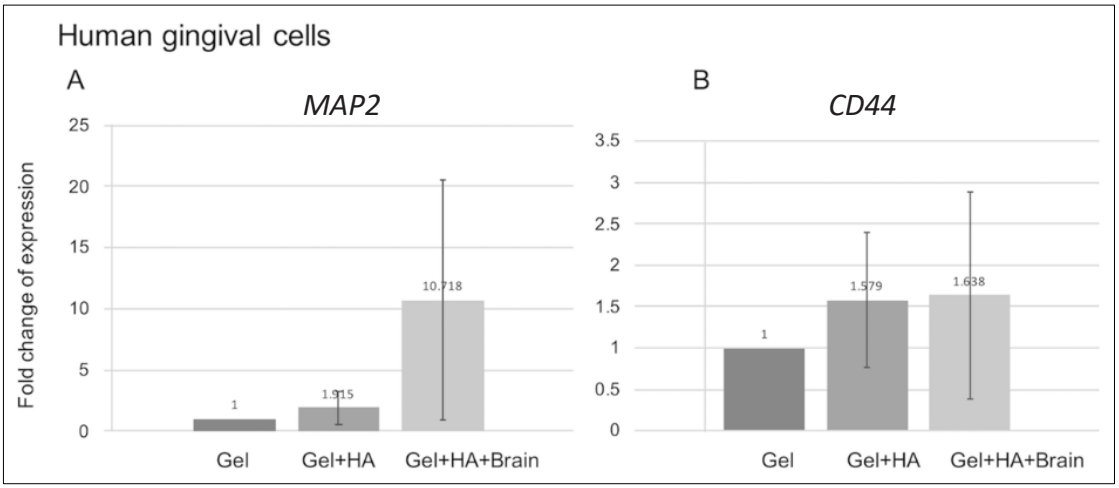

Figure 5. *Human gingival cells cultured on Gel+HA and Gel+HA+Brain showed up-regulation of MAP2 (A) and CD44 genes without statistically significance compared to 10% gelatin (B).*

Discussion

In the first step, the researchers aimed to screen for the impact of biomaterial compared with conventional tissue culture plate using RNA sequencing. In the next step, the researchers investigated the effects of the add up components such as nano-hydroxyapatite and pig brain extract.

Human gingival cells culture on Gel+HA+Brain presented dramatically change of transcriptome compared to human gingival cells cultured on tissue culture plate using RNA sequencing. The expression of antioxidant protein in Table 2 indicated that the cells were protecting themselves from oxidative stress and trying to survive. Increased expression of thioredoxin reductase 1 helped to maintain the sufficient amount of reduced thioredoxin for oxidative stress resistance.[31, 32] Microsomal glutathione S-transferase 1 protected the intracellular macromolecules from reactive electrophiles by accelerating the conjugation of glutathione with electrophilic compounds.[33] Glutathione peroxidase 3 in combination with reduced glutathione eliminated hydrogen peroxide in cells.[34]

Expression of histone genes and cell cycle-related genes were shown in Table 3. Histone gene expression dramatically occurs during the synthetic (S) phase of the eukaryotic cell cycle.[35] Increase chromatin during S phase occurs in DNA replication.[36] Somehow, increased histone expression might be related to increased lifespan and slowing the aging process of cells.[37] Gene that involved with self-renewal such as histone *H2A.2, KLF2, KLF4, NKX3-1* were also up-regulated in this study. Increased expression of the cell cycle proteins was also shown in Table 3. The regulator of cell cycle was associated with stimulation of cell cycle progression. The CDKN1A or p21 was related to cell growth, cell differentiation and apoptosis. In addition, p21 plays an important role in the cell cycle arrest at G1/S checkpoint.[38] When the expression of CDKN1A was suppressed, increases the cell division was occurred.[39] CDKN2B maintained the cells in a state of growth-arrested premalignant state.[40] The expression of Cyclin D2 related to self-renewal properties that controlled stem cells to differentiate without becoming cancer cells.[41] Down-regulation of *CDC20* and centrosome proteins were detected. *CDC20* is important as spindle assembly checkpoint protein and a key component of the mammalian cell cycle mechanism that activates the anaphase-promoting complex.[42] Some centrosomal proteins were down-regulated during DNA synthesis.[43]

Most of the top upregulated KEGG pathways was lysosome (Table 4S). Lysosome activity helped to maintain the youthfulness of cells.[44] Increased expression of lysosomal protein could also be found in the neuronal development because it reflected the increase degradation by lysosomal pathway.[45] Key pro-inflammatory cytokines and chemokines were upregulated in this study (Table 3S). A group of innate immune cells that synthesized and secreted various cytokines and chemokines were macrophages, neutrophils, mast cells, eosinophils, dendritic cells, and epithelial cells.[46] KEGG phagosome had increased significantly. Normally, the phagosome could be found in professional phagocytic cells, including macrophage monocyte neutrophil and dendritic cell. Cells engulfed certain substances that into cells such as amino acid by phagocytosis.[47] It could be possible that the hydrogels were in the biodegradable process and the cells engulfed the degraded particles into cells because the KEGG pathway showed decreased in ECM-receptor interaction and focal adhesion.

Upregulation of some neural-related genes was found i.e. *leucine-rich repeat neuronal 3 (LRRN3)* was relatively specific gene expressed in brain. LRRN3 plays an important role in brain development.[15] The expression of *NPDC-1* was very specific in the brain and controlled neural proliferation and differentiation.[9] Increased expression of solute carrier family 6 (neurotransmitter transporter) indicated that human gingival cells were trying to develop into a functional neuron because SLC6A8 acts as a GABA transporter.[12] Semaphorin 3C (Sema3C) was secreted from nerve cells and had a stimulating effect on the growth of axon in dopaminergic neurons.[21] GABARAPL1 was highly expressed in the brain, and restricted

to neurons which was required for maintaining normal autophagic flux.[18] *APLP1* were upregulated during postnatal development coinciding with synaptogenesis.[20] Neuronal pentraxin receptor was related to the synapse formation.[29] *B-cell translocation gene 2 (Btg2)* played important roles in cholinergic neuronal differentiation of BMSCs.[22] Down-regulation of *Btg2* inhibited neurite outgrowth.[48] TMEM132 molecules were considered as novel immunoglobulin-like domain containing proteins of the CNS23 which were important for cell survival in regulating certain ER stress-related gene expression in neuronal cells.[49] TRPA1 was predominantly expressed in peripheral nerve terminals, dorsal root ganglia, and central nerve terminals of primary sensory neurons in the spinal dorsal horn. TRPA1 was up-regulated in developing intervertebral disc and played roles in matrix homeostasis and inflammation.[24] Increase expression of solute-carrier gene (*SLC*) superfamily SLC was involved in the uptake of small molecules into cells such as amino acids, urea, nucleotide sugars, vitamin, neurotransmitters and etc.[50] Although the neuronal-related genes were found, neuronal differentiation could not be concluded. The gelation biomaterials used in this study showed the supportive roles for cultivation of adult somatic cells. The improvement of gelatin biomaterial properties might be useful for the application in induction of cell differentiation and the further study was continued in our laboratory.

Conclusion

Human gingival cells cultured on 42 gelatin biomaterials for 21 days showed increased oxidative stress protection and cells were in S-phase of cell cycle. Decreased cell-ECM interaction and ECM remodeling were occurred together with expression of some neuronal-related genes but neuronal-specific genes, *GFAP* and *NFL*, were not detected by RT-PCR. Immunomodulation was presented by up-regulation of chemokine and cytokine genes in human gingival cells cultured on gelatin biomaterials without microorganism infection under microscopic observation. This study aimed to investigate the biocompatibility of biomaterial. However, the physical properties such as pore size is very important and should be study in the further study.

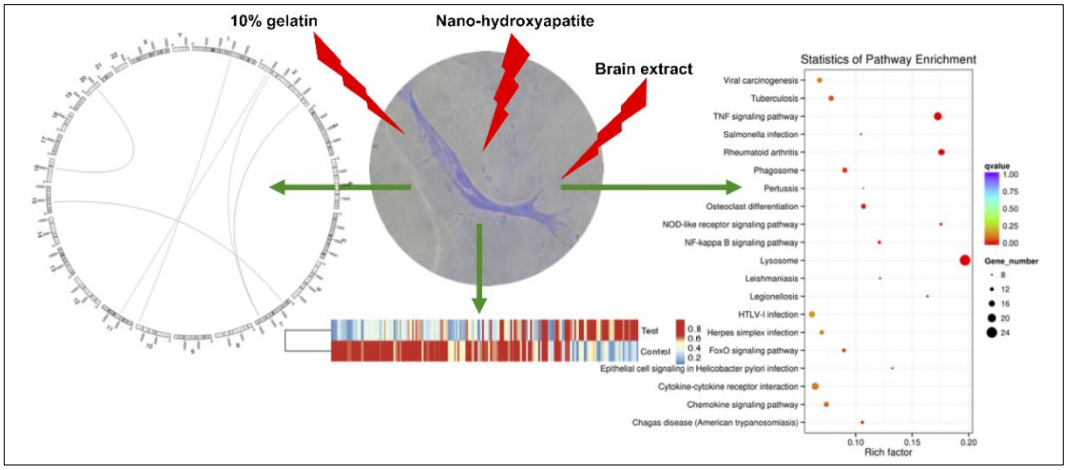

Figure 6. *Highlights of this study. Gelatin with hydroxyapatite and pig brain extract can be used in the modulation of somatic cells. Up-regulation of neuronal and antioxidant genes were found upon cultivation on the scaffold. Decreased of genes related to ECM remodeling were occurred upon cultivation on the scaffold.*

Acknowledgements

The author is very grateful for some reagents from Faculty of Associated Medical Sciences, Chiang Mai University.

Conflicts of Interest

The authors declare that there is no conflict of interest. The funders had no role in the design of the study; in the collection, analyses, or interpretation of data; in the writing of the manuscript, or in the decision to publish the results.

Ethic approval

Human gingival cells were obtained according to Ethical approval by the Ethics Committee of the Faculty of Dentistry, Chiang Mai University (21.1/2018).

References

[1] Xu X, Chen C, Akiyama K, Chai Y, Le AD, Wang Z, et al. Gingivae contain neural-crest- and mesoderm-derived mesenchymal stem cells. J Dent Res. 2013; 92(9): 825-32. doi: 10.1177/0022034513497961.

[2] Górski B. Gingiva as a new and the most accessible source of mesenchymal stem cells from the oral cavity to be used in regenerative therapies. Postepy Hig Med Dosw (Online). 2016; 70(0): 858-71.

[3] Gugliandolo A, Diomede F, Scionti D, Bramanti P, Trubiani O, Mazzon E. The Role of Hypoxia on the Neuronal Differentiation of Gingival Mesenchymal Stem Cells: A Transcriptional Study. Cell Transplant. 2019:963689718814470. doi: 10.1177/0963689718814470.

[4] Zhang X, Huang F, Li W, Dang JL, Yuan J, Wang J, et al. Human Gingiva-Derived Mesenchymal Stem Cells Modulate Monocytes/Macrophages and Alleviate Atherosclerosis. Front Immunol. 2018; 9: 878. doi: 10.3389/fimmu.2018.00878.

[5] Kantawong F, Kuboki T, Kidoaki S. Redox gene expression of adipose-derived stem cells in response to soft hydrogel. Turk J Biol. 2015; 39(5): 682-91.

[6] Kantawong F, Saksiriwisitkul C, Riyapa C, Limpakdee S, Wanachantararak P, Kuboki T. Reprogramming of mouse fibroblasts into neural lineage cells using biomaterials. Bioimpacts. 2018; 8(2): 129-38. doi: 10.15171/bi.2018.15.

[7] Kantawong F, Tanum J, Wattanutchariya W, Sooksaen P. Variation of Hydroxyapatite Content in Soft Gelatin Affects Mesenchymal Stem Cell Differentiation. Brazilian Archives of Biology and Technology. 2016;59. doi: 10.1590/1678-4324-2016150650.

[8] Lambrichts I, Driesen RB, Dillen Y, Gervois P, Ratajczak J, Vangansewinkel T, et al. Dental Pulp Stem Cells: Their Potential in Reinnervation and Angiogenesis by Using Scaffolds. J Endod. 2017; 43(9S): S12-S6. doi: 10.1016/j.joen.2017.06.001.

[9] Spencer ML, Theodosiou M, Noonan DJ. NPDC-1, a novel regulator of neuronal proliferation, is degraded by the ubiquitin/proteasome system through a PEST degradation motif. J Biol Chem. 2004; 279(35): 37069-78. doi: 10.1074/jbc.M402507200.

[10] Sansal I, Dupont E, Toru D, Evrard C, Rouget P. NPDC-1, a regulator of neural cell proliferation and differentiation, interacts with E2F-1, reduces its binding to DNA and modulates its transcriptional activity. Oncogene. 2000; 19(43): 5000-9. doi: 10.1038/sj.onc.1203843.

[11] Dupont E, Sansal I, Evrard C, Rouget P. Developmental pattern of expression of NPDC-1 and its interaction with E2F-1 suggest a role in the control of proliferation and differentiation of neural cells. J Neurosci Res. 1998; 51(2): 257-67. doi: 10.1002/(SICI)1097-4547(19980115)51:2<257::AID-JNR14>3.0.CO;2-5.

[12] Bröer S, Gether U. The solute carrier 6 family of transporters. Br J Pharmacol. 2012; 167(2): 256-78. doi: 10.1111/j.1476-5381.2012.01975.x.

[13] Kristensen AS, Andersen J, Jørgensen TN, Sørensen L, Eriksen J, Loland CJ, et al. SLC6 neurotransmitter transporters: structure, function, and regulation. Pharmacol Rev. 2011; 63(3): 585-640. doi: 10.1124/pr.108.000869.

[14] Yang J, Li F, Qiu L, Luo X, Huang H. [Role of LRRN3 in the cerebellum postnatal development in rats]. Zhong Nan Da Xue Xue Bao Yi Xue Ban. 2011; 36(5): 424-9. doi: 10.3969/j.issn.1672-7347.2011.05.009.

[15] Kochunov P, Charlesworth J, Winkler A, Hong LE, Nichols TE, Curran JE, et al. Transcriptomics of cortical gray matter thickness decline during normal aging. Neuroimage. 2013; 82: 273-83. doi: 10.1016/j.neuroimage.2013.05.066.

[16] Ehling S, Fukuyama T, Ko MC, Olivry T, Bäumer W. Neuromedin B Induces Acute Itch in Mice via the Activation of Peripheral Sensory Neurons. Acta Derm Venereol. 2019. doi: 10.2340/00015555-3143.

[17] Su W, Foster SC, Xing R, Feistel K, Olsen RH, Acevedo SF, et al. CD44 Transmembrane Receptor and Hyaluronan Regulate Adult Hippocampal Neural Stem Cell Quiescence and Differentiation. J Biol Chem. 2017; 292(11): 4434-45. doi: 10.1074/jbc.M116.774109.

[18] Boyer-Guittaut M, Poillet L, Liang Q, Bôle-Richard E, Ouyang X, Benavides GA, et al. The role of GABARAPL1/GEC1 in autophagic flux and mitochondrial quality control in MDA-MB-436 breast cancer cells. Autophagy. 2014; 10(6): 986-1003. doi: 10.4161/auto.28390.

[19] Le Grand JN, Bon K, Fraichard A, Zhang J, Jouvenot M, Risold PY, et al. Specific distribution of the autophagic protein GABARAPL1/GEC1 in the developing and adult mouse brain and identification of neuronal populations expressing GABARAPL1/GEC1. PLoS One. 2013; 8(5): e63133. doi: 10.1371/journal.pone.0063133.

[20] Schilling S, Mehr A, Ludewig S, Stephan J, Zimmermann M, August A, et al. APLP1 Is a Synaptic Cell Adhesion Molecule, Supporting Maintenance of Dendritic Spines and Basal Synaptic Transmission. J Neurosci. 2017; 37(21): 5345-65. doi: 10.1523/JNEUROSCI.1875-16.2017.

[21] Carballo-Molina OA, Sánchez-Navarro A, López-Ornelas A, Lara-Rodarte R, Salazar P, Campos-Romo A, et al. Semaphorin 3C Released from a Biocompatible Hydrogel Guides and Promotes Axonal Growth of Rodent and Human Dopaminergic Neurons. Tissue Eng Part A. 2016; 22(11-12): 850-61. doi: 10.1089/ten.TEA.2016.0008.

[22] Shao J, Sun C, Su L, Zhao J, Zhang S, Miao J. Phosphatidylcholine-specific phospholipase C/heat shock protein 70 (Hsp70)/transcription factor B-cell translocation gene 2 signaling in rat bone marrow stromal cell differentiation to cholinergic neuron-like cells. International Journal of Biochemistry & Cell Biology. 2012; 44(12): 2253-60. doi: 10.1016/j.biocel.2012.09.013.

[23] Sanchez-Pulido L, Ponting CP. TMEM132: an ancient architecture of cohesin and immunoglobulin domains define a new family of neural adhesion molecules. Bioinformatics. 2018; 34(5): 721-4. doi: 10.1093/bioinformatics/btx689.

[24] Kameda T, Zvick J, Vuk M, Sadowska A, Tam WK, Leung VY, et al. Expression and Activity of TRPA1 and TRPV1 in the Intervertebral Disc: Association with Inflammation and Matrix Remodeling. Int J Mol Sci. 2019; 20(7). doi: 10.3390/ijms20071767.

[25] Förstner P, Rehman R, Anastasiadou S, Haffner-Luntzer M, Sinske D, Ignatius A, et al. Neuroinflammation after Traumatic Brain Injury Is Enhanced in Activating Transcription Factor 3 Mutant Mice. J Neurotrauma. 2018; 35(19): 2317-29. doi: 10.1089/neu.2017.5593.

[26] Taniguchi H, Mohri I, Okabe-Arahori H, Aritake K, Wada K, Kanekiyo T, et al. Prostaglandin D2 protects neonatal mouse brain from hypoxic ischemic injury. J Neurosci. 2007; 27(16): 4303-12. doi: 10.1523/JNEUROSCI.0321-07.2007.

[27] Uezu A, Kanak DJ, Bradshaw TW, Soderblom EJ, Catavero CM, Burette AC, et al. Identification of an elaborate complex mediating postsynaptic inhibition. Science. 2016; 353(6304): 1123-9. doi: 10.1126/science.aag0821.

[28] Fusco G, Pape T, Stephens AD, Mahou P, Costa AR, Kaminski CF, et al. Structural basis of synaptic vesicle assembly promoted by α-synuclein. Nat Commun. 2016; 7: 12563. doi: 10.1038/ncomms12563.

[29] Farhy-Tselnicker I, van Casteren ACM, Lee A, Chang VT, Aricescu AR, Allen NJ. Astrocyte-Secreted Glypican 4 Regulates Release of Neuronal Pentraxin 1 from Axons to Induce Functional Synapse Formation. Neuron. 2017; 96(2): 428-45.e13. doi: 10.1016/j.neuron.2017.09.053.

[30] Lee SJ, Wei M, Zhang C, Maxeiner S, Pak C, Calado Botelho S, et al. Presynaptic Neuronal Pentraxin Receptor Organizes Excitatory and Inhibitory Synapses. J Neurosci. 2017; 37(5): 1062-80. doi: 10.1523/JNEUROSCI.2768-16.2016.

[31] Bobba A, Casalino E, Petragallo VA, Atlante A. Thioredoxin/thioredoxin reductase system involvement in cerebellar granule cell apoptosis. Apoptosis. 2014; 19(10): 1497-508. doi: 10.1007/s10495-014-1023-y.

[32] Arodin L, Miranda-Vizuete A, Swoboda P, Fernandes AP. Protective effects of the thioredoxin and glutaredoxin systems in dopamine-induced cell death. Free Radic Biol Med. 2014; 73: 328-36. doi: 10.1016/j.freeradbiomed.2014.05.011.

[33] Townsend DM, Tew KD. The role of glutathione-S-transferase in anti-cancer drug resistance. Oncogene. 2003; 22(47): 7369-75. doi: 10.1038/sj.onc.1206940.

[34] Chung SS, Kim M, Youn BS, Lee NS, Park JW, Lee IK, et al. Glutathione peroxidase 3 mediates the antioxidant effect of peroxisome proliferator-activated receptor gamma in human skeletal muscle cells. Mol Cell Biol. 2009; 29(1): 20-30. doi: 10.1128/MCB.00544-08.

[35] Kurat C, Lambert J, Petschnigg J, Friesen H, Pawson T, Rosebrock A, et al. Cell cycle-regulated oscillator coordinates core histone gene transcription through histone acetylation. Proceedings of the National Academy of Sciences of the United States of America. 2014; 111(39): 14124-9. doi: 10.1073/pnas.1414024111.

[36] Mei Q, Huang J, Chen W, Tang J, Xu C, Yu Q, et al. Regulation of DNA replication-coupled histone gene expression. Oncotarget. 2017; 8(55): 95005-22. doi: 10.18632/oncotarget.21887.

[37] Feser J, Truong D, Das C, Carson JJ, Kieft J, Harkness T, et al. Elevated histone expression promotes life span extension. Mol Cell. 2010; 39(5): 724-35. doi: 10.1016/j.molcel.2010.08.015.

[38] Ouellet S, Vigneault F, Lessard M, Leclerc S, Drouin R, Guérin SL. Transcriptional regulation of the cyclin-dependent kinase inhibitor 1A (p21) gene by NFI in proliferating human cells. Nucleic Acids Res. 2006; 34(22): 6472-87. doi: 10.1093/nar/gkl861.

[39] Kim MK, Jeon BN, Koh DI, Kim KS, Park SY, Yun CO, et al. Regulation of the cyclin-dependent kinase inhibitor 1A gene (CDKN1A) by the repressor BOZF1 through inhibition of p53 acetylation and transcription factor Sp1 binding. J Biol Chem. 2013; 288(10): 7053-64. doi: 10.1074/jbc.M112.416297.

[40] McNeal AS, Liu K, Nakhate V, Natale CA, Duperret EK, Capell BC, et al. CDKN2B Loss Promotes Progression from Benign Melanocytic Nevus to Melanoma. Cancer Discov. 2015; 5(10): 1072-85. doi: 10.1158/2159-8290.CD-15-0196.

[41] Tschen SI, Zeng C, Field L, Dhawan S, Bhushan A, Georgia S. Cyclin D2 is sufficient to drive β cell self-renewal and regeneration. Cell Cycle. 2017; 16(22): 2183-91. doi: 10.1080/15384101.2017.1319999.

[42] Wang S, Chen B, Zhu Z, Zhang L, Zeng J, Xu G, et al. CDC20 overexpression leads to poor prognosis in solid tumors A system review and meta-analysis. Medicine. 2018; 97(52). doi: 10.1097/MD.0000000000013832.

[43] Kim G, Lee I, Kim J, Hwang D. The Replication Protein Cdc6 Suppresses Centrosome Over-Duplication in a Manner Independent of Its ATPase Activity. Molecules and Cells. 2017; 40(12): 925-34. doi: 10.14348/molcells.2017.0191.

[44] Simic MS, Dillin A. The Lysosome, Elixir of Neural Stem Cell Youth. Cell Stem Cell. 2018; 22(5): 619-20. doi: 10.1016/j.stem.2018.04.017.

[45] Frese CK, Mikhaylova M, Stucchi R, Gautier V, Liu Q, Mohammed S, et al. Quantitative Map of Proteome Dynamics during Neuronal Differentiation. Cell Rep. 2017; 18(6): 1527-42. doi: 10.1016/j.celrep.2017.01.025.

[46] Lacy P. Editorial: secretion of cytokines and chemokines by innate immune cells. Front Immunol. 2015; 6: 190. doi: 10.3389/fimmu.2015.00190.

[47] Levin R, Grinstein S, Canton J. The life cycle of phagosomes: formation, maturation, and resolution. Immunol Rev. 2016; 273(1): 156-79. doi: 10.1111/imr.12439.

[48] Miyata S, Mori Y, Tohyama M. PRMT1 and Btg2 regulates neurite outgrowth of Neuro2a cells. Neuroscience Letters. 2008; 445(2): 162-5. doi: 10.1016/j.neulet.2008.08.065.

[49] Oh-hashi K, Imai K, Koga H, Hirata Y, Kiuchi K. Knockdown of transmembrane protein 132A by RNA interference facilitates serum starvation-induced cell death in Neuro2a cells. Mol Cell Biochem. 2010; 342(1-2): 117-23. doi: 10.1007/s11010-010-0475-9.

[50] Lin L, Yee S, Kim R, Giacomini K. SLC transporters as therapeutic targets: emerging opportunities. Nature Reviews Drug Discovery. 2015; 14(8): 543-60. doi: 10.1038/nrd4626.

Supplementary data

Figure 1. *Lyophilized biomaterials made from 10% gelatin, 1 mg/mL nano-hydroxyapatite and pig brain extract (Gel + Ha + Brain).*

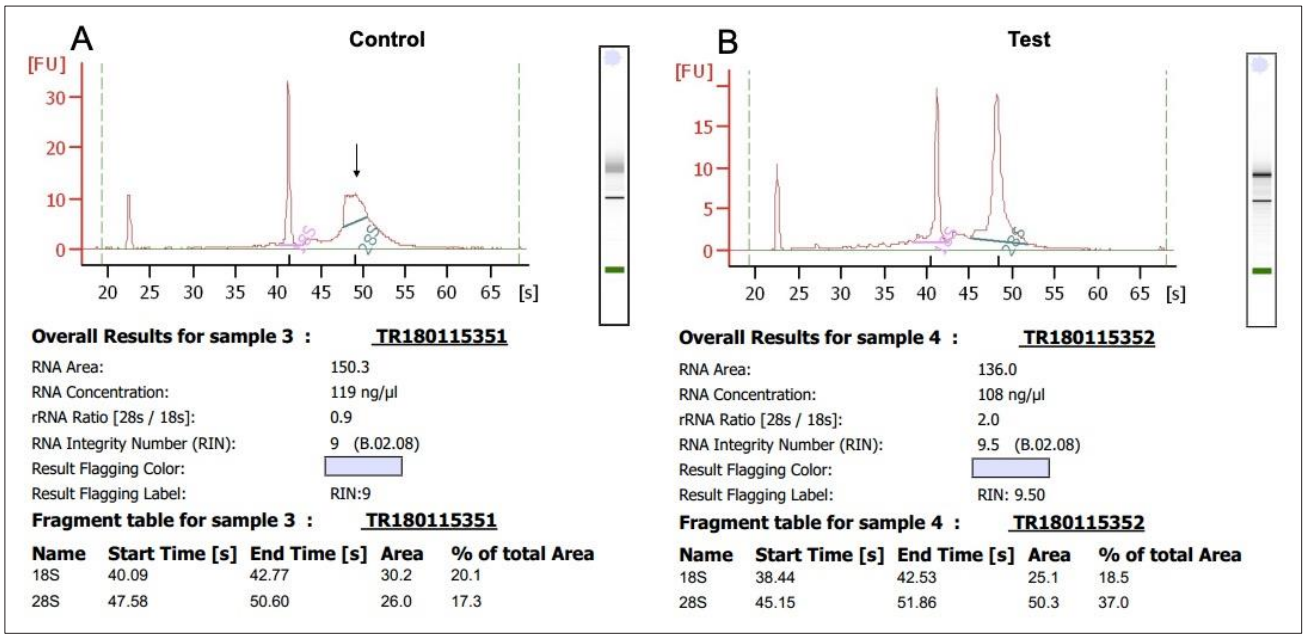

Figure 2S. *RNA QC report showed no degradation of 28 srRNA. A: control group showed a degradation of 28 srRNA, B: cells cultured on hydrogel.*

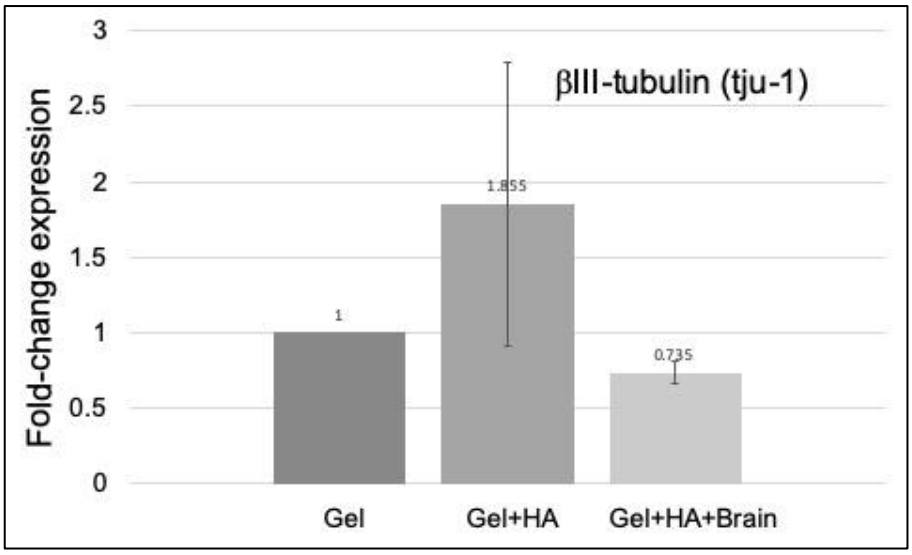

Figure 3S. *Expression of tju-1 gene was not significant between each type of biomaterials.*

Table 1S Sequences of primers used in real-time PCR.

Target genes	Primer sequences (5'->3')
1. Klf4	F: GAAATTCGCCCGCTCCGATGA
	R: CTGTGTGTTTGCGGTAGTGCC
2. βIII-tubulin	F: CGCACGACATCTAGGACTGA
	R: TGAGGCCTCCTCTCACAAGT
3. CD44	F: AGCAGCGGCTCCACCATCGAGA
	R: TCGGATCCATGAGTCACAGTG
4. MAP2	F: CCAAGGAGTCTGATTGCAGGA
	R: CCTCAACCACAGCTCAAATGC
5. ACAN	F: CTACGACGCCATCTGCTACA
	R: ACGAGGTCCTCACTGGTGAA
6. VCAN	F: AACATTTTTCAGGTGGTGAG
	R: GATGCAGAACTTGGAACTAT
7. OCN	F: GGACAGCCAGGACTCCATTG
	R: TGTGGGGACAACTGGAGTGAA
8. 18s rRNA	F: GGCCCTGTAATTGGAATGAGTC
	R: CCAAGATCCAACTACGAGCTT
9. GAPDH (Glyceraldehyde 3-phosphate dehydrogenase)	F: AAATCCCATCACCATCTTCCAGGAGC
	R: CATGGTTCACACCCATGACGAACA

Table 2S Solute-carrier gene (SLC) superfamily.

SLC gene superfamily	log2.Fold change*	Note	Function
1. Solute carrier family 6	1.0865	increased	Na^+- and Cl^--dependent neurotransmitter symporter family
2. solute carrier family 3	1.1069	increased	Heavy subunits of the heteromeric amino acid transporters
3. Solute carrier family 11	1.3954	increased	Proton-coupled metal ion transporter family
4. solute carrier family 40	1.5438	increased	Basolateral iron transporter family
5. Solute carrier family 7	1.6839	increased	Cationic amino acid transporter/glycoprotein- associated amino acid transporter family
6. Solute carrier family 25	1.7743	increased	Mitochondrial carrier family
7. Solute carrier family 43	1.8382	increased	Na+-independent system-L-like amino acid transporter family
8. Solute carrier family 12	2.5553	increased	Electroneutral cation/Cl- co-transporter family
9. Solute carrier family 39	2.7085	increased	Metal (M_2^+) ion transporter family
10. Solute carrier family 16	3.6315	increased	Monocarboxylate transporter family

**** adjusted p<0.001***

Table 3S Key pro-inflammatory cytokines and chemokines.

Gene	log2.Fold_ change*	Function
1 Chemokine (C-X-C motif) ligand 5 (CXCL5)	7.1949	*Chemokine which recruits and activates leukocytes*
2. Chemokine (C-X-C motif) ligand 1 (CXCL1)	6.4068	*Plays a role in inflammation and acts as a chemoattractant for neutrophils*
3. Interleukin 8 (IL8)	6.2294	*A major mediator of the inflammatory response serves as a chemotactic factor by guiding the neutrophils to the site of infection* *Direct regulation of adaptive T cell reactivity*
4. Chemokine (C-X-C motif) ligand 2 (CXCL2)	5.7015	*Chemotactic for neutrophils and elevated expression of CXCL2 is associated with many inflammatory and autoimmune diseases*
5. Chemokine (C-X3-C motif) ligand 1 (CX3CL1)	5.3254	*A membrane-bound chemokine* *Has a dual function as an adhesion molecule and a chemoattractant* *A neuronal cytokine that acts on microglial CX3CR1 receptor involved in the maturation of GABAergic synapses*
6. I6 (IL6)	5.2299	*Cytokine that functions in inflammation and the maturation of B cells*
7. Complement component 3 (C3)	5.2134	*Plays a central role in the activation of complement system*
8. Chemokine (C-X-C motif) ligand 6 (CXCL6)	5.0382	*Chemokine expressed by macrophages and epithelial and mesenchymal cells during inflammation*
9. Chemokine (C-X-C motif) ligand 3 (CXCL3)	5.0317	*Plays a role in inflammation and acts as a chemoattractant for neutrophils*
10. Tumor necrosis factor, alpha-induced protein 3 (TNFAIP3)	4.3074	*Inhibit NF-kappa B activation as well as TNF-mediated apoptosis*
11. Chemokine (C-C motif) ligand 2 (CCL2)	4.174	*Displays chemotactic activity for monocytes and basophils but not for neutrophils or eosinophils*
12. Chemokine (C-X-C motif) ligand 10 (CXCL10)	4.1312	*Stimulation of monocytes, natural killer and T-cell migration, and modulation of adhesion molecule expression*
13. Prostaglandin D2 synthase 21kDa (brain) (PTGDS)	4.093	*Catalyzes the conversion of prostaglandin H2 (PGH2) to postaglandin D2 (PGD2).* *PGD2 functions as a neuromodulator as well as a trophic factor in the central nervous system*

Table 3S Key pro-inflammatory cytokines and chemokines. (continues)

Gene	log2.Fold_change*	Function
14. Intercellular adhesion molecule 1 (ICAM1)	4.0847	*Typically expressed on endothelial cells and cells of the immune system*
15. Kynureninase (KYNU)	3.9303	*Biosynthesis of NAD cofactors from tryptophan*
16. Prostaglandin-endoperoxide synthase 2 (PTGS2 or COX-2)	3.9002	*Prostaglandin biosynthesis*
17. v-maf musculoaponeurotic fibrosarcoma oncogene homolog B (MAFB)	3.5467	*Transcription factor that plays an important role in the regulation of lineage-specific hematopoiesis*
18. Interleukin 32 (IL32)	3.3573	
19. Tumor necrosis factor, alpha-induced protein 6 (TNFAIP6)	3.2914	*Extracellular matrix stability and cell migration*
20. Nuclear factor of kappa light polypeptide gene enhancer in B-cells inhibitor, alpha (NFKBIA)	2.8315	*Involved in inflammatory responses*
21. Interferon regulatory factor 1 (IRF1)	2.7041	*Involved in both innate and acquired immune responses*
22. Retinoic acid receptor responder 2 (RARRES2)	2.6768	*Chemotactic protein that initiates chemotaxis*
23. POU class 2 homeobox 2 (POU2F2)	2.5773	*Transcriptional activator of immunoglobulin (Ig) in B lineage cells*
24. BTG family, member 2 (BTG2)	2.5507	*Involved in the regulation of the G1/S transition of the cell cycle*
25. Interleukin-1 receptor-associated kinase 2 (IRAK2)	2.4458	*Participate in the IL1-induced upregulation of NF-kappaB*
26. Chemokine (C-X-C motif) ligand 14 (CXCL14)	2.3953	*Regulation of immune cell migration, also executes antimicrobial immunity*
27. Major histocompatibility complex, class I, B (HLA-B)	2.2969	*Express on most of the somatic cells in the body* *Play a central role in the immune system by presenting peptides derived from the endoplasmic reticulum lumen* *Display peptides that result from the degradation of cytosolic proteins to T lymphocytes and natural killer (NK) cells*
28. Beta-2-microglobulin (B2M)	1.1334	*Serum protein found in association with the major histocompatibility complex (MHC) class I heavy chain on the surface of nearly all nucleated cells*
29. Interferon gamma receptor 2 (IFNGR2)	1.1464	*Non-ligand-binding beta chain of the gamma interferon receptor*
30. MHC class I polypeptide-related sequence A (MICA)	1.2047	*A membrane-bound protein acting as a ligand to stimulate an activating receptor expressed on the surface of essentially all human natural killer (NK), T and CD8(+) T cells*
31. Sema domain, immunoglobulin domain (Ig) (SEMA3C)	1.2086	*Soluble proteins that are well recognized for their role in guiding axonal migration during neuronal development.* *In the immune system, Sema3A has been shown to influence murine dendritic cell (DC) migration by signaling through a neuropilin (NRP)-1/plexin-A1 coreceptor axis*

Table 3S Key pro-inflammatory cytokines and chemokines. (continues)

Gene	log2.Fold_change*	Function
32. Major histocompatibility complex, class I, C (HLA-C)	1.2341	*Express on most of the somatic cells in the body* *Play a central role in the immune system by presenting peptides derived from the endoplasmic reticulum lumen* *Display peptides that result from the degradation of cytosolic proteins to T lymphocytes and natural killer (NK) cells*
33. Major histocompatibility complex, class I, A (HLA-A)	1.5698	*Express on most of the somatic cells in the body* *Play a central role in the immune system by presenting peptides derived from the endoplasmic reticulum lumen* *Display peptides that result from the degradation of cytosolic proteins to T lymphocytes and natural killer (NK) cells*
34. Interferon gamma receptor 1 (IFNGR1)	1.5842	*IFN-gamma and its receptor subunit, IFNGR1, in direct contact with the promoter region of IFN-gamma-activated genes*

**** adjusted p<0.001***

Table 4S KEGG pathway.

KEGG up	Corrected *p* value	Cell type
1. Lysosome (hsa04142)	7.34×10^{-9}	Any
2. TNF-signaling pathway (hsa04668)	2.53×10^{-6}	Any
3. Rheumatoid arthritis (hsa05323)	1.69×10^{-5}	Synovial macrophages
4. NOD-like receptor signaling pathway (hsa04621)	0.0022	Macrophages Dendritic cells Peripheral blood Leukocytes Interstitial epithelial cells Paneth cells
5. Legionellosis (hsa05134)	0.0068	Macrophages Epithelial cells
6. Osteoclast differentiation (hsa04380)	0.0069	Bone marrow derived monocyte/macrophage precursor cells
7. NF-kappa B signaling pathway (hsa04064)	0.0107	Any
8. Epithelial cell signaling in Helicobacter pylori infection (hsa05120)	0.0172	Epithelial cells
9. Phagosome (hsa04145)	0.0206	Phagocytic cells
10. Chagas disease (American trypanosomiasis) (hsa05142)	0.0206	Macrophage Fibroblast Skeletal muscle cell Cardiac muscle cell
11. Leishmaniasis (hsa05140)	0.0215	Macrophage
12. FoxO signaling pathway (hsa04068)	0.0385	Any
13. Salmonella infection (hsa05132)	0.0466	Interstitial epithelial and M cells
14. Tuberculosis (hsa05152)	0.0479	Macrophages Dendritic cells
15. Pertussis (hsa05133)	0.0604	Phagocytic cells
16. Chemokine signaling pathway (hsa04062)	0.0653	Eosinophil Neutrophil Macrophages T lymphocytes

Table 4S KEGG pathway. (continues)

KEGG up	Corrected *p* value	Cell type
17. ECM-receptor interaction (hsa04512)	0.000000195	Any
18. Focal adhesion (hsa04510)	0.00000743	Any
19. PI3K-Akt signaling pathway (hsa04151)	0.0000497	Any
20. Arrhythmogenic right ventricular cardiomyopathy (ARVC) (hsa05412)	0.000650596	Cardiac myocyte
21. Protein digestion and absorption (hsa04974)	0.001761442	Small intestinal epithelial cell
22. Hypertrophic cardiomyopathy (HCM) (hsa05410)	0.006059177	Cardiac myocyte
23. Dilated cardiomyopathy (hsa05414)	0.000423057	Cardiac myocyte
24. Regulation of actin cytoskeleton (hsa04810)	0.022123169	Any

Journal of Associated Medical Sciences 2021; 54 (3): 125-134

JAMS
Journal of Associated Medical Sciences

Thai-Journal Citation Index Centre (TCI) & ASEAN Citation Index (ACI)

Journal of Associated Medical Sciences

Journal homepage: https://www.tci-thaijo.org/index.php/bulletinAMS/index

Expression of preadipocyte genes in apical papilla cells after treatment with crude water extract of *Cuscuta japonica* Choisy

Fahsai Kantawong [1*] Peeraya Wongsit [1] Jianghua Yang [1] Penpitcha Wanachantararak [2] Jiang Nan [3] Jianming Wu [4]

[1]*Department of Medical Technology, Faculty of Associated Medical Sciences, Chiang Mai University, Chiang Mai Province, Thailand*
[2]*The Dental Research Center, Faculty of Dentistry, Chiang Mai University, Chiang Mai Province, Thailand*
[3]*International Education School, Southwest Medical University, Luzhou, China*
[4]*School of Pharmacy, Southwest Medical University, Luzhou, China*

ARTICLE INFO

Article history:
Received 17 July 2021
Accepted as revised 26 August 2021
Available online 26 August 2021

Keywords:
Cuscuta japonica Choisy, flavonoids; phenolic acids, gene expression

ABSTRACT

Background: *Cuscuta japonica* Choisy (Japanese dodder) is a well-known traditional Chinese herbal medicine that has been used since ancient times as longevity and rejuvenation remedies, especially, in the southern part of China. The effects of this herb are widely known and can be applied for the treatment of a number of physiological diseases, but there is a lack of evidence describing its effects.

Objectives: This study focused on observing global change of gene expression after long-term treatment with high dose of crude water extract from *Cuscuta japonica* Choisy.

Materials and methods: In this research, dodder seeds were blended and boiled in distilled water before freeze drying to preserve as dried powder. UHPLC-QTOF-MS/MS was employed to test for important compounds in the extract of *Cuscuta japonica* Choisy. The extract at the concentration of 250 µg/mL was tested with apical papilla cells for 10 days to screen for change of gene expression by RNA sequencing before confirmation with real-time PCR.

Results: UHPLC-QTOF-MS/MS result found glycosides, phenolic acids and flavonoids as the main components in dodder seed water extract. Results from next-generation sequencing showed that dodder seed water extract significantly altered expression of 19 genes in apical papilla cells treated with the extract for 10 days (11 genes were increased while 8 genes were decreased). RT-PCR result of *CD36* and *SCARA5* genes showed correlated results with RNA sequencing.

Conclusion: The active compounds found in dodder seed water extract were phenolic acid, flavonoids, polysaccharide, lignan and volatile oil. The RNA sequencing studied in apical papilla cells showed that dodder seed water extract affected only a few genes that played roles in metabolism which correlated to the properties of this herb that was described as supplementary in metabolic diseases.

* **Corresponding author.**
Author's Address: *Department of Medical Technology, Faculty of Associated Medical Sciences, Chiang Mai University, Chiang Mai Province, Thailand.*
** **E-mail address:** fahsai.k@cmu.ac.th
doi: 10.14456/jams.2021.32
E-ISSN: 2539-6056

Introduction

Cuscuta chinensis, *Cuscuta australis* and *Cuscuta japonica* Choisy were important species of *Cuscutae Semen* recorded in Chinese Pharmacopoeia.[1] The *Cuscuta chinensis* Lam., *Cuscuta japonica* Choisy, and *Cuscutae* Semen seeds are well-known traditional medicinal herbs, commonly used for improving reproductive system, supporting liver and kidney functions, reducing pain in joints and knees, and treating pharyngitis.[2] *Cuscuta* Semen is a crude drug prepared from the seeds of *Cuscuta chinensis* Lam., and used as a tonic liver and kidney. Nowadays, the seeds of *Cuscuta australis* and *Cuscuta japonica* Choisy are used as substitutes for *Cuscuta chinensis* , which is not readily available. *Cuscuta japonica* is a unique parasitic plant widely distributed in eastern Asian countries.[3] Extract of *Cuscuta japonica* Choisy is a well-known traditional Chinese herbal medicine that has been used since ancient times as longevity and rejuvenation remedies, especially, in the southern part of China. Effects of this herb are widely known and can be applied for the treatment of a number of physiological diseases, but there is a lack of evidence describing its effects. However, few evidences have been elucidated as mechanisms for the action of *Cuscuta japonica* Semen. The study by Moon *et al*. demonstrated that *Cuscuta japonica* Choisy had an enhancing effect on cognitive function and the histological mechanisms that support this improvement in cognitive function may be mediated by an increased level of neurogenesis in the mouse hippocampus.[4] Mushroom Tyrosinase inhibitory activity of *Cuscuta japonica* Choisy was presented by Suk *et al*.[5] The study of Jang et al indicated that aqueous fraction from *Cuscuta japonica* seeds inhibited p38 MAPK phosphorylation with suppressed cAMP levels and subsequently down-regulated MITF and TRP expression, which resulted in a marked reduction of melanin synthesis and tyrosinase activity in α-MSH-stimulated murine melanoma cells.[6] The content of polysaccharide in *Cuscuta japonica* was high, which has higher medical value.[7] *Cuscuta chinensis* polysaccharide showed benefits on glucose-lipid metabolism in diabetic rats induced by streptozotocin. *Cuscuta* chinesis plant was effective in reduced blood glucose of type 1 diabetes mellitus rats.[8] *Cuscuta chinensis* showed anti-obesity properties by modulating hepatic arginase and nitric oxide production and metabolic pathways related to hepatic triglyceride metabolism.[9]

This study presented the simple method for crude extraction by blending and boiling in water which still provided the active components such as phenolic acids and flavonoids that can be used for prevention of diseases. Most of the previous studies employed solvent extractions which were not common in daily life use. More over the effect of crude water extract on global gene expression in primary cell culture was performed.

Apical papilla cells were used as a model for study of gene expression in this study because they contained a population of mesenchymal stem cells[10] and other type of cells[11] which were easy to obtain from routine tooth extraction. Apical papilla cells could be used to test for global change of gene expression in according to the long-term treatment with crude water extract from *Cuscuta japonica* Choisy. In the parallel study, human gingival cells were treated with 250 µg/mL *Cuscutus japonica* Choisy water extract. The result from real-time PCR indicated that this amount clearly regulated *CD36* and *SCARA5* genes. We followed the previous treatment protocol to observe these 2 genes with apical papilla cells.

Materials and methods

Preparation of dodder seeds water extracts

Dodder seeds were obtained from local trader in Sichuan (Sichuan Shamgracy Pharmaceutical Co., LTD). Commercial *Cuscutae Semen* was *Cuscuta japonica* Choisy as indicated on the package (Figure 1). The voucher specimen of commercial *Cuscuta japonica* Choisy from Sichuan was previously identified by Prof. Yu-lin Lin (Institute of Medicinal Plant Development (IMPLAD), Chinese Academy of Medical Science and Peking Union Medical College) and deposited at the herbarium of IMPLAD, Chinese Academy of Medical Sciences and Peking Union Medical College. 1 Dried dodder seeds amount of 200 grams were blended in a blender for 2 minutes with 3,000 mL of distilled water before boiling for 5 minutes. After that, the boiled solution was cooled down at 4 °C overnight. The next day, the solution was filtered through white gauze. The filtrate was aliquoted in lyophilized flasks and frozen at -20 °C before lyophilized into powder for 7 days.

Figure 1. *Cuscutae Semen. Seeds of Cuscuta japonica Choisy bought from Sichuan Shamgracy Pharmaceutical Co., LTD.*

UHPLC-QTOF-MS/MS analyses

The UHPLC analyses were carried out on an AB Sciex ExionLC system (AB SCIEX, Foster City, CA, USA), equipped with an ExionLC Solvent Delivery System, an ExionLC AD Auto-sampler, an ExionLC AD Column oven, an ExionLC Degasser, an ExionLC AD Pump, an ExionLC PDA Detector, and an ExionLC Controller. Analytical column was a Shim-pack XR-ODSII column (2.0 mm i.d. × 75 mm). Column oven temperature was set at 30 °C. The mobile phases consisted of water containing 0.1% formic acid (solvent A) and acetonitrile (solvent B). The flow rate was set at 0.3 mL/min.

Binary gradient was applied with linear interpolation as follows: 18.00 min, 45.0% B; 23.00 min, 100.0% B; 24.00 min, 100.0% B; 24.01 min, 5.0% B; 27.00 min, 5.0% B; The UHPLC-QTOF-MS/MS detection was conducted on a Sciex QTOFTM X500R system with a TurboIonSpray source both in the positive and negative electrospray ion mode (AB SCIEX, Foster City, CA, USA). Parameters of the electrospray ionization applied in the positive mode are: ion spray voltage, 5500V; ion source temperature, 550 °C; curtain gas, 35 psi; Ion source gas 1 (GS 1), 55 psi; Ion source gas 2 (GS 2), 55 psi; and declustering potential (DP), 50V. The mass ranges were set at m/z 60-2000 Da for the TOF-MS scan and 50-2000 Da for the TOF MS/MS experiments. In IDA-MS/MS experiment, the collision energy (CE) was set at 35 eV, and the collision energy spread (CES) was 0 eV for the UHPLC-QTOF-MS/MS detection. Parameters of electrospray ionization applied in the negative mode are: ion spray voltage, -4500V; ion source temperature, 550 °C; curtain gas, 35 psi; Ion source gas 1 (GS 1), 55 psi; Ion source gas 2 (GS 2), 55 psi; and declustering potential (DP), -80V. The mass ranges were set at m/z 60-2000 Da for the TOF-MS scan and 50–2000 Da for the TOF MS/MS experiments. In the IDA-MS/MS experiment, the collision energy (CE) was set at -35 eV, and the collision energy spread (CES) was 0 eV for the UHPLC-QTOF-MS/MS detection. The most intensive 10 ions from each TOF-MS scan were selected as MS/MS fragmentation. Dynamic background subtraction (DBS) was applied to match the information dependent acquisition (IDA) tests for UHPLC-QTOF-MS/MS detection. The LC-MS/MS data was analyzed using PeakView® 1.2 software (AB SCIEX, Foster City, CA, USA).

Qualitative assay for glycosides by Molisch's test

Dried dodder seed water extract was dissolved in distilled water to the concentrations of 5000, 2500, 1250 and 625 µg/mL. Two mL of each concentration was prepared in the test tube and 2 drops of Molisch's reagent were added and mixed. One mL of conc. sulfuric acid was slowly overlayered without any mixing. The purple ring was observed in positive sample. Glucose diluted in distilled water at the concentrations 5000 µg/mL, 2500 µg/mL, and 1250 µg/mL were used as positive controls.

Apical papilla cell culture

Molar teeth were collected in routine tooth extraction according to a protocol approved by the Ethics Committee, Faculty of Dentistry, Chiang Mai University (68/2019). Apical papilla cells were obtained from apical papilla tissues of non-carious molars. The 18- to 25-year-old healthy patients were recruited (n=2). The apical papilla tissues were detached and digested by using 3 mg/mL collagenase I and 4 mg/mL dispase II for 45 minutes at 37 °C. Cells were cultured in complete α-Modified Eagle medium (α-MEM) at 37°C and 5% CO_2. Cells at the third passage with 80% confluent were used. Apical papilla cells were seeded into 6 well plates at the density of $1x10^5$ cells per well and maintained in 5% CO_2 at 37 °C for 24 hours to allow cell attachment. In the next day, medium was discarded and replaced with complete DMEM containing 250 µg/mL dodder extract. Apical papilla cells were seeded into 6 well plates at cell density of $1x10^5$ cells per well cultured in plain complete DMEM were used as control groups. Cultured media was changed every 3 days. Cells were treated for 10 days.

Cell staining

4% formaldehyde was added onto cell cultures and left for 10 minutes at room temperature. After that, 4% formaldehyde was discarded and replaced with methylene blue solution for 5 minutes. Methylene blue was washed out with tap water and cell morphology was observed under the inverted microscope.

RNA Sequencing (Transcriptomic assay)

The RNA sequencing was performed to observe Differential Gene Expression (DGE). Total RNA extraction was performed following the instruction from Nucleospin Kit. RNA samples were analyzed by Illumina platform, Novogene, Hong Kong. Differentially expressed genes between control sample and test sample at 10 days culture were analyzed by log2 fold change of Fragments Per Kilobase Million (FPKM) value of treated sample compared with FPKM value of control sample with adjusted p(padj)<0.05.

Real-time PCR

Total RNA amounts were measured with Nanodrop 2000. The reaction solutions were prepared with 6 µL of RNA, 4 µL of 5x RT Master Mix and 10 µL of DEPC water. The RNA was converted to cDNA in the thermocycler using the following program: 37 °C 15 minutes, 50 °C for 5 minutes, 98 °C for 5 minutes. cDNA was stored at -20 °C. NO-RT control was prepared with the same method using 5x RT buffer. Real-time PCR reaction were prepared with 8 µL RNA, 10 µL SYBR Green Mastermix and 2 µL primer (the final concentration of each the primer was 1.0 µM) in the total volume of 20 µL. The PCR program was set as following: (1) Pre-incubation at 95 °C for 2 minutes. (2) PCR consisted of denature at 95 °C, annealing at 60 ºC and extension at 72 °C. Real-time PCR was performed for 40 cycles. The reference gene; *GAPDH* was used for normalization. The sequences of primers used in this study were; *GAPDH*: (F) 5'-AAATCCCATCACCATCTTCCAGGAGC-3', (R) 5'-CATGGTTCACACCCATGACGAACA-3', *CD36*: (F) 5'-ATGTAACCCAGGACGCTGAG-3', (R) 5'-GTCGCAGTGACTTTCCCAAT-3', *SCARA5* (F) 5'-GGAACATCTCCCTCGCGAAA-3', (R) 5'-CTCGGTCACCTTTGAACCCA-3'. The experiment was divided into 2 groups: the control (cells cultured in complete DMEM) and the treatment (cells cultured in DMEM containing 250 µg/mL dodder seed extract). Duplicate pool samples of controls and tests were prepared. Fold change of gene expressions were presented in the form of mean±SD.

The relative quantification for the gene expression was normalized to *GAPDH* using Light Cycler®480 software release 1.5.0 SP4. This program used Advanced Relative Quantification which is a highly reliable results due to the extended range of parameters called the E-Method (Efficiency Method). The E-Method data are based on the true efficiency of each reaction and the final results are automatically calculated from the crossing point (Cp) values of the target (unknowns and calibrator) and the reference (unknowns and calibrator).

Results

Extraction

Dried powder of dodder seed water extract 14.97 g was obtained when 200 grams of dried dodder seeds were used in the extraction and %yield was equal to 7.5% (Figure 2).

Figure 2. *Dodder seed extract powder obtained after lyophilized.*

The composition of dodder seed extract by UHPLC-QTOF-MS/MS analysis

Mass spectrum of the active components was shown in Figure 3. The important chemical constituents in dodder seed extract were shown in Table 1 including phenolic acids, flavonoids, polysaccharides, lignan and volatile oil.

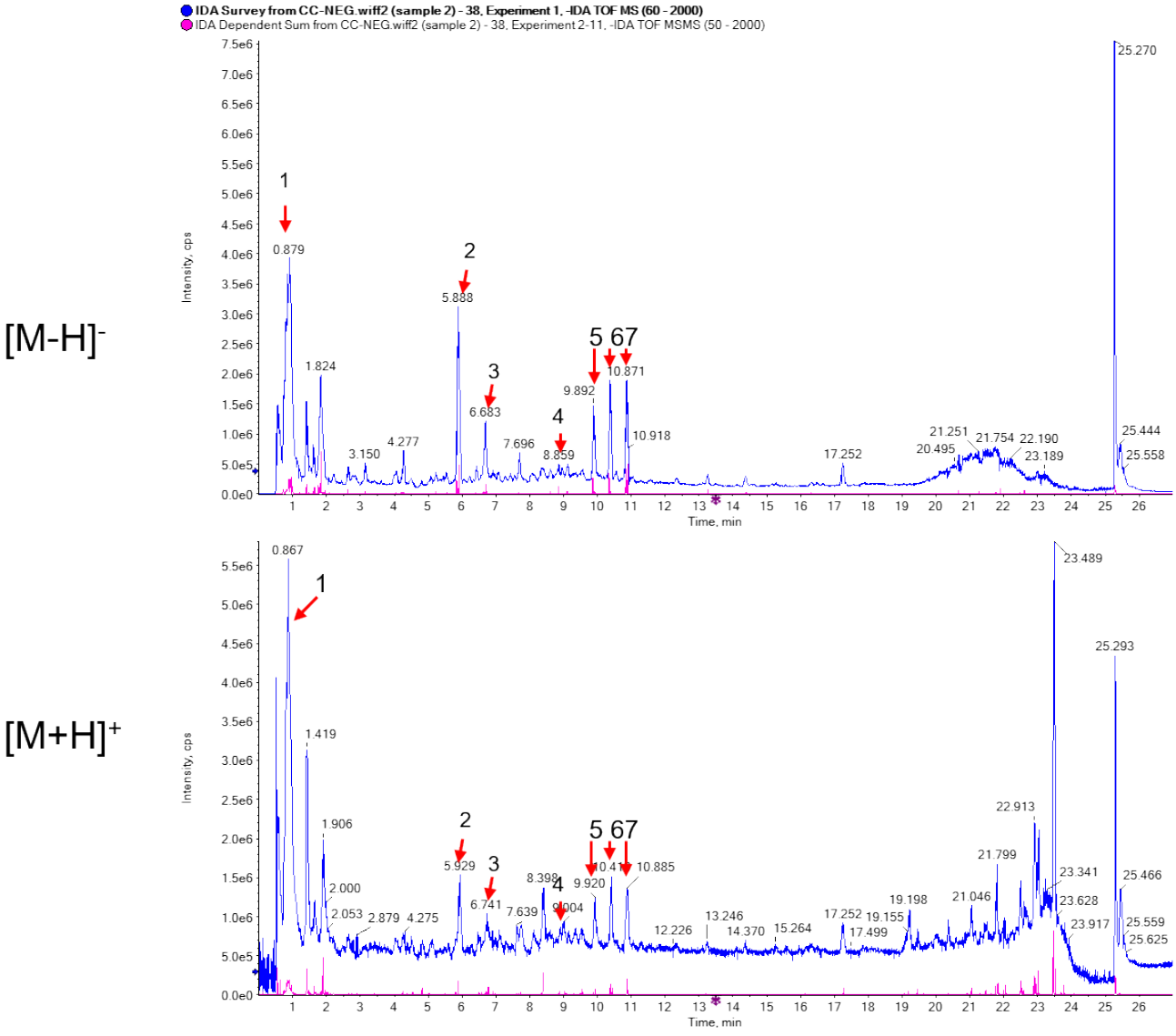

Figure 3. *Mass spectra of dodder seed water extract. The m/z of negative ion mode [M-H]- and positive mode [M+H]+ ions generated by electrospray were detected by positive and negative full scans.*

Table 1 Active compounds found in dodder seed extract.

Peak	Class	$[M-H]^-$ time	$[M-H]^-$ m/z	$[M+H]^+$ time	$[M+H]^+$ m/z	Name
1	Polysaccharides			0.73515	151.0256638	L-Arabinose
1	Lignans	0.8895	357.12945			Pinoresinol
2	Volatile oil	5.8217	137.034759	5.87393	139.0298671	2-Pentylfuran
2	Phenolic acid	5.8348	353.113443	5.88572	355.0795712	Chlorogenic acid
3	Phenolic acid	6.6975	179.047401	6.72505	181.0370603	Caffeic acid
4	Phenolic acid	8.603	163.051903	8.63547	165.0437828	P-coumaric acid
4	flavonoids			8.86682	303.0308298	Quercetin
4	flavonoids	8.8549	609.188342	8.87522	611.1220516	Rutin
4	flavonoids	8.7412	463.25218	8.89603	465.0731793	Hyperoside
5	flavonoids			9.92977	317.0441563	Isorhamnetin
5	Phenolic acid	9.8595	515.155518	9.94663	517.1002181	3,4-Dicaffeoylquinic acid
6	Phenolic acid	10.345	515.155256	10.354	517.1027363	3,5-Dicaffeoylquinic acid
7	Phenolic acid	10.836	515.155166	10.8821	517.1022455	4,5-Dicaffeoylquinic acid

Qualitative assay for glycosides by Molisch's test

Qualitative analysis of glycosides was confirmed using Molish's test. The result was shown in Figure 4. The observed purple rings in test tubes revealed that dodder seed extract contained glycosides.

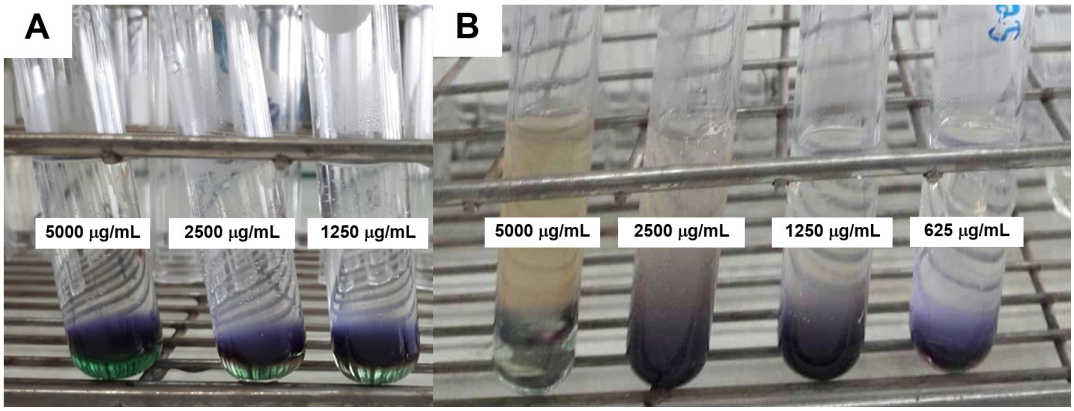

Figure 4. *(A) Formation of purple rings of glucose at concentrations of 5,000 2,500 and 1,250 µg/mL, which were used as positive control (B) Formation of purple rings of extracts at concentrations of 5,000 2,500 1,250 and 625 µg/mL respectively.*

Cell staining

Cell staining with methylene blue indicated that cells proliferated to form monolayer and the morphologies were not different between control and test as shown in Figure 5.

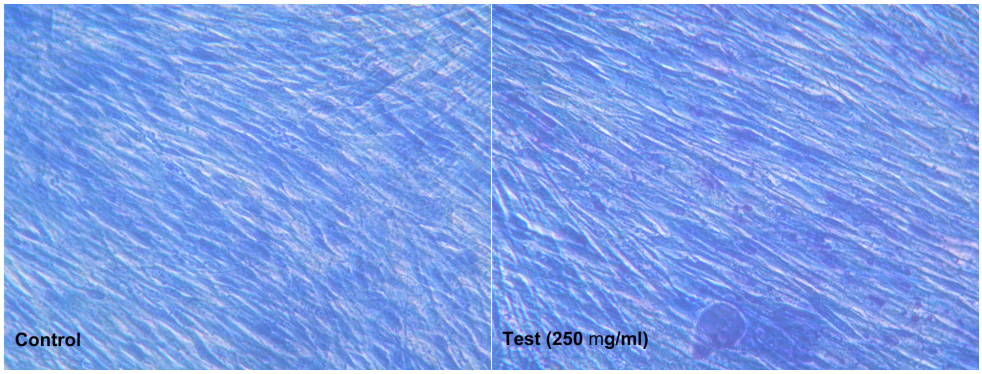

Figure 4. *Methylene blue staining of 10-day cultivation of apical papilla cells.*

Next-generation sequencing results in apical papilla cells

RNA quality control indicated that the RNA samples were passed with good purity and integrity. Next-generation sequencing identified more than 20,000 genes. However, when considering the adjusted *p*-value less than 0.05, only 19 genes were changed significantly. Differential gene expression was shown in Table 2.

Table 2 Differential gene expression.

Gene Name	*C. japonica* extract	Control	log2Fold Change	padj
SAMD11	0.041029	1.194022	-4.7066	0.02409
SCARA5	0.205143	4.55221	-4.4395	1.98E-06
WNT2	0.533371	4.55221	-3.0817	0.001073
RGS18	0.451314	3.320875	-2.8659	0.016795
DMKN	2.995085	13.47006	-2.1673	0.022233
CXCL14	5.046513	20.9327	-2.0513	0.02409
CHL1	3.856685	15.14916	-1.9724	0.041304
CXCL12	96.86843	352.2366	-1.8624	0.040733
C3	52.4345	13.76857	1.9288	0.033529
SFTPC	15.05748	3.880572	1.9548	0.045014
IL32	9.641712	2.462671	1.9669	0.065823
CTNND2	8.082627	2.014913	2.0015	0.063881
PIP	13.66251	3.246248	2.0717	0.030333
PLCXD3	12.0624	2.761177	2.1252	0.02409
SFTPB	6.56457	1.417901	2.2071	0.033529
KISS1	6.85177	0.93283	2.8703	0.000907
CD36	2.954056	0.373132	2.9686	0.011623
TM4SF4	0.8616	0	7.4706	0.040733
IGHA1	0.8616	0	7.4706	0.040733

Confirmation of *CD36* and *SCARA5* by real-time PCR

Apical papilla cells were treated with 250 µg/mL of dodder seed extract for 10 days. Replicate controls and tests were prepared. The expressions of both *CD36* and *SCARA5* were correlated with the result from Next-generation sequencing (Figure 6). *CD36* showed increased expression. *CD36* was a free fatty acid carrier.[12] It was possible that the increased expression of *CD36* was the effect of phytoestrogen because estrogen was reported to increase the expression of free fatty acid transporter (*CD36*) in the plasma membrane of the cardiomyocyte.[13] Scavenger receptor class A member 5 (*SCARA5*) showed increased expression. *SCARA5* also played a role as ferritin receptor.[14]

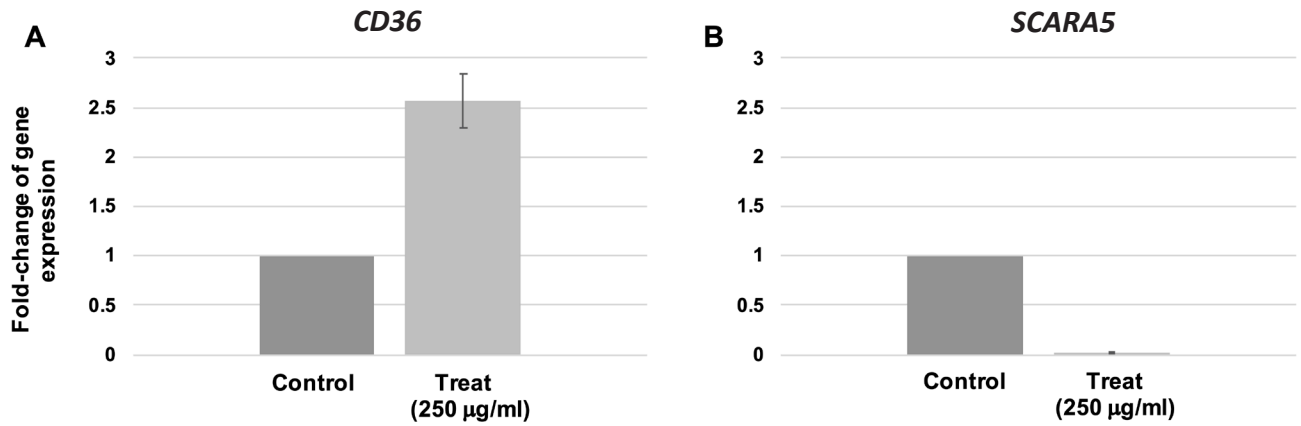

Figure 6. *(A) CD36 gene expression in duplicate experiments showed that the expression of CD36 increased by 2.6 times compared with the control group at 10 days. (B) SCSRA5 gene expression in duplicate experiments indicated that the expression of SCARA5 was dramatically reduced compared to the control group at 10 days. Real-time PCR results of CD36 and SCSRA5 gene expressions were correlated with the result from RNA sequencing.*

Discussion

The main substances found in dodder seed water extract were polysaccharides, phenolic acids and flavonoids. The phenolic acids found in dodder seed extract were chlorogenic acid, caffeic acid, p-coumaric acid, 3,4-dicaffeoylquinic acid, 3,5-dicaffeoylquinic acid and 4,5-dicaffeoylquinic acid. In the previous studies, phenolic acids showed important roles in oxidative prevention and metabolism. 3,5-Dicaffeoylquinic acid was a potent α-glucosidase inhibitor which contributed to the antihyperglycemic action of the compound.[15] The beneficial effects of 3,5-dicaffeoylquinic acid support the traditional use of *Cuscuta japonica* Choisy for the treatment of diabetes.[16] 4,5-Dicaffeoylquinic acid maintained prostate cancer cell line in the S-phase.[17] 4,5-Dicaffeoylquinic acid was an inhibitor of pigmentation which could be developed as an active component for formulations to treat pigmentation disorders[18] and it might be concordant with the use as skin whitening product.

Chlorogenic acid possessed vital roles on regulation of glucose and lipid metabolic disorders, which are associated with the occurrence and progression of diabetes, obesity, hepatic steatosis, cardiovascular disease, and cancer.[19] Coumaric acid inhibited the differentiation of skeletal muscle cell and preadipocyte cells by inhibiting the genes that are responsible for myogenesis and adipogenesis.[20]

Quercetin, rutin, hyperoside and isorhamnetin were flavonoids found in dodder seed extract. These substances prevented cancer and oxidative stress. Isorhamnetin and quercetin were anti-acetylcholinesterase[21] while pinoresinol was a phytoestrogen with antitumor activity, inhibiting breast cancer cells.[22]

Studies in apical papilla cells (Table 2) showed that dodder seed extract clearly affected the expression of genes involved with metabolism and the transportation of substances across cell membrane. Some genes involved with signal transduction while some genes played roles as tumor promoter genes and tumor suppressor genes.

Increased expression of *CD36* indicated that cells were trying to uptake fatty acids into the cells because *CD36* controlled the transport of long-chain fatty acids into fatty acids-requiring organ including heart, skeletal muscle, and adipose tissue.[12, 23, 24] *CD36*-deficiency attenuates the development of high fat diet (HFD)-induced obesity and insulin-mediated inhibition of lipolysis was more potent in *CD36*(-/-) mice.[25] Upregulation of *CD36* in preadipocytes may contribute to the development of adipose tissue inflammation.[26] Elevated levels of *CD36* with a concomitant increase in adipocyte number.[27] *CD36* could promote adipogenesis in vitro as well as in vivo.[28] It seemed like the expression of *CD36* in this study indicated disadvantage of *Cuscuta japonica* water extract.

Significantly reduce expression of *SCARA5* was observed. Menssen et al. identified *SCARA5* as a new candidate gene possibly related to adipogenesis.[29] *SCARA5* was a positive regulator in fat tissue formation,[30] therefore, reduced expression of *SCARA5* should inhibit adipogenesis which concordant with the previous that coumaric acid inhibited adipogenesis. The concern of this study was that *SCARA5* was a tumor suppressor gene. The reduced expression may increase the risk of developing different types of cancer.[31] *SCARA5* could modulate the expression of epithelial-mesenchymal transition-related proteins.[32] Knockdown of *SCARA5* inhibits human aortic smooth muscle cells proliferation and migration through suppression of the PDGF signaling pathway. Thus, *SCARA5* may be a therapeutic target for preventing or treating vascular diseases involving vascular smooth muscle cell proliferation and migration.[33]

Both *CD36* and *SCARA5* were scavenger receptors.[34] *SCARA5* was a scavenger receptor class A found in epithelial, testis, heart and brain tissues as a receptor for ferritin. *SCARA5* bound to serum ferritin and stimulated endocytosis. *CD36* was a scavenger receptor class B which functioned as a receptor for thrombospondin-1, oxidized LDL, and long-chain fatty acid. Even though the expression of both *CD36* and *SCARA5* were ambiguous in this study, they indicated change in the regulation of lipid metabolism.

Change of other genes were found in differential gene expression but they were not confirmed by RT-PCR in this study. Upregulation of the *KISS-1* gene indicated that kisspeptin, encoded by the *KISS-1* gene may account for both reproductive and metabolic abnormalities reported in obese and diabetic rats.[35, 36] Kisspeptin-1 receptor involved in regulation of energy metabolism, obesity and adipocyte differentiation.[37] *PLCDXD3* gene correlated positively with insulin secretion and correlated negatively with HbA1c.[38] *TM4SF4* induced thiamine uptake which was important for cell survival because thiamine pyrophosphate played a vital role in metabolism and energy production.[39] The catenin-δ2 gene (*CTNND2*, encoding catenin-δ2) was associated with anxiety-disorder.[40] There was a report about using dodder seeds with other herbs to relieve anxiety. Additionally, many previous studies indicated that giant dodder (*Cuscuta reflexa*) could be promising for the development of phytomedicines for anxiety.[41] It was possible the related species like *Cuscuta japonica* Choisy might contain the same property on anxiety.

In addition, epithelial marker was also found upregulated. Dodder seed water extract increased the expression of *SFTPB* and *SFTPC* expression in the apical papilla cells. They were classified as differentiation markers of the alveolar and bronchiolar epithelial cells[42] which were lung-specific genes.[43] It was unclear whether differentiation of epithelial cells occurred or not which requires more detailed studies. Another important point was that some of the genes in Table 2 played roles as tumor promoter genes and tumor suppressor genes. Significant increase in *TM4SF4* was found in apical papilla cells treated with dodder seed extract. This gene was used as a prognostic marker for many types of cancer such as colon cancer,[44] stomach cancer[45] and lung cancer.[46]

At the same time reduced expression of immunoglobulin (*IGHA1*) was often found in metastatic or poor prognosis cancer.[47] In this experiment, the *IGHA1* gene showed a significantly increased expression. This gene was also used as a prognostic marker for cancer but as a preventive gene.[48] The increased expression of *IGHA1* causes tumor suppressor effect.[49]

Genes in some signaling pathways were changed. SMAD family was an intermediary in TGF-β signaling.[50] In

this experiment, *SMAD11* was reduced by 5 times in the group that was treated with dodder seed extract. Down-regulation of *WNT2* related to some signaling pathway and cancer. This gene produces cysteine-rich secreted glycoprotein, which acts as a paracrine[51] and autocrine.[52]

The important point of tumor promoter genes and tumor suppressor genes expression was the balanced effect between each other. Crude extracts contained several compounds and when total crude extract was applied to treat cells there could be a balance between expression of tumor promoter genes and tumor suppressor genes. Although more than 20,000 genes were identified but only 19 genes were changed significantly. It could be concluded that dodder seed water extract slightly altered transcriptome of apical papilla cells. Most of gene expressions indicated regulation of metabolism which concordant with the properties of this herb.

Conflicts of Interest

The authors declare no conflicting interests.

Acknowledgements

We would like to give a special thank you to The Faculty of Associated Medical Sciences for funding support.

References

[1] Gao Z, Wang L, Wang X, Liu Y, Han J. Authenticity Survey of Cuscutae Semen on Markets Using DNA Barcoding. Chinese Herbal Medicines. 2017; 9(3): 218-25.

[2] Cheng J, Liaw C, Lin M, Chen C, Chao C, Chao C, et al. Anti-Influenza Virus Activity and Chemical Components from the Parasitic Plant Cuscuta japonica Choisy on Dimocarpus longans Lour. Molecules. 2020; 25(19). doi: 10.3390/molecules25194427.

[3] Oh H, Kang DG, Lee S, Lee HS. Angiotensin converting enzyme inhibitors from Cuscuta japonica Choisy. J Ethnopharmacol. 2002; 83(1-2): 105-8. doi: 10.1016/s0378-8741(02)00216-7.

[4] Moon M, Jeong HU, Choi JG, Jeon SG, Song EJ, Hong SP, et al. Memory-enhancing effects of Cuscuta japonica Choisy via enhancement of adult hippocampal neurogenesis in mice. Behav Brain Res. 2016; 311: 173-82. doi: 10.1016/j.bbr.2016.05.031.

[5] Suk K, LEE S, Bae J. Inhibitory Effects of Cuscuta japonica Extract and C. australis Extract on Mushroom Tyrosinase Activity. Korean Journal of Pharmacognosy. 2004; 35(4): 380-3.

[6] Jang JY, Kim HN, Kim YR, Choi YH, Kim BW, Shin HK, et al. Aqueous fraction from Cuscuta japonica seed suppresses melanin synthesis through inhibition of the p38 mitogen-activated protein kinase signaling pathway in B16F10 cells. J Ethnopharmacol. 2012; 141(1): 338-44. doi: 10.1016/j.jep.2012.02.043.

[7] Hu Y, Wang L. Extraction and content determination of polysaccharide in Cuscuta japonica Choisy in Changbai mountain area. Med Plant 2010; 1(2): 42-4.

[8] Al-Sultany F, Al-Hussaini I, Al- Saadi A. Studying Hypoglycemic Activity of Cuscuta chinesis Lam. on Type 1 Diabetes Mellitus in White Male Rats. Journal of Physics: Conf. Series 1294. 2019; 062020. doi:10.1088/1742-6596/1294/6/062020.

[9] Moon J, Ha MJ, Shin MJ, Kim OY, Yoo EH, Song J, et al. Semen Cuscutae Administration Improves Hepatic Lipid Metabolism and Adiposity in High Fat Diet-Induced Obese Mice. Nutrients. 2019; 11(12). doi: 10.3390/nu11123035.

[10] Nada OA, El Backly RM. Stem Cells From the Apical Papilla (SCAP) as a Tool for Endogenous Tissue Regeneration. Front Bioeng Biotechnol. 2018; 6: 103. doi: 10.3389/fbioe.2018.00103.

[11] Huang GT, Sonoyama W, Liu Y, Liu H, Wang S, Shi S. The hidden treasure in apical papilla: the potential role in pulp/dentin regeneration and bioroot engineering. J Endod. 2008; 34(6): 645-51. doi: 10.1016/j.joen.2008.03.001.

[12] Wang W, Yan Z, Hu J, Shen WJ, Azhar S, Kraemer FB. Scavenger receptor class B, type 1 facilitates cellular fatty acid uptake. Biochim Biophys Acta Mol Cell Biol Lipids. 2019:158554. doi: 10.1016/j.bbalip.2019.158554.

[13] Liu Q, Li R, Chen G, Wang J, Hu B, Li C, et al. Inhibitory effect of 17 beta-estradiol on triglyceride synthesis in skeletal muscle cells is dependent on ESR1 and not ESR2. Molecular Medicine Reports. 2019; 19(6): 5087-96. doi: 10.3892/mmr.2019.10189.

[14] Li JY, Paragas N, Ned RM, Qiu A, Viltard M, Leete T, et al. Scara5 is a ferritin receptor mediating non-transferrin iron delivery. Dev Cell. 2009; 16(1): 35-46. doi: 10.1016/j.devcel.2008.12.002.

[15] Simeonova R, Vitcheva V, Zheleva-Dimitrova D, Balabanova V, Savov I, Yagi S, et al. Trans-3,5-di-caffeoylquinic acid from Geigeria alata Benth. & Hook.f. ex Oliv. & Hiern with beneficial effects on experimental diabetes in animal model of essential hypertension. Food Chem Toxicol. 2019; 132: 110678. doi: 10.1016/j.fct.2019.110678.

[16] Noureen S, Noreen S, Ghumman SA, Batool F, Bukhari SNA. The genus. Iran J Basic Med Sci. 2019; 22(11): 1225-52. doi: 10.22038/ijbms.2019.35296.8407.

[17] Lodise O, Patil K, Karshenboym I, Prombo S, Chukwueke C, Pai SB. Inhibition of Prostate Cancer Cells by 4,5-Dicaffeoylquinic Acid through Cell Cycle Arrest. Prostate Cancer. 2019; 2019: 4520645. doi: 10.1155/2019/4520645.

[18] Tabassum N, Lee JH, Yim SH, Batkhuu GJ, Jung DW, Williams DR. Isolation of 4,5-O-Dicaffeoylquinic Acid as a Pigmentation Inhibitor Occurring in Artemisia capillaris Thunberg and Its Validation In Vivo. Evid Based Complement Alternat Med. 2016; 2016: 7823541. doi: 10.1155/2016/7823541.

[19] Meng S, Cao J, Feng Q, Peng J, Hu Y. Roles of chlorogenic Acid on regulating glucose and lipids metabolism: a review. Evid Based Complement Alternat Med. 2013; 2013: 801457. doi: 10.1155/2013/801457.

[20] Ilavenil S, Kim dH, Srigopalram S, Arasu MV, Lee KD, Lee JC, et al. Potential Application of p-Coumaric Acid on Differentiation of C2C12 Skeletal Muscle and 3T3-L1 Preadipocytes-An in Vitro and in Silico Approach. Molecules. 2016; (8). doi: 10.3390/molecules21080997.

[21] Olennikov DN, Kashchenko NI, Chirikova NK, Akobirshoeva A, Zilfikarov IN, Vennos C. Isorhamnetin and Quercetin Derivatives as Anti-Acetylcholinesterase Principles of Marigold (Calendula officinalis) Flowers and Preparations. Int J Mol Sci. 2017; 18(8). doi: 10.3390/ijms18081685.

[22] López-Biedma A, Sánchez-Quesada C, Beltrán G, Delgado-Rodríguez M, Gaforio JJ. Phytoestrogen (+)-pinoresinol exerts antitumor activity in breast cancer cells with different oestrogen receptor statuses. BMC Complement Altern Med. 2016; 16: 350. doi: 10.1186/s12906-016-1233-7.

[23] Kim Y, Ryu R, Choi J, Choi M. Platycodon grandiflorus Root Ethanol Extract Induces Lipid Excretion, Lipolysis, and Thermogenesis in Diet-Induced Obese Mice. Journal of Medicinal Food. 2019; 22(11): 1100-9. doi: 10.1089/jmf.2019.4443.

[24] Wang J, Hao J, Wang X, Guo H, Sun H, Lai X, et al. DHHC4 and DHHC5 Facilitate Fatty Acid Uptake by Palmitoylating and Targeting CD36 to the Plasma Membrane. Cell Reports. 2019; 26(1): 209-21.e5. doi: 10.1016/j.celrep.2018.12.022.

[25] Vroegrijk IO, van Klinken JB, van Diepen JA, van den Berg SA, Febbraio M, Steinbusch LK, et al. CD36 is important for adipocyte recruitment and affects lipolysis. Obesity (Silver Spring). 2013; 21(10): 2037-45. doi: 10.1002/oby.20354.

[26] Luo X, Li Y, Yang P, Chen Y, Wei L, Yu T, et al. Obesity induces preadipocyte CD36 expression promoting inflammation via the disruption of lysosomal calcium homeostasis and lysosome function. EBioMedicine. 2020; 56: 102797. doi: 10.1016/j.ebiom.2020.102797.

[27] Huang KT, Hsu LW, Chen KD, Kung CP, Goto S, Chen CL. Decreased PEDF Expression Promotes Adipogenic Differentiation through the Up-Regulation of CD36. Int J Mol Sci. 2018; 19(12). doi: 10.3390/ijms19123992.

[28] Christiaens V, Van Hul M, Lijnen HR, Scroyen I. CD36 promotes adipocyte differentiation and adipogenesis. Biochim Biophys Acta. 2012; 1820(7): 949-56. doi: 10.1016/j.bbagen.2012.04.001.

[29] Menssen A, Häupl T, Sittinger M, Delorme B, Charbord P, Ringe J. Differential gene expression profiling of human bone marrow-derived mesenchymal stem cells during adipogenic development. BMC Genomics. 2011; 12: 461. doi: 10.1186/1471-2164-12-461.

[30] Lee H, Lee Y, Choi H, Seok J, Yoon B, Kim D, et al. SCARA5 plays a critical role in the commitment of mesenchymal stem cells to adipogenesis. Scientific Reports. 2017;7(1):14833.doi: 10.1038/s41598-017-12512-2.

[31] Ryu S, Howland A, Song B, Youn C, Song PI. Scavenger Receptor Class A to E Involved in Various Cancers. Chonnam Med J. 2020; 56(1): 1-5. doi: 10.4068/cmj.2020.56.1.1.

[32] Zheng C, Xia EJ, Quan RD, Bhandari A, Wang OC, Hao RT. Scavenger receptor class A, member 5 is associated with thyroid cancer cell lines progression via epithelial-mesenchymal transition. Cell Biochem Funct. 2020. doi: 10.1002/cbf.3455.

[33] Zhao J, Jian L, Zhang L, Ding T, Li X, Cheng D, et al. Knockdown of SCARA5 inhibits PDGF-BB-induced vascular smooth muscle cell proliferation and migration through suppression of the PDGF signaling pathway. Mol Med Rep. 2016; 13(5): 4455-60. doi: 10.3892/mmr.2016.5074.

[34] Zani IA, Stephen SL, Mughal NA, Russell D, Homer-Vanniasinkam S, Wheatcroft SB, et al. Scavenger receptor structure and function in health and disease. Cells. 2015; 4(2): 178-201. doi: 10.3390/cells4020178.

[35] Dudek M, Kołodziejski PA, Pruszyńska-Oszmałek E, Sassek M, Ziarniak K, Nowak KW, et al. Effects of high-fat diet-induced obesity and diabetes on Kiss1 and GPR54 expression in the hypothalamic-pituitary-gonadal (HPG) axis and peripheral organs (fat, pancreas and liver) in male rats. Neuropeptides. 2016; 56: 41-9. doi: 10.1016/j.npep.2016.01.005.

[36] Castellano JM, Navarro VM, Fernández-Fernández R, Roa J, Vigo E, Pineda R, et al. Expression of hypothalamic KiSS-1 system and rescue of defective gonadotropic responses by kisspeptin in streptozotocin-induced diabetic male rats. Diabetes. 2006; 55(9): 2602-10. doi: 10.2337/db05-1584.

[37] Wang T, Cui X, Xie L, Xing R, You P, Zhao Y, et al. Kisspeptin Receptor GPR54 Promotes Adipocyte Differentiation and Fat Accumulation in Mice. Front Physiol. 2018; 9: 209. doi: 10.3389/fphys.2018.00209.

[38] Taneera J, Fadista J, Ahlqvist E, Atac D, Ottosson-Laakso E, Wollheim CB, et al. Identification of novel genes for glucose metabolism based upon expression pattern in human islets and effect on insulin secretion and glycemia. Hum Mol Genet. 2015; 24(7): 1945-55.

doi: 10.1093/hmg/ddu610.

[39] Subramanian VS, Nabokina SM, Said HM. Association of TM4SF4 with the human thiamine transporter-2 in intestinal epithelial cells. Dig Dis Sci. 2014; 59(3): 583-90. doi: 10.1007/s10620-013-2952-y.

[40] Nivard MG, Mbarek H, Hottenga JJ, Smit JH, Jansen R, Penninx BW, et al. Further confirmation of the association between anxiety and CTNND2: replication in humans. Genes Brain Behav. 2014; 13(2): 195-201. doi: 10.1111/gbb.12095.

[41] Thomas SS, S Velmurugan,C Ashok Kumar, B.S. Evaluation of anxioltic effect of whole plant of " Cuscuta reflexa ". World J Pharm Pharm Sci. 2015; 4(8): 1245-53.

[42] Nakamura N, Kobayashi K, Nakamoto M, Kohno T, Sasaki H, Matsuno Y, et al. Identification of tumor markers and differentiation markers for molecular diagnosis of lung adenocarcinoma. Oncogene. 2006; 25(30): 4245-55. doi: 10.1038/sj.onc.1209442.

[43] Xiong M, Heruth DP, Zhang LQ, Ye SQ. Identification of lung-specific genes by meta-analysis of multiple tissue RNA-seq data. FEBS Open Bio. 2016; 6(7): 774-81. doi: 10.1002/2211-5463.12089.

[44] Li H, Zhong A, Li S, Meng X, Wang X, Xu F, et al. The integrated pathway of TGF beta/Snail with TNF alpha/NF kappa B may facilitate the tumor-stroma interaction in the EMT process and colorectal cancer prognosis. Scientific Reports. 2017;7. doi: 10.1038/s41598-017-05280-6.

[45] Wei Y, Shen X, Li L, Cao G, Cai X, Wang Y, et al. TM4SF1 inhibits apoptosis and promotes proliferation, migration and invasion in human gastric cancer cells. Oncology Letters. 2018; 16(5): 6081-8. doi: 10.3892/ol.2018.9411.

[46] Choi SI, Kim SY, Lee J, Cho EW, Kim IG. TM4SF4 overexpression in radiation-resistant lung carcinoma cells activates IGF1R via elevation of IGF1. Oncotarget. 2014; 5(20): 9823-37. doi: 10.18632/oncotarget.2450.

[47] Jorissen R, Gibbs P, Christie M, Prakash S, Lipton L, Desai J, et al. Metastasis-Associated Gene Expression Changes Predict Poor Outcomes in Patients with Dukes Stage B and C Colorectal Cancer. Clinical Cancer Research. 2009; 15(24): 7642-51. doi: 10.1158/1078-0432.CCR-09-1431.

[48] Liu Z, Li M, Hua Q, Li Y, Wang G. Identification of an eight-lncRNA prognostic model for breast cancer using WGCNA network analysis and a Cox-proportional hazards model based on L1-penalized estimation. International Journal of Molecular Medicine. 2019; 44(4): 1333-43. doi: 10.3892/ijmm.2019.4303.

[49] Hsu HM, Chu CM, Chang YJ, Yu JC, Chen CT, Jian CE, et al. Six novel immunoglobulin genes as biomarkers for better prognosis in triple-negative breast cancer by gene co-expression network analysis. Sci Rep. 2019; 9(1): 4484. doi: 10.1038/s41598-019-40826-w.

[50] Zi Z, Chapnick DA, Liu X. Dynamics of TGF-β/Smad signaling. FEBS Lett. 2012; 586(14): 1921-8. doi: 10.1016/j.febslet.2012.03.063.

[51] Petrov NS, Popov BV. Study of Wnt2 secreted by A-549 cells in paracrine activation of β-catenin in co-cultured mesenchymal stem cells. Biochemistry (Mosc). 2014; 79(6): 524-30. doi: 10.1134/S0006297914060054.

[52] Klein D, Demory A, Peyre F, Kroll J, Augustin HG, Helfrich W, et al. Wnt2 acts as a cell type-specific, autocrine growth factor in rat hepatic sinusoidal endothelial cells cross-stimulating the VEGF pathway. Hepatology. 2008; 47(3): 1018-31. doi: 10.1002/hep.22084.

Instructions for Authors

Instructions for Authors

Original article/thesis can be submitted through the on-line system via website https://www.tci-thaijo.org/index.php/bulletinAMS/

General Principles

Journal of Associated Medical Sciences is a scientific journal of the Faculty of Associated Medical Sciences, Chiang Mai University. The articles submitted to the journal that are relevant to any of all aspects of Medical Technology, Physical Therapy, Occupational Therapy, Radiologic Technology, Communication Disorders, and other aspects related to the health sciences are welcome. Before publication, the articles will go through a system of assessment and acceptance by at least three experts who are specialized in the relevant discipline. All manuscripts submitted to Journal of Associated Medical Sciences should not have been previously published or under consideration for publication elsewhere. All publications are protected by the Journal of Associated Medical Sciences' copyright.

Manuscript categories

1. **Review articles** must not exceed 20 journal pages (not more than 5,000 words), including 6 tables/figures, and references (maximum 75, recent and relevant).
2. **Original articles** must not exceed 15 journal pages (not more than 3,500 words), including 6 tables/figures, and 40 reference (maximum 40, recent and relevant).
3. **Short communications** including technical reports, notes, and letter to editor must not exceed 5 journal pages (not more than 1,500 words), including 2 tables/figures, and references (maximum 10, recent and relevant).

Manuscript files

To submit your manuscript, you will need the following files:

1. A Title page file with the names of all authors and corresponding authors*
2. Main document file with abstract, keywords, main text and references
3. Figure files
4. Table files
5. Any extra files such as Supplemental files or Author Biographical notes

Manuscript Format

1. **Language**: English, Caribri 10 for text and 7 for all symbols. PLEASE be informed that the Journal only accept the submission of English manuscript.
2. **Format**: One-side printing, double spacing. Use standard program and fonts and, add page and line number for all pages.
3. **A Title page**: Include article title, names of all authors and co-authors, name of the corresponding author and acknowledgements. Prepare according to following contents;
   - *Title of the article*: Concise and informative. Titles are often used in information-retrieval systems. Avoid abbreviations and formulate where possible.
   - *Author names and affiliation*: Where the family name may be ambiguous (e.g. a double name), please indicate this clearly. Present the authors' affiliation addresses (where the actual work was done) below the names. Indicate all affiliations with superscript number immediately after author's name and in front of appropriate address. Provide the full postal address of each affiliation, including the province, country and, if available, the e-mail address of each author.
   - *Corresponding author*: Clearly indicate who will handle correspondence at all stages of refereeing and publication, also post-publication, ensure that telephone and fax numbers (with postal area code) are provided in addition to the e-mail address and the complete postal address. Contact details must be kept up to date by the corresponding author.
   - *Acknowledgements*: Acknowledgements will be collated in a separate section at the end of the article before the references in the stage of copyediting. Please, therefore, include them on the title page, List here those individuals who provided help during the research (e.g. providing language help, writing assistance or proof reading the article, etc.)
4. **Main article structure**: The manuscripts should be arranged in the following headings: Title, Abstract, Introduction, Materials and Methods, Results, Discussion and Conclusion, and Reference. Prepare according to following contents;
   - *Abstract*: Not exceeding 400 words, abstract must be structured with below headings in separated paragraph:
     - Background,
     - Objectives,
     - Materials and methods,
     - Results,
     - Conclusion, and
     - Keywords (3-5 keywords should be included)
   - *Introduction*: State the objectives of work and provide an adequate background, avoiding a detailed literature survey or a summary of the results.
   - *Materials and Methods*: Provide sufficient detail to allow the work to be reproduced. Methods already published should be indicated by a reference, only relevant modifications should be described. Ensure that each table, graph, or figure is referred in the text. According to the policy of ethical approval, authors must state the ethical approval code and conduct informed consent for human subject research (If any) and for animal research, authors must include a statement or text describing the experimental procedures that affirms all appropriate measures (if any) in this section.
   - *Results*: Results should be clear and concise. Present the new results of the study such as tables and figures mentioned in the main body of the article and numbered in the order in which they appear in the text or discussion.
   - *Discussion*: This should explore the significance of the results of the work, not repeat them. A combined Results and Discussion

section is often appropriate. Avoid extensive citations and discussion of published literature.
- *Conclusion*: The main conclusions of the study may be presented in a short Conclusions section, which may stand alone or form a subsection of a "Discussion" or "Results and Discussion".
- *Conflict of interes*t: All authors must declare any financial and personal relationship with other people or organization that could inappropriately influence (bias) their work. If there is no interest to declare, then please state this: "The authors declare no conflict of interest".
- *Ethic approval*: Ethic clearance for research involving human and animal subjects.
- *References*: Vancouver's style.

5. **Artwork Requirements**
   - Each table, graph and figure should be self-explanatory and should present new information rather than duplicating what is in the text. Prepare one page per each and submit separately as supplementary file(s).
   - Save the figures as high resolution JPEC or TIFF files.

Note: Permission to reprint table(s) and/or figure(s) from other sources must be obtained from the original publishers and authors and submitted with the typescript.

Ensuring a blind peer review

To ensure the integrity of the double-blinded peer-review for submission to this journal, every effort should be made to prevent the identities of the authors and reviewers from being known to each other. The authors of the document have deleted their names from the main text, with "Author" and year used in the references and footnotes, instead of the authors' name, article title, etc. After the journal was accepted, the name of authors and affiliation and the name of the corresponding author must be included into the document and re-submitted in the copyediting stage.

Proof correction

The Proofs of final paper approved for publication are to be returned by email to the researcher before publication.

Page charge

No page charge.

References Format

1. References using the Vancouver referencing style (see example below).
2. In-text citation: Indicate references by number(s) in the order of appearance in the text with superscript format. Reference numbers are to be placed immediately after the punctuation (with no spacing). The actual authors can be referred to, but the reference number(s) must always be given. When multiple references are cited at a given place in the text, use a hyphen to join the first and last numbers that are inclusive. Use commas (with no spacing) to separate non-inclusive numbers in a multiple citation e.g. (2-5,7,10). Do not use a hyphen if there are no citation numbers in between inclusive statement e.g. (1-2). Use instead (1,2).
3. References list: number the references (numbers in square brackets) in the list must be in the order in which they are mentioned in the text. In case of references source from non-English language, translate the title to English and retain "in Thai" in the parentheses.
4. Please note that if references are not cited in order the manuscript may be returned for amendment before it is passed on to the Editor for review.

Examples of References list

Multiple Authors: List up to the first 6 authors/editors, and use "et al." for any additional authors.

Journal Articles (print): In case of reference source contains DOI, retain doi: at the end of reference. Vancouver Style does not use the full journal name, only the commonly-used abbreviation: "Physical Therapy" is cited as "Phys Ther". As an option, if a journal carries continuous pagination throughout a volume (as many medical journals do) the month and/or issue number may be omitted. Allow one space after semi-colon and colon and end each reference with full stop after page number.

- Pachori P, Gothalwal R, Gandhi P. Emergence of antibiotic resistance Pseudomonas aeruginosa in intensive care unit; a critical review. Genes Dis. 2019; 6(2): 109-19. doi: 10.1016/j.gendis.2019.04.001.
- Hung Kn G, Fong KN. Effects of telerehabilitation in occupational therapy practice: A systematic review. Hong Kong J Occup Ther. 2019; 32(1): 3-21. doi: 10.1177/1569186119849119.
- Wijesooriya K, Liyanage NK, Kaluarachchi M, Sawkey D. Part II: Verification of the TrueBeam head shielding model in Varian VirtuaLinac via out-of-field doses. Med Phys. 2019; 46(2): 877-884. doi: 10.1002/mp.13263.
- Velayati F, Ayatollahi H, Hemmat M. A systematic review of the effectiveness of telerehabilitation interventions for therapeutic purposes in the elderly. Methods Inf Med. 2020; 59(2-03): 104-109. doi: 10.1055/s-0040-1713398.
- Junmee C, Siriwachirachai P, Chompoonimit A, Chanavirut R, Thaweewannakij T, Nualnetr N. Health status of patients with stroke in Ubolratana District, Khon Kaen Province: International Classification of Functioning, Disability and Health-based assessments. Thai J Phys Ther. 2021; 43(1): 45-63 (in Thai).

Book / Chapter in an Edited Book References

PLEASE be informed that references of books and chapter in edited book should not be include in the research article, but others manuscript categories.

- Grove SK, Cipher DJ. Statistics for Nursing Research: A Workbook for Evidence-Based Practice. 3rd Ed. St. Louis, Missouri: Elsevier; 2019.
- Perrin DH. The evaluation process in rehabilitation. In: Prentice WE, editor. Rehabilitation techniques in sports medicine. 2nd Ed. St Louis, Mo: Mosby Year Book; 1994: 253–276.

E-book

- Dehkharghani S, editor. Stroke [Internet]. Brisbane (AU): Exon Publications; 2021 [cited 2021 Jul 31]. Available from: https://www.ncbi.nlm.nih.gov/books/NBK572004/ doi: 10.36255/exonpublications.stroke.2021.
- Tran K, Mierzwinski-Urban M. Serial X-Ray Radiography for the Diagnosis of Osteomyelitis: A Review of Diagnostic Accuracy, Clinical Utility, Cost-Effectiveness, and Guidelines [Internet]. Ottawa (ON): Canadian Agency for Drugs and Technologies in Health; 2020 [cited 2021 Jul 31]. Available from: https://www.ncbi.nlm.nih.gov/books/NBK562943/

Dissertation/Thesis

- Borkowski MM. Infant sleep and feeding: a telephone survey of Hispanic Americans [Dissertation]. Mount Pleasant (MI): Central Michigan University; 2002.
- On-Takrai J. Production of monoclonal antibody specific to recombinant gp41 of HIV-1 subtype E [Term paper]. Faculty of Associated Medical Sciences: Chiang Mai University; 2001 [in Thai].

Conference Proceedings

- Lake M, Isherwood J, Clansey. Determining initial knee joint loading during a single limb drop landing: reducing soft tissue errors. Proceedings of 34th International Conference of Biomechanics in Sport; 2016 Jul 18-22; Tsukuba, Japan, 2016. Available from: https://ojs.ub.uni-konstanz.de/cpa/article/view/7126.
- Ellis MD, Carmona C, Drogos J, Traxel S, Dewald JP. Progressive abduction loading therapy targeting flexion synergy to regain reaching function in chronic stroke: preliminary results from an RCT. Proceedings of the 38th Annual International Conference of the IEEE Engineering in Medicine and Biology Society; 2016: 5837-40. doi: 10.1109/EMBC.2016.7592055.

Government Organization Document

- Australian Government, Department of Health. Physical activity and exercise guidelines for all Australian. 2021 [updated 2021 May 7; cited 15 Jul 2021]. Available from: https://www.health.gov.au/health-topics/physical-activity-and-exercise/physical-activity-and-exercise-guidelines-for-all-australians.
- Department of Health. Situation survey on policy and implementation of physical activity promotion in schools for first year 2005. (in Thai). Nonthaburi: Ministry of Public Health; 2005.
- Department of Local Administration, Ministry of Interior Affairs. Standard of Sports Promotion. (in Thai). Bangkok. 2015:7–9.
- World Health Organization. WHO guidelines on physical activity and sedentary behaviour. Geneva: World Health Organization; 2020. Licence: CC BY-NC-SA 3.0 IGO.

Journal History

Established in 1968

- 1968-2016 As the Bulletin of Chiang Mai Associated Medical Sciences
  - Vol1, No1 - Vol.49, No3
- 2017, the Journal of Associated Medical Sciences
  - Vol.50, No1 and forward.

Journal Sponsorship Publisher

Faculty of Associated Medical Sciences, Chiang Mai University

Sponsors

Faculty of Associated Medical Sciences, Chiang Mai University

Sources of support

Faculty of Associated Medical Sciences, Chiang Mai University